Università degli Studi della Tuscia di Viterbo

Dipartimento di Scienze Agrarie e Forestali (DAFNE)

PhD Program "Plant and Animal Science"

XXXV ciclo

Development and characterization of durum wheat genotypes with improved nutritional and technological properties

AGR/07

Ph.D. Student:
Dott.ssa Arianna Frittelli

Ph.D. Coordinator
Prof.ssa Roberta Bernini

Supervisor
Prof. Francesco Sestili

Co-tutors
Dott. Mirko Volpato

Dott.ssa Ermelinda Botticella

Dott.ssa Samuela Palombieri

A.Y. 2021/22

CHAPTER 1

1. General Introduction

1.1 Wheat

Wheat, along maize and rice, represents the most cultivated and consumed cereal. Nowadays, wheat is grown from Scandinavia and Russia to Argentina, in mainly temperate, but also tropical, sub-tropical and desert environmental conditions. Wheat represents a staple food in more than 40 countries around the world, providing over 20% of calories and protein in human nutrition. The adaptability to cultivation in different climatic and environmental conditions, the good nutritional profile, the versatility of processing and its easy and safe storage are the main reasons for its worldwide spread (**Figure 1.1**) (**Ranhotra, 1995**; **Bushuk, 1996**; **Shewry, 2009**). Of the total production about 65% is destined for human food, 21% for animal feed, 8% for seeds and the remaining 6% for other uses including industrial ones (**Orth and Shellenberger, 1988**). FAO's latest forecast regarding global cereal production in 2023 is equal to 2 765 million tonnes, of which about 794 million tonnes represent wheat production (**Figure 1.2**) (**FAOSTAT, 2023**).

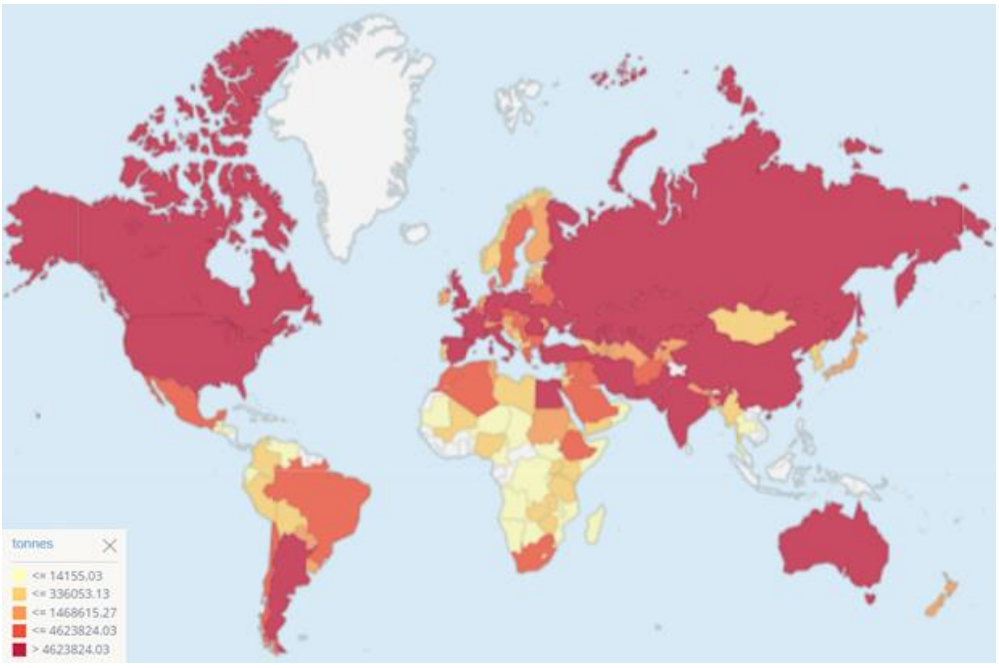

Figure 1.1 Wheat production by Country (FAOSTAT data 2021).

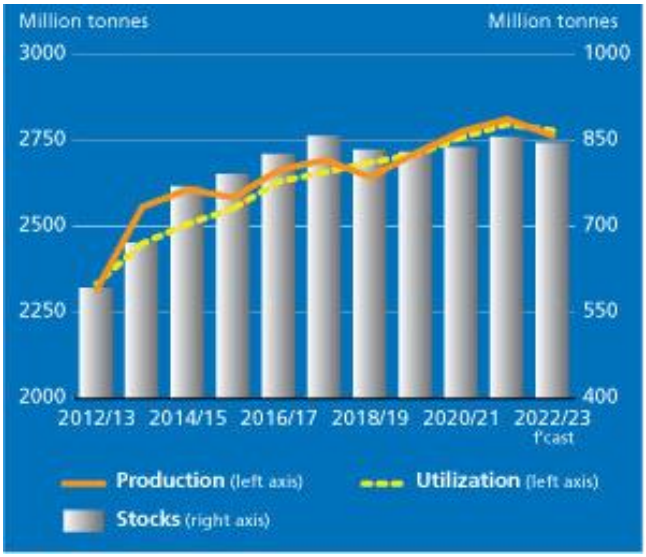

Figure 1.2 Cereal production, utilization and stocks from 2013 to 2023 (FAOSTAT data 2023).

Asia represents the continent with the highest production (43.5%), followed by Europe (33%), America (17%), Africa (3.3%) and Oceania (3.2%) (**Figure 1.3**) (**FAOSTAT, 2021**).
In Europe, Russia is the first producer followed by France and Ukraine. In 2021 Italy produced about 7 million tonnes of wheat compared to the 270 million tonnes produced by Europe (**FAOSTAT, 2021**).

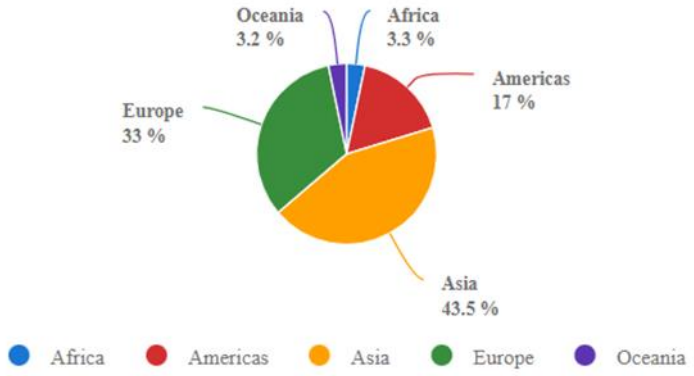

Figure 1.3 Production share of Wheat by region (FAOSTAT data 2021).

Currently about 95% of world wheat production is represented by bread wheat, *Triticum aestivum* ssp. *aestivum* (hexaploid with AABBDD genome) used mainly for the production of bread, biscuits, crackers and pastry products; the remaining 5% is durum wheat, *Triticum*

turgidum ssp. *durum* (tetraploid with AABB genome) used for the production of pasta, couscous, bulgur and bread in some regions of southern Italy (**Kolster, 1992**; **Shewry, 2009**).

1.1.1 Durum Wheat

Durum wheat is the 10th most important and cultivated cereal worldwide with a production of 40 million tonnes. Despite accounting for only 5% of total production, on global scale, durum wheat has significant economic relevance (**FAOSTAT, 2021**).

Durum wheat is adapted to more diverse environments than bread wheat and it performs very well in semiarid regions. It is grown primarily in the Mediterranean basin supported mainly by Italy, Egypt, Spain, France, Greece, Morocco, Algeria, Tunisia, Turkey and Syria accounting for 75% of global production. The major producers outside the Mediterranean basin are Canada, Mexico, the USA, Russia, Kazakhstan, Azerbaijan, and India (**De Vita and Taranto, 2019**; **Martínez-Moreno et al., 2022**).

The typical durum kernel is hard, translucent, vitreous, and amber-colored with high protein content. These characteristics determine the suitability of durum wheat for milling into semolina. Durum wheat is used to produce a range of food products, such as pasta, couscous and bulgur and some traditional local dishes and desserts (**Kadkol and Sissons, 2016**; **Tidiane Sall et al., 2019**; **Beres et al., 2020**).

Furthermore, durum wheat constitutes the main food source for 1.2 billion poor people, providing 20-50% of daily calories and is considered a strategic crop for food security. However, the ongoing climate change along with increased consumption threatens production and leads to the need for genetic improvement.

Climate forecasts for the 2040-2070 period in the Mediterranean and Western Europe warn that extreme drought events will become more frequent and severe due to decreased winter precipitations and increasingly drier springs (**Spinoni et al., 2018**). According to recent projections, global warming may reduce the world's suitable areas for durum wheat cultivation by 19% in 2050 and 48% in 2100, with the greatest losses occurring in the Mediterranean area (**Shayanmehr et al., 2020; Martínez-Moreno et al., 2022**). The main environmental constraints affecting durum wheat yield in this area are drought, high temperatures and salinity (**De Vita and Taranto, 2019**), overall if they occur in some growth stages such as flowering, pollination, and grain filling.

To guarantee the production considering the above cited factors and in climate change scenarios, numerous breeding programmes are focused on current topics, such as 1) resistance to biotic disease, 2) improvement of grain protein content, grain weight, semolina yield, semolina color, 3) improvement of dough characteristics and pasta-making properties. World durum production has a potential to expand despite the challenges from the changing climate, loss of arable land to other uses, and competition from other crops (**Morris and Sands, 2006**; **Kadkol and Sissons, 2016**; **Beres et al., 2020; Xynias et al., 2020**).

1.2 Origin and Phylogeny of *Triticum*

Wheat belongs to the genus *Triticum*, tribe *Triticeae*, family *Poaceae*. The center of origin and differentiation is represented by the area of the Middle East, between the Mediterranean coast and the Tigris and Euphrates, known as the Fertile Crescent area.
The first cultivation of wheat dates back to about 10.000 years ago, during the 'Neolithic Revolution', when there was the transition from hunter-gatherers to a sedentary life (**Dubcovsky and Dvorak, 2007**; **Shewry, 2009**; **Faris, 2014**).
The cultivated wheat consists of several species with different degrees of ploidy originated through the phenomenon of amphiploidy, a process in which fertile polyploids were formed as a result of spontaneous crossings between species with different chromosome structure (hybridization) followed by spontaneous chromosomal doubling. Wheat genome is arranged into seven chromosomes (1x = 7) and grouped in diploid (2n = 2x = 14), tetraploid (2n = 4x = 28) and hexaploid wheats (2n = 6x = 42) (**Shewry et al., 2003**; **Feldman et al., 2012**; **Faris, 2014**).
Given the high number of species and the high capacity of interspecific crossing, the classification of wheat is still in continuous revision. One of the first classifications dates back to 1913 when Schulz divided the genus *Triticum* into three main groups (eikorn-*Triticum monococcum*, emmer- *Triticum dicoccum*, dinkel- *Triticum spelta*) based on morphological traits. The proposed division was then confirmed by cytogenetic studies conducted by **Sakamura (1918)** determining the correct chromosomal number of the three groups of wheat. In 1924 Kihara, analyzing the chromosomal pairing during meiosis in hybrids of species considered more or less similar, identified different types of genome and grouped wheat in diploid (2n = 2x = 14) with AA genome, tetraploid (2n = 4x = 28) with AABB genome and hexaploid species (2n = 6x = 42) with AABBDD genome (**Feldman et al., 2012**).
Diploids (AA genome) comprise *T. urartu* and *T. monococcum* that includes *T. monococcum* ssp. *boeoticum* and *T. monococcum* ssp. *monococcum* (derived from domestication of the previous one). Tetraploids include the species *T. turgidum* and *T. timopheevii* originating from spontaneous interspecific crossing between *T. urartu* and a wild species belonging to the genus *Aegilops*, donor of the BB genome and the GG genome respectively (most likely *Aegilops speltoides*). *T. turgidum* is constituted by different subspecies that comprehends *T. turgidum* ssp. *dicoccoides* from whose was domesticated *T. turgidum* ssp. *dicoccum*, from which is then derived the current durum wheat *T. tugidum* ssp. *durum*. *T. timopheevii* is constituted by the wild *T. timopheevi* ssp. *araraticum* and the cultivated *T. timopheevii* ssp. *timopheevii*. Hexaploid wheats include the species *T. aestivum* and *T. zhukovskyi*. *T. aestivum* originated from hybridization between *T. turgidum* ssp. *dicoccoides* and *Aegilops tauschii* (also called *Aegilpos squarrosa*) donor of the genome DD. *T. zhukovskvi* instead derives from the hybridization between *T. timopheevii* and the cultivated diploid *T. monococcum* (**Figure 1.4**).

The species currently most cultivated by economic importance are *T. aestivum* ssp. *aestivum* (hexaploid with AABBDD genome) and *T. tugidum* ssp. *durum* (tetraploid with AABB genome). However, the species *T. monococcum* (diploid with AA genome) and *T. timopheevii* (tetraploid with YYDD genome) are also cultivated (**Dvorak et al., 1988**; **Dvorak et al., 1993**; **Huang et al., 2002**; **Shewry et al., 2003**; **Shewry, 2009**; **Faris, 2014**; **Levy and Feldman, 2022**).

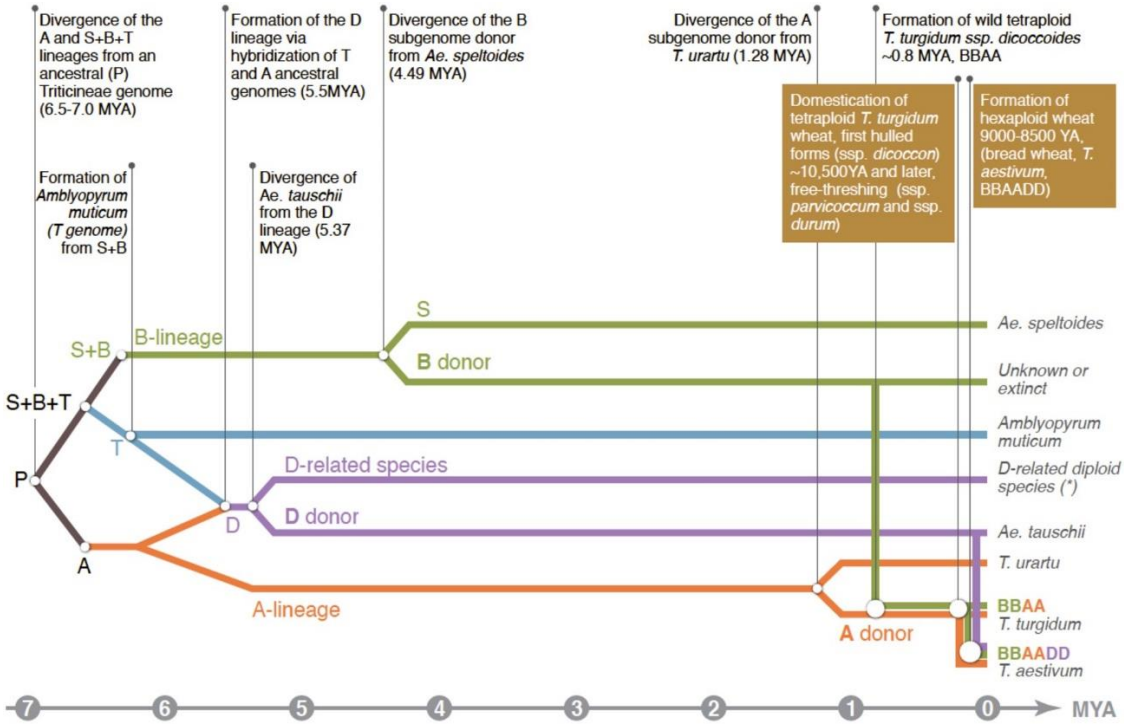

Figure 1.4 Representation of wheat evolution (Levy and Feldman, 2022).

1.3 Wheat Kernel Composition

Wheat kernel is an indehiscent dry fruit with an average length of 8-9 mm and a weight between 20 and 50 mg. It represents the site of accumulation of the products of photosynthesis and nitrogen metabolism and contains proteins (7-15%), lipids (2-9%) and a high content of carbohydrates (65-75%) mainly in the form of starch. It represents a good source of minerals, vitamins and molecules with antioxidant activity such as phenolic acids, lignans and carotenoids.

The wheat grain is composed of three parts: bran (13-17%), embryo (3%) and endosperm (80-85%) (**Figure 1.5**). The bran is formed by the covering layers (pericarp outside and residues of the seminal teguments inside) and by the aleuronic layer, made up of parenchyma cells, which surrounds the endosperm. In particular, the aleuronic layer contains high levels of β-glucans which represent the major components of soluble dietary fiber, arabinoxylans, appreciable quantities of ferulic acid which has antioxidant activity, proteins, vitamins, minerals and lignans with antioxidant and anticancer activity. The embryo presents a high lipid and protein content, with minerals such as potassium (K), calcium (Ca), magnesium (Mg) and zinc (Zn) and both water-soluble and fat-soluble vitamins including vitamin A, tocopherols and tocotrienols. The endosperm is contained within the aleuronic layer and represents the source of nutrition for the developing embryo; rich in starch it also contains proteins, lipids, minerals and soluble fiber (**Evers and Millars, 2002**; **Surget and Barron, 2005**; **Hemery et al., 2007**; **Seal et al., 2016**). During milling process the embryo, aleurone, and pericarp are removed, leaving the starchy endosperm as the principal contributor to white flour.

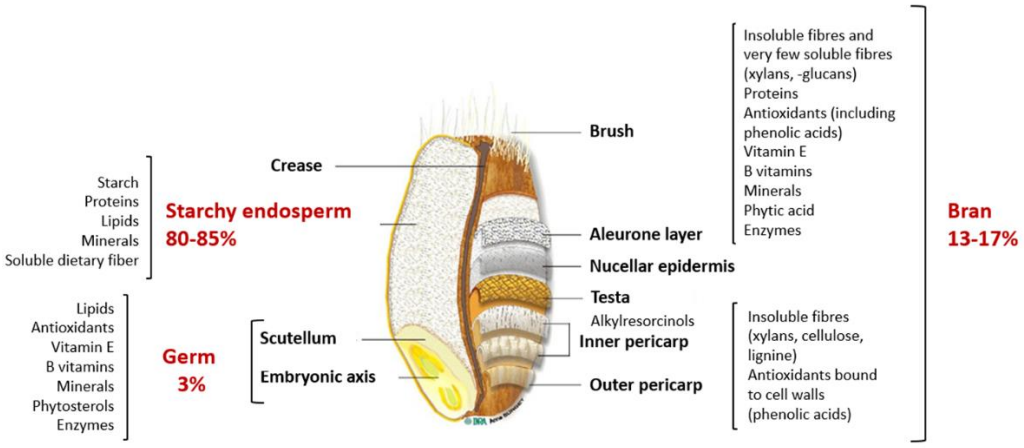

Figure 1.5 Composition and structure of wheat kernel (Modified by Hemery et al., 2007).

1.3.1 Starch

Starch is the most abundant storage carbohydrate in wheat and comprises about 60–75% of grain and 70–80% of flour. It consists of two different glucose polymers, amylose and amylopectin. They differ in the degree of polymerization. Amylose is a linear polymer with α(1→4) linkages and a degree of polymerization of 10^3-10^4 glucose units. Amylopectin presents a higher degree of polymerization of 10^5-10^7 glucose units; the structure is larger and more

branched as it contains more branch points connected to the linear chain by α(1→6) linkages (**Shevkani et al., 2017**).
Typically wheat starch contains 20–30% of amylose and 70–80% of amylopectin. The amylose/amylopectin ratio together with the size and ramification of the polymers represent the factors that determine the chemical-physical properties and functional characteristics of starch. The modification of the starch composition in the amylose/amylopectin ratio represents an important strategy to develop new starch properties suitable for novel end uses (**Sestili et al., 2014**).

1.3.2 Lipids

The lipids present in the wheat kernels are mainly found in the embryo, but in moderate quantities also inside endosperm and bran. Most polar lipids are represented by glycolipids and phospholipids derived from the cell wall and located in the starchy endosperm. Non-polar lipids are mainly present within the embryo and aleuronic layer.
Part of the lipids are bound to starch to form starch-lipid complexes, while another part binds to proteins during dough processing by increasing gas retention and influencing the technological qualities of wheat flour (**Šramková et al., 2009**; **Pareyt et al., 2011**; **Cornell, 2012**).

1.3.3 Proteins

Proteins present in wheat grains were classified by Osborne in 1924 into four different groups according to their extractability and solubility in various solvents:
• Albumins: water-soluble low molecular weight proteins;
• Globulins: low molecular weight proteins soluble in saline solutions (NaCl);
• Gliadins: monomeric proteins soluble in alcoholic solutions (70% EtOH);
• Glutenins: polymeric proteins soluble in acidic solutions.
In general, albumins and globulins constitute about 20% of the wheat kernel, they are mainly present in the aleuronic layer and germ. They are physiologically active proteins, in particular globulins promote the hydrolysis of starch by producing the substrates necessary for fermentation during the leavening of wheat dough. Albumins and globulins have dual roles as nutrient reserves for the germinating embryo and as inhibitors of pathogens before germination (**Dupont and Altenbach, 2003**).
Gliadins and glutenins account for 80-85% of wheat grain proteins. These proteins are accumulated exclusively in the endosperm and have the role of storage proteins. Since their high content in proline and glutamine, they are referred as prolamins, proteins that form gluten.

The technological properties of wheat flour and in particular the visco-elastic properties of the doughs depend on the quality of gluten proteins, gliadins and glutenins, which confer respectively extensibility strength and elasticity (**Shewry et al., 1995**).

1.3.4 Fiber

Dietary fiber represents a food component not digested in the human gastrointestinal tract and can be divided into two categories: soluble dietary fiber and insoluble dietary fiber. The first is characterized by water-soluble components and includes pectic and hydrocolloid substances; the second is made up of components that are insoluble in water and include cellulose, hemicellulose and lignin.
The main components of fiber are represented by β-glucans and arabinoxylans. Localized in the aleuronic layer and in the endosperm, they seem to have an immunostimulant activity and positive effects on the containment of the glycaemic, insulin and cholesterol response. A component of arabinoxylans constitutes the insoluble fiber, and is localized in the aleuronic layer and pericarp and considered an excellent substrate for the production of short-chain fatty acids (SCFA), specifically butyrate in the colon which appears to improve intestinal health and reduce the risk of cancer (**Dalmo and Bøgwald, 2008**; **Chen and Raymond, 2008**; **Šramková et al., 2009**).

1.3.5 Vitamins and Minerals

The vitamins are found in the aleuronic layer and the germ. They represent essential micronutrients for humans and perform various biochemical functions such as coenzymes or their precursors (niacin, thiamin, biotin, vitamin B6, vitamin B12 and folate), antioxidants (vitamin C, vitamin E, carotenoids), factors involved in gene regulation (folic acid, vitamin B12, vitamin B6, vitamin C, D and E) or have specific functions such as vitamin A and ascorbate. The minerals such as potassium (K), calcium (Ca), magnesium (Mg), zinc (Zn), iron (Fe) and selenium (Se) present in the wheat kernels depend on the mineral content present in the soil, but the accumulation is also influenced by genetic factors. Deficiency in the diet causes serious nutritional problems that lead to serious health, economic and social consequences (**Šramková et al., 2009**).

1.4 Wheat genetic improvement

Agriculture, which arose independently in different places about 10.000 years ago, played a central role in human evolution. Man has always selected phenotypically plants present in nature to preserve interesting traits and, at the same time, to create new varieties with better characteristics. Therefore genetic improvement has developed at the same time as agriculture itself.

Domesticated wheat, transferred from a natural growth situation to artificial cultivation conditions, presents distinct genetic traits from their wild progenitors. One of these traits is represented by the loss of seed shattering at maturity which prevents the dispersion of the seeds and facilitates harvesting; the trait is determined by a mutation at the *Br* (*brittle rachis*) locus (**Nalam et al., 2006**). The second important trait selected is represented by the development of free-threshing naked seeds, in which the glumes no longer adhere to the kernel. The free forms arose by a dominant mutant at the *Q* locus which modified the effects of recessive mutations at the *Tg* (*tenacious glume*) locus (**Simons et al., 2006**; **Dubcovsky and Dvorak, 2007**). Other traits of the domestication syndrome in wheat are related to grain size, uniformity in germination, increase in seeds per spike, plant height, seed hardness, and reduced seed dormancy (**Feldman, 2001**; **Kilian et al., 2010**).

Wheat genetic improvement has multiple objectives that have emerged over time based on demographic development and consumer demand. While in the past the main objectives concerned the increase in production and therefore yield, today particular attention is given to genetic improvement for quality understood in its overall sense as organoleptic, nutritional, technological and hygienic-sanitary quality.

1.4.1 Conventional Breeding and Mutagenesis

Conventional methods of genetic improvement are based on the crossing and the subsequent selection of the desired characteristics. However, the classic approach presents the limitation of not ignoring sexual compatibility and the timing of obtaining the new variety is long.

The development of biotechnology has made important progress in the field of genetic improvement, since it has been possible to overcome the limitations of traditional technologies. Crop breeding programmes generally rely on germplasm resources, the first source of genetic variation, essential to produce a progeny with suitable agronomic traits (**Hua et al., 2019**). Considering that crop breeding programmes could take several years due to the availability of beneficial alleles, several approaches have been developed during the last 40 years to face this problem (**Oladosu et al., 2016**). In particular, new allelic variants can be generated by the use of physical and chemical mutagenesis. At present, over 3000 commercial varieties of food crops have been produced by mutagenesis (IAEA Mutant Variety Database) (**Chaudhary et al., 2019**).

Mutagenesis uses chemical (ethyl methane sulphonate, sodium azide) or physical (X-ray, γ-ray, UV, accelerated neutron and ion beam) mutagens which increase the rate of mutations transmitted to progeny to improve genetic variability. The mutants obtained can be used for functional studies or the development of new varieties with superior characteristics to the starting ones.

Classical mutagenesis has been widely used in breeding programs in the last 60 years, but the progress made in genome sequencing, the greater availability of gene sequences and the

development of new technologies allowed the use of reverse genetic techniques; in this way, from the sequence of a gene it is possible to trace the corresponding phenotype, therefore to the gene function and improve the traits of interest (**Parry et al., 2009**; **Gilchrist and Haughn, 2010**).

1.4.2 TILLING

Targeting Induced Local Lesions IN Genomes (TILLING) is a highly processive reverse genetics technique that combines chemical mutagenesis with PCR-based screening for mutant identification in the gene of interest (**McCallum et al., 2000**; **Till et al., 2003**; **Till et al., 2007**). TILLING exploits classical mutagenesis, sequence availability and high-throughput screening for nucleotide polymorphisms in a targeted sequence; moreover it can be applied to any plant species, regardless of its genome size, ploidy level or method of propagation. The use of chemical mutagens, usually ethyl methane sulphonate (EMS), provides a high frequency of point mutations distributed on a specific gene of interest. This chemical agent produces point mutations through the alkylation of a guanine residue, mainly causing G → A and C → T transitions which lead to a high probability of causing the formation of nonsense codons. The mutations are stably introduced in the genome, which is not always the case with alternative reverse genetics such as RNA interference (RNAi) silencing, and genetic transformation is not required. TILLING is the only reverse genetics strategy applicable for species that are not transformable or recalcitrant. It is recommended as non-GMO technology, so GMO controversies are avoided. Moreover, TILLING is not technically demanding and can be performed at relatively low cost (**Kurowska et al., 2011**).

The creation of a TILLING platform is characterized by three main steps: development of a mutagenized population; extraction of DNA and creation of pools; screening of mutations for the selection of mutants of interest.

Although over time many techniques have been developed for the screening of mutations in mutagenized populations, the use of High Resolution Melting (HRM) remains one of the best high-throughput strategies (**Wittwer et al., 2003**).

This technique represents a valid strategy for the improvement of cereal species through the introduction of new variability, without resorting to traditional breeding techniques or genetic transformation. The recalcitrant nature of these species to transformation and *in vitro* regeneration causes significant limitations to the approaches of insertional mutagenesis and silencing through transgenic technology. Polyploidy also allows greater tolerance to mutagenesis due to the effect of compensation of homoeologous genes present in another genome, allowing the development of populations with high mutation density (**Singh et al., 2014**).

2. Objectives

Climate change and the need to feed an increasing population affect food production and security, fostering the development of new agriculture, more sustainable, productive, and accessible worldwide.

Among staple crops, cereal species represent the most important in terms of cultivated area, production and consumption. Wheat and derived foods play an important role in human nutrition as they represent a good source of carbohydrates, proteins, dietary fiber and micronutrients providing 20% of the global calorie requirement. Despite this, it is necessary to consider that the kernel compartmentation and its constituents, together with the transformation processes it undergoes in the food industry, strongly influence the nutritional and technological profile.

Scientific research focused on the cereals genetic improvement is therefore called to develop varieties that are both productive and sustainable. It is also important to consider that while it is necessary to increase production to feed the growing population, on the other hand, it should be remembered that hidden hunger involves than 3 billion people around the world and the incidence of non-communicable diseases such as type II diabetes, obesity, some cardiovascular diseases and cancer is growing in industrialised countries.

Therefore, it is essential to develop new varieties that are more productive but at the same time able to bring benefits to human health.

The purpose of the Ph.D. project is to develop and characterize new durum wheat genotypes with improved yield, nutritional and technological properties than current varieties. The project includes three activities.

The first activity focused on the modulation of the phytic acid (PA) content in durum wheat. Depending on its chemical structure, PA binds important mineral cations such as iron (Fe), zinc (Zn), potassium (K), calcium (Ca) and magnesium (Mg) precipitating in the form of phytate salts poorly digested by monogastric animals, including humans, due to the lack of phytases in the digestive tract. A reduced bioavailability of microelements in the raw materials is considered one of the main causes of mineral deficiency in populations whose diet is largely based on the consumption of staple crops. In this regard, the genetic modulation of PA in cereal grains represents a valid strategy of biofortification in essential minerals.

The second activity concerns the development of three durum wheat genotypes in which novel properties have been combined both in the health-functional profile of the derived foods and in the milling characteristics of the grain. The project involves a group of durum wheat genotypes, in which the starch composition (amylose/amylopectin ratio) has been modified (**Lafiandra et al., 2010**; **Sestili et al., 2015**; **Botticella et al., 2016**). In detail, genotypes with a high and low amylose content showing mutations in the *SSIIa, SBEIIa* and *GBSSI* genes were crossed with a soft durum wheat (**Morris et al., 2011**). This activity was performed as the high amylose

genotypes exhibited a higher kernel hardness, that reduced the milling performance. The introduction of the soft trait in these genotypes is expected to improve the efficiency and sustainability of milling along with the quality of the end products.

Although the SSIIa genotype presents a good nutritional profile due to the elevated amount of amylose in the grain, it shows negative effects in terms of grain yield. Recently some authors demonstrated that the silencing of *TaGW2-A1* allele has positive effects on grain size, weight and yield (**Simmonds et al., 2016**). In the third activity a Kronos GW2-A1^{-} mutant was crossed with the high amylose Svevo SSIIa mutant in order to develop durum wheat lines with improved yield and study the effects of the *GW2* gene on the grain size with the aim to increase yield in high amylose genotypes.

A TILLING approach has been undertaken to achieve these objectives to create new genetic variability that can be used in future breeding programs without legislative limitations.

CHAPTER 2

The suppression of *TdMRP3* genes reduces the phytic acid and increases the nutrient accumulation in durum wheat grain

Modified by Frittelli et al., 2023 doi: 10.3389/fpls.2023.1079559

Frittelli A.[1], Botticella E.[2], Palombieri S.[1], Masci S.[1], Celletti S.[1], Fontanella M.C.[3], Astolfi S.[1], De Vita P.[4], Volpato M.[5] and Sestili F.[1]

[1]Department of Agriculture and Forest Science (DAFNE) - University of Tuscia, Via Camillo de Lellis snc, 01100 Viterbo ,Italy
[2]Institute of Sciences of Food Production (ISPA) - CNR. via Provinciale Lecce-Monteroni, 73100 Lecce ,Italy
[3]Department for Sustainable Process, Faculty of Agriculture, Food and Environmental Science (DiSTAS), Università Cattolica, Via Emilia Parmense 84, 29122 Piacenza ,Italy
[4]Council for Agricultural Research and Economics, Research Centre for Cereal and Industrial Crops (CREA-CI), S.S. 673, Km 25,200, 71122 Foggia ,Italy
[5]Grandi Molini Italiani, Via Elettricità, 13, 30175 Venezia ,Italy

Abstract

Micronutrient malnutrition affects more than half of the world population. Reduced bioavailability of microelements in the raw materials is considered one of the main causes of mineral deficiency in populations whose diet is largely based on the consumption of staple crops. In this context, the production of low phytic acid (*lpa*) cereals is a main goal of the breeding programs, as phytic acid (PA) binds essential mineral cations such as iron (Fe), zinc (Zn), manganese (Mn), potassium (K), calcium (Ca) and magnesium (Mg) precipitating in the form of phytate salts poorly digested by monogastric animals, including humans, due to the lack of phytases in the digestive tract. Since PA limits the bioavailability of microelements, it is widely recognized as an anti-nutritional compound. A Targeting Induced Local Lesions IN Genomes (TILLING) approach has been undertaken to silence the genes encoding the TdABCC13 proteins, known as Multidrug-Resistance associated Proteins 3 (TdMRP3), transporters involved in the accumulation of PA inside the vacuole in durum wheat. The TdMRP3 complete null genotypes showed a significant reduction in the content of PA and were able to accumulate a higher amount of essential micronutrients (Fe, Zn, Mn) compared to the control. The number of spikelets and seeds per spike, traits associated with the agronomic performances, were reduced compared to the control, but the negative effect was in part balanced by the increased grain weight. The TdMRP3 mutant lines showed morphological

differences in the root apparatus such as a significant decrease in the number of root tips, root length, volume and surface area and an increase in root average diameter compared to the control plants. These materials represent a promising basis for obtaining new commercial durum wheats with higher nutritional value.

KEYWORDS

Durum Wheat, Genetic Biofortification, Micronutrients, Mutagenesis, Phytic Acid, TILLING

2.1 Introduction

Wheat, along with rice and maize, is one of three major cereals cultivated worldwide. The adaptability to a wide range of conditions, the good nutritional profile, along with its unique dough visco-elastic properties are the main reasons for its success (**Shewry, 2009**).
Durum wheat (*Triticum turgidum* ssp. *durum*), the second wheat species most cultivated worldwide, is a key raw material in a wide variety of traditional foods largely consumed in the Mediterranean basin as a part of a diet style recognized as one of the healthiest in absolute terms (**Willett et al., 1995**; **Sofi et al., 2010**).
Where diets rely on plant-derived foods, it is crucial to increase the amount of health-promoting compounds (i.e. fibres, proteins, vitamins, antioxidants, minerals) in durum wheat as a valuable strategy to maintain good health and to prevent important non- communicable diet-related diseases (obesity, diabetes, cardiovascular disorders, osteoporosis, cancer), along with those associated to "hidden hunger". In this regard, hidden hunger indicates a particular form of undernutrition that occurs when the intake and absorption of micronutrients are not enough for the daily requirement. This pathology affects almost one-third of the population, triggering serious diseases such as anaemia, weak bones, fatigue and weakened immune system and a few hidden impacts on the general well-being, lowering the life quality and increasing the risk of new pathologies (**Lockyer et al., 2018**; **Vitamin and Mineral Nutrition Information System (VMNIS), 2022**).
Genetic biofortification of staple crops represents an effective and sustainable strategy to boost essential minerals (i.e. iron, magnesium, calcium, potassium and zinc) in the human diet as it does not require the addition of fertilizers during the cultivation or additives in food production giving, as result, a stable over generations crop enriched in the target compound (**Vasconcelos et al., 2017**; **Roberts and Mattoo, 2019**).

2.1.1 Phytic Acid as anti-nutritional factor

Myo-inositol-1,2,3,4,5,6-hexakisphosphate ($InsP_6$) is a ubiquitous component of eukaryotic cells that plays several regulatory roles (**Shears, 2001**). Also known as phytic acid (PA), it is the major phosphorus storage sink within the plant seeds and other plant tissues and organs such as pollen, roots, tubers and turions. The amount and distribution of PA within the kernel depend on the plant species. In barley, rice and wheat about 80% of PA is stored in the aleuronic layer and bran, whereas in maize and Arabidopsis mainly in the embryo and scutellum (**O'Dell et al., 1972**). Differently from cereals and Arabidopsis, about 95% of PA is accumulated in the cotyledons in legumes (**Ariza-Nieto et al., 2007**).
Due to its negative charges, PA binds important mineral cations such as zinc, iron, potassium, magnesium and calcium precipitating in the form of phytate salts poorly digested by monogastric animals, including humans, due to the lack of phytases inside the digestive tract.

As it chelates ions, the bioavailability of phosphorus and minerals is decreased and PA is considered an anti-nutritional compound. In addition, the excretion of undigested phosphate contributes to environmental pollution by accelerating the eutrophication of the soil (**Raboy, 2009**; **Secco et al., 2017**).

In plants, phytic acid biosynthesis is carried out through two metabolic pathways (**Sparvoli and Cominelli, 2015**). The lipid-dependent pathway acts in all plant tissues using precursors that include phosphatidylinositol (PtdIns) and PtdIns phosphates, while the lipid-independent pathway is mainly active in seeds consisting of the sequential phosphorylation of the 6-carbon myo-inositol and soluble inositol phosphates (InsPs) (**Figure 2.1**). In the first step, glucose-6-phosphate is converted into myo-inositol-3-phosphate ($Ins(3)P_1$) by myo-inositol-3-phosphate synthase (MIPS). The subsequent steps involve sequential phosphorylation of the inositol ring through various enzymes (inositol phosphate kinase 2, IPK2; inositol 1,3,4-trisphosphate 5-/6 kinase, ITPK; inositol polyphosphate 2- kinase, IPK1). The synthesized phytic acid is accumulated into globoids, spherical inclusions found within protein bodies (**Krishnan, 2008**; **Regvar et al., 2011**), and stored inside the vacuoles where it is transported by specific PA protein transporters, such as the *Multidrug-Resistance associated Proteins* (MRPs) (**Sparvoli and Cominelli, 2014**; **Colombo et al., 2020**; **Cominelli et al., 2020a**).

Previous breeding programs focused on the reduction of PA to increase the mineral content of food and the sustainability of agricultural production in different crops (**Raboy, 2020**). Low phytic acid (*lpa*) genotypes have been produced in all major grain crops using different strategies. In this regard, *lpa* mutants can be divided into three classes according to the step where the mutations affect the PA biosynthetic pathway or transport: 1) the first biosynthetic step in which glucose-6-phosphate is converted into $Ins(3)P_1$ by MIPS; 2) the last biosynthetic step in which IPK1 phosphorylates $InsP_5$ in the 2-position to synthesize PA; 3) the transport and storage of phytic acid into the vacuole through the targeting of MRP transporters (**Sparvoli and Cominelli, 2015**; **Colombo et al., 2020**).

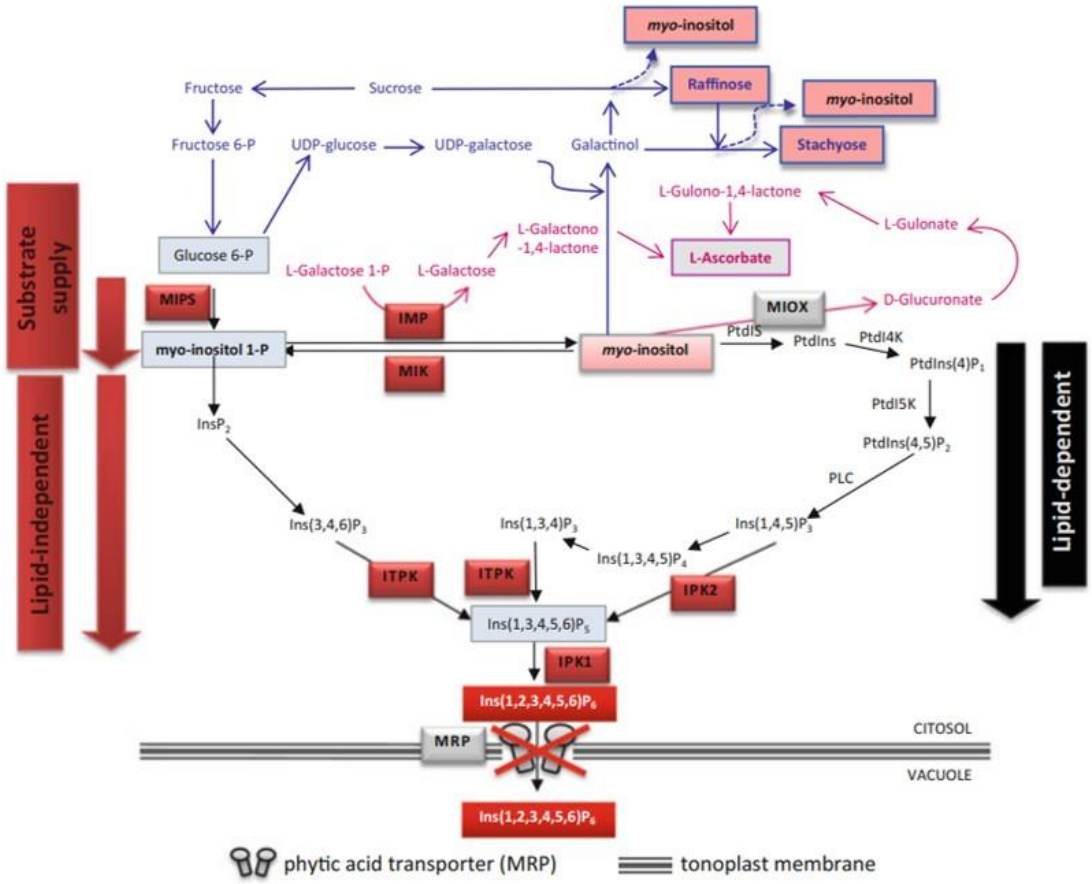

Figure 2.1 Representation of phytic acid biosynthesis (Sparvoli and Cominelli, 2014). The black lateral arrow indicates the lipid-dependent pathway, the red lateral arrow indicates the lipid-independent pathway. genes involved in the two biosynthetic pathways represented: MIPS myo-inositol-3-phosphate synthase, IMP bifunctional enzyme: myo-inositol-phosphate monophosphatase and galactose-1-phosphate phosphatase, MIOX myo-inositol monooxygenase, MIK myo-inositol kinase, IPK2 inositol 1,4,5-tris-phosphate kinase, ITPK inositol 1,3,4-triphosphate 5/6-kinase, IPK1 inositol 1,3,4,5,6 pentakisphosphate 2-kinase, PtdIS phosphatidyl inositol phosphate synthase, PtdI4K phosphatidyl inositol 4-kinase; PtdI5K phosphatidyl inositol 5-kinase, PtdIns phosphatidyl inositol; PtdIns(4)P_1 phosphatidyl inositol 4-phosphate; PtdIns(4,5)P_2, phosphatidyl inositol 4,5-biphosphate, PLC phospholipase C.

2.1.2 MRP3 Transporters

In bread wheat *TaMRP3* homeoalleles are located on the long arm of the 5A, 4B and 4D chromosomes and encode multidrug resistance-associated proteins belonging to the ABCC cluster of plant ATP-binding cassette (ABC) transporters (**Bhati et al., 2014**). ABC transporters are plant transmembrane transporters involved in the transport of molecules necessary for plant

growth (hormones, lipids, metabolites, and defence compounds) and involved in different plant processes (**Klein et al., 2006**; **Hwang et al., 2016**).

MRP proteins are characterized by a common structure consisting of two hydrophobic transmembrane domains (TMD1 and TMD2, containing six transmembrane α-helices) arranged with two cytosolic domains, referred as nucleotide-binding domains (NBD1 and NBD2) containing the Walker A and B motifs. PA transporters as other members of the ABCC cluster, contain an additional hydrophobic N-terminal extension (TMD0, containing five transmembrane α-helices) connected by a cytosolic loop to the rest of protein (**Figure 2.2**) (**Sparvoli and Cominelli, 2014**; **Colombo et al., 2020**). *Lpa* mutants were produced by targeting *MRP* genes in *Arabidopsis thaliana*, rice, soybean and common beans (**Colombo et al., 2020**), demonstrating that MRP proteins are involved in the transport of PA within the vacuole (**Shi et al., 2007**; **Nagy et al., 2009**).

Interestingly, **Bhati et al. (2016)** previously reported a partial suppression of *TaMRP3* genes by RNA interference (RNAi) and demonstrated its functional role in bread wheat. Due to its central role in PA transport, TdMRP3 is an attractive target for increasing the accumulation of minerals in durum wheat through a non-transgenic genetic approach focused on its inactivation. In this paper, the genes encoding TdABCC13 (TdMRP3) were completely disrupted at DNA level through a Targeting Induced Local Lesions in Genomes (TILLING) strategy, a highly processive non-transgenic reverse genetics technique that combines chemical mutagenesis with a PCR-based screening for the identification of mutations in the gene of interest (**McCallum et al., 2000**).

We show that the effect of *TdMRP3* silencing was a significant reduction in PA content, resulting in an improved capability to accumulate micronutrients (Fe, Zn, Mn) in wheat seeds. In addition, it was tested whether the suppression of *TdMRP3* genes in durum wheat generates modifications in root system architecture with significant consequences on root ability to acquire water and nutrients.

To the best of our knowledge, this study represents the first example of a genetic approach that successfully reduced the accumulation of phytic acid and increased the bioavailability of essential minerals in durum wheat kernel.

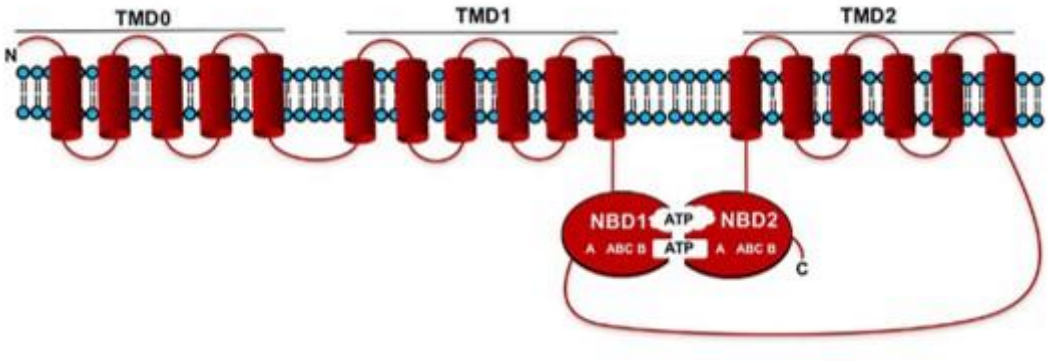

Figure 2.2 Schematic representation of ABCC transporters (Colombo et al., 2020).

2.2 Material and methods

2.2.1 Isolation of genes coding TdMRP3 from genomic databases

To identify the sequences of the *TdMRP3* genes, the orthologous genes of *T. aestivum* (TraesCS5A02G512500 and TreasCS4B02G343800) were used as queries in two independent approaches. In the first approach the two queries were blasted against *Triticum turgidum* ssp *durum* cv. Svevo genome in Ensembl Plants database (https://plants.ensembl.org/index.html). In the second one the orthologous query sequences were individually blasted against the Svevo Platinum genome available at the Svevo Platinum Genome Consortium (data unpublished). The exon/intron structure of the two identified durum wheat homeoalleles (*TdMRP3-A1* and *TdMRP3-B1*) was predicted by GENESCAN web tool (**Burge and Karlin, 1997**).

2.2.2 Bioinformatic analysis of TdMRP3 proteins

Domain topology and organization were predicted by analyzing and comparing the full-length amino acid sequence of each TdMRP3 protein in the UniProt database.
The orthologous sequences of the major grass species were identified by blasting the TdMRP3 protein sequences in NCBI BLASTP software (https://blast.ncbi.nlm.nih.gov/Blast.cgi). The orthologous sequence of *Arabidopsis thaliana*, used as an outsider, was isolated from TAIR database.
The multiple sequence alignment of MRP proteins (orthologous of TdMRP3) was performed by accurate Multiple Sequence Alignment (MSA) with PSI-Coffee 11.0 tool (**Chang et al., 2012**).
The phylogenetic analysis of MRP proteins was carried out by MEGA11 software (**Tamura et al., 2021**). The evolutionary history and distance among the selected taxa were deduced using

the Neighbor-Joining (NJ) method with p-distance method and pairwise deletion option. The bootstrap consensus tree was inferred from 1000 replicates.

2.2.3 Plant materials

A preliminary *in silico* study allowed the identification of two durum wheat mutant lines possessing deleterious mutations on the two *TdMRP3* homeoalleles through the platform WheatTILLING available at the University of Davis (https://dubcovskylab.ucdavis.edu/home; **Krasileva et al., 2017**). In detail, the line Kronos 3179 has a splice site mutation located in the 5' region of the intron 4 of *TdMRP3-A1*, while the line Kronos 4443 has a nonsense mutation in the exon 4 of *TdMRP3-B1* (**Supplementary Figure S1**). The presence of the two mutations was confirmed by Sanger sequencing.
The pyramiding of the two mutations was carried out by crossing the identified mutant lines TdMRP3-A1^{-} and TdMRP3-B1^{-}. The partial and complete null mutants along with the controls (cv. Kronos and wild-type sib lines derived by the cross) were grown in a controlled growth chamber with initial vernalization at 4-5°C for 3 weeks, followed by 18-26°C day and 16-18°C night temperature with a 16 h light period.

2.2.4 DNA extraction

Genomic DNA was extracted from leaves using the commercial kit NucleoSpin® Plant II (Macherey-Nagel, Düren, Germany) according to the manufacturer's instructions. The DNA was used as template for the genotyping analysis.

2.2.5 High resolution melting genotyping

High Resolution Melting (HRM) analysis was performed on *TdMRP3* gene amplicons including the targeted mutations, amplified from the genomic DNA of F_2 progeny of the cross described in the "Plant materials" paragraph. Amplicons were produced by a nested PCR strategy. The first PCR was carried out to amplify genome-specific fragments of 460 bp and 780 bp for *TdMRP3-A1* and *TdMRP3-B1* homeoalleles, respectively, using the primer pairs reported in **Supplementary Table S1**. The reaction was performed in a 20 µl volume using the following conditions: 10 µl of 2X GoTaq® G2 Hot Start Colorless Master Mix (Promega, Madison, USA), 0.5 µM of each primer, 20 ng of template DNA and nuclease- free water up to 20 µl volume, with the following conditions: 95°C for 2 min, followed by 38 cycles at 95°C for 30 sec, 58°C for 30 sec, 72°C for 1 min and a final extension at 72°C for 5 min. The first PCR reaction was diluted 60-fold and 2 µl were used as a template for the second PCR reaction for HRM analysis. The second reaction was carried out using the primer pairs reported in **Supplementary Table S1** and was prepared as follows: 2 µl of diluted DNA template, 5 µl of 2X GoTaq® G2 Hot Start Colorless Master Mix (Promega), 0.5 µM of each primer, 1 µL LC

Green Plus (Idaho Technology Inc., Salt Lake City, USA) and nuclease-free water up to 10 µl volume. The PCR program was carried out following these conditions: 95°C for 2 min, followed by 39 cycles at 95°C for 30 sec, 60°C for 20 sec, 72°C for 20 sec and a final extension at 72°C for 5 min. At the end of the final extension step, the reaction was held at 95°C for 30 sec, then at 25°C for 60 sec. The PCR reaction was carried out in 96-well Frame-Star plates (4titude Ltd., Surrey, UK) overlaid with 10 µl of mineral oil (Sigma-Aldrich, St. Louis, MO, USA). The Light Scanner instrument (Idaho Technology, Inc.) was used to analyse the melting curves.

2.2.6 Determination of phytic acid

PA was determined in mature seeds of the selected F_4 partial and complete null mutant lines (TdMRP3-A1$^-$, TdMRP3-B1$^-$ and TdMRP3-A1$^-$B1$^-$) along with the controls (cv. Kronos and WT sibling lines) using a commercial kit (K-PHYT kit, Megazyme Inc, Bray, Ireland). The grains were grounded to fine powder by a laboratory Cycline Mill (Cyclotec 1093, FOSS, Hilleröd, Sweden). One gram of the powder was suspended in 20 ml of 0.66 M HCl with continuous stirring overnight. The supernatant was then used for the colorimetric procedure according to the manufacturer's protocol. PA content has been expressed in the form of mean values of three biological replicates ± standard error. Three technical replicates were carried out for each biological replicate. Significant differences between mean values were identified by applying a one-way analysis of variance and the post hoc Tukey's HSD test, p-value< 0.01.

2.2.7 Visualization of iron deposits in seeds using the Perls stain

The *Perls* method is used to determine the localization of ferric iron (Fe^{3+}) deposits stained in blue in the tissues (**Krishnan et al., 2001**; **Prom-u-Thai et al., 2003**). Briefly, the mature F_4 seeds were soaked in dH_2O for 5 hours. Then, the seeds were cut transversely and longitudinally and placed in Petri dishes, submerged in freshly prepared Perls staining solution (2% hydrochloric acid mixed with 2% potassium ferrocyanide) for 30 min. The seeds were then gently washed continuously in dH_2O for 5 min. The intensity of staining was rated under a stereo microscope.

2.2.8 Determination of nutrients concentration

Mature F_4 seeds of the selected mutant lines along with controls (cv. Kronos and WT sibling lines) were grounded to fine powder and oven-dried at 80°C to constant weight. Samples were introduced in polypropylene tubes (digiTUBES, SCP Science, Champlain, NY, USA) with 3 mL of concentrated nitric acid and 1 mL of concentrated hydrogen peroxide and heated in a block system (DIGIPREP, SCP Science, Champlain, NY, USA) for 120 min at 95°C. After digestion, the extracts were filtered by a 0.45 µm teflon filter (DigiFILTER, SCP Science,

Champlain, NY, USA). After cooling down, the digests were diluted with dH_2O and analysed by inductively coupled plasma-mass spectrometry (ICP-MS 7900, Agilent Technologies, Santa Clara, CA, USA) with Octopole Reaction System (ORS). Phosphorous and sulfur in the digested solutions were determined by inductively coupled plasma-optical emission spectrometer (ICP-OES 5100 Agilent Technologies, Santa Clara, CA, USA). Data have been expressed as mean values of three biological replicates ± standard error. Three technical replicates were carried out for each biological replicate. The ICP-MS operating conditions are summarized in **Supplementary Table S2**.

2.2.9 Analysis of root morphological traits

The mature F_4 seeds of the selected mutant lines along with control plants (cv. Kronos and WT sibling lines) were soaked in dH_2O for 1 hour. Then they were transferred in Petri dishes and left to germinate for 5 days in the dark at room temperature. After germination, uniform seedlings were transferred to a plastic pot filled with 2 L of a continuously aerated nutrient solution (**Celletti et al., 2016**) and were placed in a growth chamber under 27/20°C and 14/10 h day/night cycles with a relative humidity of 80% and 200 mmol m^{-2} s^{-1} PAR at leaf level for 5 days. Roots were excised from the stem and subsequently placed in a Perspex tray with a shallow film of water to minimize root overlapping. Root systems were analysed using the WinRHIZO™ scanning equipment and software (EPSON1680, WinRHIZO Pro2003b Software; Regent Instruments Inc., Quebec, Canada) to determine their volume and surface area, total root length, root diameter and number of root tips. Data have been expressed as mean values of three biological replicates ± standard error. Three technical replicates were carried out for each biological replicate.

2.2.10 Field trial evaluation of yield-related traits

The experimental field trial was carried out at CREA-CI (Foggia, Italy) during the 2021-2022 growing season using standard agronomic practices. For this experiment, grains from two different genotypes were used: wild-type (cv. Kronos) and double null TdMRP3 mutant. Each genotype was seeded in single plots, consisting of 1-m rows, 30 cm apart, with 30 germinating seeds per plot, and following a randomized complete block design with three replications. Plots were hand-harvested at maturity and yield-related traits (i.e. Spike weight, g; Spike length, cm; Spikelets number per spike; Kernels per spike and Kernel weight per spike, g), measured from ten randomly selected spikes per row, were recorded.

2.3 Results

2.3.1 *In silico* analysis of TdMRP3 transporters

A blast search of *TaMRP3-A1* and *TaMRP3-B1* (TraesCS5A02G512500 and TraesCS4B02G343800) run against the durum wheat genome in Ensembl Plants revealed a high identity with TRITD5Av1G244640 and TRITD4Bv1G193220 both coding for proteins with ATP binding and ABC-type transporter activity. The comparison of the deduced protein sequences with TaMRP3 proteins showed that both TdMRP3 proteins lack the TDM0 domain and present a shorter IPR011527 ABCC1_TM domain (data not shown). A second blast of the orthologous *TaMRP3* homeoalleles was performed against the Svevo Platinum Genome and allowed the identification of two sequence hits with high identity values, located on the chromosomes 5A and 4B, respectively. The *TdMRP3* sequences of Svevo include 11 exons and 10 introns (**Supplementary Figures S1A**, **S2**). The deduced amino acid sequences contain 1510 and 1505 aa for TdMRP3-A1 and TdMRP3-B1, respectively; both proteins showed five domains in the forward orientation typical of ABCC transporters: TMD0-TMD1-NBD1_TMD2-NBD2 (**Supplementary Figures S1B**, **S3**). The analysis performed by I-TASSER 3D model program confirmed the presence of five transmembrane α-helices in TMD0, six α-helices in each TMD1 and TMD2 and the presence of Walker A and B motifs in the two cytosolic nucleotide-binding domains NBD1 and NBD2 (**Supplementary Figure S1B**).

A Multiple Sequence Alignment (MSA) of MRP proteins of major cereals and the model species *Arabidopsis thaliana* highlighted that the five domains of TdMRP3-A1 and TdMRP3-B1 were highly conserved among the orthologous proteins of the different species except for TDM0 (**Supplementary Figure S3**). In **Figure 2.3** the phylogenetic tree shows the evolutionary relationships of MRP transporters (orthologous of TdMRP3) among the grasses. TdMRP3 transporters showed phylogenetic proximity with other *Triticinae* (*Triticum aestivum*, *Triticum dicoccoides*) and barley (*Hordeum vulgare*). Noteworthy the amino acid sequences of the TdMRP3-A1 and TdMRP3-B1 were identical to those of bread wheat (TaMRP3-A1 and TaMRP3-B1, respectively). In addition, a higher homology was observed between the homeologous sequences of the genomes B and D compared to that of the A genome.

A second phylogenetic cluster was constituted by the MRP proteins isolated from *Oryza sativa*, *Zea mays*, *Sorghum bicolor*, *Panicum hallii*, *Panicum virgatum*, *Setalia italica*, *Setaria viritis*. Although the last cluster was more divergent from durum wheat sequences, the structure (domains) and the amino acid composition were strongly conserved among the different species considered for the phylogenetic tree (**Figure 2.3**; **Supplementary Figure S3**).

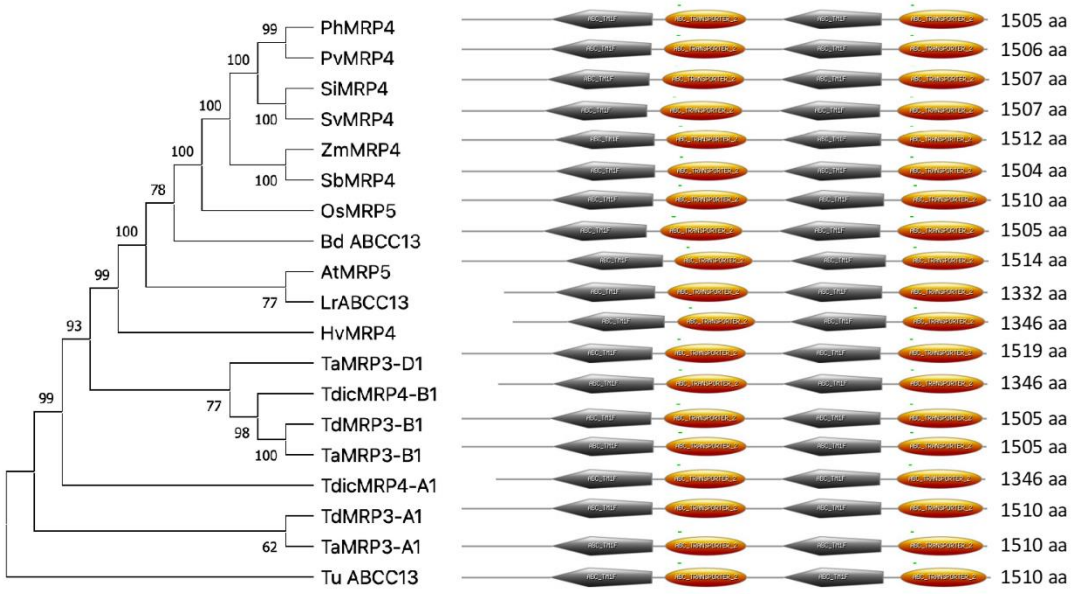

Figure 2.3 Phylogenetic tree of the ABCC multidrug resistance-associated protein (ABCC-MRP) in different plant species. Td: *Triticum turgidum* ssp *durum* MRP3-A1 (SVEVO PLATINUM SEQUENCE), MRP3-B1 (SVEVO PLATINUM SEQUENCE), Ta: *Triticum aestivum* MRP3-A1 (XP_044384038 _TraesCS5A02G512500), MRP3-B1 (XP_044371728 TraesCS4B02G343800), MRP3-D1 (XP_044377018_TraesCS4D02G339000); Tu: *Triticum urartu* ABCC13 XP_048531007.1; Tdic: *Triticum dicoccoides* MRP4-A1 (XP_037437166.1), MRP4-B1 (XP_037426738.1); Hv: *Hordeum vulgare* MRP4 (XP 044983147.1); Bd: *Brachypodium distachyon* ABCC13 (XP_003558836.1); Zm: *Zea mays* MRP4 (EF586878); Sb: *Sorghum bicolor* MRP4 (XP 002468528.2); Pah: *Panicum hallii* MRP4 (XP 025794868.1); Pav: *Panicum virgatum* MRP4 (XP_039780041.1); Si: *Setaria italica* MRP4 (XP 004985744.1); Os: *Oryza sativa Japonica group* MRP5 (XP 015630971.1); At: *Arabidopsis thaliana* MRP5 (AT1G04120.1); Sv: *Setaria viridis* MRP4 (XP_034572896.1); Lr: *Lolium rigidum* ABCC13 like (XP_047089394.1). The tree constructed by the Neighbor-joining (NJ) method with pairwise deletion option and p-distance matrix in MEGA XI (Tamura et al., 2021). Bootstrap values (1000 replicates) were shown at each node.

2.3.2 Identification and pyramiding of TdMRP3 mutations: selection of *lpa* mutants

Two knock out mutant lines for *TdMRP3* genes (one for each homeoallele), described in the "Material and methods" section, were identified through an *in silico* search on the "Wheat TILLING" platform (**Krasileva et al., 2017**). The single null mutant lines Kronos 3179 (TdMRP3-A1^{-}) and Kronos 4443 (TdMRP3-B1^{-}) were crossed to pyramid the two mutations and the F_2 progenies genotyped by an HRM-genotyping assay (**Wittwer et al., 2003**), able to

distinguish among heterozygous, homozygous and wild type genotypes for both the homeoalleles (**Supplementary Figure S4**). The analysis led to identifying four F_2 homozygous double null mutants. In addition, three independent sister lines were identified for each single null mutant genotype (TdMRP3-A1$^-$ and TdMRP3-B1$^-$) and for the control line (wild type at each *MRP3* homeoallele -WT sibling lines). The different genotypes were confirmed by Sanger sequencing (**Supplementary Figure S4**).

2.3.3 Effect of the TdMRP3 suppression on the accumulation of phytic acid and nutrients in the kernel

To evaluate the effect of silencing of *TdMRP3* genes, mature grains were assessed for PA content in the whole set of mutants plus the controls. The complete null genotypes (TdMRP3-A1$^-$B1$^-$) showed a strong reduction in PA compared to the control (cv. Kronos) and WT sibling lines (-84.5% and -86.5%, respectively), while no differences were observed in the single mutants (**Figure 2.4**).

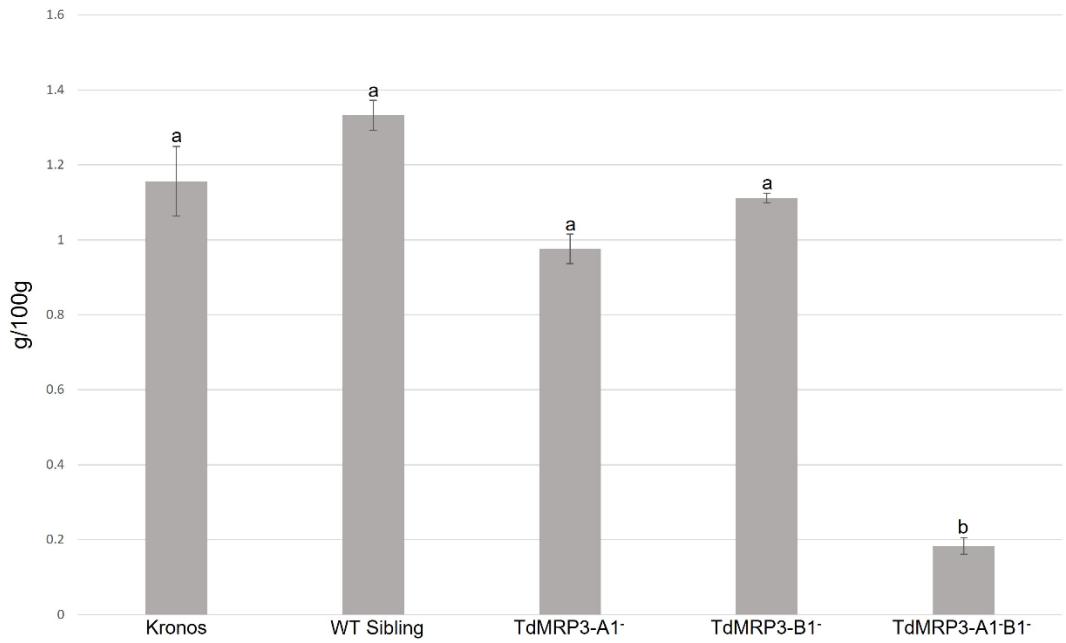

Figure 2.4 Phytic acid content in *lpa* mutants, WT sibling lines and cv. Kronos. Mean values of three biological replicates, error bars indicate standard error. Values followed by different letters differ significantly from one another (one-way ANOVA, Tukey HSD test, $p<0.01$).

In light of the interaction between PA and cationic nutrients, the localization of iron deposits and micro/macronutrient accumulation were analysed in the mature seeds of the set of TdMRP3 mutants compared to the control. The intensity of iron deposits appeared strongly increased in

the double null TdMRP3 mutants, interesting the scutellum, even more in the aleuronic layer and also evident in the endosperm (**Figure 2.5**). The single null genotypes (TdMRP3-A1$^-$ and TdMRP3-B1$^-$) also revealed visible differences in respect to the control, but less pronounced than the completely null genotypes (**Figure 2.5**).

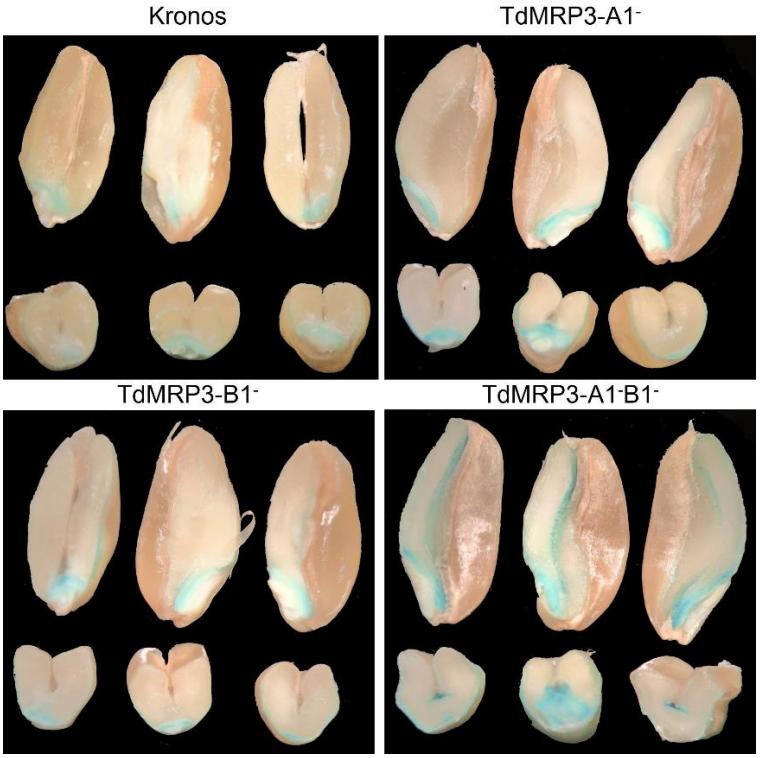

Figure 2.5 Visualization of iron deposits within the kernel using the Perls staining. In each image there are the longitudinal sections (top) and the transversal sections (bottom), of the seeds of cv. Kronos, TdMRP3-A1$^-$, TdMRP3-B1$^-$, TdMRP3-A1$^-$B1$^-$.

The analysis of macro- and micro-nutrients in seeds highlighted differences among the genotypes. With regard to macronutrients, a higher accumulation of Mg and S was observed in the complete null TdMRP3 genotype compared to both the partial mutants and the controls (**Figure 2.6**). In detail, the whole grain of the complete null TdMRP3 genotypes showed a raise of 38.4% for Mg and 32.6% for S compared to the cv. Kronos.
No significant differences were detected for K in the mutant lines (either for partial or complete null genotypes), except for TdMRP3- A1$^-$, which showed a slight decrease (-23.5%).
More interesting, a significant raise in micronutrient accumulation was recorded in the TdMRP3-A1$^-$B1$^-$ genotype (Fe +186.3%, Zn +78.4%, and Mn +36.3%), with the exception of Cu that maintained a concentration similar to the control (**Figure 2.6**). On the other hand, the accumulation pattern of micronutrients in partial genotypes was non-uniform. In particular, the

accumulation of Fe did not change in the TdMRP3-B1$^-$ mutant, whereas it increased by 89.3% in the other partial mutant TdMRP3-A1$^-$. A different trend was also observed for Zn accumulation: it was reduced in the TdMRP3-B1$^-$ genotype (-30.3%) and not significantly affected in TdMRP3-A1$^-$.

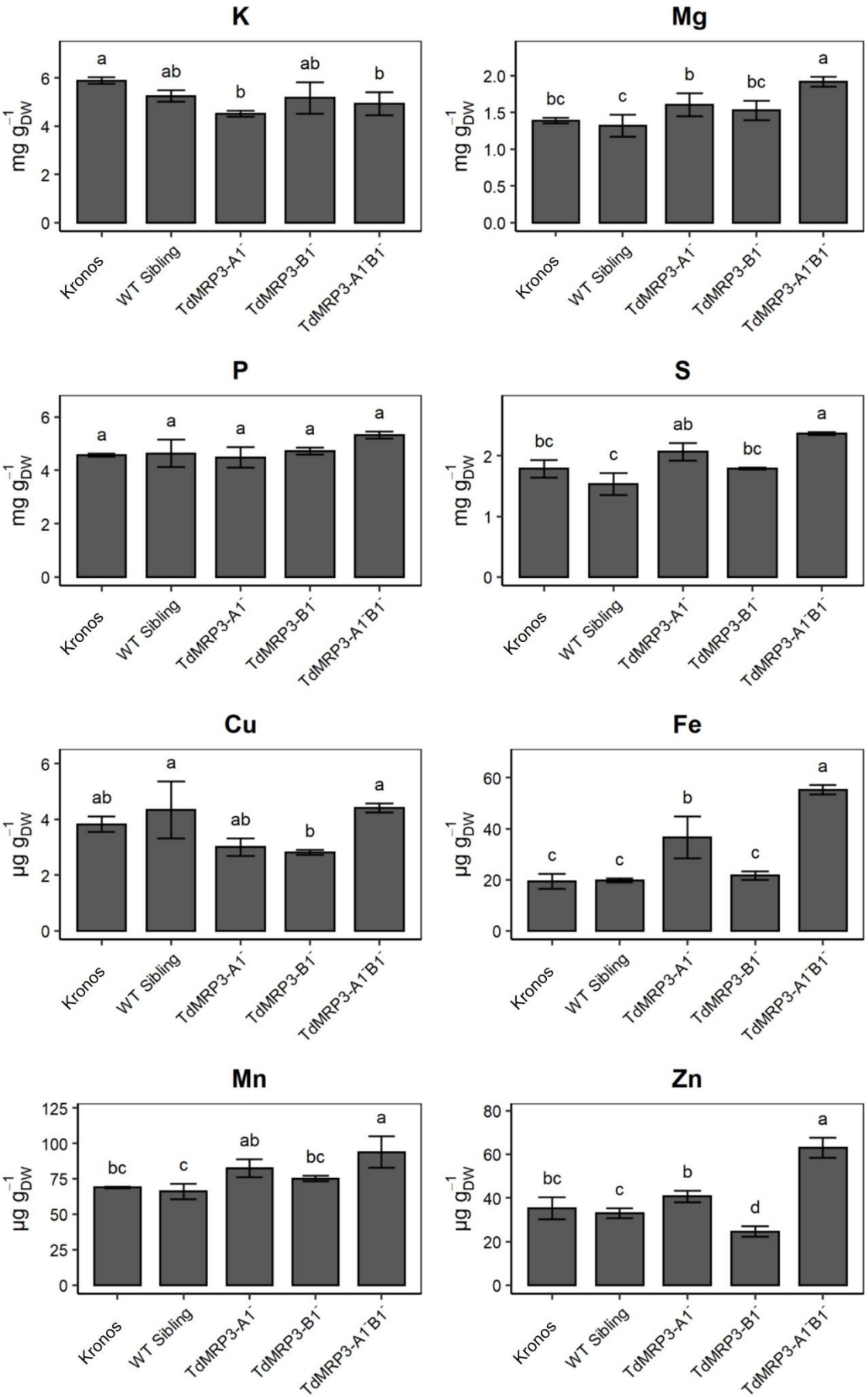
K
mg g$^{-1}_{DW}$
a
ab
b
ab
b
Mg
mg g$^{-1}_{DW}$
bc
c
b
bc
a
P
mg g$^{-1}_{DW}$
a
a
a
a
a
S
mg g$^{-1}_{DW}$
bc
c
ab
bc
a
Cu
µg g$^{-1}_{DW}$
ab
a
ab
b
a
Fe
µg g$^{-1}_{DW}$
c
c
b
c
a
Mn
µg g$^{-1}_{DW}$
bc
c
ab
bc
a
Zn
µg g$^{-1}_{DW}$
bc
c
b
d
a
Kronos
WT Sibling
TdMRP3-A1$^-$
TdMRP3-B1$^-$
TdMRP3-A1$^-$B1$^-$

Figure 2.6 Concentration of nutrients in *lpa* mutants, WT sibling lines and cv. Kronos. Mean values of three biological replicates ± St. Dev. One-way ANOVA, LSD post hoc test, $p < 0.05$.

2.3.4 Effects of TdMRP3 silencing on the agronomic performance and root morphology

The agronomic performances of TdMRP3 mutant lines were evaluated in field by measuring a set of yield-related parameters of plant growth. No significant differences were registered for spike weight, spike length and kernel weight for spike between the control and TdMRP3 complete null mutant genotypes (**Figure 2.7**). Otherwise, TdMRP3-A1$^-$B1$^-$ mutant lines showed a reduction in the number of spikelets per spike (-17.7%) and a more significant reduction in the number of kernels per spike (-34.5%), while no significant differences for the grain weight per spike were recorded. Single kernel weight was increased by 34.2% in the TdMRP3-A1-B1- mutant lines. No significant differences were observed between the single null lines and the wild type (data not shown).

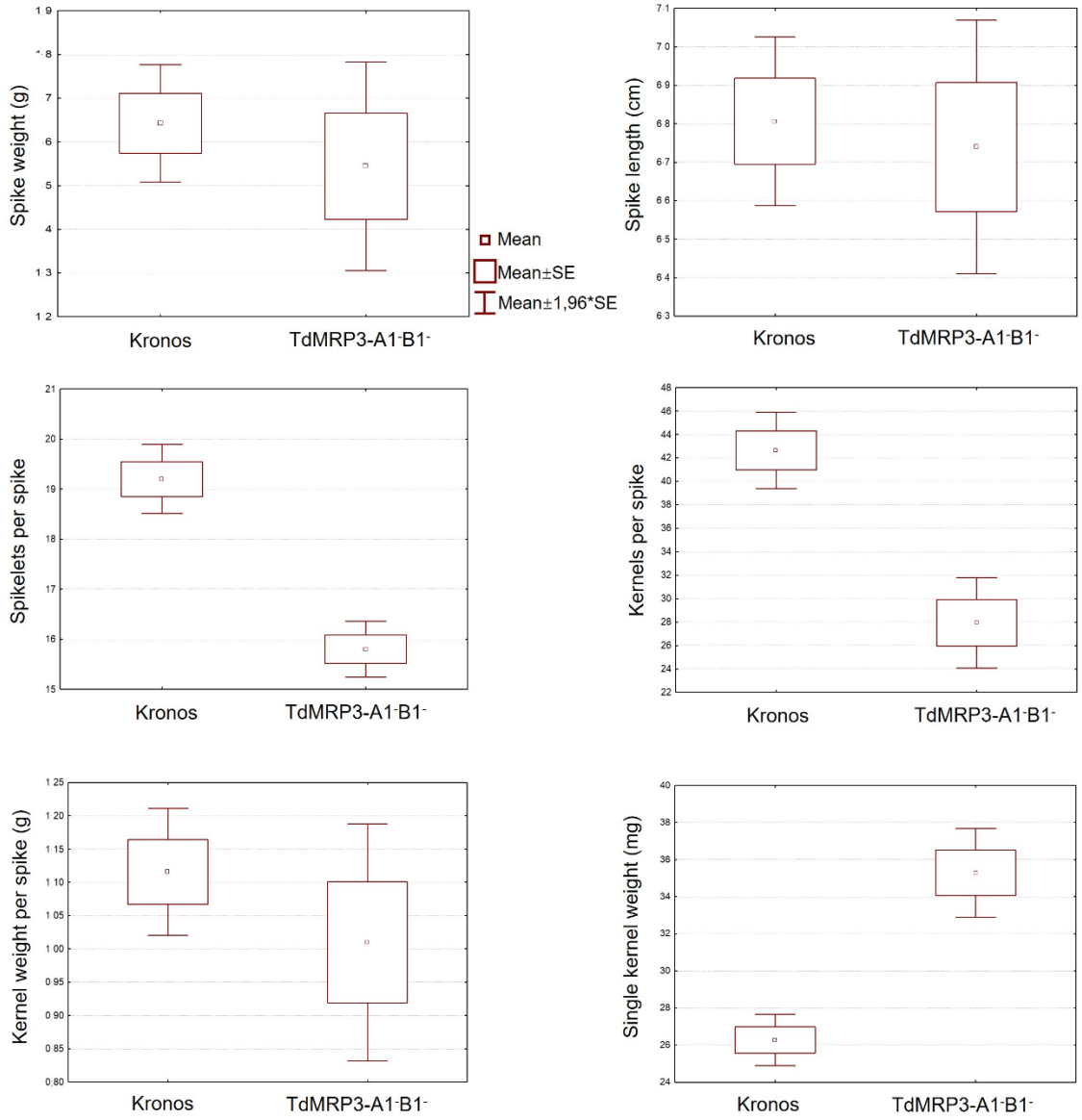

Figure 2.7 Agronomic traits analysis performed on: Spike weight (g), Spike length (cm), Spikelets per spike, Kernels per spike, Kernel weight per spike (g), Single kernel weight (mg). In each image there is the analysis of the seeds of cv. Kronos compared to TdMRP3-A1^{-}B1^{-}.

As ABCC proteins are involved in several aspects of plant growth and root development, the root architecture of the set of mutant lines was analysed and compared to the control, considering the following parameters: root length, number of root tips, root surface area,

volume and diameter (**Figure 2.8**). The mutant plants TdMRP3-A1^{-}B1^{-} showed a significant decrease in the number of root tips (-83.5%), root length (-61.2%), volume (-16.8%), and surface area (-40.6%) compared to the cv. Kronos. A decrease in the number of root tips and an increase in root volume were observed in both the partial mutant genotypes, while no significant differences were detected in the root length and root surface area. Noteworthy, root average diameter significantly increased in all the mutants and increased by 45.8% in the TdMRP3-A1^{-}B1^{-} (**Figure 2.8**).

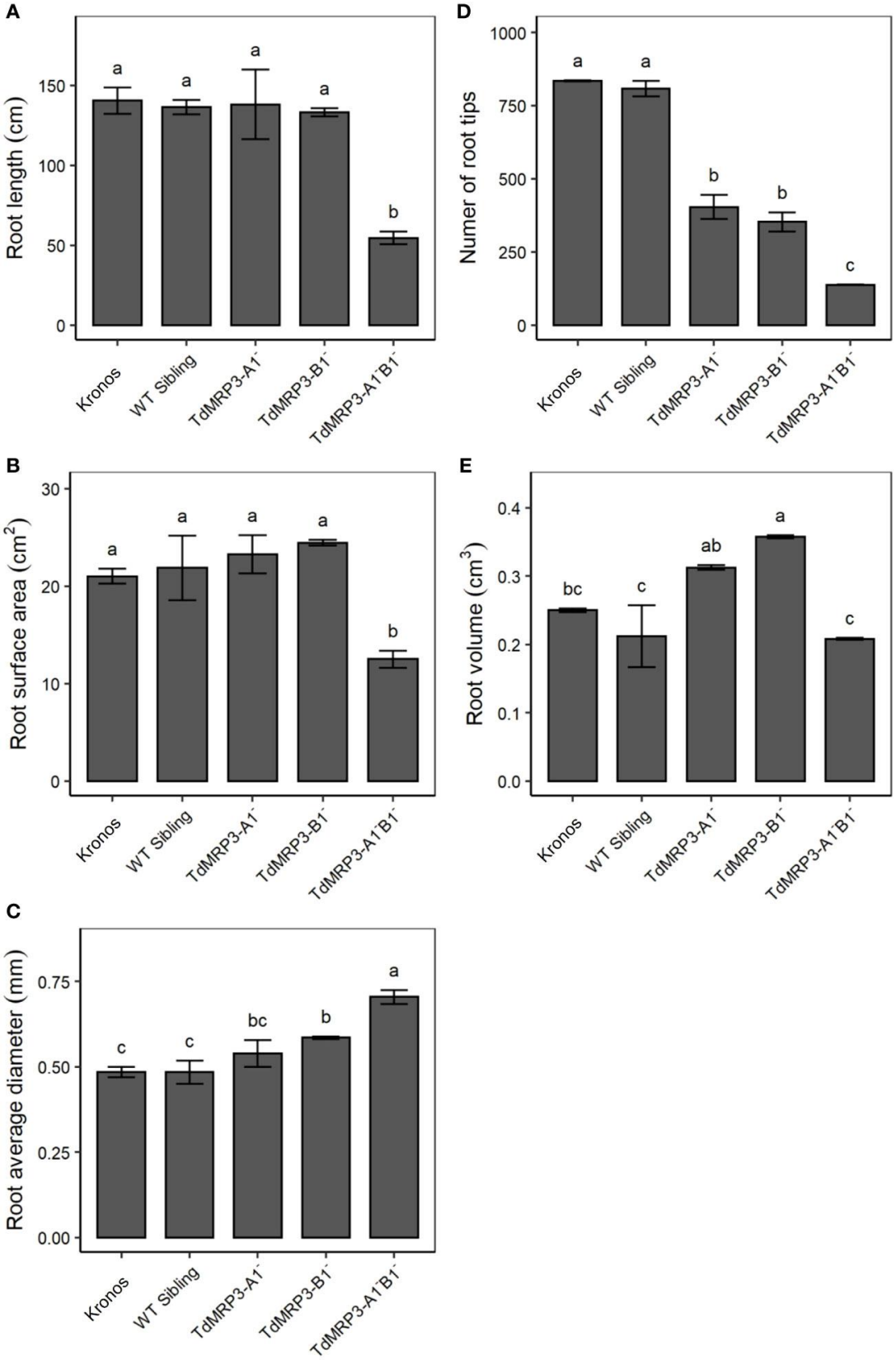
A
Root length (cm)
0
50
100
150
a
a
a
a
b
Kronos
WT Sibling
TdMRP3-A1-
TdMRP3-B1-
TdMRP3-A1-B1-
D
Numer of root tips
0
250
500
750
1000
a
a
b
b
c
Kronos
WT Sibling
TdMRP3-A1-
TdMRP3-B1-
TdMRP3-A1-B1-
B
Root surface area (cm2)
0
10
20
30
a
a
a
a
b
Kronos
WT Sibling
TdMRP3-A1-
TdMRP3-B1-
TdMRP3-A1-B1-
E
Root volume (cm3)
0.0
0.1
0.2
0.3
0.4
bc
c
ab
a
c
Kronos
WT Sibling
TdMRP3-A1-
TdMRP3-B1-
TdMRP3-A1-B1-
C
Root average diameter (mm)
0.00
0.25
0.50
0.75
c
c
bc
b
a
Kronos
WT Sibling
TdMRP3-A1-
TdMRP3-B1-
TdMRP3-A1-B1-

Figure 2.8 Root morphological traits: length (A), surface area (B), diameter (C), number of root tips (D) and volume (E) in *lpa* mutants, WT sibling lines and cv. Kronos. Mean values of three biological replicates ± St. Dev. One-way ANOVA, LSD post hoc test, $p < 0.05$.

2.4 Discussion and conclusions

Hidden hunger is a global health issue, that involves more than 3 billion people around the world, mostly in Africa, Asia, and Latin America. Diets poor in essential vitamins and minerals (micronutrients), typical of some countries of the above-cited continents, are the main driver of the hidden hunger. The development of biofortified staple crop varieties is an effective and low-cost strategy pursued by several major public and private sector organizations (such as Universities, INRA, CIMMYT and ICARDA) in Southern America, Asia and Africa. In this context, Harvest Plus is a big initiative focused on the development of bio-fortified wheat varieties, that involves partners from dozens of countries (**Wani et al., 2022**). Although numerous efforts have been focused on the realization of biofortified wheat genotypes, it remains still challenging.

In plants, PA is stored in the vacuole and functions as a Pi sink to aid plant growth upon seed germination. Due to its negative charge, PA chelates the cations forming poorly bioavailable phytate salts and limiting mineral ion bioavailability, thus promoting mineral deficiencies in the body (**Grases et al., 2017**; **Samtiya et al., 2020**). For this reason, boosting the bioavailability of minerals in plant food can be achieved by reducing PA. *Lpa* mutants can be produced by the impairment of the transport and storage of PA into the vacuole: in the cytosol PA is exposed to a dephosphorylation process carried out by cytosolic phosphatases, decreasing the final amount of phytates and increasing free Pi and cations (**Sparvoli and Cominelli, 2015**; **Colombo et al., 2020**). *Lpa* mutants were developed in wheat *via* ethyl methane sulfonate mutagenesis, and germplasm derived from these mutants was used for breeding purposes (**Guttieri et al., 2004**; **Guttieri et al., 2006**; **Venegas et al., 2022**).

Here, *lpa* mutants were generated in durum wheat targeting *TdMRP3* genes by TILLING, thereby causing the impairment of PA into the vacuole. TILLING strategy (**McCallum et al., 2000**) is a reverse genetics approach widely used in functional studies and breeding programs in numerous species, including bread and durum wheat (**Slade et al., 2005**; **Botticella et al., 2011**; **Hazard et al., 2014**; **Sestili et al., 2015**; **Sestili et al., 2019**; **Garcia Molina et al., 2021**) as it offers the big advantage to expand the genetic variability and to produce nontransgenic plants, that can be used for commercial purposes.

Our *in silico* analysis showed that the protein structure of MRP transporters was highly conserved among the major cereals. In detail, all the analysed sequences had the typical domains of ABCC transporters in forward orientation (**Colombo et al., 2020**), with a high identity degree in according to previous studies (**Bhati et al., 2016**; **Cominelli et al., 2020b**).

Preliminary analysis on Ensembl database highlighted that durum wheat MRP3 proteins from Svevo genome v1 were different in length with respect to bread wheat and other cereal sequences. These durum wheat proteins missed an N- terminal region that included the TMD0 domain and part of the TMD1. Differently, the two durum wheat MRP3 sequences isolated by means of the new Svevo Platinum sequence showed the same length of TaMRP3 proteins (1510 and 1505 aa) and a perfect amino acid identity, sharing high phylogenetic proximity with other cereal species.

TdMRP3-A1 and -B1 were clustered into the same subgroup and were closer to the MRP proteins of *Triticinae* and barley and more divergent from other species, including the major cereals (rice and maize). Our data are in agreement with previous comparative studies that showed a high level of synteny in several gene loci among wheat, barley and other members of the *Triticeae* (**Linde-Laursen et al., 1997**; **Mayer et al., 2011**). Although the MRP3 sequences are highly conserved among the A, B, and D genomes of wheat, small amino acidic differences were identified. Unexpectedly a higher synteny was observed between the homeologous sequences encoded by the B and D genomes compared to MRP3-A1. In this regard, previous studies demonstrated higher synteny levels between A and D genome homeologues compared to those of the B genome (**Akhunov et al., 2003**; **Pont et al., 2013**).

In TdMRP3 double null mutants, PA was reduced by roughly 85% compared to the control in line with what was observed in *lpa* genotypes produced in legumes and other cereals, like maize and rice that showed a reduction of 80 and 90%, respectively (**Silva et al., 2021**). Differently, partial suppression of *TaMRP3* genes targeted by RNAi resulted in a modest reduction of PA content (in the range from -22 to -34%) in bread wheat. These differences can be explained by the different efficiency of silencing of the two approaches: full silencing in TILLING mutants, and reduction in the range of 40-72% of *TaMRP3* transcripts in the case of RNAi plants (**Bhati et al., 2016**). Accordingly, the accumulation of Fe, Zn and Mn in the grain was significantly raised in the TdMRP3 null mutants than in the transgenic RNAi lines (about +186% vs +18% for Fe; about +36% vs 0% for Mn; +78% vs +13% for Zn).

Generally, the phytic acid mutants described in many plant species were presented as agronomically poor for the low yields and for the poor germination capacity of the seeds (**Raboy, 2020**). In bread wheat, previous studies conducted on EMS mutants showed a reduction in PA of 30 to 40% (**Guttieri et al., 2004**), and a more contained loss of yield (from 8 to 25%).

In our study, the reduction in yield was comparable to bread wheat, although the reduction in PA was much higher (>85%). Actually, **Guttieri et al. (2006)** showed the absence of consistent effects on yield and yield-related traits in wheat *lpa* mutants, depending on the different genetic backgrounds in which the trait was transferred. In particular, in the soft white spring genetic background, the kernel weight of the *lpa* mutants was greater than that of the control wild type, confirming our findings, in which the partial reduction in yield, due to the reduction in the

number of spikelets and kernels for spike, was compensated by a greater kernel weight. This suggested that the negative agronomic effects of the *lpa* genotype can be mitigated by adopting an adequate genetic improvement strategy.

In maize the suppression of *ZmMRP4* was associated with ungerminability and seed weight loss (**Pilu et al., 2005**; **Cerino Badone et al., 2012**). **Pilu et al. (2005)** found a decreased content of PA in maize mutant lines and showed that kernels with less than 20% of PA are unable to germinate. The same pleiotropic effects were reported in rice with the suppression of *OsMRP5*, orthologous of *TdMRP3* and *ZmMRP4* (**Xu et al., 2009**). In detail, the T-DNA knock out line, in which *OsMRP5* was disrupted, showed a strong reduction of PA (>90%) and an inability to germinate.

Non-lethal *lpa* mutants were obtained in soybean and common bean through the silencing of the orthologous genes of *TdMRP3* (**Oltmans et al., 2005**; **Cominelli et al., 2018**). PA dropped between 75 and 90% in both the species but only in common bean no pleiotropic effect on yield traits and plant phenotype was observed.

The morphology of the root apparatus was markedly altered in our complete null TdMRP3 mutant line. In detail, the root length, volume and surface area and the number of tips, were decreased, while the root diameter was increased compared to the control plants. The morphological alteration of the root apparatus is a common adaptive strategy used by plants to cope with suboptimal nutrients (mainly nitrogen, sulfur and phosphate) and water availability (**Aiken and Smucker, 1996**; **López-Bucio et al., 2003**; **Péret et al., 2011**). The root diameter generally matches the elongation rate, which stops when the root reaches the minimal diameter (**Pagès et al., 2020**). Accordingly, shorter roots generally have a larger diameter.

It is well known that the plants face phosphate starvation by modifying the root system architecture through the inhibition of primary root growth, the increase of the lateral root formation and the growth and production of root hairs, thus allowing their root systems to efficiently utilize Pi from soils (**Vance et al., 2003**; **Hinsinger et al., 2009**; **Péret et al., 2011**). Besides soil P concentration, also plant Pi status can trigger morphological root responses (**Vance et al., 2003**; **Lambers et al., 2006**). Thus, the short-root phenotype showed by our mutants could be attributed to changes in Pi homeostasis induced by *TdMRP3* silencing resulting in increased availability of free phosphate in the cells and lower Pi demand from the soil. Moreover, MRP3 transporters are known to be expressed in several plant tissues including roots. So, we cannot rule out the possibility that the silencing of MRP3 transporter may have a more direct effect on anatomical root differences known to impact tolerance to Pi deficiency.

From a future perspective, it could be interesting to develop novel approaches able to limit the silencing of the *TdMRP3* expression to the seed to minimize the pleiotropic effects associated with *lpa* mutants. **Bhati et al. (2016)**, using a different silencing technology, did not find a significant difference in the root length between the control and the RNAi transgenic plants. Moreover, they observed that the number of lateral roots was higher in the transgenic lines

compared to the control plants. We could interpret these contrasting results by considering that the critical P supply and plant status for the activation of P-deficiency response, including root alterations, differ among plant species (**Teng et al., 2013**).

In conclusion, this study shed light on the functional role of *TdMRP3* in durum wheat. In detail, it confirmed that the reduction of PA through the silencing of MRP transporters is a good strategy to obtain durum wheat genotypes biofortified in essential minerals and with acceptable agronomic performances. To date, to the best of our knowledge, this represents the first study in wheat allowing at the same time to increase the accumulation of essential minerals such as Zn, Fe and Mn. Noteworthy, the plant lines can be used as starting material in breeding programs focused on mineral biofortification without any legal restriction associated with genetically modified organisms.

Supplementary material

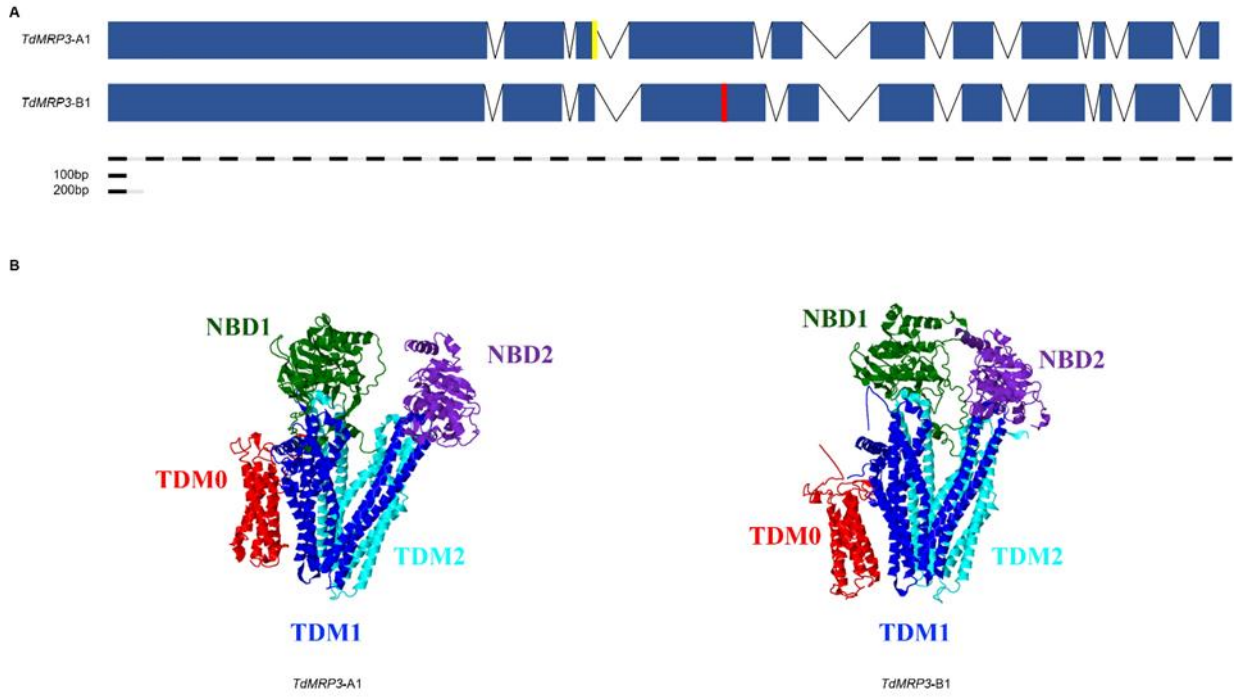

Supplementary Figure S1 *TdMRP3* gene and protein structures. (A) Gene structures of *TdMRP3* homeoalleles. Blue rectangles represent exons, the yellow box indicates the splice site mutation located in the 5′ region of the intron 4 on the homeoallele *TdMRP3-A1* (mutant line Kronos 3179). The red box indicates the premature stop codon located on the exon 4 of the homeoallele *TdMRP3-B1* (mutant line Kronos 4443). (B) Domain representation of modelled

TdMRP3 protein [Colour code: Red-TMD0, Blue-TMD1, Green-NBD1, Light blue-TMD2, Violet-NBD2].

>TdMRP3-A1 gene

ATGCCGCGCCTCCGCGCCCACACCCCCCTCCCCCTCACGGAGGCCGCCGCCGCCGCCGCGCACGCCGCGCTGCTCGCCCTCGCGCTCCT
CCTCCTGCTCCTCCGCGGCGCGCGCGCCCTCGCCTCCCGCTGCGCCTCCTGCCTCAAGCCGCCCCGCCGCGCCCGCAACCTCGTCCACG
ATGGGCCGCCCCTCGCCTCCCCGCCGCCCGCCGCCGGGGGCGCCTGGTTCAGGGCCGCCCTCGCCTGCTGCGCCTACGTCCTGCTGGCG
CAGCTCGCCGCGCTGACCTACGAGGTCGCGGCCGCGCCGCCGCCCGTCGAGGCCGAGGCGCTGCTGCTGCCGGCCGTGCAGGCGCTGGC
CTGGGCGGCCCTGCTGGCGCTCGCGCTGCGGGCGCGCGCCGGGGGCCGCGGCAGGTTCCCGGCGCTCGTCCGGGTCTGGTGGGTGCTCG
CCTTCGCGCTCTCCGTCGCCATCGCCTTCGACGACTCCAGGCGCCTCATGGGCGCCGACGACCGTGATGCGGACTACGCGCACATGGTC
GCCAACTTCGCGTCGCTGCCGGCCCTCGGCTTCCTCTGCTTGGTTGGTGTGATGGGTTCCAGCGGTGTCGAGTTGGAGTTCAGTGATGA
CGACACCGGTGTCCACGAGCCCCTGTTGCTCGGCGGCCAGCGCAGAGGTGCCGAGGAGGAGCCCGGCTGCCTGCGGGTGACTCCCTACG
GCGATGCCGGGATCCTCAGCCTTGCAACGCTCTCATGGCTCAGTCCGCTGCTCTCGGTTGGGGCCAAGAGGCCGCTCGAGCTGGCTGAC
ATACCCTTGCTGGCTCACAAGGATCGTGCCAAGTTCTGCTACAAGGCCATGAGCAGTCACTATGAGCGCCAACGGCTGGAGTGCCCTGA
CAAGGAGCCATCGCTGGCATGGGCAATACTCAAGTCCTTCTGGCGGGAGGCGGCCATCAACGGCGCCTTCGCCGCGGTGAACACCGTCG
TGTCCTATGTCGGCCCCTACCTGATCAGCTACTTTGTGGACTACCTCAGTGGCAAAATTGCCTTCCCCCATGAAGGTTACATCCTTGCC
TCCGTATTTTTTGTATCAAAGTTGATTGAGACGCTCACTGCTCGCCAGTGGTACCTGGGCGTGGACGTCATGGGGATCCATGTCAAGTC
CGGGCTGACGGCCATGGTGTACCGGAAGGGCCTCAGGCTGTCGAATGCCTCAAAGCAGAGCCATACGAGCGGTGAGATTGTGAATTACA
TGGCGGTCGATGTGCAGCGGGTGGGGGACTATGCGTGGTACTTTCATGACATATGGATGCTTCCACTGCAGATCATCCTTGCGCTCGCC
ATCCTGTACAAGAATGTCGGGATCGCCACTGTCTCGACATTGATAGCCACCGCGCTGTCAATTGCTGCCTCGGTTCCTGTGGCGAAGCT
GCAGGAGCACTACCAAGATAAGCTGATGGCAGCAAAGGATGAGCGAATGCGCAAGACTGCAGAGTGCTTGAAGAGTATGAGAATTCTCA
AGTTGCAGGCATGGGAGGACCGGTATAGGATAATGCTTGAAGAGATGAGGAACGTTGAATGCAGGTGGCTCAAGTGGGCTTTGTACTCA
CAGGCCGCAGTTACGTTTGTTTTCTGGAGTTCGCCAATCTTTGTCTCGGTCATAACTTTCGGCACTTGTATATTGCTTGGTGGCGAGCT
CACTGCCGGAGGTGTTCTCTCTGCATTAGCTACCTTTAGGATCCTTCAAGAGCCTCTGAGGAATTTCCCTGATCTCATCTCCATGATAG
CTCAGACGAGGGTGTCTTTGGACAGGTTGTCTCACTTCTTACGGCAAGAAGAGTTGCCGGATGATGCAACAATAAGTGTTCCACAGGGT
AGTACAGACAAGGCAATCGATATCAGGGATGGCAGTTTCTCTTGGAACCCATCTTGCTCAAACCCTACGCTCTCTGATATACAACTTAG
TGTGGTGAGAGGCATGAGAGTAGCAGTCTGTGGTGTGATTGGTTCTGGCAAATCAAGTCTATTGTCCTCTATACTTGGGGAGATACCCA
AGCTGTCTGGCCAAGTAAGTACACGCATAAAAATAAAGAGAGTTGATGCTAACTTGAATGACAGTTTAATTACATTTTCCTTCTGCTCC
TTATTCAGGTTAGGATCAGTGGTACAGCAGCATATGTTTCTCAGACTGCCTGGATACAGTCTGGAAATATTGAGGAGAACGTTCTTTTC
GGCACTCCAATGGACAGACCGCGTTATAAGAGAGTACTTGAGGCTTGCTCCCTGAAGAAAGATCTTCAGTTGCTCCAGTATGGAGATCA
GACCATCATTGGTGACAGAGGCATTAATTTGAGTGGAGGTCAGAAACAGAGAGTGCAGCTTGCGAGAGCATTGTACCAAGATGCTGATA
TTTATTTGCTTGATGACCCCTTCAGTGCTGTTGATGCTCATACTGGAAGCGATCTATTTAAGGTCTGTATCGATGTTGCCTTATTCTAT
TTTTTTTAAAGGTGCTTCTGTTTCATAACATGTCAGATTTTGTGTTGCAGGACTATATATTGGGGGCACTAGCTAGCAAAACAGTAATT
TATGTAACCCATCAAGTCGAGTTCCTACCAGCTGCTGACTTGATATTGGTAATACTACTTTTCTCACAAAATCTATTAGCCTATTGAGT
TGTTCAATTTGACGTGTTGTTTATCCATGTTTCCTGATTAGAAAAACCAGCAGATTCTGCATGAAAGTTGCGCTATCTTTTCTAATACT
TCTCATTGGACTGTTCATGGGATAATGGGCCCTTGATCTCTCATTGTGTGTTTTTTTTTGTCATGGCACAGGTTCTTAAGGATGGTCAT
ATCACCCAAGCTGGAAAATATGATGATCTTCTCCAAGCTGGAACCGATTTCAATGCTCTGGTTTCTGCTCATAATGAAGCTATCGAGAC
CATGGATTTTGGCGAAGATTCTGATGGAGATATCGCTCCTTCCGTTCCTAACAAAAGATTGACACCAAGTGTTAGCAATATCGATAACC
TGAAAAATAAAGTATCTGAAAATGGGAAGTCATCTAATACACGTGGAATTAAGGACAAGAAAAAGAGTGAAGAACGTAAGAAGAAGCGT
ACTGTTCAGGAAGAGGAGAGGGAGCGAGGAAGAGTTAGCTTAAATGTTTATTTAACATACATGGGGGAAGCCTACAAAGGTTCACTGAT
TCCACTCATTGTCTTGGCGCAAACCCTGTTCCAAGTTCTTCAGATTGCCAGTAACTGGTGGATGGCATGGGCAAACCCACAAACAGAAG
GAGATGCACCTAAGACAAGTAGTGTGGTCCTTCTTGTTGTTTATATGTGCCTTGCTTTCGGGAGTTCATTGTTTGTGTTTGTGAGAAGC
CTTCTTGTAGCTACATTTGGTTTAGCAGCTGCTCAGAAACTATTTATAAAAATGCTAAGGTGTGTGTTTCGAGCGCCAATGTCATTCTT
CGATACTACACCATCTGGACGGATTCTGAATCGAGTAAGTTTAGATCATGCTCTTGCTCCTAATTTGTATTTGACACCTGTGTGGCTTT
TCTAATTTGCATACTCTAATCTTCTTCAATCATACTTCATATCAGGTTTCTGTAGATCAAAGTGTTGTGGACCTTGATATAGCATTCAG
GCTAGGGGGGTTTGCATCAACAACAATTCAACTCCTTGGAATCGTTGCTGTCATGAGCAAAGTCACATGGCAAGTTCTGTTTCTTATAG
TTCCTATGGCTATGGCATGCATGTGGATGCAGGTAAATTGCTAAACTTTCAGGTTTTCTTTTAGGGCTAACATTACCTGGGATCCTTAA
TTTCTTTAATGGAAATTGTAATACAAATAAGGCAGATAGCAAGGGTAGATACACCTAAATGGCTAAATGAATCACTAAAGAATTATGCG
CACATAATTTTTTTGGCTGCCTTTGTCATTTAACTAGCAGCCAATTAACCAGAGAACATATGCATATGTTCAGCATGAAAGTATCGAAA
GTTGTGAAGTAAGCTTATTATTCTTAAAGCACGAGGCCTGTGTTCAAGATAGCTTGATGATTTTGTGTACCAAAAGACTTTTAAAGATC
TTCATCACACAATAGATAATGGATGTCCTTGCTACCATGAACTTGCAGAGATATTACATTGCTTCATCGAGGGAGCTGACTAGGATCTT
GAGTGTTCAGAAGTCTCCAGTGATCCATTTGTTTAGCGAGTCAATCGCTGGTGCTGCTACTATCAGAGGATTTGGTCAGGAGAAAAGAT
TCATGAAAAGAAATCTTTACCTCCTTGATTGTTTTGCTCGGCCTTTGTTTTCCAGCCTTGCAGCTATTGAATGGCTCTGCCTGCGAATG
GAATTGCTCTCAACCTTTGTGTTTGCTTTCTGCATGGCAATACTTGTGAGCTTTCCTCCTGGAACAATTGAACCAAGTATGTCTTATCT
GCTGTCTCACACACCGTTCTGTTGCATTTTATGATCTTGCCTTACCCAATAGATCACTTGTTAGGTGCACTAGAAAACTTGCATATCTT
TTTCAATAAAATATGGCAATATGCTTCTCAATCTAAACAAGCTTTCCAATTGATAGGCATGGCTGGGCTTGCTGTCACATATGGACTCA
ACTTAAATGCTCGGATGTCAAGGTGGATATTGAGCTTCTGTAAATTAGAGAACAGAATCATCTCTGTTGAGCGTATTTATCAGTATTGC
AAGATTCCTAGTGAAGCACCACTGATTATCGAGAATTGCCGTCCCCCTTCCTCATGGCCTGAGAATGGAAACATTGAATTGATTGATCT
CAAGGTAAACTTAGCCCGTAGCCATTATTTATTTGTCATTATCCATTTGCTCTTCGTTATATATATTCACCAAAAGTAGTATGTAATCT
ATTTTTCTTCTTCTAAGCTGAACATACTTCTGTTTTATTTACGGCATCTTATTGTGCTTTTGCTAAATATCATAGGTTCGCTACAAGGA
TGACCTTCCCTTTGTTCTACATGGAGTCAGTTGTATTTTTCCTGGTGGGAAAAAGATTGGGATTGTAGGACGAACTGGAAGTGGTAAAT

CTACTCTCATTCAGGCTCTTTTCCGTCTAATTGAACCAGCAGGAGGGAAAATTATCATTGACAACATCGATGCTTCTGCGATTGGCCTT
CATGATCTGCGGTCACGGTTGAGCATCATTCCTCAGGACCCTACATTGTTCGAGGGTACTATCAGAATGAATCTTGACCCTCTTGAAGA
GCGTTCTGATCAAGAAATTTGGGAGGTATGCCATGGTCGCTTTTATGCTATCCTCATGTTAAATGTGCCATGATCTTTATGGAAGAGAA
TTCTTTTCTTTCAGGCACTAGAGAAGTGCCAGCTAGGAGAGGTCATTCGTTCGAAGGAAGAAAAACTGGACAGTCCAGGTTTGTTCTAA
TTTTGAATATTCAAACACTTCTTCAAAGAGTGAGCATGACACTTCGTAAAGCATGACACCTCGTAAAACAAAATTATATTTTCCTGGAT
ATTTGTGGTGCCATTGCAGTACTGGAGAATGGGGATAACTGGAGTGTGGGACAGCGCCAGCTTATTGCATTGGGTAGGGCGCTGCTTAA
GCAGGCAAGAATTTTGGTGCTTGATGAGGCAACGGCATCAGTTGACACAGCTACAGATAATCTCATCCAGAAGATCATCCGCAGCGAAT
TCAGGGATTGCACTGTCTGTACAATTGCACACAGGATCCCAACGGTTATCGACAGTGACCTAGTCATGGTGCTTAGCGACGGTACATGC
TCCTTCACACGATTAACCAAGACCATCACATGTTTTGTTTCTTACTGATCGTATGTTGAATTATCCGAGTAACACTCCTAGCTAAACAC

TGTTCTTGGAGCAACAGCCTTTACGGTGAATTCACCTTGTTCTTGTTTATTTCAGGTAAAATTGCGGAGTTCGACACACCCCAGAGGCT
TCTGGAGGACAAGTCCTCGATGTTCATGCAGCTAGTATCCGAGTACTCCACCAGGGCGAGCTGTATATAG

>TdMRP3-A1 protein
MPRLRAHTPLPLTEAAAAAAHAALLALALLLLLLRGARALASRCASCLKPPRRARNLVHDGPPLASPPPAAGGAWFRAALACCAYVLLA
QLAALTYEVAAAPPPVEAEALLLPAVQALAWAALLALALRARAGGRGRFPALVRVWWVLAFALSVAIAFDDSRRLMGADDRDADYAHMV
ANFASLPALGFLCLVGVMGSSGVELEFSDDDTGVHEPLLLGGQRRGAEEEPGCLRVTPYGDAGILSLATLSWLSPLLSVGAKRPLELAD
IPLLAHKDRAKFCYKAMSSHYERQRLECPDKEPSLAWAILKSFWREAAINGAFAAVNTVVSYVGPYLISYFVDYLSGKIAFPHEGYILA
SVFFVSKLIETLTARQWYLGVDVMGIHVKSGLTAMVYRKGLRLSNASKQSHTSGEIVNYMAVDVQRVGDYAWYFHDIWMLPLQIILALA
ILYKNVGIATVSTLIATALSIAASVPVAKLQEHYQDKLMAAKDERMRKTAECLKSMRILKLQAWEDRYRIMLEEMRNVECRWLKWALYS
QAAVTFVFWSSPIFVSVITFGTCILLGGELTAGGVLSALATFRILQEPLRNFPDLISMIAQTRVSLDRLSHFLRQEELPDDATISVPQG
STDKAIDIRDGSFSWNPSCSNPTLSDIQLSVVRGMRVAVCGVIGSGKSSLLSSILGEIPKLSGQVRISGTAAYVSQTAWIQSGNIEENV
LFGTPMDRPRYKRVLEACSLKKDLQLLQYGDQTIIGDRGINLSGGQKQRVQLARALYQDADIYLLDDPFSAVDAHTGSDLFKDYILGAL
ASKTVIYVTHQVEFLPAADLILVLKDGHITQAGKYDDLLQAGTDFNALVSAHNEAIETMDFGEDSDGDIAPSVPNKRLTPSVSNIDNLK
NKVSENGKSSNTRGIKDKKKSEERKKKRTVQEEERERGRVSLNVYLTYMGEAYKGSLIPLIVLAQTLFQVLQIASNWWMAWANPQTEGD
APKTSSVVLLVVYMCLAFGSSLFVFVRSLLVATFGLAAAQKLFIKMLRCVFRAPMSFFDTTPSGRILNRVSVDQSVVDLDIAFRLGGFA
STTIQLLGIVAVMSKVTWQVLFLIVPMAMACMWMQRYYIASSRELTRILSVQKSPVIHLFSESIAGAATIRGFGQEKRFMKRNLYLLDC
FARPLFSSLAAIEWLCLRMELLSTFVFAFCMAILVSFPPGTIEPSMAGLAVTYGLNLNARMSRWILSFCKLENRIISVERIYQYCKIPS
EAPLIIENCRPPSSWPENGNIELIDLKVRYKDDLPFVLHGVSCIFPGGKKIGIVGRTGSGKSTLIQALFRLIEPAGGKIIIDNIDASAI
GLHDLRSRLSIIPQDPTLFEGTIRMNLDPLEERSDQEIWEALEKCQLGEVIRSKEEKLDSPVLENGDNWSVGQRQLIALGRALLKQARI
LVLDEATASVDTATDNLIQKIIRSEFRDCTVCTIAHRIPTVIDSDLVMVLSDGKIAEFDTPQRLLEDKSSMFMQLVSEYSTRASC

>TdMRP3-B1 gene
ATGCCGCGCCGCGCCCTCCCCCTCGCCGAGGCCGCCGCCGCCGCCGCGCACGCCGCGCTGCTCGCCCTCGCGCTCCTCCTCCTGCTCCT
CCGCGGCGCGCGCGCCCTCGCCTCCCGCTGCGCCTCCTGCCTCAAGCCGCCCCGCCGCGCCCGCAACCCCGCCCTCGCCGGCGATGGGG
CGCCCCTCGCCCCCTCGCCGCCCGCCGCCGGGGGCGCCTGGTACCGGGCCGCCCTCGCCTGCTGCGCCTACGCCCTGCTGGCGCAGCTC
GCCGCGCTGAGCTACGAGGTCGCGGCCGCCGCGCCGCCCGCCGAGGCCGAGGCGCTGCTGCTGCCGGCCGTGCAGGCGCTGGCCTGGGC
GGCCCTGCTAGCGCTCGCGCTGCGGGCCCGCGCCGGCAGGTTCCCGGCGCTCGTGCGGGTCTGGTGGGTGCTCGCCTTCGCGCTCTCCC
TCGCCATCGCCTTCGACGACTCCAGGCGCCTCATGGGCGCCGACGACCACGATGCGGACTACGCGCACATGGTCGCCAACTTCGCGTCG
CTGCCGGCCCTCGGCTTCCTCTGCTTGGTTGGTGTGATGGGTTCCAGCGGTGTCGACTTGGAGTTTAGTGACGACGACACCGGTGTCCA
CGAGCCCCTGTTGCTCGGCGGGCAGCGCAGAGGCGCCGAGGAGGAGCCCGGCTGCCTGCGGGTGACTCCCTACGGCGACGCCGGGATCC
TCAGCCTTGCAACACTCTCATGGCTCAGTCCTTTGCTCTCGGTTGGGGCCAAGAGGCCGCTCGAGCTGGCTGACATACCCTTGCTGGCT
CACAAGGATCGTGCCAAGTTCTGCTACAAGGCCATGAGCAGTCACTATGAGCGCCAACGGCTGGAGTGCCCTGACAAGGAGCCGTCGCT
GGCATGGGCAATACTCAAGTCCTTCTGGCGGGAGGCGGCCATCAACGGCGCCTTCGCCGCGGTGAACACCGTCGTGTCCTATGTCGGCC
CCTACCTGATCAGCTACTTTGTGGACTACCTCAGTGGCAAAATTGCCTTCCCCCATGAAGGTTACATCCTTGCCTCAGTATTTTTCGTA
TCAAAGTTGATTGAGACGCTCACTGCTCGCCAGTGGTACCTGGGCGTGGACGTCATGGGGATCCATGTCAAGTCCGGGCTGACGGCCAT
GGTGTACCGGAAGGGCCTCAGGCTGTCGAATGCCTCAAAGCAGAGCCATACGAGCGGTGAGATTGTGAATTACATGGCGGTTGATGTGC
AGCGGGTGGGGGACTATGCATGGTACTTTCATGACATATGGATGCTTCCACTGCAGATCATCCTTGCGCTCGCCATCCTGTACAAGAAT
GTCGGGATCGCCACCGTCTCGACATTGATAGCCACCGCGCTGTCAATTGCTGCCTCGGTTCCTGTGGCCAAGCTGCAGGAACACTACCA
AGATAAGCTAATGGCAGCAAAGGATGAGCGAATGCGCAAGACTGCAGAGTGCTTGAAGAGTATGAGAATTCTCAAGCTGCAGGCATGGG
AGGACCGGTACAGGATAATGCTTGAAGAGATGAGGAACGTTGAATGCAGGTGGCTCAAGTGGGCTTTGTACTCGCAGGCCGCAGTTACG
TTTGTTTTCTGGAGCTCACCAATCTTTGTCTCGGTCATAACTTTCGGCACTTGTATATTGCTTGGTGGCGAGCTCACTGCCGGAGGTGT
TCTCTCTGCTTTAGCAACTTTTAGGATCCTTCAAGAGCCTCTGAGGAATTTCCCTGATCTCATCTCCATGATAGCTCAGACGAGGGTGT
CCTTGGACAGGTTGTCACACTTTTTGCGGCAAGAAGAGTTGCCGGATGATGCAACAATAAGTGTTCCACAGGGTAGCACAGACAAGGCA
ATCGATATCAAGGATGGCAGTTTCTCTTGGAACCCGTCTTGCTCAACCCCTACACTATCTCATATACAACTTAGTGTGGTGAGAGGCAT
GAGAGTAGCAGTCTGTGGTGTGATTGGCTCTGGCAAATCAAGTCTATTGTCCTCTATACTTGGGGAGATACCCAGACTGTCTGGCCAAG
TAAGTACATGCGTAAAAAAAGAGTTCATGCTAACTTGAGTGACCGTCTAATTACATTTTCCTTCTGCTCCTTATTCAGGTTAGGGTCAG
TGGTACAGCAGCATATGTTTCACAGACTGCCTGGATACAGTCTGGAAATATTGAGGAGAACGTTCTTTTCGGCACTCCAATGGACAGAC
CGCGCTATAAGAGAGTACTTGAGGCTTGCTCCCTGAAGAAGGATCTTCAGTTGCTCCAGTATGGTGATCAGACCATCATCGGTGACAGA
GGCATCAATTTGAGTGGAGGCCAGAAACAGAGAGTGCAGCTTGCGAGAGCACTGTACCAGGATGCTGATATTTATTTGCTTGATGACCC
CTTCAGTGCTGTTGATGCTCATACTGGAAGTGATCTATTTAAGGTCTGTATAGTTGTTGCCTTATTCTAGTTCTTTCTTGAAGGTGCTT
CTGTTTCGTAACATGTCAGCTTTTGTGTTGCAGGACTATATATTGGGGGCACTAGCTAGTAAAACAGTAATTTATGTGAACTCATCAAGT
CGAGTTCCTACCAGCTGCTGACTTGATATTGGTAATAACATTTTTCTCACAATCTAAGCACTAGTACATTTAGTGGCTAATGTACATAG
ATATGCTGTTTCAAATTTCTAACAGCCTATTAAGTTGTTCAATTCGACATATTGTTTATCCATGTTTCTTAATGAGAATAAAACAGCAG
ATTCTGCATGAAAGTTTCGCTATCTTCTATGTACAATACTTCTGATAGGATAATGGGCCCTTGATCACTCGTTTGTGCTTTCTTTTTAT

CATGGCATAGGTTCTTAAGGATGGTCATATCACCCAAGCTGGAAAATATGATGATCTTCTCCAAGCTGGAACCGATTTCAATGCTCTGG
TTTCTGCTCACAATGAAGCTATCGAAACCATGGATTTCGGCGAAGATTCTGATGGAGATATTGCTCCTTCTGTTCCTAACAAAAGATTG
ACACCAAGTGTTAGCAATATCGATAACCTGAAAAATAAAGTATCTGAAAATGGTAAGTCATCTAATACACGTGGAATTAAGGACAAGAA
AAAGAGTGAAGAACGTAAGAAGAAGCGTACTGTTCAGGAAGAGGAGAGGGAGCGAGGAAGAGTTAGCTTAAATGTTTATTTGACATACA
TGGGGGAAGCCTACAAAGGTTCACTTATACCACTCATTGTCTTGGCACAAACCCTGTTCCAAGTTCTTCAGATTGCCAGTAACTGGTGG
ATGGCATGGGCAAACCCACAAACAGAAGGAGATGCACCTAAGACAAGTAGTGTGGTCCTTCTTGTTGTTTATATGTGCCTTGCTTTCGG
GAGTTCATTGTTTGTGTTTGTGAGAAGCCTTCTTGTAGCTACATTTGGTTTAGCAGCTGCTCAGAAACTATTTATAAAAATGCTAAGGT
GTGTGTTTCGAGCGCCAATGTCATTCTTCGATACTACACCATCTGGACGGATTCTGAATCGAGTAAGTTTAGATCATGCTCTTGCTCCT
AAATTGTGTTTTTCACTCTCGCGTGTGCCTTTTCTATTTTGCACATCCTAATCTTCTTCAATCATACTTCATATCAGGTTTCTGTAGAT

CAAAGTGTTGTGGACCTTGATATAGCATTCAGGCTAGGGGGATTTGCCTCAACAACAATTCAACTCCTTGGAATTGTTGCTGTCATGAG
TAAAGTCACATGGCAAGTTCTGTTTCTTATAGTCCCTATGGCTATGGCATGCATGTGGATGCAGGTAAATTGCTAAACTTTCAGGTTTC
TTTTAGTGTTGGCATTAACCTGGGATACTTAATTTTTTCAATGGAGATCGTAATGCAAGTAAAGTAGATAGCAAGGGTAGGTACACCTA
AATGAATCAATAAAAGAACTATGCGCGCATAAATTTGGCCACCTCTGTTAGTTAACTAGCCAATTAACCAGAAAACAGATGTATATGTT
CAGCATGAAAGTATTGAAACTTGTGAAGTAAGCTCATTCTTAAAGCATGAGCTTTCAAGATAGCTTGATGATTTATGTACCAAAGACTT
TTAAAGATCTTTATCATCACACAATAGTTAATGAATGTCCTTGCTACCATGAACTTGCAGAGATATTACATTGCTTCATCAAGGGAGCT
GACTAGGATCTTGAGTGTTCAGAAGTCTCCAGTGATCCATTTGTTTAGCGAGTCAATCGCTGGTGCTGCTACTATCAGAGGATTTGGTC
AGGAAAAAAGATTCATGAAAAGAAATCTTTACCTCCTTGATTGTTTTGCTCGGCCTTTGTTTTCCAGCCTTGCAGCTATTGAATGGCTC
TGCCTGCGAATGGAATTGCTCTCGACTTTTGTGTTTGCTTTCTGCATGGCAATACTCGTGAGCTTTCCTCCTGGAACAATTGAACCAAG
TATGTCTTATCTGCTATCTCACAGGCCGTTCTGTTACATTTTATGATCTTGCTTTACCCAATAGATCACTTGTTAGGTGCACTAGAAAA
CTTGCATATCTTTTTCAATAAAATATGGCAATGTGCTTCTCAATCTAAACAAGCTTTCCAATTGATAGGTATGGCTGGGCTTGCTGTCA
CATATGGACTCAACCTAAATGCTCGGATGTCAAGGTGGATATTGAGCTTCTGTAAATTAGAGAACAGAATCATCTCTGTTGAGCGTATT
TATCAGTACTGCAAGATTCCTAGTGAAGCACCACTGATTATTGAGAATTGTCGTCCCCCGGCCTCATGGCCTGAGAATGGAAACATTCA
ATTGATTGATCTCAAGGTAAACTTAGTCCGTAGCCATTTATTTGTGACTATCCATTTGCTCTTCGTTATACATAATCACCAGAAGTATA
TACTCTGTTTTTTCTTCTTCTAAGCTAAAAATACTTCAGTTTTATTTACGGCATCTTATTGTGCTTTTGCTAAATATCATAGGTCCGCT
ACAAGGACGACCTTCCCTTCGTTCTACATGGAGTCAGTTGTATTTTTCCTGGCGGGAAAAAGATTGGGATTGTAGGGAGAACTGGAAGT
GGTAAATCTACTCTCATTCAGGCTCTTTTCCGTCTAATTGAACCCACAGGAGGGAAAATTATCATTGACGACATCGATGTTTCTGCGAT
TGGCCTTCACGATCTGCGGTCACGGTTGAGCATCATCCCTCAGGACCCTACATTGTTCGAGGGTACTATCAGAATGAATCTTGACCCTC
TTGAAGAGCGTTCTGATCAAGAAATTTGGGAGGTACGCCATGGTCGCTTTTATGCTATCCTCATGTTAAATGTGCCATGATCTTTATGG
AAGAGAACTCTTTGTTTCAGGCACTAGAGAAGTGCCAGCTAGGAGAGGTCATTCGTTCGAAGGAAGAAAAACTGGACAGTCCAGGTTTG
TTCTAATTTTGAATATTCAAACACTTCTTCAAAGAGTGAGCATGACACTTGGTAAAGCATGACACCTCGTAAACAAAATTATATTTTCC
TGGATATTTGTGGTGCCATTGCAGTACTGGAGAATGGGGATAACTGGAGTGTGGGACAGCGCCAGCTTATTGCATTGGGTAGGGCGCTG
CTTAAGCAGGCAAGAATTTTGGTGCTTGATGAGGCGACGGCATCAGTTGACACAGCTACAGATAATCTTATCCAGAAGATTATTCGCAG
CGAATTCAGGGATTGCACTGTCTGTACAATTGCACACAGGATCCCAACGGTCATCGACAGTGACCTAGTCATGGTGCTTAGCGACGGTA
CATGCTCCTTCACACGATTAACCAAGTCATCTTTCCAGCCGTAGCTAGACCATTACATGTTTTGTTTCTTACTGATCGTATGTTGAATT
ATCTGAGTAACGCTCCTAACCAAACAGTGTTCTTTGTCACGCCCGAAAACTTGGGAGCAACAAACAGCGGTTACGGTGAATTCACCTGG
TCTTGTTTATTTTCCAGGTAAAATAGCGGAGTTCGACACACCCCAGAGGCTTGTGGAGGACAAGTCCTCCATGTTCATGCAGCTAGTAT
CCGAGTACTCCACCAGGGCGAGCTGTATATAGAGAGAGAGGCTTATTAGCTTAAATCCCCCACCGAGAATAGAGGCTGGGAGGTAAGGT
AGCCGGATCTGCCAGTCTACTCACACCATACAAGTAAGTAGCAACACCAGACAGGAGGATAGGAGGGGTATATGAACGGAAAGAAGCGC
CGGGCGCGTTCCCTGACCTGAATGGCCATGGATTCTTCTTCGAGGGAACGCGGCAGGCGATCGAACACCACGGGAGGAGTTGGCGGCAT
TAACCGAAGCTCTGATGCTTTTGTATGTATAACACTCTGTACTGCTTCTCCCCTTGCATGATGGGAAAACGAACACAAATAACGTGGGT
AATAAAGGGGGAAATTTTGCTTTC

>TdMRP3-B1 protein
MPRRALPLAEAAAAAAHAALLALALLLLLLRGARALASRCASCLKPPRRARNPALAGDGAPLAPSPPAAGGAWYRAALACCAYALLAQL
AALSYEVAAAAPPAEAEALLLPAVQALAWAALLALALRARAGRFPALVRVWWVLAFALSLAIAFDDSRRLMGADDHDADYAHMVANFAS
LPALGFLCLVGVMGSSGVDLEFSDDDTGVHEPLLLGGQRRGAEEEPGCLRVTPYGDAGILSLATLSWLSPLLSVGAKRPLELADIPLLA
HKDRAKFCYKAMSSHYERQRLECPDKEPSLAWAILKSFWREAAINGAFAAVNTVVSYVGPYLISYFVDYLSGKIAFPHEGYILASVFFV
SKLIETLTARQWYLGVDVMGIHVKSGLTAMVYRKGLRLSNASKQSHTSGEIVNYMAVDVQRVGDYAWYFHDIWMLPLQIILALAILYKN
VGIATVSTLIATALSIAASVPVAKLQEHYQDKLMAAKDERMRKTAECLKSMRILKLQAWEDRYRIMLEEMRNVECRWLKWALYSQAAVT
FVFWSSPIFVSVITFGTCILLGGELTAGGVLSALATFRILQEPLRNFPDLISMIAQTRVSLDRLSHFLRQEELPDDATISVPQGSTDKA
IDIKDGSFSWNPSCSTPTLSHIQLSVVRGMRVAVCGVIGSGKSSLLSSILGEIPRLSGQVRVSGTAAYVSQTAWIQSGNIEENVLFGTP
MDRPRYKRVLEACSLKKDLQLLQYGDQTIIGDRGINLSGGQKQRVQLARALYQDADIYLLDDPFSAVDAHTGSDLFKDYILGALASKTV
IYVTHQVEFLPAADLILVLKDGHITQAGKYDDLLQAGTDFNALVSAHNEAIETMDFGEDSDGDIAPSVPNKRLTPSVSNIDNLKNKVSE
NGKSSNTRGIKDKKKSEERKKKRTVQEEERERGRVSLNVYLTYMGEAYKGSLIPLIVLAQTLFQVLQIASNWWMAWANPQTEGDAPKTS
SVVLLVVYMCLAFGSSLFVFVRSLLVATFGLAAAQKLFIKMLRCVFRAPMSFFDTTPSGRILNRVSVDQSVVDLDIAFRLGGFASTTIQ
LLGIVAVMSKVTWQVLFLIVPMAMACMWMQRYYIASSRELTRILSVQKSPVIHLFSESIAGAATIRGFGQEKRFMKRNLYLLDCFARPL
FSSLAAIEWLCLRMELLSTFVFAFCMAILVSFPPGTIEPSMAGLAVTYGLNLNARMSRWILSFCKLENRIISVERIYQYCKIPSEAPLI
IENCRPPASWPENGNIQLIDLKVRYKDDLPFVLHGVSCIFPGGKKIGIVGRTGSGKSTLIQALFRLIEPTGGKIIIDDIDVSAIGLHDL
RSRLSIIPQDPTLFEGTIRMNLDPLEERSDQEIWEALEKCQLGEVIRSKEEKLDSPVLENGDNWSVGQRQLIALGRALLKQARILVLDE
ATASVDTATDNLIQKIIRSEFRDCTVCTIAHRIPTVIDSDLVMVLSDGKIAEFDTPQRLVEDKSSMFMQLVSEYSTRASCI

Supplementary Figure S2 Genomic sequences of TdMRP3 homeoalleles and their deduced amino acid sequences. Exons are highlighted in light grey.

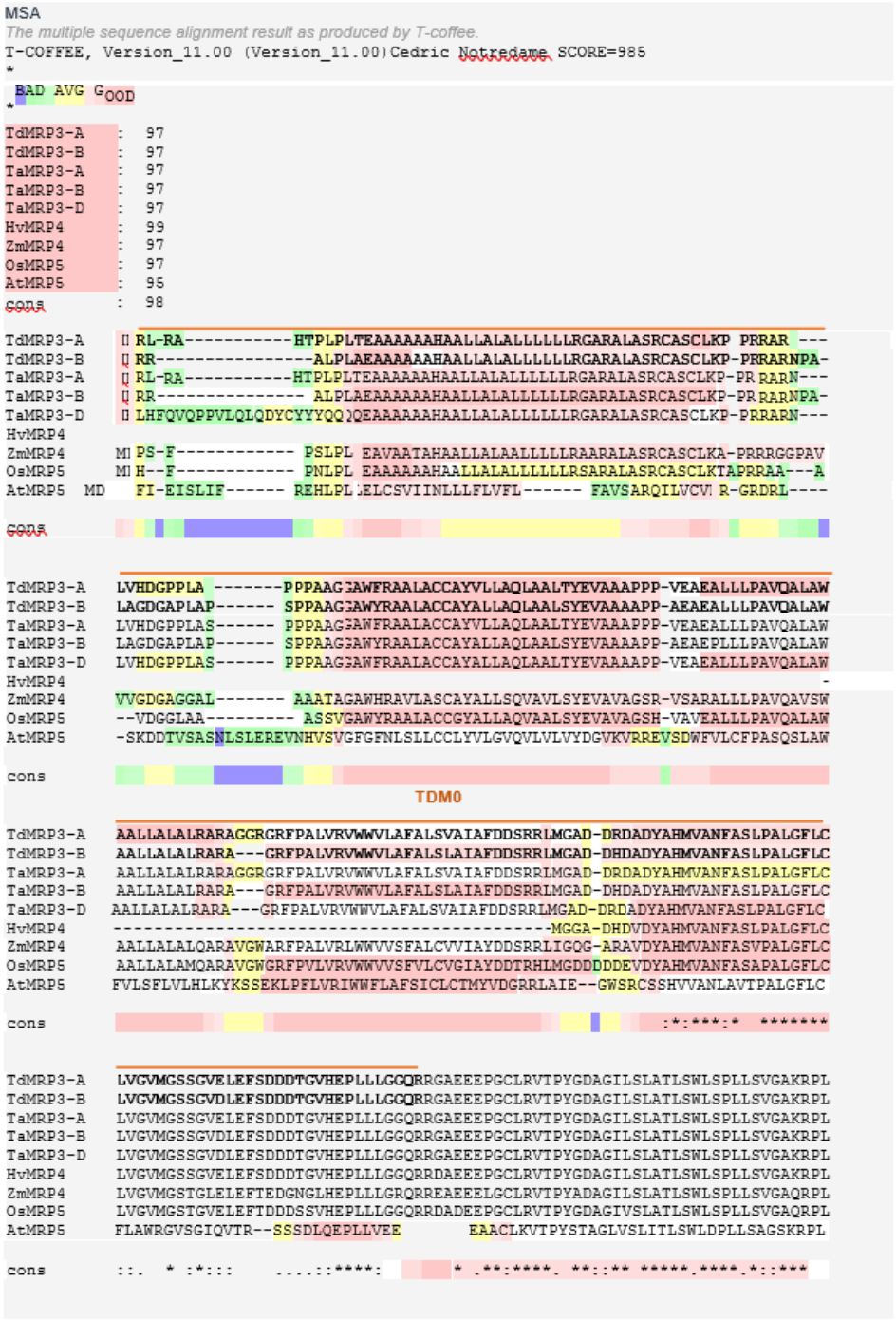

```
TdMRP3-A    ELADIPLLAHKDRAKFCYKAMSSHYERQRLECPDKEPSLAWAILKSFWREAAINGAFAAVNTVVSYVGPYLI
TdMRP3-B    ELADIPLLAHKDRAKFCYKAMSSHYERQRLECPDKEPSLAWAILKSFWREAAINGAFAAVNTVVSYVGPYLI
TaMRP3-A    ELADIPLLAHKDRAKFCYKAMSSHYERQRLECPDKEPSLAWAILKSFWREAAINGAFAAVNTVVSYVGPYLI
TaMRP3-B    ELADIPLLAHKDRAKFCYKAMSSHYERQRLECPDKEPSLAWAILKSFWREAAINGAFAAVNTVVSYVGPYLI
TaMRP3-D    ELADIPLLAHKDRAKFCYKAMSSHYERQRLECPDKEPSLAWAILKSFWREAAMNGAFAAVNTVVSYVGPYLI
HvMRP4      ELADIPLLAHKDRAKFCYKAMSSHYERQRIECPDKEPSLAWAILKSFWREAAINGCFAAVNTVVSYVGPYLI
ZmMRP4      ELADIPLLAHKDRAKSCYKAMSAHYERQRLEYPGREPSLTWAILKSFWREAAVNGTFAAVNTIVSYVGPYLI
OsMRP5      ELADIPLMAHKDRAKSCYKAMSSHYERQRMERPGSEPSLAWAILKSFWREAAINGAFAAVNTIVSYVGPYLI
AtMRP5   ELKDIPLLAPRDRAKSSYKVLKSNWKRCKSENPSKPPSLARAIMKSFWKEAACNAVFAGLNTLVSYVGPYLI

cons        ** ****:* :**** _**.:.:::::* : * *.  ***: **:****:*** *. **.:**:**********


TdMRP3-A    SYFVDYLSGKIAFPHEGYILASVFFVSKLIETLTARQWYLGVDVMGIHVKSGLTAMVYRKGLRLSNASKQSH
TdMRP3-B    SYFVDYLSGKIAFPHEGYILASVFFVSKLIETLTARQWYLGVDVMGIHVKSGLTAMVYRKGLRLSNASKQSH
TaMRP3-A    SYFVDYLSGKIAFPHEGYILASVFFVSKLIETLTARQWYLGVDVMGIHVKSGLTAMVYRKGLRLSNASKQSH
TaMRP3-B    SYFVDYLSGKIAFPHEGYILASVFFVSKLIETLTARQWYLGVDVMGIHVKSGLTAMVYRKGLRLSNASKQSH
TaMRP3-D    SYFVDYLSGKIAFPHEGYILASVFFVSKLIETLTARQWYLGVDVMGIHVKSGLTAMVYRKGLRLSNASKQSH
HvMRP4      SYFVDYLSGKIAFPHEGYILASVFFVSKLIETLTARQWYLGVDVMGIHVKSGLTAMVYRKGLRLSNASKQSH
ZmMRP4      SYFVDYLSGNIAFPHEGYILASIFFVAKLLETLTARQWYLGVDIMGIHVKSGLTAMVYRKGLRLSNASRQSH
OsMRP5      SYFVDYLSGKIEFPHEGYILASVFFVAKLLETLTARQWYLGVDVMGIHVKSGLTAMVYRKGLRLSNSSRQSH
AtMRP5   SYFVDYLGGKEIFPHEGYVLAGIFFTSKLIETVTTRQWYMGVDILGMHVRSALTAMVYRKGLKLSSIAKQNH

cons        *******_*:  ******:**_:**_:**:**:*:****:***::*:**:*_**********:**_ ::*_*


TdMRP3-A    TSGEIVNYMAVDVQRVGDYAWYFHDIWMLPLQIILALAILYKNVGIATVSTLIATALSIAASVPVAKLQEHY
TdMRP3-B    TSGEIVNYMAVDVQRVGDYAWYFHDIWMLPLQIILALAILYKNVGIATVSTLIATALSIAASVPVAKLQEHY
TaMRP3-A    TSGEIVNYMAVDVQRVGDYAWYFHDIWMLPLQIILALAILYKNVGIATVSTLIATALSIAASVPVAKLQEHY
TaMRP3-B    TSGEIVNYMAVDVQRVGDYAWYFHDIWMLPLQIILALAILYKNVGIATVSTLIATALSIAASVPVAKLQEHY
TaMRP3-D    TSGEIVNYMAVDVQRVGDYAWYFHDIWMLPLQIILALAILYKNVGIATVSTLIATALSIAASVPVAKLQEHY
HvMRP4      TSGEIVNYMAVDVQRVGDYAWYFHDIWMLPLQIILALAILYKNVGIATVSTLIATALSIAASVPVAKLQEHY
ZmMRP4      TSGEIVNYMAVDVQRVGDYAWYFHDIWMLPLQIILALAILYKNVGIAMVSTLVATVLSIAASVPVAKLQEHY
OsMRP5      TSGEIVNYMAVDVQRVGDYAWYFHDIWMLPLQIILALAILYKNVGIAMVSTLVATVLSIAASVPVAKLQEHY
AtMRP5   TSGEIVNYMAVDVQRIGDYSWYLHDIWMLPMQIVLALAILYKSVGIAAVATLVATIISILVTIPLAKVQEDY

cons        ****************:***:**:********:**:*********_**** *:**:** :** .::*:**:**_*
                                  IPR011527 ABCC1_TM_dom

TdMRP3-A    QDKLMAAKDERMRKTAECLKSMRILKLQAWEDRYRIMLEEMRNVECRWLKWALYSQAAVTFVFWSSPIFVSV
TdMRP3-B    QDKLMAAKDERMRKTAECLKSMRILKLQAWEDRYRIMLEEMRNVECRWLKWALYSQAAVTFVFWSSPIFVSV
TaMRP3-A    QDKLMAAKDERMRKTAECLKSMRILKLQAWEDRYRIMLEEMRNVECRWLKWALYSQAAVTFVFWSSPIFVSV
TaMRP3-B    QDKLMAAKDERMRKTAECLKSMRILKLQAWEDRYRIMLEEMRNVECRWLKWALYSQAAVTFVFWSSPIFVSV
TaMRP3-D    QDKLMAAKDERMRKTAECLKSMRILKLQAWEDRYRIMLEEMRNVECRWLKWALYSQAAVTFVFWSSPIFVSV
HvMRP4      QDKLMAAKDERMRKTAECLKSMRILKLQAWEDRYRIMLEEMRNVECRWLKWALYSQAAVTFVFWSSPIFVSV
ZmMRP4      QDKLMASKDERMRKTSECLKNMRILKLQAWEDRYRLQLEEMRNVECRWLRWALYSQAAVTFVFWSSPIFVAV
OsMRP5      QDKLMASKDERMRKTSECLKNMRILKLQAWEDRYRLKLEEMRNVECKWLRWALYSQAAVTFVFWSSPIFVAV
AtMRP5   QDKLMTAKDERMRKTSECLRNMRVLKLQAWEDRYRVRLEEMREEEYGWLRKALYSQAFVTFIFWSSPIFVAA

cons        *****::*********:***:_**:************: *****: *  **: ****** ***:********:.


TdMRP3-A    ITFGTCILLGGELTAGGVLSALATFRILQEPLRNFPDLISMIAQTRVSLDRLSHFLRQEELPDDATISVPQG
TdMRP3-B    ITFGTCILLGGELTAGGVLSALATFRILQEPLRNFPDLISMIAQTRVSLDRLSHFLRQEELPDDATISVPQG
TaMRP3-A    ITFGTCILLGGELTAGGVLSALATFRILQEPLRNFPDLISMIAQTRVSLDRLSHFLRQEELPDDATISVPQG
TaMRP3-B    ITFGTCILLGGELTAGGVLSALATFRILQEPLRNFPDLISMIAQTRVSLDRLSHFLRQEELPDDATISVPQG
TaMRP3-D    ITFGTCILLGGELTAGGVLSALATFRILQEPLRNFPDLISMIAQTRVSLDRLSHFLRQEELPDDATISVPQG
HvMRP4      ITFGTCILLGGELTAGGVLSALATFRILQEPLRNFPDLISMIAQTRVSLDRLSHFLRQEELPDDATISVPQG
ZmMRP4      ITFGTCILLGGQLTAGGVLSALATFRILQEPLRNFPDLISMMAQTRVSLDRLSHFLQQEELPDDATINVPQS
OsMRP5      ITFGTCILLGGELTAGGVLSALATFRILQEPLRNFPDLISMIAQTRVSLDRLSHFLQQEELPDDATITVPHG
AtMRP5   VTFATSIFLGTQLTAGGVLSALATFRILQEPLRNFPDLVSMMAQTKVSLDRISGFLQEEELQEDATVVIPRG

cons        :**_*.*:** :**************************:**:***:*****:* **::*** :***: :*:.
                                                  NBD1 (Walker A)

TdMRP3-A    STDKAIDIRDGSFSWNPSCSNPTLSDIQLSVVRGMRVAVCGVIGSGKSSLLSSILGEIPKLSGQVRISGTAA
TdMRP3-B    STDKAIDIKDGSFSWNPSCSTPTLSHIQLSVVRGMRVAVCGVIGSGKSSLLSSILGEIPRLSGQVRVSGTAA
TaMRP3-A    STDKAIDIRDGSFSWNPSCSNPTLSDIQLSVVRGMRVAVCGVIGSGKSSLLSSILGEIPKLSGQVRISGTAA
TaMRP3-B  STDKAIDIKDGSFSWNPSCSTPTLSHIQLSVVRGMRVAVCGVIGSGKSSLLSSILGEIPRLSGQVRVSGTAA
```

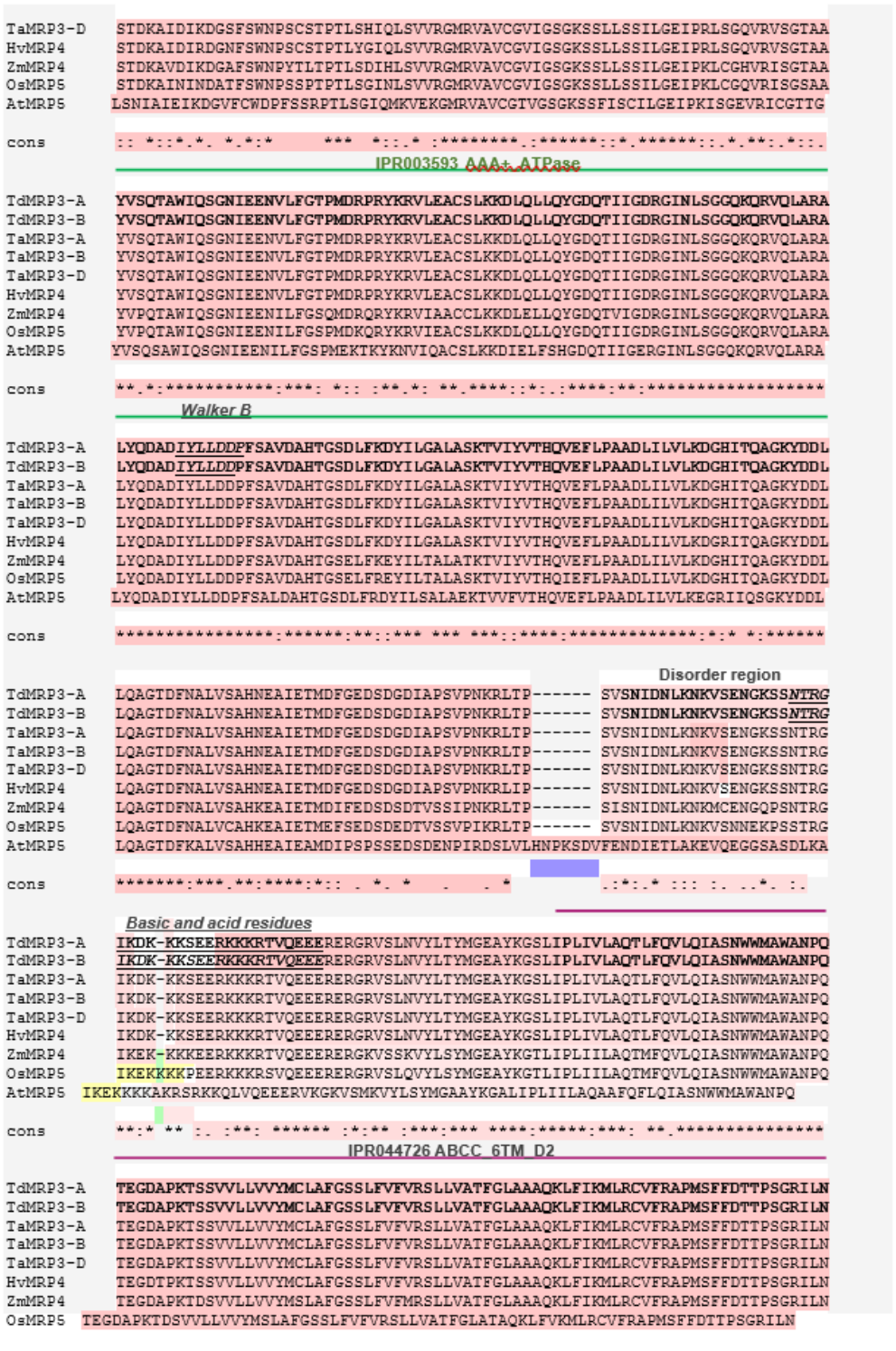
IPR003593 AAA+ ATPase
Walker B
Disorder region
Basic and acid residues
IPR044726 ABCC_6TM_D2

```
AtMRP5      TEGDESKVDPTLLLIVYTALAFGSSVFIFVRAALVATFGLAAAQKLFLNMLRSVFRAPMSFFDSTPAGRILN

cons        **** .*....:**:** .******:*:*:*: ********:*****::***.**********:**:*****

TdMRP3-A    RVSVDQSVVDLDIAFRLGGFASTTIQLLGIVAVMSKVTWQVLFLIVPMAMACMWMQRYYIASSRELTRILSV
TdMRP3-B    RVSVDQSVVDLDIAFRLGGFASTTIQLLGIVAVMSKVTWQVLFLIVPMAMACMWMQRYYIASSRELTRILSV
TaMRP3-A    RVSVDQSVVDLDIAFRLGGFASTTIQLLGIVAVMSKVTWQVLFLIVPMAMACMWMQRYYIASSRELTRILSV
TaMRP3-B    RVSVDQSVVDLDIAFRLGGFASTTIQLLGIVAVMSKVTWQVLFLIVPMAMACMWMQRYYIASSRELTRILSV
TaMRP3-D    RVSVDQSVVDLDIAFRLGGFASTTIQLLGIVAVMSKVTWQVLFLIVPMAMACMWMQRYYIASSRELTRILSV
HvMRP4      RVSVDQSVVDLDIAFRLGGFASTTIQLLGIVAVMSKVTWQVLFLIVPMAMACMWMQRYYIASSRELTRILSV
ZmMRP4      RVSVDQSVVDLDIAFRLGGFASTTIQLLGIVAVMSKVTWQVLILIVPMAVACMWMQRYYIASSRELTRILSV
OsMRP5      RVSVDQSVVDLDIAFRLGGFASTTIQLLGIVAVMSKVTWQVLILIVPMAVACMWMQRYYIASSRELTRILSV
AtMRP5      RVSIDQSVVDLDIPFRLGGFASTTIQLCGIVAVMTNVTWQVFLLVVPVAVACFWMQKYYMASSRELVRIVSI

cons        ***:*********.************* ******::*****::*:**:*:**:***:**:******.**:*:

TdMRP3-A    QKSPVIHLFSESIAGAATIRGFGQEKRFMKRNLYLLDCFARPLFSSLAAIEWLCLRMELLSTFVFAFCMAIL
TdMRP3-B    QKSPVIHLFSESIAGAATIRGFGQEKRFMKRNLYLLDCFARPLFSSLAAIEWLCLRMELLSTFVFAFCMAIL
TaMRP3-A    QKSPVIHLFSESIAGAATIRGFGQEKRFMKRNLYLLDCFARPLFSSLAAIEWLCLRMELLSTFVFAFCMAIL
TaMRP3-B    QKSPVIHLFSESIAGAATIRGFDQEKRFMKRNLYLLDCFARPLFSSLAAIEWLCLRMELLSTFVFAFCMAIL
TaMRP3-D    QKSPVIHLFSESIAGAATIRGFGQEKRFMKRNLYLLDCFARPLFSSLAAIEWLCLRMELLSTFVFAFCMAIL
HvMRP4      QKSPVIHLFSESIAGAATIRGFGQEKRFMKRNLYLLDCFARPLFSSLAAIEWLCLRMELLSTFVFAFCMAIL
ZmMRP4      QKSPVIHLFSESIAGAATIRGFGQEKRFMKRNLYLLDCFARPLFSSLAAIEWLCLRMELLSTFVFAFCMAIL
OsMRP5      QKSPVIHLFSESIAGAATIRGFGQEKRFMKRNLYLLDCFARPLFSSLAAIEWLCLRMELLSTFVFAFCMAIL
AtMRP5      QKSPIIHLFGESIAGAATIRGFGQEKRFIKRNLYLLDCFVRPFFCSIAAIEWLCLRMELLSTLVFAFCMVLL

cons        ****:****.************.*****:**********.**:*.*:****************:******.:*

TdMRP3-A    VSFPPGTIEPSMAGLAVTYGLNLNARMSRWILSFCKLENRIISVERIYQYCKIPSEAPLIIENCRPPSSWPE
TdMRP3-B    VSFPPGTIEPSMAGLAVTYGLNLNARMSRWILSFCKLENRIISVERIYQYCKIPSEAPLIIENCRPPASWPE
TaMRP3-A    VSFPPGTIEPSMAGLAVTYGLNLNARMSRWILSFCKLENRIISVERIYQYCKIPSEAPLIIENCRPPSSWPE
TaMRP3-B    VSFPPGTIEPSMAGLAVTYGLNLNARMSRWILSFCKLENRIISVERIYQYCKIPSEAPLIIENCRPPASWPE
TaMRP3-D    VSFPPGTIEPSMAGLAVTYGLNLNARMSRWILSFCKLENRIISVERIYQYCKIPSEAPLIIENCRPPSSWPE
HvMRP4      VSFPPGTIEPSMAGLAVTYGLNLNARMSRWILSFCKLENRIISVERIYQYCKIPSEAPLIIENCRPPSSWPE
ZmMRP4      VSFPPGTIEPSMAGLAVTYGLNLNARMSRWILSFCKLENRIISVERIYQYCRLPSEAPLIIENCRPPSSWPQ
OsMRP5      VSFPPGTIEPSMAGLAVTYGLNLNARMSRWILSFCKLENRIISVERIYQYCKLPSEAPLIIENSRPSSSWPE
AtMRP5      VSFPHGTIDPSMAGLAVTYGLNLNGRLSRWILSFCKLENKIISIERIYQYSQIVGEAPAIIEDFRPPSSWPA

cons        **** ***:***************.*:************:***:******.:: .*** ***: **.:***

                                    NBD2

TdMRP3-A    NGNIELIDLKVRYKDDLPFVLHGVSCIFPGGKKIGIVGRTGSGKSTLIQALFRLIEPAGGKIIIDNIDASAI
TdMRP3-B    NGNIQLIDLKVRYKDDLPFVLHGVSCIFPGGKKIGIVGRTGSGKSTLIQALFRLIEPTGGKIIIDDIDVSAI
TaMRP3-A    NGNIELIDLKVRYKDDLPFVLHGVSCIFPGGKKIGIVGRTGSGKSTLIQALFRLIEPAGGKIIIDNIDASAI
TaMRP3-B    NGNIQLIDLKVRYKDDLPFVLHGVSCIFPGGKKIGIVGRTGSGKSTLIQALFRLIEPTGGKIIIDDIDVSAI
TaMRP3-D    NGNIELIDLKVRYKDDLPFVLHGVSCIFPGGKKIGIVGRTGSGKSTLIQALFRLIEPSGGKIIIDNIDVSAI
HvMRP4      NGNIELIDLKVRYKDDLPFVLHGVSCIFPGGKKIGIVGRTGSGKSTLIQALFRLIEPAGGKIIIDDIDVSAI
ZmMRP4      NGNIELIDLKVRYKDDLPLVLHGVSCMFPGGKKIGIVGRTGSGKSTLIQALFRLIEPTGGKIIIDNIDISAI
OsMRP5      NGNIELVDLKVRYKDDLPLVLHGISCIFPGGKKIGIVGRTGSGKSTLIQALFRLIEPTGGKVIIDDVDISRI
AtMRP5      TGTIELVDVKVRYAENLPTVLHGVSCVFPGGKKIGIVGRTGSGKSTLIQALFRLIEPTAGKITIDNIDISQI

cons        .*.*:*:*:**** ::** ****:**:*******************************:.**: **::* * *

                                    IPR003593 AAA+ ATPase

TdMRP3-A    GLHDLRSRLSIIPQDPTLFEGTIRMNLDPLEERSDQEIWEALEKCQLGEVIRSKEEKLDSPVLENGDNWSVG
TdMRP3-B    GLHDLRSRLSIIPQDPTLFEGTIRMNLDPLEERSDQEIWEALEKCQLGEVIRSKEEKLDSPVLENGDNWSVG
TaMRP3-A    GLHDLRSRLSIIPQDPTLFEGTIRMNLDPLEERSDQEIWEALEKCQLGEVIRSKEEKLDSPVLENGDNWSVG
TaMRP3-B    GLHDLRSRLSIIPQDPTLFEGTIRMNLDPLEERSDQEIWEALEKCQLGEVIRSKEEKLDSPVLENGDNWSVG
TaMRP3-D    GLHDLRSRLSIIPQDPTLFEGTIRMNLDPLEERSDQEIWEALEKCQLGEVIRSKEEKLDSPVLENGDNWSVG
HvMRP4      GLHDLRSRLSIIPQDPTLFEGTIRMNLDPLEERSDQEIWEALEKCQLGEVIRSKEEKLDSPVLENGDNWSVG
ZmMRP4      GLHDLRSRLSIIPQDPTLFEGTIRMNLDPLEECTDQEIWEALEKCQLGEVIRSKEEKLDSPVLENGDNWSVG
OsMRP5      GLHDLRSRLSIIPQDPTLFEGTIRMNLDPLEECTDQEIWEALEKCQLGEVIRSKDEKLDSPVLENGDNWSVG
AtMRP5      GLHDLRSRLGIIPQDPTLFEGTIRANLDPLEEHSDDKIWEALDKSQLGDVVRGKDLKLDSPVLENGDNWSVG

cons        *********.*************** ******* :*::*****:*.***:*:*.*: *****************
```

Supplementary Figure S3 Multiple sequence alignment (MSA) of the ABCC multidrug resistance associated protein (ABCC-MRP) in different plant species. Td: *Triticum turgidum* ssp. *durum* MRP3-A1, MRP3-B1, Ta: *Triticum aestivum* MRP3-A (TraesCS5A02G512500), MRP3-B (TraesCS4B02G343800), MRP3-D (TraesCS4D02G339000); Hv: *Hordeum vulgare* MRP4 (XP 044983147.1); Zm: *Zea mays* MRP4 (EF586878); Os: *Oryza sativa Japonica group* MRP5 (XP 015630971.1); At: *Arabidopsis thaliana* MRP5 (AT1G04120.1). The MSA alignment is coloured according to the T-Coffee TCS scheme. Dark pink bits are very reliable, while blue and green bits are unreliable based on the T-Coffee library.

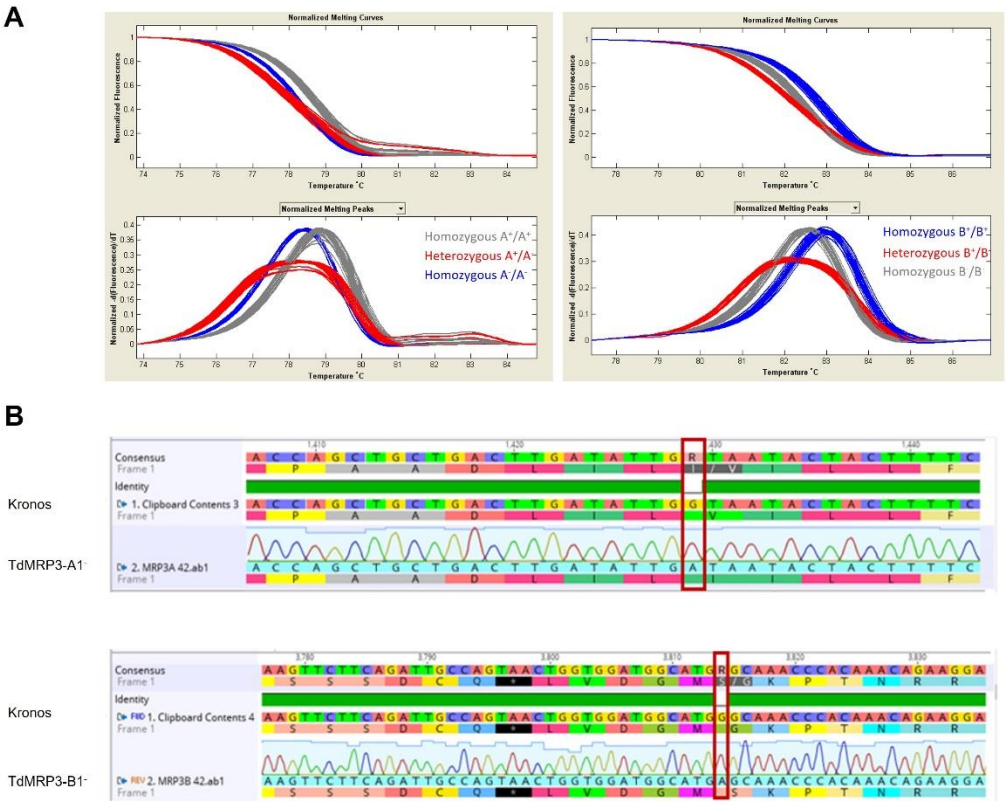

Supplementary Figure S4 Selection of the mutant genotypes by MAS and Sanger sequencing. (A) HRM genotypingof F_2 and F_3 progenies from the cross TdMRP3-A1$^-$ x TdMRP3-B1$^-$. The different melting curve profiles show the heterozygous plants and homozygous mutant or wild type lines. On the left HRM analysis of the *TdMRP3-A1* homeoallele; on the right HRM analysis of the *TdMRP3- B1* homeoallele. (B) Example of the sequencing of a double null homozygous mutant for the *TdMRP3* genes selected by HRM genotyping in the F_2 progeny. On the top sequences related to the *TdMRP3-A1* homeoallele. On the bottom sequences of the *TdMRP3-B1*.

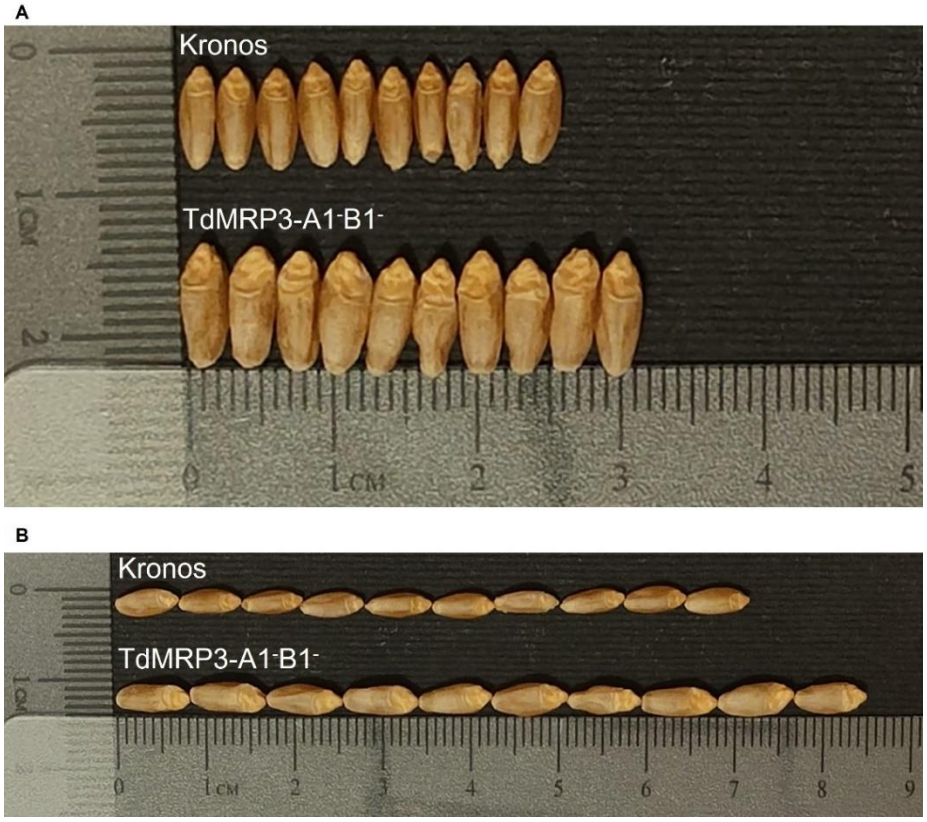

Supplementary Figure S5 Grain size comparison between the control (cv. Kronos) and the complete null TdMRP3 mutant lines.

Supplementary Table S1 List of primers used for HRM genotyping

Id primer	Sequence	T Annealing	Amplicon Size	Use	Genome
MRP3A_F	TTGCGAGAGCATTGTACCAAG	58°C	460 bp	1st round PCR	A
MRP3A_R	CATGAACAGTCCAATGAGAAG				
MRP3Aex3F1	AACCCATCAAGTCGAGTTCC	60°C	89 bp	2nd round PCR	
MRP3Aex3R	GAACAACTCAATAGGCTAATAG				
MRP3B_F	ATGTACAATACTTCTGATAGG	58°C	780 bp	1st round PCR	B
MRP3B_R	GAAAAGGCACACGCAAGAGTG				
4443_F	GTTCCAAGTTCTTCAGATTG	60°C	92 bp	2nd round PCR	
4443_R2	GGACCACACTACTTGTCTTA				

Supplementary Table S2 ICP-MS operating conditions.

ICP-MS parameters	**Setting**
RF power	1550 W
RF Matching	1.80 V
Carrier gas flow rate (Argon)	0.90 L min^{-1}
Dilution Mode	ON
Dilution Gas (Argon)	0.30 L min^{-1}
Sampling depth	8.0 mm
S/C temp	2°C
Collision Gas	He
Collision gas flow rate	4.0 L min^{-1} (*10 L min^{-1})
Isotope monitored	^{23}Na, ^{24}Mg, ^{39}K, ^{44}Ca, ^{55}Mn, ^{59}Co, ^{56}Fe, ^{60}Ni, ^{63}Cu, ^{66}Zn, ^{78}Se*, ^{95}Mo
Internal standards	^{6}Li, ^{45}Sc, ^{72}Ge, ^{89}Y, ^{115}In, ^{159}Tb
Integration Time/Mass	0.3 sec

CHAPTER 3

Development of *lpa* durum wheat genotypes by silencing *TdIPK1* genes

In submission

Frittelli A.[1], Palombieri S.[1], Quagliata G.[1], Celletti S.[1], Astolfi S.[1], Botticella E.[2], Masci S.[1], De Vita P.[3], Volpato M.[4], Sestili F.[1]

[1] Department of Agriculture and Forest Sciences, University of Tuscia. Via S. Camillo de Lellis, SNC 01100 Viterbo, Italy
[2] Institute of Sciences of Food Production (ISPA) - CNR. Via Provinciale Lecce-Monteroni, 73100 Lecce, Italy
[3] Council for Agricultural Research and Economics, Research Centre for Cereal and Industrial Crops (CREA-CI), S.S. 673, Km 25,200, 71122 Foggia, Italy
[4] Grandi Molini Italiani. Via Elettricità, 13, 30175 Venezia, Italy

Abstract

Phytic acid (PA) is the main storage form of phosphorus in kernel and is considered an anti-nutritional compound because of its ability to bind to essential minerals such as iron (Fe), zinc (Zn), potassium (K), calcium (Ca) and magnesium (Mg), thus limiting their availability, especially for populations whose diet is largely based on staple crops.
In this study, a promising nutrient biofortification approach of durum wheat is reported. The approach was based on the silencing of the gene encoding the *inositol pentakisphosphate 2-kinase 1* (*IPK1*), involved in the last step of the PA biosynthetic pathway, through a Targeting Induced Local Lesions IN Genomes (TILLING) approach. Single knock out mutants for the *IPK1* homeoalleles were identified and crossed to pyramid the two mutations. Although an elevated number of plants (F_2 and F_3 progenies) were analysed, it was not possible to identify genotypes lacking both the homeoalleles, suggesting that the expression of *IPK1* is crucial for seed formation in the spike and/or for plant germination and development.
The characterization of the single null genotypes highlighted that the partial TdIPK1-B1$^-$ mutants showed a lower accumulation of PA in the kernel along with a higher content of essential microelements (Fe, Mn, Zn) compared to the control wild-type. The pattern of accumulation was different for the TdIPK1-A1$^-$ mutants which only presented a greater accumulation of K.

KEYWORDS

Durum Wheat, Genetic Biofortification, Phytic Acid, Microelements, *TdIPK1* genes, TILLING

3.1 Introduction

3.1.1 Hidden hunger

Over the past decade, the international research community has faced challenges in reducing malnutrition, often referred to as the 'triple burden of malnutrition', including overnutrition, undernutrition and micronutrient deficiencies.

In 2015, the countries of the United Nations committed to the 2030 Agenda for Sustainable Development, with the aim to eliminate all forms of malnutrition and guarantee that all people have access to safe, nutritious and sufficient food (**Lowe, 2021**).

Micronutrient malnutrition, or hidden hunger, is one of the major impediments to proper growth, development, and overall health, and usually results from inadequate intake of vitamins and minerals due to poor diet, limited food availability or reduced absorption (**Von Grebmer et al., 2014**).

The Food and Agriculture Organization (FAO) estimates that 11% of the current world population is suffering extreme food shortages, and 17% suffers from micronutrient deficiencies (**FAO et al., 2019**).

Therefore, micronutrient deficiencies affect 3 billion people (**Figure 3.1**), resulting in deleterious impacts on human health especially in low- and middle-income countries with already high levels of food insecurity mainly due to staple crops-based diet (**Muthayya et al., 2013**). Although these crops can satisfy the daily caloric requirement, they do not provide the right quantities of essential nutrients required for the maintenance of optimal health, physiological function and well-being (**Lockyer et al., 2018**; **Sestili et al., 2019**; **Vitamin and Mineral Nutrition Information System (VMNIS), 2022**).

The most common micronutrient deficiencies include iron (Fe), zinc (Zn), iodine (I) and vitamins deficiency and affect especially women and children by weakening the immune system, leading to infections such as diarrhoea, stunting, blindness, anemia, fetal malformations and developmental difficulties. For these reasons, they are a serious health, economic and social concern in vulnerable countries.

The UN's Sustainable Development Objective 2 is to "End hunger, achieve food security and better nutrition and promote sustainable agriculture". Within this goal, several internationally agreed targets to be achieved by 2030 have been identified. In this scenario, specific indicators have been used to allow individual countries to monitor their progress (**Global indicator framework for the Sustainable Development Goals and targets of the 2030 Agenda for Sustainable Development**).

Over time, various strategies have been employed to improve micronutrient intake including diet supplementation, fortification and diversification (**Sheoran et al., 2022**). Each of these

interventions can bring benefits, but all have limitations depending on the context and available resources.

Supplementation programs to improve micronutrient status have been developed for Fe (**Thompson et al., 2013**; **Pasricha et al., 2014**) and Zn (**Stammers et al., 2015**; **Liu et al., 2018**). Despite this, the use of supplementation to address hidden hunger remains little practised as the strategy is too expensive and its effectiveness depends on the ability to reach vulnerable populations. Moreover, the supplementation may provide a short-term solution but does not solve the long-term problem of a nutrient-poor diet.

Fortification consists in the approach of raising the content of one or more micronutrients in food to improve the nutritional quality providing public health benefits. Despite its potential, food fortification faces challenges due to a lack of national laws; moreover, fortification projects tend to favour metropolitan areas and places with greater socioeconomic standing than rural areas (**WHO, 2006**; **Olson et al., 2021**).

Another strategy adopted to combat malnutrition concerns the development of diversified diets. Indeed, the greater the diversity of a diet, the lower the risk that the diet is insufficient in terms of micronutrient supply, therefore understanding dietary patterns is important to plan the right approach to overcome hidden hunger. The main limit of this strategy is the difficulty of providing a balanced diet accessible to low-income populations.

Since it is not practicable either to provide diversified diets, or to adopt fortification and supplementation programs for the entire world population, staple crop biofortification is now the most concrete option for addressing the problem of hidden hunger (**Sheoran et al., 2022**).

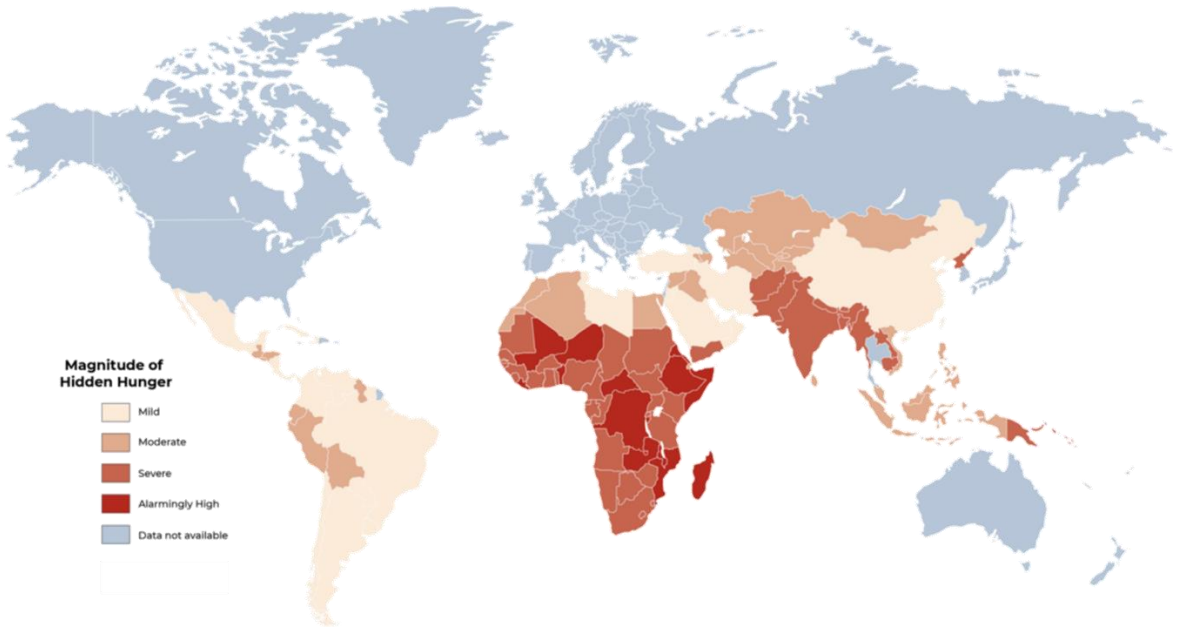

Figure 3.1 Diffusion of Hidden Hunger in the World (Muthayya et al., 2013).

3.1.2 Crop Biofortification

The biofortification process focuses on improving crops' content of Fe, Zn, and vitamins, whose deficiencies account for the majority of the health burden from hidden hunger through agronomic practices, conventional breeding techniques or genetic modification.
The most common approach to improve micronutrient content in the edible parts of plants, and thus to increase human intake, is soil or foliar application of fertilizers. Although previous studies have revealed the successful application of this approach (**Ludwig and Slamet-Loedin, 2019**; **Ramzan et al., 2020**), results are dependent on crop and the soil mineral availability. Moreover, the application is expensive, as fertilizers must be applied regularly, it is not possible to direct the micronutrients towards the edible parts and excessive usage of fertilizers can lead to environmental concerns.
With the need to overcome these limitations, attempts have been made to use genetic biofortification by exploiting the genetic variability of crops and conventional breeding techniques. To date, modern biotechnologies represent the most interesting perspective for biofortification. The transgenic approach appears to be the best option in cases where genetic variability is limited or absent. Furthermore, this approach allows to perform multiple genetic manipulations on a single organism to direct the accumulation of micronutrients towards the edible parts of plants (**White and Broadley, 2009**; **Garg et al., 2018**; **Kiran et al., 2022**).
In recent decades, scientific studies and initiatives such as HarvestPlus focused on iron (Fe), zinc (Zn), and vitamin A biofortification because they are considered the most limited micronutrients according to the World Health Organization (**WHO, 2006**).
According to the HarvestPlus about 283 varieties of biofortified crops were released so far in 30 countries among which: zinc wheat, rice and maize; vitamin A cassava, maize, sweet potato; iron bean and pearl millet (https://www.harvestplus.org/).
Some biofortified crops have been developed using non-transgenic techniques such as rice with enhanced Zn and Se content (**Mangueze et al., 2018**), wheat with higher Fe and Zn (**Verma et al., 2016**), or maize (**Manjeru et al., 2019**) and wheat enriched with provitamin A (**Sestili et al., 2019**; **Garcia Molina et al., 2021**) and essential minerals (**Frittelli et al., 2023**).

3.1.3 Phytic acid

Phytic acid, also known as $InsP_6$ or PA, is a naturally occurring compound found in many plant-based foods, including grains, legumes, nuts, and seeds. It is particularly abundant in wheat bran and germ (**Ibrahim et al., 2022**), which are often removed during food processing. Phytic acid can bind to minerals such as Ca, Fe, Zn, and Mg, lowering their availability for absorption

in the human body (**Lopez et al., 2002; Frittelli et al., 2023**). This can be a concern for people who rely heavily on plant-based diets, as it may increase their risk of mineral deficiencies. Phytic acid is regarded an anti-nutritional compound and reducing or eliminating the PA content in grains remains a significant issue in plant breeding programs. Different strategies allowed to develop many low phytic acid (*lpa*) mutants in all major crops according to the step where the mutations affect the PA biosynthetic pathway or transport (**Sparvoli and Cominelli, 2015**; **Raboy, 2020**) .

Several experiments were made to block the PA biosynthesis by targeting different genes at various steps of the pathway. However, it was demonstrated that the disruption of the biosynthetic pathway at the early steps can affect the plant inositol metabolism and disturb related pathways. Therefore, the best strategies to develop *lpa* mutants seem to be represented by the silencing of PA biosynthesis genes involved in the final steps, such as for example the gene encoding the inositol 1,3,4,5,6-pentakisphosphate 2-kinase (IPK1) (**Colombo et al., 2020**; **Ibrahim et al., 2022**).

3.1.4 *IPK1* genes

IPK1 is a member of inositol phosphate kinase superfamily. In plants, it is implicated in various biological processes, including stress response, gene regulation, and cell signalling (**Kuo et al., 2014**). IPK1 has been shown to be involved in the regulation of plant responses to abiotic stress, such as drought, salt, and cold stress, and may play a role in the regulation of gene expression in response to these stresses (**Riemer et al., 2022**). IPK1 is expressed in various tissues in plants, including seeds, roots, leaves, and flowers. It plays a crucial role in regulating the synthesis of PA in seeds, where it controls the rate of PA accumulation during seed development in the last step of the biosynthetic pathway (**Ali et al., 2013**; **Sparvoli and Cominelli, 2015**). Mutations in the *IPK1* gene have been shown to reduce the levels of phytic acid in seeds, which can have important implications for crop nutrition and quality. The silencing of the *IPK1* gene in rice and wheat through the RNAi approach led to the development of lpa mutants able to accumulate higher amount of Fe and Zn in the kernel (**Ali et al., 2013**; **Aggarwal et al., 2018**). Similar results were obtained in bread wheat by the silencing of *TaIPK1.A* gene through the use of CRISPR/Cas9 technology (**Ibrahim et al., 2022**). The analysis of the genome-edited lines revealed a significant decrease in the PA content accompanied by 1.5 to 2.1 fold increase in the Fe concentration and 1.6 to 1.9 fold rise in Zn concentration. Phenotypic analyses revealed an altered spike architecture in transgenic plants without compromising significantly grain yield (**Ibrahim et al., 2022**).

The goal of the research here presented is the development of durum wheat genotypes biofortified in essential minerals through the silencing of *TdIPK1* genes using a non-transgenic approach known as Targenting Induced Local Lensions in Genome (TILLING) (**McCallum et al., 2000**).

3.2 Materials and methods

3.2.1 Isolation and phylogenesis of IPK1 sequences

In order to identify the sequence of *TdIPK1*, the orthologous genes of *Triticum aestivum* were used as a query and blasted against *Triticum turgidum* ssp *durum* cv. Svevo genome in Ensembl Plants database (https://plants.ensembl.org/index.html).
The IPK1 protein sequences of the major grass species were identified by blasting the protein sequences in NCBI BLASTP software (https://blast.ncbi.nlm.nih.gov/Blast.cgi) and the phylogenetic analysis was carried out by MEGA11 software (**Tamura et al., 2021**). The evolutionary history among the selected taxa were deduced using the Neighbor-Joining (NJ) method with the p-distance method and pairwise deletion option. The multiple sequence alignment of IPK1 proteins was performed by T-Coffee Expresso 11.0 tool (https://tcoffee.crg.eu/apps/tcoffee/do:expresso).

3.2.2 Plant materials

Two TdIPK1 mutant lines, deriving from the treatment with EMS mutagen, were identified through the platform WheatTILLING available at the University of Davis (https://dubcovskylab.ucdavis.edu/home; **Krasileva et al., 2017**). In detail, the lines Kronos 2700 and Kronos 1194 had a nonsense mutation in the exon II of the *TdIPK1-A1* homeoallele and in the exon IV of *TdIPK1-B1* homeoallele, respectively (**Supplementary Figure S1**). The two mutations were pyramided crossing the homozygous mutant lines (TdIPK1-A1^{-} and TdIPK1-B1^{-}). The F_1 generation was self-pollinated and the selection of the different genotypes was conducted on the derived F_2 and F_3 progenies. The partial null mutants were grown in a controlled growth chamber with initial vernalization at 4-5°C for 3 weeks, followed by 18-26°C day and 16-18°C night temperature with a 16 h light period along with the controls (cv. Kronos and wild-type sibling lines selected by the cross).

3.2.3 DNA extraction

Genomic DNA was extracted from leaves (F_2 progeny) and half seeds (F_3 progeny) using the NucleoSpin® Plant II (Macherey-Nagel) kit and according to the manufacturer's instructions. The DNA was used as template for the analysis of HRM-genotyping.

3.2.4 HRM analysis

HRM analysis was performed on the F_2 progeny of the cross TdIPK1-A1^{-} X TdIPK1-B1^{-}. Amplicons were produced by a nested PCR strategy. The first PCR was carried out to amplify genome-specific fragments for *TdIPK1-A1* and *TdIPK1-B1* homeoalleles, respectively, using the primer pairs reported in **Supplementary Table S1**. The reaction was performed in a 20 µl

volume using the following conditions: 10 µl of 2X GoTaq® G2 Hot Start Colorless Master Mix (Promega, Madison, USA), 0.5µM of each primer, 20 ng of template DNA and nuclease-free water up to 20 µl volume, with the following conditions: 95°C for 2 min, followed by 38 cycles at 95°C for 30 sec, 56°C for 30 sec, 72°C for 1 min and a final extension at 72°C for 5 min. The first PCR reaction was diluted 60-fold and 2 µl were used as a template for the second PCR reaction for HRM analysis. The second reaction was carried out using the primer pairs reported in **Supplementary Table S1** and prepared as follows: 2 µl of diluted DNA template, 5 µl of 2X GoTaq® G2 Hot Start Colorless Master Mix (Promega), 0.5µM of each primer, 1 µL LC Green Plus (Idaho Technology Inc., Salt Lake City, USA) and nuclease-free water up to 10 µl volume. The PCR program was carried out following these conditions: 95°C for 2 min, followed by 39 cycles at 95°C for 30 sec, 60°C for 20 sec, 72°C for 20 sec and a final extension at 72°C for 5 min. At the end of the final extension step, the reaction was held at 95 °C for 30 sec, then at 25 °C for 1 min. The PCR reaction was carried out in 96-well Frame-Star plates (4titude Ltd., Surrey, UK) overlaid with 10 µl of mineral oil (Sigma-Aldrich, St. Louis, MO, USA), and the analyses of the melting curves was performed by the Light Scanner instrument (Idaho Technology, Inc.).

3.2.5 Analyses of the gene expression by Quantitative Real Time PCR (qRT-PCR)

Immature seeds of the partial null mutants along with the control (cv. Kronos) at 14 Days Post Anthesis (DPA) were harvested, immediately frozen in liquid nitrogen and stored at -80°C. Total RNA was extracted using the Spectrum Plant Total RNA kit (Sigma-Aldrich, St. Louis, USA) following manufacturer's instructions. One µg of the extracted RNA was used as template for the synthesis of cDNA, following the protocol indicated in the QuantiTect Reverse Transcription Kit (Qiagen, Hilden, Germany). The analyses of qRT-PCR were performed using the CFX 96 Real-TimePCR Detection System device (Bio-Rad Hercules, CA, USA). The reaction was prepared in a final volume of 10 µl containing the following concentrations: 5 µl of 2X SsoAdvUniver SYBR GRN SMX (Bio-Rad Hercules, CA, USA), 0.5 µM of each primer and 1 µl of cDNA. The qRT-PCR program had the following conditions: 95°C for 3 min, followed by 39 cycles at 95°C for 10 sec and 60°C for 30 sec. A melting curve was generated over the range 75–95°C, with 0.5°C increments at 5 s/step. Transcript quantification was enabled by CFX manager software. Three biological replicates were analysed for each genotype, and each biological replicate was represented by three technical replicates. The list of genes analysed, along with the housekeeping β-actin gene, and the used primers are shown in **Supplementary Table S2**.

3.2.6 Determination of PA and visualization of iron deposits

PA was determined as described in **Frittelli et al. (2023)**. Briefly, mature seeds of selected F_4 partial mutant lines (TdIPK1-A1$^-$, TdIPK1-B1$^-$) along with the controls (cv. Kronos and WT sibling lines) were grounded to fine powder by a laboratory Cycline Mill (Cyclotec 1093, FOSS, Hilleröd, Sweden). PA was determined using a commercial kit (K-PHYT kit, Megazyme Inc, Bray, Ireland) and the PA content was expressed in the form of mean values of three biological replicates ± standard error. Three technical replicates were carried out for each biological replicate. A one-way analysis of variance and the post hoc Tukey's HSD test (p-value< 0.05) were used to identify significant differences among mean values.
The ferric iron (Fe^{3+}) deposits were stained in F_4 mature seeds of the same genotypes as described in **Frittelli et al. (2023),** with Perls' blue staining method (**Krishnan et al., 2001**; **Prom-u-Thai et al., 2003**) and a stereo microscope was used to assess the staining intensity.

3.2.7 Determination of macro- and micro-nutrient

Mature F_4 seeds of the selected mutant lines along with controls (cv. Kronos) were grounded to fine powder and oven-dried at 80°C. As described in **Frittelli et al. (2023)**, samples were introduced in polypropylene tubes (digiTUBES, SCP Science, Champlain, NY, USA). After the addition of 3 mL of concentrated nitric acid and 1 mL of concentrated hydrogen peroxide, samples were heated in a block system (DIGIPREP, SCP Science, Champlain, NY, USA) at 95° C for 2 hours. The extracts were then filtered by a 0.45 µm teflon filter (DigiFILTER, SCP Science, Champlain, NY, USA). The digests were diluted with dH_2O and analysed by inductively coupled plasma-mass spectrometry (ICP-MS 7900, Agilent Technologies, Santa Clara, CA, USA) with Octopole Reaction System (ORS). Phosphorous and sulfur in the digested solutions were determined by inductively coupled plasma-optical emission spectrometer (ICP-OES 5100 Agilent Technologies, Santa Clara, CA, USA) using the operating conditions described in **Frittelli et al. (2023)**. Data were expressed as mean values of three biological replicates ± standard error and three technical replicates were carried out for each biological replicate.

3.2.8 Root analysis of IPK1 mutants

The root systems of the selected TdIPK1 mutant lines along with control plants (cv. Kronos and WT sibling lines) were analysed to highlight any morphological differences. Mature seeds of F_4 progeny were left to germinate for 5 days in the dark at room temperature in Petri dishes. After germination, seedlings were transferred to a plastic pot filled with 2 L of a continuously aerated nutrient solution and were placed in a growth chamber under 27/20°C and 14/10 h day/night cycles with a relative humidity of 80% and 200 mmol m^{-2} s^{-1} PAR at leaf level for 5 days (**Quagliata et al., 2023**). Roots were cut from the stem and placed in a Perspex tray with

a film of water to reduce root overlapping. The WinRHIZO™ scanning equipment and software (EPSON1680, WinRHIZO Pro2003b Software; Regent Instruments Inc., Quebec, Canada) was employed to determine morphological root traits, such as volume and surface area, total root length, root diameter and number of root tips. Data were expressed as mean values of three technical replicates for three biological replicates ± standard error.

3.2.9 Field trial evaluation of yield-related traits

The experimental field trial was carried out at CREA-CI (Foggia, Italy) during the 2021-2022 growing season using standard agronomic practices. Cultivar Kronos and the mutant TdIPK1-B1^{-} genotypes were seeded in single plots, consisting of 1-m rows, 30 cm apart, with 30 germinating seeds per plot, and following a randomized complete block design with three replications. Plots were hand-harvested at maturity. The following yield-related traits were recorded from randomly selected spikes: Spike weight, Spike length, Spikelets number per spike, Kernels per spike and Kernel weight per spike.

3.3 Results

3.3.1 Phylogenesis of IPK1 proteins

With the aim to evaluate the evolutionary history of IPK1 enzymes in the major cereals and the model species *Arabidopsis thaliana*, a phylogenetic analysis was performed using MEGA11 software. A blast search of *TaIPK1-A1* (TraesCS2A02G497700) and *TaIPK1-B1* (TraesCS2B02G525900) run against the durum what genome in Ensembl Plants showed a high identity with TRITD2Av1G270440 and TRITD2Bv1G233570, respectively annotated as *TdIPK1-A1* and *TdIPK1-B1*. The IPK1 protein sequences used in phylogenetic tree were identified by blasting the protein sequences in NCBI BLASTP software. The phylogenetic analysis highlighted that TdIPK1 proteins were evolutionally close to *Triticum aestivum*, *Aegilops tauschii*, *Triticum dicoccoides*, *Hordeum vulgare*, *Brachypodium distachyon* and *Lolium rigidum*. Among the considered sequences, a second cluster was constituted by the IPK1 proteins isolated from *Oryza sativa*, *Oryza glaberrima*, *Zea mays*, *Panicum hallii* and *Setaria italica* (**Figure 3.2**).

The multiple sequence alignment performed using T-Coffee Expresso tool showed a high level of identity among the sequences confirming the conservation of typical motifs among the species analysed (**Supplementary Figure S2**). TdIPK1 proteins had four typical motifs (GEG(G/A)ANL, RxxMHQxLK, LDxLDIEGx4Y, and EXKPK) (reported in bold letter in **Supplementary Figure S2**) that are strongly conserved in wheat, rice and maize species as already reported in previous works (**Ali et al., 2013**; **Bhati et al., 2014**).

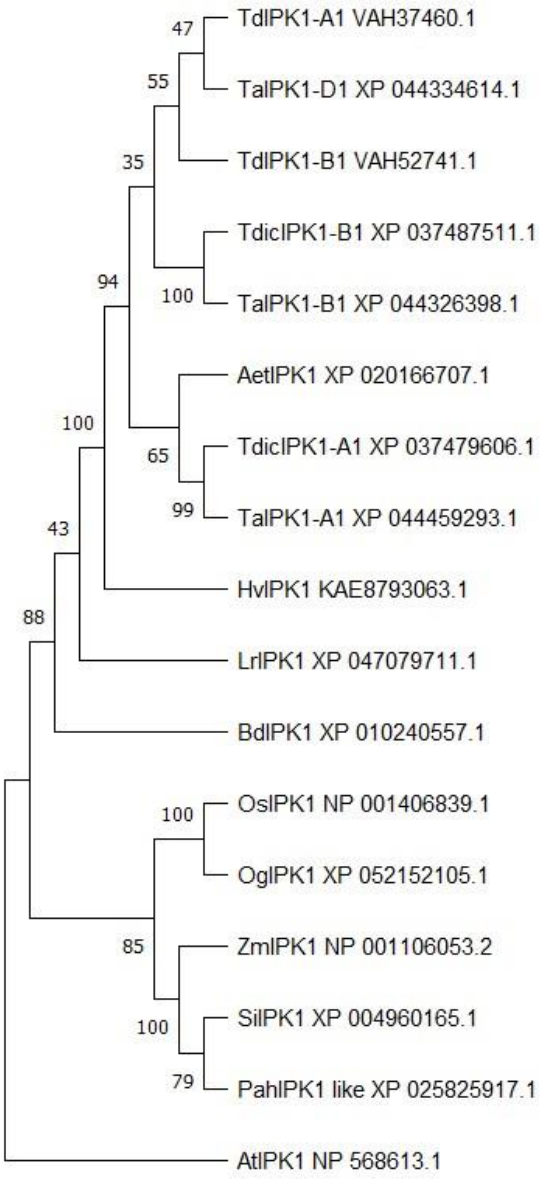

Figure 3.2 Phylogenetic tree of IPK1 proteins in different plant species. At: *Arabidopsis thaliana* IPK1 (NP_568613.1); Lr: *Lolium rigidum* IPK1 like (XP_047079711.1); Og: *Oryza glaberrima* IPK1 (XP_052152105.1); Os: *Oryza sativa Japonica Group* IPK1 (NP_001406839.1); Pah: *Panicum hallii* IPK1 (XP_025825917.1); Bd: *Brachypodium distachyon* IPK1 (XP_010240557.1); Hv: *Hordeum vulgare* IPK1 (KAE8793063.1); Aet: *Aegilops tauschii* subsp. *strangulata* IPK1 (XP_020166707.1); Tdic: *Triticum dicoccoides* IPK1-A1 like (XP_037479606.1), IPK1-B1 like (XP_037487511.1); Ta: *Triticum aestivum* IPK1-A1 (XP_044459293.1), IPK1-B1 (XP_044326398.1), IPK1-D1 (XP_044334614.1); Td:

Triticum durum ssp. *durum* IPK1-A1 (VAH37460.1); IPK1-B1 (VAH52741.1); Zm: *Zea mays* IPK1 (NP_001106053.2); Si: *Setaria italica* IPK1 (XP_004960165.1). The phylogenetic tree was constructed by the Neighbor-joining (NJ) method with pairwise deletion option and p-distance matrix in MEGA XI (Tamura et al., 2021). Bootstrap values (1000 replicates) were shown at each node.

3.3.2 Selection of TdIPK1 mutants

With the dual objective of evaluating the function of *TdIPK1* in durum wheat and obtaining new genotypes able to accumulate a higher content of essential minerals in the grain, a TILLING strategy was carried out to silence both the *TdIPK1* homeoalleles. Single null mutants in the two homeoalleles (*TdIPK1-A1* and *TdIPK1-B1*) were selected in the TILLING platform available at the University of Davis and the mutations were pyramided by crossing the two selected mutant lines. The mutations were followed in F_2 progeny of the cross (29 lines) through HRM-genotyping (**Supplementary Figure S3**). No double null mutants for the *TdIPK1* genes were identified in the F_2 generation. The analyses were, therefore, conducted on F_3 progenies of genotypes homozygous null mutants for one homeoallele and heterozygous for the second one. A total of 249 genotypes were analysed, of which only two complete null mutants were identified and confirmed by sequencing out of 62 expected for a Mendelian segregation.
From the molecular screening, 46 and 68 single null lines TdIPK1-A1$^-$ and TdIPK1-B1$^-$ were selected, respectively (**Supplementary Table S3**).

3.3.3 Expression analysis of key genes involved in PA biosynthetic pathway

The expression analyses performed on *TdIPK1-A1* and *TdIPK1-B1* revealed a significant down-regulation (>70%) of the two genes in TdIPK1-A1$^-$ and TdIPK1-B1$^-$ mutant lines, respectively (**Figure 3.3**). A significant reduction (>50%) of transcript level in the two mutant lines was also observed using the primer pair that amplifies both *IPK1* homeoalleles.
To investigate if the silencing of the single homeoalleles can cause pleiotropic effects on the expression of the major genes involved in PA biosynthetic pathway, qRT-PCR was carried out on the mRNA (extracted from immature grain at 14 DPA) of the three genotypes (Kronos wild-type, TdIPK1-A1$^-$ and TdIPK1-B1$^-$).
In detail, the expression analyses were performed on the following genes: *inositol monophosphate phosphatase* (*IMP*), involved in the production of free myo-inositol (Ins) from myo-inositol 3-phosphate (Ins(3) P_1); *myo-inositol kinase* (*MIK*), involved in the first phosphorylation step, consisting in the conversion of Ins to $InsP_1$; *inositol 1,3,4-triphosphate 5/6-kinase* (*ITPK*), involved in the phosphorylation of $InsP_3$ to $InsP_5$. In addition, it was investigated the expression level of a non-biosynthetic gene, encoding the multidrug-resistance associated proteins 3 (MRP3), involved in the transport and storage of PA in the vacuole. The

data showed that the silencing of the *IPK1* genes in the TdIPK1-A1$^-$ and TdIPK1-B1$^-$ mutants did not determine changes in the expression levels of the analysed genes, except for the *IMP1* gene that resulted up-regulated (2.8 fold) in TdIPK1-B1$^-$ mutant lines (**Figure 3.3**).
The expression analyses were extended to other two genes, *Gle1* and *LOS4*. *Gle1* encodes an essential multifunctional protein that plays a direct role in both mRNA export and translation (**Lee et al., 2015**). In plants *Gle1* seems to be associated to the *osmotically responsive genes 4* (*LOS4*) and PA. In fact, several amino acidic residues of Gle1 are involved in the interaction with the phosphate groups of PA (**Montpetit e al., 2011**). The modification of these residues determined the development of Gle1 variants with different binding pockets for PA. In detail, Gle1 (IS1) and Gle1 (IS2) mutants, which presented a single mutation from Ala-437 to Lys and a double mutation of Glu-433 to Lys and Ala-437 to Lys, respectively, were able to reduce the negative effects associated to IPK1 low phytic mutant in *Arabidopsis* (**Lee et al., 2015**). Here, the expression analysis revealed an up-regulation of *Gle1* (2.1 fold) and *LOS4* (2.8 fold) in the TdIPK1-B1$^-$ mutants compared to TdIPK1-A1$^-$ and control Kronos (**Figure 3.3**).

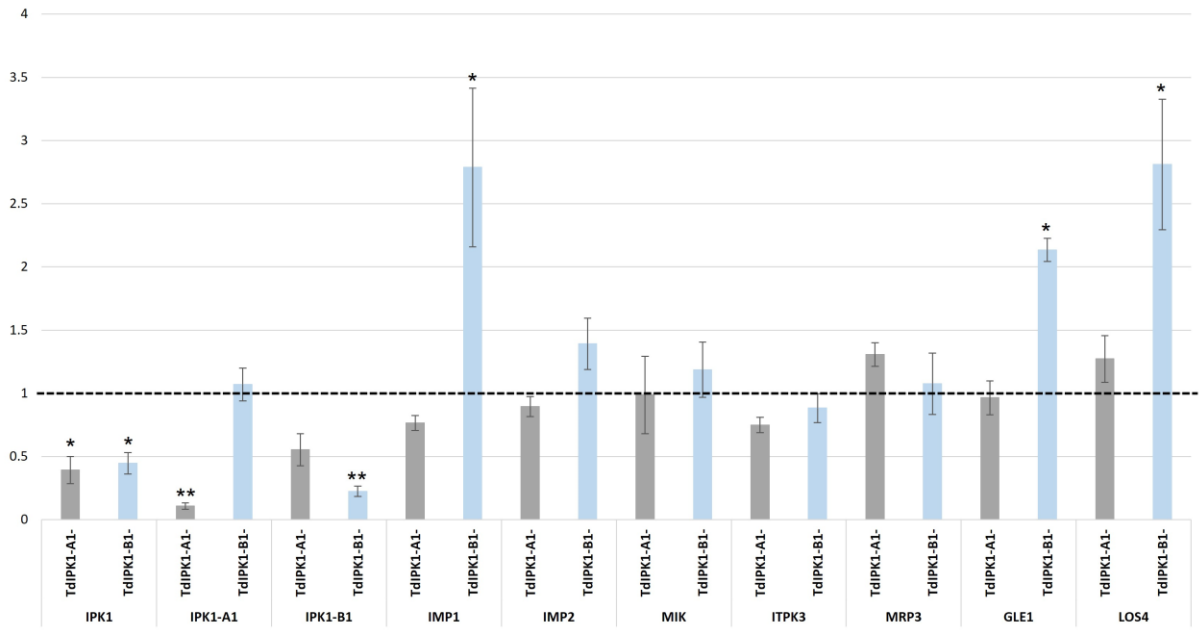

Figure 3.3 Relative expression of TdIPK1 mutant lines compared to the control Kronos wild-type. The levels of gene expression were determined in relation to the transcription levels of

the housekeeping gene β-actin. The bar graph represents the mean of three biological replicates, each one made of three technical replicates. The dotted line indicates the relative transcription value of the control Kronos wild-type. Standard error is indicated above each bar. Two-tailed Student's t-tests showed relative expression values with significant (*p≤0.05) and highly significant (**p≤0.01) differences compared to the control.

3.3.4 Biochemical characterization of TdIPK1 mutants

The analysis of PA content revealed significant differences among the controls (cv. Kronos and WT sibling lines) and the partial null mutant genotypes (TdIPK1-A1$^-$ and TdIPK1-B1$^-$)selected from the F_3 segregating progenies grown in field at the Experimental Farm of University of Tuscia in the season 2022-2023. In detail, PA content was reduced of about 19% and 17% in the TdIPK1-A1$^-$ and TdIPK1-B1$^-$ mutants, respectively (**Figure 3.4**). No difference was found comparing the Kronos wild-type with the F_3 wild-type sibling lines.

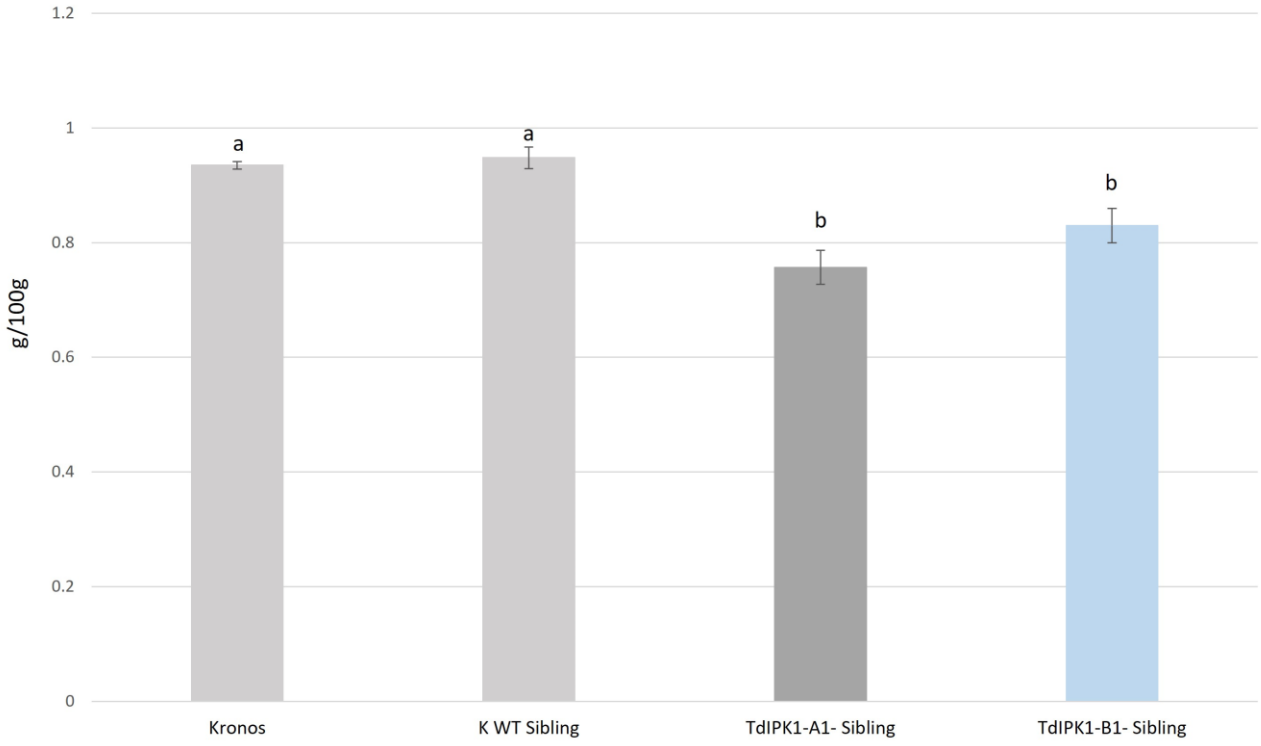

Figure 3.4 Phytic acid content in *lpa* mutants along with the control genotypes (cv. Kronos and K WT sibling lines). Mean values of three biological replicates, error bars indicate standard errors. Values followed by different letters differ significantly from one another (one-way ANOVA, Tukey HSD test, p<0.05).

Since PA acts as a chelator of essential mineral cations, the modulation of PA accumulation in seeds can be associated with an increased bioavailability of nutrients.
To evaluate at qualitative level if the reduction of PA observed in the single null TdIPK1 mutant affected the amount of iron in the kernel, the *Perls* staining was carried out on longitudinal sections of mature caryopsides. Results highlighted that the signal of Fe deposition was stronger in both the mutant lines compared to the control Kronos wild-type. In this regard the intensity of stained Fe increased in the scutellum and aleuronic layers of the TdIPK1-A1$^-$ and TdIPK1-B1$^-$ single null homozygous mutants (**Figure 3.5**).

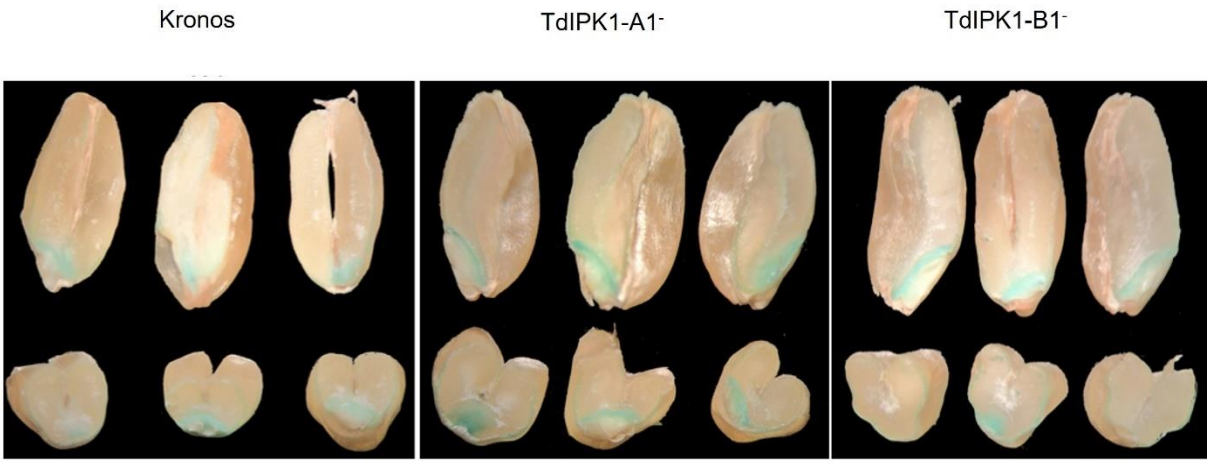

Figure 3.5 Localization of Fe deposits within the kernel with Perls' blue staining. In each image there are the longitudinal sections (top) and the transversal sections (bottom), of the seeds of cv. Kronos, TdIPK1-A1$^-$, TdIPK1-B1$^-$.

The analysis of macro- and micro-nutrients concentration confirmed differences among the different genotypes analysed (**Figure 3.6**). With regard to macronutrients, an increase of Mg (+60%), P (+40%) and S (+25%) was observed in the TdIPK1-B1$^-$ mutant compared to the control Kronos. Differently, the TdIPK1-A1$^-$ mutant presented a greater accumulation for K (+20%) compared to the control, whereas the other macronutrients were not differentially accumulated. Noteworthy, the grain of TdIPK1-B1$^-$ contained a significantly higher content of important microelements compared to the control Kronos wild-type, i.e. Fe (+72%), Mn (+30%) and Zn (+126%) contents.

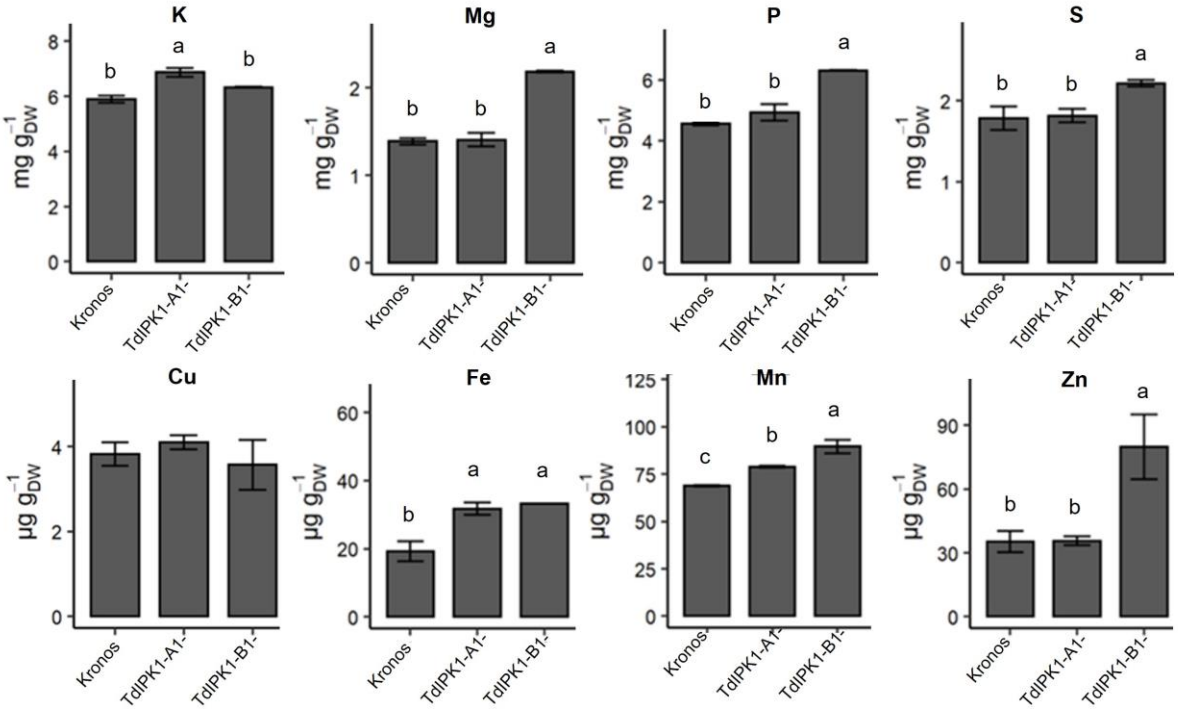

Figure 3.6 Concentration of macro-and micro-nutrients in *lpa* mutants and Kronos wild-type kernels. Mean values of three biological replicates ± Dev. St. One-way ANOVA, LSD post hoc test, $p < 0.05$.

3.3.5 Agronomic performance and roots morphological analyses

The agronomic performances of TdIPK1-B1$^-$ mutant were measured in field by evaluating a set of yield-related parameters compared to the control cv. Kronos. Significant differences were registered for Spike weight (-14%), Spike kernel weight (-17%) and Single kernel weight (-12%) which were lower in the TdIPK1-B1$^-$mutant genotype compared to the control. No difference was observed for Spike length, Spikelets number per spike and Kernels per spike (**Figure 3.7**).

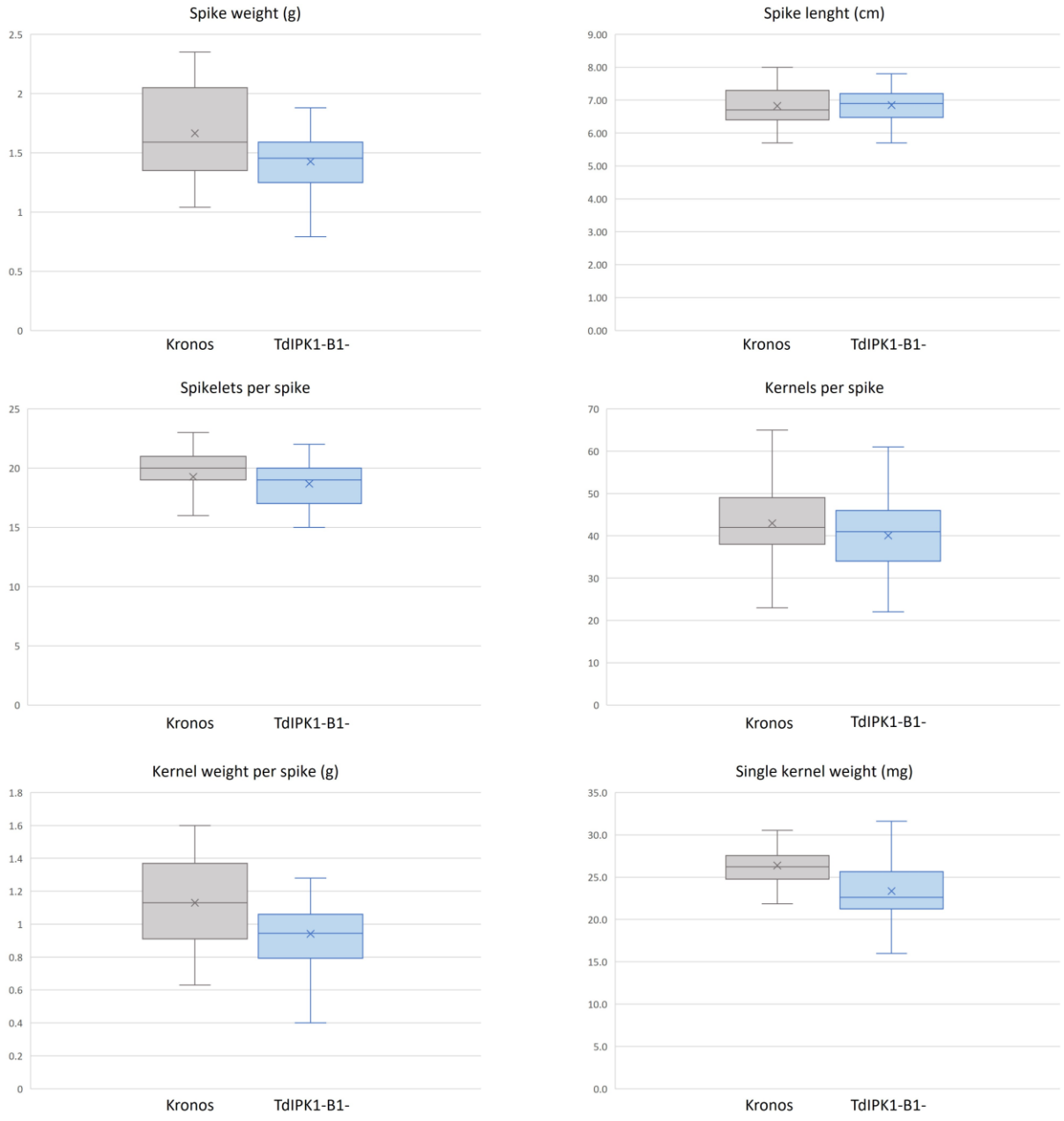

Figure 3.7 Analyses of agronomical yield-related traits of TdIPK1-B1^{-} mutants compared to the control Kronos wild-type.

In order to evaluate if the silencing of *IPK1* genes affected the root architecture, the root apparatus of the set of selected mutant lines was analysed by measuring root length, root surface area, volume, diameter and number of root tips (**Figure 3.8**). No differences were found for all

measured parameters comparing the single null mutants TdIPK1-A1^{-} and TdIPK1-B1^{-} to the control plants (Kronos wild-type) (**Figure 3.8**).

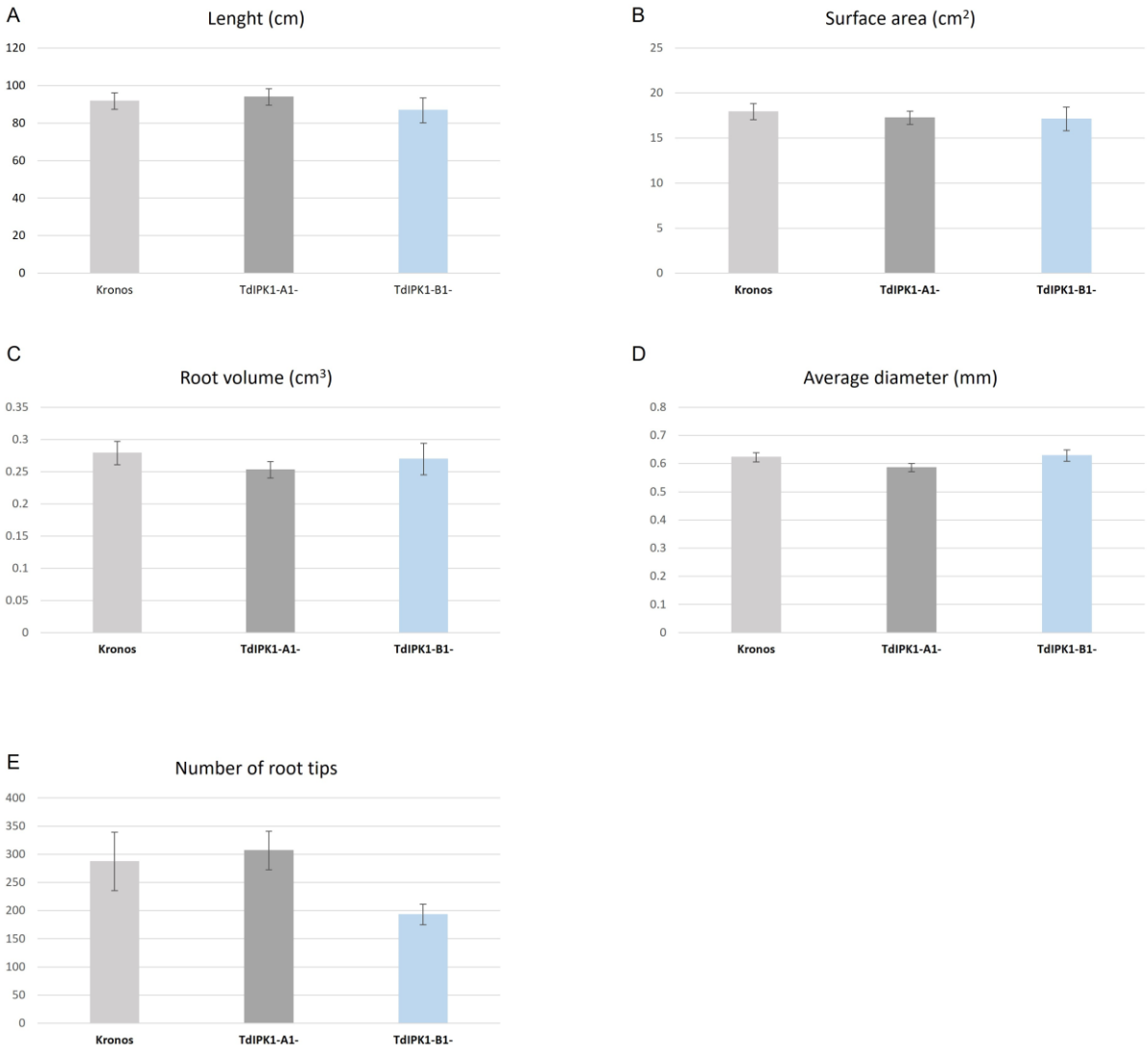

Figure 3.8 Root morphological traits: length (A), surface area (B), volume (C), diameter (D) and number of root tips (E) in *lpa* mutants and cv. Kronos. Mean values of three biological replicates ± St. Err. One-way ANOVA, LSD post hoc test, $p < 0.05$.

3.4 Discussion and conclusions

Micronutrient deficiencies affect 3 billion people, leading to serious health, economic and social consequences especially in low- and middle-income countries (**FAO et al., 2019**). Since it is unrealistic to fight malnutrition only through a balanced and varied diet for the entire world population, the biofortification of staple crops represents the most valid solution (**Sheoran et al., 2022**).

Although durum wheat kernels are rich in micronutrients, their bioavailability in semolina is limited due to the presence of anti-nutritional compounds (**Raboy, 2009**). Among them, PA [$InsP_6$] is one of the major anti-nutrients limiting the micronutrient bioavailability in durum wheat. In fact, PA is a strong chelator of cations important for nutrition such as Ca, Fe, Zn, and Mg, making them less available for the body absorption. Therefore, to address the issue of low nutrient bioavailability, the modulation of PA in seeds and the development of *lpa* mutants represent valid strategies that can lead to micronutrients biofortification. In the last decades, several *lpa* mutants have been developed in barley, maize, rice, and wheat with different strategies (**Sparvoli and Cominelli, 2015**; **Raboy, 2020**). In this paper, we focused on the silencing of *inositol 1,3,4,5,6-pentakisphosphate 2-kinase* (*IPK1*), a member of inositol phosphate kinase superfamily. In literature, it has been reported that the suppression of this gene is one of the most effective methods for developing *lpa* crops (**Ali et al., 2013**; **Aggarwal et al., 2018**; **Ibrahim et al., 2022**).

In detail, the research here presented focused on the development and characterization of durum wheat genotypes where *TdIPK1* genes were silenced through a TILLING approach.

In silico analysis of TdIPK1 proteins showed phylogenetic closeness among cultivated and wild wheat and the major crops in the following order: *T. durum*, *T. dicoccoides*, *T. aestivum*, *Ae. tauschii*, barley, *L. rigudum*, *B. distachyon*. More divergence was observed for *Zea mays*, *P. hallii*, *S. italica* and rice. The comparison of IPK1 amino acid sequences confirmed the high degree of conservation of proteins among plant species. The phylogenetic analysis regrouped in the same cluster wheat, barley, *L. rigidum* and *B. distachyon* confirming high relatedness among these species as previously reported (**Bhati et al.,2014**; **Sestili et al., 2019**; **Garcia Molina et al., 2021**). These results agree also with the study of **Wicker et al. (2009)**, which demonstrated that gene structure, order and content are highly conserved between barley and wheat providing evidence of a parallel evolution of their genome. The multiple sequence alignment performed using T-Coffee Expresso tool confirmed the conservation of typical motifs among wheat, rice and maize species as previously reported by **Ali et al. (2013)** and **Bhati et al. (2014)**.

The unexpected segregation, along with the difficulty of germination of the two complete null genotypes, suggests that *TdIPK1* genes have an essential role for pollen fertility, seed formation or plant development. Almost all *lpa* mutations, described during the last decades, were

associated with negative pleiotropic effects regarding germination frequency, seedling emergence, seed viability and plant development (**Meis et al., 2003**; **Guttieri et al., 2004**; **Pilu et al., 2005**; **Xu et al., 2009**; **Kuo et al., 2014)** confirming that PA plays regulatory roles in plants (**Shears, 2001**). In bread wheat the expression of *TaIPK1* homeoalleles was modulated either though transgenic approach or genome editing, but nobody described genotypes with a full suppression of this gene, demonstrating its crucial role in plant development and growth (**Ali et al., 2013**; **Aggarwal et al., 2018**; **Ibrahim et al., 2022)**. In this regard, **Ali et al. (2013)** reduced *IPK1* transcripts of 3.8-fold in T4 RNAi transgenic lines; **Aggarwal and colleagues (2018)** obtained similar results using the same technique.

As expected, the expression analyses performed on *TdIPK1-A1* and *TdIPK1-B1* genes revealed that there is a significant down-regulation of the target genes in TdIPK1-A1$^-$ and TdIPK1-B1$^-$ mutant lines, respectively, confirming that the presence of premature stop codons on the two *IPK1* homeoalleles affects their expression level. The degradation of non-functional transcripts is due to the activation of a mechanism of quality control preventing the accumulation of truncated proteins, which is known as nonsense-mediated decay (NMD) (**Frischmeyer and Dietz, 1998**). Similar results were already observed in durum wheat TILLING mutants (**Sestili et a., 2015**; **Garcia Molina et al., 2021**). The investigation of the main PA biosynthetic genes did not detect significant pleiotropic effects at the gene expression level in the immature grain of the two mutant lines, except for *IMP1* which was strongly up-regulated in the TdIPK1-B1$^-$ mutants. IMP1 plays important roles in many metabolic and signaling pathways in plants. Besides being essential for the de novo synthesis of myo-Inositol, and for recycling of Ins in Ins(1,4,5)P_3, it also is involved in ascorbic acid synthesis, indicating a bifunctionality that links these two branches of carbon metabolism (**Fu et al., 2008**).

In addition to its role as a reservoir for phosphate, $InsP_6$ has been associated with other functions in mammals, such as mRNA export, translational control, RNA editing and DNA repair (**Lee et al., 2015**). Similarly in plants, $InsP_6$ has been also associated with hormonal and signaling processes.

Lee et al. (2015) reported that Gle1 in conjunction with $InsP_6$ actives the ATPase/RNA helicase LOS4, which plays a role in the export of mRNA in *Arabidopsis*. $InsP_6$ acts as a cofactor linking and stabilizing the Gle1-LOS4 interaction by binding to a pocket at the interface between Gle1 and LOS4 (**Lee et al., 2015**). The same authors demonstrated that the expression of Gle1 variant with enhanced $InsP_6$ sensibility stimulated the expression of LOS4 rescuing the defects in mRNA export identified in IPK1 $InsP_6$ deficient mutants. Here, the expression analyses performed on *Gle1* and *LOS4* genes revealed an up-regulation of these genes in TdIPK1-B1$^-$ mutants. The drastic reduction of *TdIPK1-B1* transcript levels (-78% compared to the control) due to the silencing of *TdIPK1-B1* homeoallele seems to activate the expression of both genes (*Gle1* and *LOS4*). This alteration of the gene expression can in part explain the low number

(compared to expected) of homozygous mutant genotypes identified during the screening of F_2 and F_3 progenies.

The significant reduction of the PA content in the mature grain, was accompanied by an increase of Fe depositions in the scutellum and aleuronic layer in both single null homozygous mutants. This observation was confirmed by the increase of some macro and micronutrients in the TdIPK1 mutant kernels (overall in the single null TdIPK1-B1$^-$) compared to the controls. In detail, TdIPK1-B1$^-$ lines showed an increase in macronutrients, such as Mg (+60%), P (+40%) and S (+25%), and micronutrients as Fe (+72%), Mn (+30%) and Zn (+126%) contents. Previous studies performed on bread wheat revealed similar results. In detail, the silencing of *TaIPK1* genes through RNAi strategy led to an increase in Fe (1.2 to 1.7-fold), and Zn (1.3 to 2.2-fold) (**Aggarwal et al., 2018**). The increase in micronutrients content was accompanied by a drastic reduction of PA (-56% in RNAi mutant lines). Analysis of a set of TaIPK1-A1 genome-edited lines revealed a significant decrease in the PA (-72%) content accompanied by 1.5 to 2.1 fold increase in the Fe concentration and 1.6 to 1.9 fold rise in Zn (**Ibrahim et al., 2022**). A similar behaviour, but more modest, was observed in the single null TdIPK1 mutant lines.

The *lpa* mutants described in **Aggarwal et al. (2018)** and **Ibrahim et al. (2022)** showed less drastic pleiotropic effects in terms of germinability, and yield compared to other studies in which genes involved in the early stages of the PA biosynthetic pathway had been mutated in different crops (**Colombo et al., 2020; Raboy, 2020**), probably due to a partial silencing of the gene. The agronomical analyses performed on the TdIPK1-B1$^-$ genotypes revealed pleiotropic yield-related traits associated with the *TdIPK1* silencing in contrast to what was observed in rice and *Arabidopsis thaliana* where the IPK1 silencing did not affect the seed development (**Stevenson-Paulik et al., 2005**; **Ali et al., 2013**). According to **Aggarwal et al. (2018)**, the silencing of the *TdIPK1* homealleles determined a significant reduction in Spike weight, Kernel weight per spike and Single kernel weight. However, no alterations in spike architecture were observed as previously found in genome edited lines produced by **Ibrahim et al. (2022)**. Finally, both single null TdIPK1 mutant lines did not exhibit significant differences for all measured root characteristics compared to the wild-type, suggesting that the TdIPK1 silencing did not affect the exploitation potential of the root system.

Although the transgenic approach has been found to be a powerful tool for minerals biofortification (**Aggarwal et al., 2018**; **Ibrahim et al., 2022**), genetically modified organisms are still subjected to law restrictions which limit their cultivation, processing and marketing. In this work, the use of TILLING strategy allowed to develop non GMO durum wheat lines potentially useful in future biofortification breeding programs without legal restrictions. Our results demonstrated that *Td-IPK1-B1* has a main role compared to its homeoallele (*Td-IPK1-A1*), as only the suppression of the former has produced a genotype able to accumulate higher amounts of micronutrients in the grain. Our study suggests that the complete absence of both

homeoallele is lethal for the plant development. The introduction of Gle1 variants could be a successful strategy in future breeding program to mitigate the pleiotropic effects caused by the complete suppression of this gene.

Supplementary material

Supplementary Figure S1 Exon/intron structures of *TdIPK1* homeoalleles. Light blue rectangles represent exons, light blue lines introns, red boxes the premature stop codon mutation located in the two homeoalleles on exon II and exon IV, respectively.

```
MSAThe multiple sequence alignment result as produced by T-coffee.

T-COFFEE, Version_11.00 (Version_11.00)
Cedric Notredame
SCORE=97
*
 BAD AVG GOOD
*
AtIPK1          :  97
AetIPK1         :  97
TdicIPK1-A1     :  98
TdicIPK1-B1     :  97
TdIPK1-A1       :  97
TdIPK1-B1       :  97
TaIPK1-A1       :  98
TaIPK1-B1       :  96
TaIPK1-D1       :  97
OsIPK1          :  97
OgIPK1          :  96
ZmIPK1          :  96
HvIPK1          :  97
BdIPK1          :  97
LrIPK1          :  97
SiIPK1          :  97
PahIPK1         :  97
cons            :   9
```

```
AtIPK1          --MEMI------LE----------------------------------------------------EK
AetIPK1         --MEVA------LQ----------------------------------------------------AG
TdicIPK1-A1     --MEVV------LH----------------------------------------------------AG
TdicIPK1-B1     ---MEV-----ALQ----------------------------------------------------AC
TdIPK1-A1       --MEVV------LH----------------------------------------------------AG
TdIPK1-B1       ---MEV-----ALQ----------------------------------------------------AC
TaIPK1-A1       --MEVV------LH----------------------------------------------------AG
TaIPK1-B1       ---MSIGSLSVSLEPHASAPSAWRPLFLHVSASRESAAFLFLPPGPDSSNRATGAAAAAAASAARASER
TaIPK1-D1       --MEVA------LQ----------------------------------------------------AG
OsIPK1          M--EVV------LH----------------------------------------------------EG
OgIPK1          M--EVV------LH----------------------------------------------------EG
ZmIPK1          MEMDGV------LQ----------------------------------------------------AA
HvIPK1          --MEAV------LQ----------------------------------------------------AG
BdIPK1          --MEAV------LQ----------------------------------------------------AG
LrIPK1          --MDVV------LQ----------------------------------------------------AG
SiIPK1          MEMEGV------LQ----------------------------------------------------AG
PahIPK1         M--EGV------LQ----------------------------------------------------AG

cons                        *.                                                    

AtIPK1          ----------------------------------------------------------DASDWIYRGEGG
AetIPK1         ----------------------------------------------------------DAADWVYKGEGA
TdicIPK1-A1     ----------------------------------------------------------DAEDWVYKGEGA
TdicIPK1-B1     ----------------------------------------------------------DAADWVYKGEGA
TdIPK1-A1       ----------------------------------------------------------DAEDWVYKGEGA
TdIPK1-B1       ----------------------------------------------------------DAADWVYKGEGA
TaIPK1-A1       ----------------------------------------------------------DAEDWVYKGEGA
TaIPK1-B1       AAAAATRASAGPSPPRAAAARLSSGHRGSALRRQRPRSSAPRLRRFRAAMEVALQACDAADWVYKGEGA
TaIPK1-D1       ----------------------------------------------------------DAADWVYKGEGA
OsIPK1          ----------------------------------------------------------DAKDWVYKGEGA
OgIPK1          ----------------------------------------------------------DAKDWVYKGEGA
ZmIPK1          ----------------------------------------------------------DAKDWVYKGEGA
HvIPK1          ----------------------------------------------------------DAANWVYKGEGA
BdIPK1          ----------------------------------------------------------DAEDWVYKGEGA
LrIPK1          ----------------------------------------------------------DAGDWVYKGEGA
SiIPK1          ----------------------------------------------------------DAKDWVYKGEGA
PahIPK1         ----------------------------------------------------------DAKDWVYKGEGA

cons                                                                        ** :*:*:***.


AtIPK1          ANLVLAYAGSSP-LFVGKVIRIQKARRNDKA---IKNANGVVS--------VLTSDEQHLWRENNELIS
```

```
AetIPK1         ANLILSYTGNSPSMF-GKVLRAKKVLN-DKA-QPAPN---CVN---------FSSYEQLVWGDIPELIE
TdicIPK1-A1     ANLILSYTGSSP-SMLGKVLRAKKVLN-DKA-QPAPN---CVN---------FSSYEQLVWGDIPELIE
TdicIPK1-B1     ANLILSYTGSSP-SMLGKVLRAKKVLN-DKA-QPAPN---CVN---------FSSYEQLVWGDIPELIE
TdIPK1-A1       ANLILSYTGSSP-SMLGKVLRAKKVLN-DKA-QPAPN---CVN---------FSSYEQLVWGDIPELIE
TdIPK1-B1       ANLILSYTGSSP-SMLGKVLRAKKVLN-DKA-QPAPN---CVN---------FSSYEQLVWGDIPELIE
TaIPK1-A1       ANLILSYTGSSP-SMLGKVLRAKKVLN-DKA-QPAPN---CVN---------FSSYEQLVWGDIPELIE
TaIPK1-B1       ANLILSYTGSSP-SMLGKVLRAKKVLN-DKA-QPAPN---CVN---------FSSYEQLVWGDIPELIE
TaIPK1-D1       ANLILSYTGNSPSMF-GKVLRAKKVLN-DKA-QPAPN---CVN---------FSSYEQLVWGDIPELIE
OsIPK1          ANLILSYTGSSP-SMLGKVLRVKKILK-DKG-QPAPN---CI---------VFSSHEEHLWGKIPGLLE
OgIPK1          ANLILSYTGSSP-SMLGKVLRVKKILK-DKGQPAPNC---IV----------FSSHEEHLWGKIPGLLE
ZmIPK1          ANLILSYTGSSP-SMLGKVLRLKKILK-NKS-------------QRAPSCIVFSSHEQLLWGHIPELVE
HvIPK1          ANLILSYTGSSP-SMLGKVLRAKKVLN-DKA-QPAPN---CVN---------FSSYEQLVWGQIPELVE
BdIPK1          ANLILSYTGSSP-SMLGKVLRAKKILN-DKA-QPAPN---CVV---------FSSFEQLLWGEIPELVE
LrIPK1          ANLILSYTGSSP-SMLGKVLRAKKILN-DKA---QPS--PTCE--------VFSTSEQLVWGEIPGLVE
SiIPK1          ANLILSYTGTSP-AMLGKVLRVKKILK-DKSQ----P---APSCMV------FSSYEQLLWGHIPELVD
PahIPK1         ANLILSYTGSSP-SMHGKVLRIKKILK-DKSL----P---APSCMV------FSSYEQLLWGHIPELLD

cons            ***:*:*:*.**  : ***:* :*  . :*.                 ::: *: :* .   *:.


AtIPK1          SPNKEVLEQRYVKNVIIPLLGPKHVDAGVRVSVSKEFLECVDKKVTKQRPLWRVNAANVDTSHDSALIL
AetIPK1         SVKQGSVAQAYAVHVMSQHLGHDHVDGGVRVSVSKDFLEIVGKNVLSSRPAWRVNASAIDTNADSALLI
TdicIPK1-A1     SVKQGSVAQAYAVHVMSQHLGHDHVDGGVRVSVSKDFLEIVGKNVLSARPAWRVNASAIDTNADSALLI
TdicIPK1-B1     SVKQGSVAQAYAVHVMSQHLGHDHVDGGVRVSVSKDFLEIVGKNVLSARPAWRVNASAIDTKADSALLI
TdIPK1-A1       SVKQGSVAQAYAVHVMSQHLGHDHVDGGVRVSVSKDFLEIVGKNVLSARPAWRVNASAIDTNADSALLI
TdIPK1-B1       SVKQGSVAQAYAVHVMSQHLGHDHVDGGVRVSVSKDFLEIVGKNVLSARPAWRVNASAIDTKADSALLI
TaIPK1-A1       SVKQGSVAQAYAVHVMSQHLGHDHVDGGVRVSVSKDFLEIVGKNVLSARPAWRVNASAIDTNADSALLI
TaIPK1-B1       SVKQGSVAQAYAVHVMSQHLGHDHVDGGVRVSVSKDFLEIVGKNVLSARPAWRVNASAIDTKADSALLI
TaIPK1-D1       SVKQGSVAQAYAVHVMSQHLGHDHVDGGVRVSVSKDFLEIVGKNVLSARPAWRVNASAIDTNADSALLI
OsIPK1          SVKNDCLPQAYATIVMSQHLGANHVDGGVRVRVSKNFFELAGKNVLDNRPAWRVNASAIDAGADSALLI
OgIPK1          SVKNDCLPQAYATIVMSQHLGANHVDGGVRVRVSKNFFELAGKNVLDNRPAWRVNASAIDAGADSALLI
ZmIPK1          SVKQDCLAQAYAVHVMSQHLGANHVDGGVRVRVSRDFLELVEKNVLSSRPAGRVNASSIDNTADAALLI
HvIPK1          SVKQGSVAQAYAVHVMSPHLGHDHVDGGVRVPVSKDFLEIVGKNVLSARPSWRVNASAIDTSADSALLI
BdIPK1          SVKQDLLPQAYAVHVMSQHLGANHVDGGVRVRVSKDFLEIVGKNVLSARPTWRVNASAIDTSADSALLI
LrIPK1          SLKQDCLPQAYAQ-VMSQHLGANHVDGGVRARVSKEFLEIVGKNVLSSRPAWRVTASAIDTSADSALLI
SiIPK1          SVKQDSLAQAYVMHVMSKHLGANHVDGGVRVCVSRDFLELVEKNVLNSRPAWRVNASSIDNTADAALLI
PahIPK1         SVKQDCLAQAYAVHVMSKHLGANHVDGGVSVGVSRDFLELVEKNVLDSRPAWRVNASSIDNTADAALLI

cons            * ::  : * *.  *:   ** .***.** . **::*:* . *:* . **  **.*: :*   *:**::


AtIPK1          NDHSLFSQGISSGGD-CISVEIKPKCGFLPTSRFIGKENMLKTSVSRFKMHQLLKLEYN-EISEESEYD
AetIPK1         SDHSLFS-GKPRGSS-CIAVEIKAKCGFLPSSEYISKENAIKKQVTRYKMHQHLKFHQG-QISKTSEYD
TdicIPK1-A1     SDHSLFS-GKPRGSS-CIAVEIKAKCGFLPSSEYISKENAIKKQVTRYKMHQHLKFHQG-QISKTSEYD
```

```
TdicIPK1-B1   SDHSLFS-GKPRGSS-CIAVEIKAKCGFLPSSEYISKENVIKKQVTRYKMHQHLKFHQG-QISKTSEYD
TdIPK1-A1     SDHSLFS-GKPRGSS-CIAVEIKAKCGFLPSSEYISKENAIKKQVTRYKMHQHLKFHQG-QISKTSEYD
TdIPK1-B1     SDHSLFS-GKPRGSS-CIAVEIKAKCGFLPSSEYISKENVIKKQVTRYKMHQHLKFHQG-QISKTSEYD
TaIPK1-A1     SDHSLFS-GKPRGSS-CIAVEIKAKCGFLPSSEYISKENAIKKQVTRYKMHQHLKFHQG-QISKTSEYD
TaIPK1-B1     SDHSLFS-GKPRGSS-CIAVEIKAKCGFLPSSEYISKENVIKKQVTRYKMHQHLKFHQG-QISKTSEYD
TaIPK1-D1     SDHSLFS-GKPRGSS-CIAVEIKAKCGFLPSSEYISKENAIKKQVTRYKMHQHLKFHQG-QISKTSEYD
OsIPK1        SDHTLFS-GNPRGSS-CIAVEIKAKCGFLPSSEYISKENSIKKQVTRYKMHQHLKFHLG-EISKTSEYD
OgIPK1        SDHTLFS-G-NPRGSSCIAVEIKAKCGFLPSSEYISKENSIKKQVTRYKMHQHLKFHLG-EISKTSEYD
ZmIPK1        ADHSLFS-GNPKGSS-CIAVEIKAKCGFLPSSEYISEDNTIKKQVTRYKMHQHLKF-YQGEISKTSEYN
HvIPK1        SDHSLFS-GKPRGSS-CIAVEIKAKCGFLPSSEYISRENAIKKQVTRYKMHQHLKFHQG-QISKTSEYD
BdIPK1        SDHSLFS-GKSRGSS-CIAVEIKAKCGFLPSSEYISKENSIKKQVTRYKMHQHLKFHQG-EVSKTSEYD
LrIPK1        SDHSLFS-GKPRGSS-CIAVEIKAKCGFLPSSEYISQENSIKKQVTRYKMHQQLKFHQG-QISKISDYN
SiIPK1        PDHSLFS-GNPRGNS-CIAVEIKAKCGFLPSSEYISKENSIKKQVTRYKMHQHLKFHQG-EISTPSEYN
PahIPK1       ADHSLFS-GNPRGSS-CIAVEIKAKCGFLPSSEYISKENYIKKQVTRYKMHQHLKFHQG-QISRTSEYN

cons           **:*** *    .. **:****.******:*.:*..:* :*..*:*:**** **:    ::*  *:*:

AtIPK1        PLDLFSGSKESVLEAIKALYSTPQNNFRVFLNGSLILGGSGESTGRT-SP-EIGYAFEDA--LKG--FI
AetIPK1       PLDLFSGSKERIRTAIKSFFSTPQNNFRIFVNGSLGFGGMGGGADKILAN-ETEKCLEDL--RKVSGL-
TdicIPK1-A1   PLDLFSGSKERIRTAIKSFFSTPQNNFRIFVNGSLGFGGMGGGADKVLAN-ETEKCLEDL--RKVSGL-
TdicIPK1-B1   PLDLFSGSKERIRTAIKSFFSTPQNNFRIFVNGSLGFGGMGGGADKVLAN-ETEKCLEDL--RKVSGL-
TdIPK1-A1     PLDLFSGSKERIRTAIKSFFSTPQNNFRIFVNGSLGFGGMGGGADKVLAN-ETEKCLEDL--RKVSGL-
TdIPK1-B1     PLDLFSGSKERIRIAIKSFFSTPQNNFRIFVNGSLGFGGMGGGADKVLAN-ETEKCLEDL--RKVSGL-
TaIPK1-A1     PLDLFSGSKERIRTAIKSFFSTPQNNFRIFVNGSLGFGGMGGGADKVLAN-ETEKCLEDL--RKVSGL-
TaIPK1-B1     PLDLFSGSKERIRTAIKSFFSTPQNNFRIFVNGSLGFGGMGGGADKVLAN-ETEKCLEDL--RKVSGL-
TaIPK1-D1     PLDLFSGSKERICTAIKSFFSTPQNNFRIFVNGSLGFGGMGGGADKILAN-ETEKCLEDL--RKVSGL-
OsIPK1        PLDLFSGSKERIHMAIKSFFSTPQNNFRIFVDGSLVFGGMGGGADSV-HPNETEKCLEDL--SKVTGL-
OgIPK1        PLDLFSGSKERIHMAIKSFFSTPQNNFRIFVDGSLVFGGMGGGADSV-HPNETEKCLEDL--SKVTGL-
ZmIPK1        PLDLFSGSKERICMAIKSLFSTPQNNLRIFVNGSLAFGGMGGGADSV-HP-------ADT--LK-----
HvIPK1        PLDLFSGSKERIRTAIKSFFSTPQNNFRIFVNGSLGFGGMGGGADKVLAN-ETEKCLEDL--RKVSGL-
BdIPK1        PLDLFSGSKERIHTAIKSFFSTPQNNFRIFVNGSLVFGGMGGGADKV-HPNETEKCLEDL--SKVSGL-
LrIPK1        PLDLFSGSKERIRTAIKSFFSTPQNNFRIFVDGSLHFGGMGGGADTV-HPDETEKCLVDL--TKVSGL-
SiIPK1        PLDLFSGSKERICIAIKSFFSTPQNNFRVFVNGSLVFGGMGGGADNV-HPAETDKCLQDL--SKVSGL-
PahIPK1       PLDLFSGSKERICMAIKSFFSTPQNNFRIFVDGSLVFGGMGGGADNV-LPAEKDKCLEDLSKLS--GL-

cons          ********** :  ***:::******:*:*::*** :** * .:.    *   .

AtIPK1        QSED-----GHRTECFLQLVSDAVYGSGVLDRLLEIQKLDKLDIEGAIHSYYDLINQPCPICKEGKPLE
AetIPK1       QLSD-----------FIELLSEAISKSGALDKLLATQKLDDHDIEAAIHLYYNIISQPCLVCKNITD--
TdicIPK1-A1   QLSD-----------FIELLSEAISKSGVLDKLLATQKLDDHDIEGAIHLYYNIISQPCLVCKNITD--
TdicIPK1-B1   QLSD-----------FIELLSEAISKSGVLDKLLATQKLDDHDIEGAIHLYYDIISQPCLVCKNITD--
TdIPK1-A1     QLSD-----------FIELLSEAISKSGVLDKLLATQKLDDHDIEGAIHLYYNIISQPCLVCKNITD--
```

```
TdIPK1-B1     QLSD-----------FIELLSEAISKSGVLDKLLATQKLDDHDIEGAIHLYYNIISQPCLVCKNITD--
TaIPK1-A1     QLSD-----------FIELLSEAISKSGVLDKLLATQKLDDHDIEGAIHLYYNIISQPCLVCKNITD--
TaIPK1-B1     QLSD-----------FIELLSEAISKSGVLDKLLATQKLDDHDIEGAIHLYYDIISQPCLVCKNITD--
TaIPK1-D1     QLSD-----------FIELLSEAISKSGALDKLLATQKLDDHDIEAAIHLYYNIISQPCLVCKNITD--
OsIPK1        QLSD-----------FIELLSEAIFKSGVLGKLLATQKLDDHDIEGAIHLYYNIISQPCLVCKSITD--
OgIPK1        QLSD-----------FIELLSEAIFKSGVLGKLLATQKLDDHDIEGAIHLYYNIISQPCLVCKSITD--
ZmIPK1        CLEDLSKISGLKLPDFTELLSETIFRSEVLGNLLATQKLDDHDIEGVIHLYYNIISQPCLVCKNLTD--
HvIPK1        QLSD-----------FIELLSEAISKSGVLDKLLATQKLDDHDIEGAIHLYYNIISQPCVVCKNITD--
BdIPK1        QLSD-----------FIELLSEAIYKSGVLDKLLATQKLDDHDIEGAIHLYYNITSQPCLVCKNISD--
LrIPK1        QPSD-----------FIELLSEAIFKSGVLDKLLVTQKLDDHDIEGAIHLYYDIISQPCLVCKNITD--
SiIPK1        ELPD-----------FIELLSEAIFRSGVLGKLLITQKLDDHDIEGAIHLYYSIISQPCLVCKNVTD--
PahIPK1       ELPD-----------FIELLSEAIFKSGVLGKLLATQKLDDHDIEGAIHLYYNIISQPCLVCKNITD--

cons           *      * :*:*:::  * .*..**  ****. ***..** **.: .*** :**. .

AtIPK1        AELS-----LHALPLDESLKIVKEYLIAATAKDCSIMISFQ----SRNAWDSEPS----GD----Y--V
AetIPK1       AELLHKYSVLHSLPLDKSCKIVRDFLISATAKDCSLMMCFR----PRE---CERTD---SE----YDSV
TdicIPK1-A1   AELLHKYSVLHSLPLDKSCKIVRDFLISATAKDCSLMMCFR----PRE---CERTD---SE----YDSV
TdicIPK1-B1   AELLHKYSVLHSLPLDKSCKIVRDFLISATAKDCSLMMCFRPRECERT----DPE----YD----S--V
TdIPK1-A1     AELLHKYSVLHSLPLDKSCKIVRDFLISATAKDCSLMMCFR----PRE---CERTD---SE----YDSV
TdIPK1-B1     AELLHKYSVLHSLPLDKSCKIVRDFLISATAKDCSLMMCFRPRECERT----DPE----YD----S--V
TaIPK1-A1     AELLHKYSVLHSLPLDKSCKIVRDFLISATAKDCSLMMCFR----PRE---CERTD---SE----YDSV
TaIPK1-B1     AELLHKYSVLHSLPLDKSCKIVRDFLISATAKDCSLMMCFRPRECERT----------DPEYDS--V
TaIPK1-D1     AELLHKYSVLHSLPLDKSCKIVRDFLISATAKDCSLMMCFR----PRE---CERTD---SE----YDSV
OsIPK1        TELLRKYSTLHSLPLDKSEKIVRDFLISATAKDCSLMISFR----PRQ----S--GTTDSE--YDS--V
OgIPK1        TELLRKYSTLHSLPLDKSEKIVRDFLISATAKDCSLMISFR----PRQ----SGTT--DSE--YDS--V
ZmIPK1        VELLRKYTFLHSLPLDKSLKIVRDFLISATAKDCSLMISFR----PRE------NGSTDSE--YDS--V
HvIPK1        AELLHKYSVLHSLPLDKSCKIVRDFLISATAKDCSLMMCFR----PRE---CERAD---SE----YDSV
BdIPK1        AELLRKYAVLHSLSLDKSCKIIRDFLISATAKDCSLMMSFQ----PRE---CEKTD---SE----YDSV
LrIPK1        AKLLHKYSVLHSLSLDKSCKIVRDFLIAATAKDCSLMMCFR----PRE----SET----TD--SEYDSV
SiIPK1        AELLRKYTLLHSLPLDKSLKIVRDFLVSATAKDCSLMISFR----PRE------SGTADSE----YDSV
PahIPK1       VELLRKYTLLHSLSLDKSLKIVRDFLVSATSKDCSLMISFR----PRE------GG--TTD--SVYDSV

cons          .:*    **:*.**:* **::::*::**:****:*:.*:     *      :    *

AtIPK1        SLKPTNQTFDYKVHFIDLSLKPLKRMESYYKLDKKIISFYNRK----------------------QK--
AetIPK1       FLQSVNRAYDYKAYFVDLDVKPLDKMTHYFKLDQKIVNFYTKSGEVGRVPCD------------SQK--
TdicIPK1-A1   FLQSVNRAYDYKAYFVDLDVKPLDKMTHYFKLDQKIVNFYTKSGEIGRVPCD------------SQK--
TdicIPK1-B1   FLQSVNRTYDYKAYFVDLDVKPLDKMTHYFKLDQKIVNFYTKS-----GEVD------------SQK--
TdIPK1-A1     FLQSVNRAYDYK-----HTL--L-------------IWM-------------------------------
TdIPK1-B1     FLQSVNRTYDYK-----HTL--L-------------IWM-------------------------------
TaIPK1-A1     FLQSVNRAYDYKAYFVDLDVKPLDKMTHYFKLDQKIVNFYTKSGEIGRVPCD------------SQK--
```

```
TaIPK1-B1     FLQSVNRTYDYKAYFVDLDVKPLDKMTHYFKLDQKIVNFYTKS-----GEVD------------SQK--
TaIPK1-D1     FLQSVNRAYDYKAYFVDLDVKPLDKMTHYFKLDQKIVNFYTKS----------------------GELM
OsIPK1        FLDSVNQSYDYKAYFIDLDVKPLDKMVHYFKLDQKIVNFYTRN----------------------G---
OgIPK1        FLDSVNQSYDYKAYFIDLDVKPLDKMVHYFKLDQKIVNFYTRN----------------------G---
ZmIPK1        FLESVKRTYEYKAYFLDLDVKPLDKMEHYFKLDQRIVNFYTRN----------------------GGG-
HvIPK1        FLQSVNRAYDYKAYFVDLDVKPLDKMEHYFKLDQKIVNFYTKSGEVGRAPCD------------APK--
BdIPK1        FLESVNRIYDYKANFVDLDVKPLDKMVHYFKLDQKIVNFYTKHGEVGRIACDSSK-GGGSTDSTKVQ--
LrIPK1        FLESVNRTYDYKAYFVDLDVKPLDKMPHYFKLDQKIVNFYTKNGEVGRVPCDSSKGGSTSGDDSKVQ--
SiIPK1        FLDSVKQTYEYKANFIDLDVKPLDKMEHYFKLDQKIVNFYSRN----------------------EEL-
PahIPK1       FLESVKQTYEYKAYFVDLDVKPLDKMEHYFALDQKIVNFYTRN----------------------QEV-

cons           *...:: ::**       :  *              : :

AtIPK1        -------------AENTAEQIGNSKPSHS-----------------------------------------
AetIPK1       ---------GVGTSDD--------TTVQPQHRGAPST---------------------------------
TdicIPK1-A1   ---------GVGTSDD--------TAVQPQH-----------------------------------------
TdicIPK1-B1   ---------GVGTSDD--------TAVQPQH-----------------------------------------
TdIPK1-A1     -----------------------------------------------------------------------
TdIPK1-B1     -----------------------------------------------------------------------
TaIPK1-A1     ---------GVGTSDD--------TAVQPQH-----------------------------------------
TaIPK1-B1     ---------GVGTSDD--------TAVQPQH-----------------------------------------
TaIPK1-D1     SGTSCIPSGWLVAAEN--------TPGIRYTDTKMLEQTFLQWQPHVAVSAADMGAQVCLVGYGVAISP
OsIPK1        ------------EVGGDPRDPPKGCGPR-----------------------------------------
OgIPK1        ------------EVGGDPRDPPKGGGPR-----------------------------------------
ZmIPK1        --------LAISKGQ-------------------------------------------------------
HvIPK1        ---------GGGTSDD--------TKVVQQH-----------------------------------------
BdIPK1        -------------PQH------------------------------------------------------
LrIPK1        -------------LEH------------------------------------------------------
SiIPK1        --------VPSLKGSNTKDASQIQLQQ-------------------------------------------
PahIPK1       --------MPSPKVTNTKDAVGSRGGPNHPLEGPTF-----------------------------------

cons                   

AtIPK1        -----
AetIPK1       -----
TdicIPK1-A1   -----
TdicIPK1-B1   -----
TdIPK1-A1     -----
TdIPK1-B1     -----
TaIPK1-A1     -----
TaIPK1-B1     -----
TaIPK1-D1     VPSTC
```

```
OsIPK1          -----
OgIPK1          -----
ZmIPK1          -----
HvIPK1          -----
BdIPK1          -----
LrIPK1          -----
SiIPK1          -----
PahIPK1         -----

cons
```

Supplementary Figure S2 Multiple sequence alignment was performed using T-Coffee Expresso tool in different plant species. At: *Arabidopsis thaliana* IPK1 (NP_568613.1); Lr: *Lolium rigidum* IPK1 like (XP_047079711.1); Og: *Oryza glaberrima* IPK1 (XP_052152105.1); Os: *Oryza sativa Japonica Group* IPK1 (NP_001406839.1); Pah: *Panicum hallii* IPK1 (XP_025825917.1); Bd: *Brachypodium distachyon* IPK1 (XP_010240557.1); Hv: *Hordeum vulgare* IPK1 (KAE8793063.1); Aet: *Aegilops tauschii* subsp. *strangulata* IPK1 (XP_020166707.1); Tdic: *Triticum dicoccoides* IPK1-A1 like (XP_037479606.1), IPK1-B1 like (XP_037487511.1); Ta: *Triticum aestivum* IPK1-A1 (XP_044459293.1), IPK1-B1 (XP_044326398.1), IPK1-D1 (XP_044334614.1); Td: *Triticum durum* ssp. *durum* IPK1-A1 (VAH37460.1); IPK1-B1 (VAH52741.1); Zm: *Zea mays* IPK1 (NP_001106053.2); Si: *Setaria italica* IPK1 (XP_004960165.1). The alignment is coloured according to the T-Coffee analysis, letter in bold represent typical conserved motifs among the different species analysed.

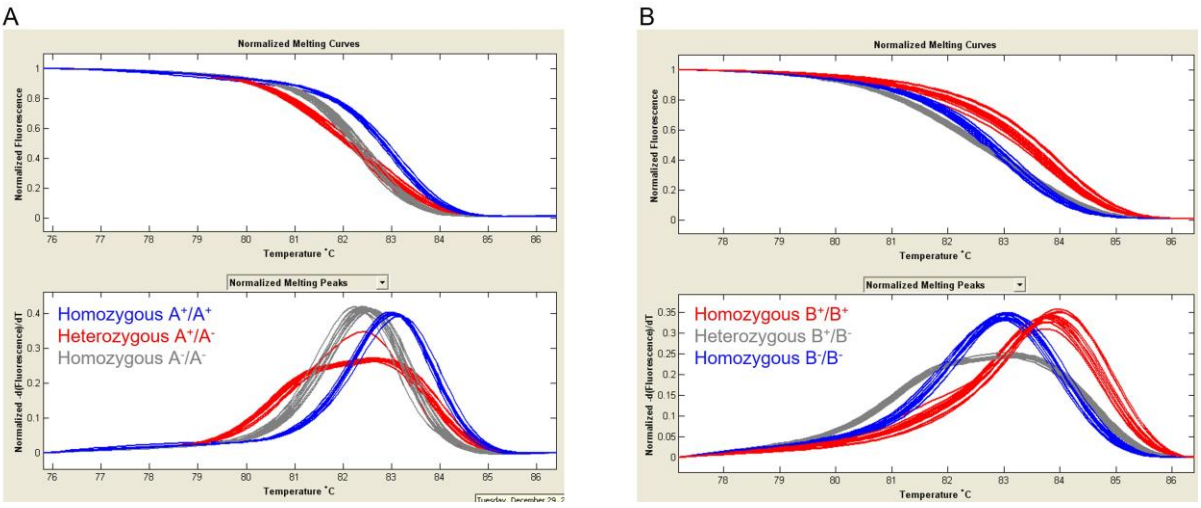

Supplementary Figure S3 Selection of the mutant genotypes through HRM-genotyping of F_2 and F_3 progenies from the cross TdIPK1-A1$^-$ x TdIPK1-B1$^-$. A) HRM analysis of *TdIPK1-A1* homeoallele; B) HRM analysis of *TdIPK1-B1* homeoallele.

Supplementary Table S1 List of primers used for HRM genotyping.

Id primer	Sequence	T Annealing	Amplicon Size	Use	Genome
IPK1A_F	GGTCAGGTGTAGCTCTTTG	56°C	511 bp	1st round PCR	A
IPK1A_R	GTGATGTTAACATTAGGAG				
IPK1Aex2F	CTGTCAAGCAAGGTTCTGTG	60°C	80 bp	2nd round PCR	
IPK1Aex2R	GCCATCAACATGATCGTG				
IPK1B_F	CCTAACGTTAGCATCACTTTG	56°C	409 bp	1st round PCR	B
IPK1B_R	CTTAAGCTAGGAAAGCTTTG				
IPK1Bex4F	GGAAAGAATGTGCTCAGT	60°C	72 bp	2nd round PCR	
IPK1Bex4R	AGAATCAGCTTTGGTATC				

Supplementary Table S2 List of genes and primers used for qRT-PCR.

ID primer	Sequence	T Annealing	Amplicon Size	Gene
IPK1_rtF	TGGATAAACTTTTGGCCACTCA	60°C	154 bp	
IPK1_rtR	GGAAGAGAATGCAACACAGAGT			
IPK1A_rtF1	TCCGGCCAAGAGAGTGTGAA	60°C	200 bp	*TdIPK1*
IPK1A_rtR1	ACAAGGAACTCGCCCGATTT			
IPK1B_rtF1	GAGAGTGTGAGAGAACAGATCCT	60°C	164 bp	
IPK1B_rtR1	AACCCCCTTCTGAGAATCGAC			
IMP1_rtF	CTGTTCGTGGAAAAGGTGCT	60°C	194 bp	
IMP1_rtR	TAGAGCCAAAGAGCCACACA			*TdIMP*
IMP2_rtF	CCCAGCAAGTACCCGAAGAT	60°C	160 bp	
IMP2_rtR	CTGTCACCAAGTCTGCAACC			
MIK_rtF	GTCGTGTCCAAGGTCGGG	60°C	185 bp	*TdMIK*
MIK_rtR	GGGTAGATCGGATCGCAGG			
ITPK3_rtF	TGACTGGAAAGGAGTGGCAA	60°C	161 bp	*TdITPK*
ITPK3_rtR	CGATAGCCCAGCCCTCATAA			
MRP3_rtF	CCAAGTTCTGCTACAAGGCC	60°C	162 bp	*TdMRP3*
MRP3_rtR	CGACATAGGACACGACGGT			
GLE1_rtF	CGTCAAACTCTATGCTGCCA	60°C	80 bp	*TdGLE1*
GLE1_rtR	ATTTCCATCCCTCGGCTAAG			
LOS4_rtF	ATCACGCTCCCCATGATCC	60°C	179 bp	*TdLOS4*
LOS4_rtR	GATTTATTCTGCTGCGCGAG			
cACT_F	GGAATGGTCAAGGCTGGTT	60°C	200 bp	*TdActin*
cACT_R	CTCCATGTCATCCCAGTTGC			

Supplementary Table S3 Segregation pattern of selected genotype from TdIPK1-A1^{-} X TdIPK1-B1^{-} crosses. The different genotypes are indicated as reported: e= heterozygous, +=wild-type, -=homozygous mutants.

	TdIPK1 A1^{e}B1^{-}	**TdIPK1 A1^{-}B1^{-}**	**TdIPK1 A1^{+}B1^{-}**	**TdIPK1 A1^{e}B1^{+}**	**TdIPK1 A1^{+}B1^{e}**	**TdIPK1 A1^{-}B1^{e}**	**TdIPK1 A1^{-}B1^{+}**	**TdIPK1 A1^{+}B1^{+}**	**TdIPK1 A1^{e}B1^{e}**	**Progeny**	**N° of seeds analysed**
TdIPK1A1^{-} X TdIPK1B1^{-}	5			2	4	5	4	3	6	F_2	29
TdIPK1 A1^{e}B1^{-}	91	1	68							F_3	160
TdIPK1 A1^{-}B1^{e}		1				17	42			F_3	60

CHAPTER 4

Modulation of kernel hardness in durum wheat genotypes with different starch compositions

Abstract

Cereals, staple crops in human nutrition, are called to face manifold challenges to encounter the urgent demand of food along with a higher nutritional value ensuring the sustainability of the supply chain. In this view, the research focused on two main topics; firstly, the rise in productivity, balancing the growing demand of food, consistent with the availability of environmental resources. The second issue regards the urgency to properly cover the nutritional needs of the population which has become more sensitive to pathologies related to high-caloric eating habits and poor in valuable nutritional compounds. Faced with such important issues, it is desirable to adopt a full approach, based on projects aimed at satisfying multiple requests at once.

The research here discussed concerns the development of three durum wheat genotypes in which novel properties have been combined both in the health-functional profile of the derived foods and in the milling characteristics of the grain. The project involves a set of durum wheat genotypes, in which the starch component has been modified in the amount of amylose, a polysaccharide that, together with amylopectin, constitutes the reserve starch. The high amylose genotypes are of interest due to the low glycaemic profile and the prebiotic functionality of the derived foods depending on the increase in “resistant starch"; the amylose-free genotype is suitable for the design of highly digestible foods ideal for specific uses, such as nutrition for infants. These genotypes were, therefore, the subject of a further improvement breeding program focused on modifying the seed hardness associated with the efficiency and sustainability of grinding and the quality of the final products.

In detail, three different genotypes of durum wheat have been selected: Soft Sv/ Sv SSIIa and Soft Sv/ Sv SBEIIa combine a high amylose content with a softer kernel that results in increased resistant starch content and energy saving during the milling process. The third genotype, Soft Sv/ Sv GBSSI, combines a softer kernel with free amylose starch following a novel starch digestibility profile suited for specific food categories.

A marker-assisted selection based on PCR and HRM-genotyping has been performed to identify the homozygous mutants in the progenies of the three different crosses.

Biochemical analyses such as the determination of amylose content, total starch, resistant starch, β-glucans and arabinoxylans were carried out to characterize the selected genotypes compared to the controls. Future analyses will be necessary to determine the technological characteristics of the developed genotypes. The set of materials here produced will be precious

to investigate the relationship between starch composition and seed texture, two important quality traits, in durum wheat.

KEYWORDS

Durum Wheat, Starch Mutants, Kernel Texture, Sustainability

4.1 Introduction

Cereals, which are staple crops in human nutrition, are facing numerous challenges in meeting the urgent demand for food while also ensuring higher nutritional value and the sustainability of the supply chain. In light of these challenges, research is focusing on two main areas. Firstly, increasing productivity to meet the growing demand for food while effectively managing environmental resources. Secondly, addressing the nutritional needs of the population, which is increasingly susceptible to health issues caused by high-calorie diets lacking valuable nutrients. Given the significance of these issues, it is desirable to adopt a comprehensive approach that addresses multiple requirements simultaneously. In this context, genetic crop improvement is expected to deliver ideotypes that meet multiple requirement in term of yield, sustainability and nutrition.

The prevalence of Non-Communicable Diseases (NCDs), which are strongly associated with unhealthy high-calorie diets, has become a major cause of mortality worldwide, as highlighted by the World Health Organization (**WHO 2022**, https://www.who.int/news-room/fact-sheets/detail/noncommunicable-diseases). This emphasizes the urgent need to develop new crops with superior nutritional value. Among cereals, durum wheat is one of the most important species grown in the Mediterranean basin and is used to produce a wide variety of foods. Therefore, improving the nutritional value of durum wheat would provide significant benefits to the human population.

Starch, the predominant component in cereal endosperm, serves as the main source of dietary carbohydrates and plays a crucial role in maintaining human health. In recent decades, there has been a growing awareness of the potential impact of "starch variability" on the quality and nutritional value of food products.

Briefly, starch consists of two glucan polymers: amylose and amylopectin. The chemical nature and quantitative ratio of these two glucans determine the final properties of starch. Amylose has a linear structure with glucose monomers linked by α(1→4) bonds. Amylose chains interact with each other through hydrogen bonds, creating a structure resistant to digestion, known as “resistant starch”. On the other hand, amylopectin has a highly branched structure due to dense patterns of α(1→6) linked glucan chains attached to the α(1→4) linear main chain. The branched nature of amylopectin makes it highly accessible to solvents and susceptible to amylolytic enzymes, resulting in highly digestible starch (**Shevkani et al., 2017**).

Given the importance of starch in the diet, there was a great interest in modulating the amylose/amylopectin ratio to enhance the nutritional value of food products and improve human metabolism. In wheat, a number of genotypes with varying amylose percentages, ranging from 0% to 70% of total starch, have been developed by targeting key enzymes involved in starch biosynthesis using natural allelic variants, mutagenesis, or transgenesis.

The synthesis of these two glucan chains shares a common substrate, ADP-glucose, but follows distinct pathways. Granule-bound starch synthase (GBSS) is solely responsible for amylose synthesis, while amylopectin is synthesized through the coordinated activities of AGPase, soluble starch synthase (SS), starch branching (BE), and starch debranching enzymes (DBE) (**Rahman et al., 2000**; **Rahman et al., 2007**; **Jeon et al., 2010**) (**Figure 4.1**).

Genotypes with low amylose content, also known as waxy genotypes, result from mutations in the granule-bound starch synthase I (*GBSSI*) genes. These waxy grains find application in feed formulation, biofuel production, and enhancing the quality of chilled and frozen food products (**Graybosch, 1998**; **Jongsutjarittam and Charoenrein, 2014**; **Morita et al., 2002**).

Conversely, high amylose genotypes have been achieved by manipulating enzymes such as SSIIa and SBEIIa involved in amylopectin synthesis. The abolishment of these enzymes leads to increased amylose content. High amylose genotypes are of interest due to their reduced digestibility, low glycaemic profile, and prebiotic functionality resulting from increased resistant starch (**Lockyer and Nugent, 2017**; **Botticella et al., 2018**).

While starch mutants offer novel nutritional profiles and improved qualities, their technological profiles are still poorly known. In this context, it has been reported that starch mutants have an impact on seed hardness in barley and bread wheat (**Clarke et al., 2008**; **Hogg et al., 2017**; **Schönhofen et al., 2017**; **Botticella et al., 2018**; **Hogg and Giroux, 2019**). However few studies have focused on the investigation of the relationship between starch properties and hardness in wheat.

Seed hardness, which measures a seed susceptibility to fracturing, has a profound impact on the milling process of wheat, affecting energy requirements and the quality of the resulting flour, including particle size and starch damage. In bread wheat, seed hardness is associated with the *Hardness* (*Ha*) locus located on chromosome 5D. Soft wheat kernels are more prone to fracturing, whereas hard types are more resistant and require more power during milling, leading to coarser and damaged starch granules. This study aims to modulate the hardness by crossing a soft durum wheat genotype from a previous breeding program with various durum starch mutants having different amylose content, establishing valuable materials for investigating the mechanisms underlying the relationship between starch composition and seed texture.

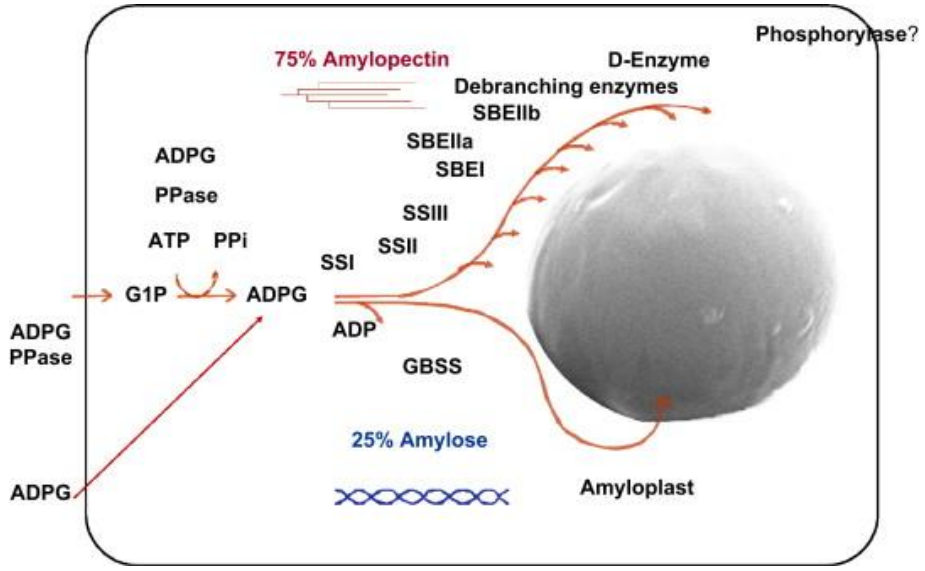

Figure 4.1 Scheme of starch synthesis in the endosperm (Rahman et al., 2007).

4.1.1 Low amylose genotypes

Low amylose genotypes, also referred as *waxy*, present mutations on the granule-bound starch synthase I (*GBSSI*) genes. In hexaploid wheat there are three GBSSI isoenzymes encoded by the *Wx-A1* gene, mapped on the short arm of chromosome 7A; *Wx-B1* gene, mapped on the arm long of chromosome 4A following a translocation from the short arm of chromosome 7B, and *Wx-D1* gene, mapped on the short arm of chromosome 7D. In durum wheat only Wx-A1 and Wx-B1 proteins are present (**Yamamori et al.,1994**). **Nakamura et al. (1995)** developed the first waxy bread wheat by crossing the natural Wx-D1 null mutant Bai-Huo and the Wx-A1/ Wx-B1 double null mutant Kanto 107. The lacking of the three isoenzymes waxy is characterized by the complete absence of amylose.
Lafiandra et al. (2010) produced the waxy genotype of the durum wheat cultivar Svevo, used in this study.
Waxy grains can be used for feed formulation and biofuel production. Furthermore, the inclusion of waxy wheat flour compensates for some of the decline in quality experienced during storage of chilled and frozen pasta-based food products (**Graybosch, 1998**), and the positive effect on water holding capacity has been promoted as a means to slow down staling of bread (**Jongsutjarittam and Charoenrein, 2014**; **Morita et al., 2002**).

4.1.2 High amylose genotypes

The biosynthesis of amylopectin is more complex and involves numerous enzymes including class I, II, and III starch synthases (SSI; SSII; SSIII), two classes of branching (BEI; BEII) and debranching enzymes (DBE).

High amylose genotypes have been produced by intervening on two classes of enzymes involved in the synthesis of amylopectin: the SSIIa and the SBEIIa. The SSIIa are mapped on the short arms of the homeologous chromosomes of group 7 (**Li et al., 1999**); the SBEII enzymes are present in two isoforms SBEIIa and SBEIIb and mapped on the long arms of the homeologous chromosomes of group 2 (**Boyer and Preiss, 1978**; **Rahman et al., 2001**; **Regina et al., 2005**).

The first high amylose genotype developed by **Yamamori et al. (2000)** through the elimination of the three isoforms of SSIIa enzymes in bread wheat presents an amylose content of about 35% against the 25% present in wild-type genotype. Subsequently, nearly isogenic lines characterized by the absence of the two isoforms SSIIa-A1 and SSIIa-B1 were developed in durum wheat cultivar Svevo, resulting in a double null genotype in which the amylose content is 43% of the total starch (**Lafiandra et al., 2010**). The investigation of the effect of the silencing of *SSIIa* genes in different lines of cultivar Svevo, allowed to identify two double null mutant lines (H795 e H806) in which semolina presents a significant increase in arabinoxylans and β-glucans, as well as resistant starch (**Botticella et al., 2016**).

As regard the silencing of SBEIIa enzymes, different strategies were used. **Regina et al. (2006)** and **Sestili et al. (2010)** used an RNAi approach to silencing the *SBEIIa* genes in bread and durum wheat, respectively, obtaining in both cases a significant increase in the percentage of amylose, with values up to 70% of the total starch. Also, the use of a TILLING approach confirmed a significant increase in amylose content in SBEIIa mutants in both bread and durum wheat (**Slade et al., 2012**; **Sestili et al., 2015**).

Starch represents the predominant source of carbohydrates dietary, but an excessive intake of calories has a negative impact on health. Thus, in food products, a high content of amylose is considered to be desirable, given that it makes the product less easily digestible. The structure of amylose is more resistant than amylopectin to the action of pancreatic enzymes, leaving it intact as a substrate for the gut microflora in the large intestine, which in turn boosts the production of short-chain fatty acids. The high amylose genotypes are of interest due to the low glycaemic profile and the prebiotic functionality of the derived foods depending on the increase in resistant starch (**Lockyer and Nugent, 2017**; **Botticella et al.,2018**).

Despite the improved nutritional qualities, information on the technological properties of high amylose wheat is still limited. In a recent work, the study of milling and bread-making quality of bread null SSIIa mutants showed a significant reduction in flour yield. Furthermore, bread made with the flour of this SSIIa mutants shows a significantly smaller volume than bread

produced with flour of the control wild-type (**Hogg and Giroux, 2019**). This negative effect on semolina yield is probably due to a harder kernel of high amylose genotypes compared to the control.

4.1.3 Seed hardness

Grain hardness represents a physical quality trait that determines the final uses and the technological properties of the flour. Based on the endosperm texture, wheat is generally classified into soft, medium-soft, medium-hard, hard, and extra-hard types (**Kent, 1994**). Soft wheat kernels are easily fractured and result in a large number of intact starch granules, whereas, hard types need relatively more power-consumption to mill and produce coarser and damaged starch granules.

Seed hardness is controlled by the expression of *Ha* locus mapped on the short arm of chromosome 5D of bread wheat. The *Ha* locus harbors the genes that encode 15-kD marker protein called friabilins that determine wheat softness. The friabilins are composed of a mixture of two lipid-binding puroindoline (PinA and PinB) polypeptides (**Sourdille et al., 1996**; **Giroux and Morris, 1997**).

The absence of the D genome in durum wheat determines the lack of these genes and consequently a very hard kernel (**Morris, 2002**). In particular, the genes responsible for this character were lost in the allotetraploidization process that led to the formation of *T. turgidum* ssp. *dicoccoides*, precursor of durum wheat (**Chantret et al., 2005**; **Li et al., 2008**).

It was demonstrated that mutations in *Pin* genes control the hardness or softness of wheat grains. Several studies were carried out on durum wheat. The hard kernel of durum wheat requires a specialized milling process requiring more energy and water use due to the increase of starch damage. The control of recombination among homeologous chromosomes, mediated by the *Ph1* (*Pairing homeologous*) gene, and the ability to tolerate homeologous substitutions represented the reasons for the development of soft durum wheat in Langdon cultivar (**Morris et al., 2011**). The soft character was then transferred to other wheat cultivars, including Svevo. Subsequent analysis of milling and technological quality allowed to demonstrate that soft durum wheat presents endosperm texture and milling properties almost identical to those of bread wheat, with reduced water absorption and unchanged quality and strength of the dough (**Morris, 2019**).

4.2 Materials and methods

4.2.1 Plant materials

Homozygous double null mutants harboring mutations on three starch biosynthetic genes (*GBSSI*, *SSIIa* and *SBEIIa*) were previously isolated in cv. Svevo (**Lafiandra et al., 2010**;

Sestili et al., 2015; **Botticella et al., 2016**). These mutants were crossed with Soft Svevo (Soft Sv) (**Morris et al., 2011**) as reported in **Figure 4.2**. The F_1 generation was self-pollinated and the selection of the different genotypes carrying the character of interest was performed on the F_2 and F_3 progenies of the three crosses. Total and partial mutants along with control plants (wild-type null segregant genotypes) were vernalized at 4°C for 15 days. The growing conditions were 20/24°C with a 16 h light period.

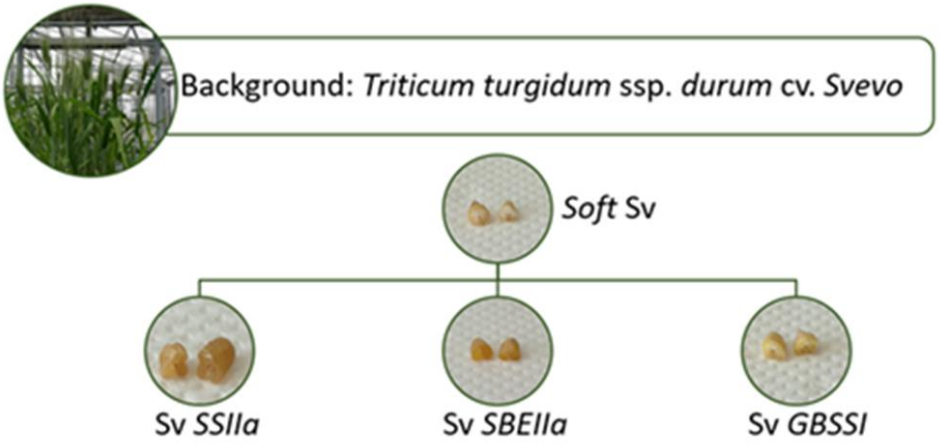

Figure 4.2 Scheme of the three crosses performed with Svevo starch mutants (Svevo SSIIa= Sv SSIIa; Svevo SBEIIa= Sv SBEIIa, Svevo GBSSI= Sv GBSSI) and Soft Svevo (Soft Sv).

4.2.2 DNA extraction

Genomic DNA was extracted from leaves of F_2 and F_3 progenies of total and partial mutants described in "Plant materials" according to **De Kochko and Hamon (1990)**, with some modifications. The samples were ground and well-homogenized in presence of liquid nitrogen to obtain a fine powder. Then, 500 µl of extraction buffer (EB) (100 mM Tris, 50 mM EDTA and 500 mM NaCl) were added to the samples along with 2% SDS. After mixed thoroughly, the samples were incubated at 65°C for 10 min enabling cellular lysis and 150 µl of 5M Potassium Acetate were added to precipitate cellular debris and SDS-protein complex. After centrifugation at 13,500 RPM for 15 min in a refrigerated centrifuge at 4°C, the supernatant was transferred to a new tube for DNA precipitation in 2-Propanol and put in the fridge for 15 min. The pellet obtained through centrifugation at 13,500 RPM for 10 min was washed twice with 70% ethanol. The dried pellet was re–suspended in 50 µl of 10 mM Tris, 1 mM EDTA, pH 8 solution and used for Polymerase Chain Reaction (PCR).

4.2.3 PCR to amplify *SSIIa*, and puroindoline genes

In order to identify the homozygous mutants from the three crosses, a Marker Assisted Selection (MAS) system based on PCR was developed. PCR were performed with different primer pairs reported in **Table 4.1**. The reactions were conducted in a final volume of 10 µl containing 5 µl 2X GoTaq® G2 Hot Start Colorless Master Mix (Promega, Madison, USA), 0.5 µM of each primer, 20 ng of template DNA and nuclease-free water up to 10 µl volume. The PCR conditions were: an initial denaturation at 95°C for 2 min, followed by 38 cycles at 95°C for 30 sec, 61°C for 30 sec, 72°C for 1 min and a final extension at 72°C for 5 min.
Touch-down PCR method was used to amplify *SSIIa-A1* homeoallele, on the following conditions: 95°C for 5 min, followed by 9 cycles at 95°C for 30 sec, 72°C for 30 sec with an increment decreasing of 1°C per cycle, 72°C for 1 min. After these steps 29 cycles at 95°C for 30 sec, 63°C for 30 sec, 72°C for 1 min and a final extension at 72°C for 5 min were performed.

Table 4.1 List of genes and primers used for PCR.

ID primer	Sequence	Gene	Reference
SSIIAF1	TGCGTTTACCCCACAGAGCAC	SSIIa-A1	Shimbata et al.,2005
SSIIAR1	ACGCGCCATACAGCAAGTCATAA		
SSIIBF1	ATTTCTTCGGTACACCATTGGCTA	SSIIa-B1	
SSIIBR1	TGCCGCAGCAGCATGCC		
PA5	GCTACATCACTAGTAATAGCCA	Pin A	This work
PA3	ATGAAGGCCCTCTTCCTCA		
PB5	ATATCATCACCAGTAATAGCC	Pin B	This work
PB3	ATGAAGACCTTATTCCTCCTA		

4.2.4 HRM-genotyping of SBEIIa mutants

Amplicons suitable for HRM analysis were produced by a nested PCR strategy using primer pairs in **Table 4.2**. Touch-down PCR method was used to amplify *SBEIIa-A1* and *SBEIIa-B1* homeoalleles, on the following conditions: 95°C for 5 min, followed by 5 cycles at 95°C for 30 sec, 65°C for 30 sec with an increment decreasing of 1°C per cycle, 72°C for 30 sec. After these steps 33 cycles at 95°C for 30 sec, 60°C for 30 sec, 72°C for 30 sec and a final extension at 72°C for 5 min were performed. The first PCR reaction was diluted 60-fold and 2 µl were used as a template for the second PCR reaction for HRM analysis. The second reaction was carried out according to **Sestili et al. (2015)**. The PCR reaction was carried out in 96-well Frame-Star plates (4titude Ltd., Surrey, UK) overlaid with 10 µl of mineral oil (Sigma-Aldrich, St. Louis,

MO, USA). The Light Scanner instrument (Idaho Technology, Inc.) was used to analyse the melting curves.

Table 4.2 List of primers used for HRM genotyping.

Id primer	Sequence	T annealing	Amplicon size	Use	Genome
A9F	AGAGGGGATAGTCCATACTGGTTG	60°C	401 bp	1st round PCR	A
A12R	CAAATATGGTGACAGAAGTCAGAG				
A66F	TGGCACTGATACACATTACTTCCAC	60°C	92 bp	2nd round PCR	
A66R	ACATACTTCCCAACTCCCATAGTT				
B15-P out F	GATTGAAAATGAGTATATTAAGGAT	60°C	552 bp	1st round PCR	B
B15-P3out R	TCGAAAGTATTGTCTTGACTCACA				
B15F	CTGTCAAGCAAGGTTCTGTG	60°C	61 bp	2nd round PCR	
B15R	GCCATCAACATGATCGTG				

4.2.5 Colorimetric assay of Waxy genotypes

The qualitative determination of the amylose content in the Waxy genotypes was determined using a rapid colorimetric assay. 300 µl of Lugol's 0.005 M were added to half seeds of Soft Sv X Sv GBSSI genotypes using Svevo wild-type and Sv GBSSI as controls. After 5 minutes, half seeds were dried and evaluated on the basis of the colour assumed. Lugol (KI/I_2) is a light brown, colorless and odorless solution in which potassium iodide dissociates according to the reaction: $I_2 + KI \rightarrow I_3^- + K^+$. The I_3^- ion binds amylose leading to the formation of a complex able to absorb light and produce a dark blue colour.

4.2.6 Isolation of starch granules and determination of amylose content

Starch granules were isolated from half seeds as described by **Zhao and Sharp (1996)** with some modifications. The half kernels without embryos were grinded and well-homogenized. The flour placed in tubes containing 1 ml of dH_2O was left at 4°C overnight. The following day the samples were vortexed and centrifuged for 5 minutes at 13,000 RPM. After the centrifugation the supernatant was removed and 300 µl of dH_2O were added to the pellet subsequently mixed with a pestle in order to form the gluten. The starch granules in suspension were transferred in a new tube containing 1 ml of 5 M NaCl and centrifuged for 5 minutes at 13,000 RPM. The supernatant was discarded and the steps repeated twice. Each sample was washed three times with 1 ml of dH_2O. After each wash the samples were vortexed, centrifuged for 5 minutes at 13,000 RPM and the supernatant removed. Finally, the pellet was washed with

1 ml of acetone and the samples centrifuged at 13,000 RPM for 3 minutes. The starch granules isolated were left to dry for about an hour in the air and stored at 4°C.
The amylose content was determined from a 15 mg of purified starch using a colorimetric assay based on the iodine–amylose reaction (**Chrastil, 1987**). Briefly 2 ml of 1M NaOH and 4 ml dH_2O were added to starch samples then placed in a boiling water bath for 30 minutes. During incubation, samples were vortexed at least three times in order to avoid gel lumps. After cooling, two tubes were prepared for each sample with 5 ml of TCA 0,5%, 100 µl of the starch solution and 50 µl of 0.01 N KI/I_2 mixture. After 20 min of incubation the absorbance of the samples was read at 610 nm. A standard curve was generated from a mixture of potato amylose (Fluka, Neu-Ulm, Germany) and amylopectin from maize (Sigma Aldrich, St. Louis, MO). Each value represents the mean of three biological replicates ± standard error. Three technical replicates were carried out for each biological replicate.

4.2.7 Analysis of total starch, resistant starch, β-glucan and arabinoxylan

The contents of total starch, resistant starch and β -glucan were determined from whole flour samples, using kits supplied by Megazyme (Irishtown, Ireland). The total starch and the resistant starch contents were determined using the protocol specified for 'samples containing also resistant starch'. Total arabinoxylan contents were determined using a colorimetric method (**Finnie et al., 2006**). 10 mg of flour were weighed in Pyrex tubes. 4 mL of dH_2O and 20 mL of freshly prepared extraction solution (Glacial acetic acid, HCl, Fluoroglucinol 20% and Glucose 1.75%) were added to each tube. The samples were placed in a boiling water bath for 25 minutes and vortexed after 10 and 20 minutes. After incubation the absorbance of the samples was read at 510/552 nm. A standard curve was generated from a mixture of D-Xilose (Sigma Aldrich, St. Louis, MO) at different concentration. Each value represents the mean of three biological replicates ± standard error. Three technical replicates were carried out for each biological replicate.

4.2.8 Single Kernel Characterization System

The Single Kernel Characterization System 4100 (SKCS 4100) (Perten Instruments North America Inc., Reno, NV) was used to determine the seed texture. SKCS crushes individual grains between a crescent-shaped slot and a toothed rotor to obtain crush-response profiles and conductivity measurements. An overview on the operation and principles of the SKCS is presented in **Osborne and Anderssen (2003)**. Kernel hardness is determined from equation developed by **Martin et al. (1993)** using various parameters. Data from 300 kernel provide hardness index (HI), weight, diameter, and moisture. Each of the measurements is indirect and must be calibrated against reference laboratory methods.

SKCS was performed on 300 seeds of the homozygous mutant lines derived from the three different crosses compared to the control Svevo and the parent lines Soft Sv, Sv SSIIa, Sv SBEIIa and Sv GBSSI.

4.3 Results

4.3.1 Production of the genotype with altered starch composition in a soft background

To modulate the hardness in the set of three available starch mutants of durum wheat cv Svevo, a classical cross was conducted with the line Soft Sv, a durum wheat variety that carries the soft trait, achieved through chromosomal engineering by introducing the *Ha* locus from chromosome 5D of bread wheat into durum wheat.
Different strategies were followed for the three F_2 progenies. The selection process of the three crosses (Soft Sv X Sv SSIIa, Soft Sv X Sv SBEIIa, Soft Sv X Sv GBSSI) initially focused on the F_2 progenies, where the soft seed phenotype was chosen. This phenotype is characterized by a waxy/opaque appearance of the grain, which is distinct from the typical vitreous appearance of durum wheat (**Figure 4.3**). Seeds displaying the soft phenotype underwent an iodometric assay using half-seed. For the Soft Sv X Sv SBEIIa cross, subsets of phenotypes exhibiting a more intense coloration, indicating a higher amylose content, were selected and bred. Regarding the Soft Sv X Sv SSIIa nulls, the selection process involved the identification of seeds with a brownish colour and shrunken appearance, which are characteristic of the SSIIa null mutation. For Soft Sv X SvGBSSI, the I_2/KI staining on half seeds led to the selection of low amylose genotype showing a red-yellow coloration; indeed it wasn't possible to distinguish hardness phenotype based on seed appearance. The selected seeds were bred, and their traits were validated using molecular assays for both characteristics in the F_3 progenies.

Figure 4.3 Example of opaque appearance of Soft Sv grain (left side) compared to the typical vitreous appearance of Sv durum wheat (right side).

4.3.2 Identification of the *Ha* locus in the progenies of the crosses Soft Sv X Sv SSIIa, Soft Sv X Sv SBEIIa, Soft Sv X Sv GBSSI

To determine the presence of puroindoline genes in the F_2 progenies of the three crosses, a PCR-based marker assay was conducted. Puroindolines, PinA and PinB, are proteins encoded by small-size associated genes located on chromosome 5B in the genotype Soft Sv that lacks introns. Thus the PCR-amplicons cover the entire length of the genes. The markers used are dominant and indicate the presence or absence of puroindoline genes, but they cannot distinguish between homozygous and heterozygous genotypes.
PCR analysis successfully identified nine lines in which the Soft background was fixed. Specifically, the molecular analyses allowed to identify three lines Soft Sv x Sv SSIIa, three lines Soft Sv x Sv BEIIa and three lines Soft Sv x Sv GBSSI (**Figure 4.4**).

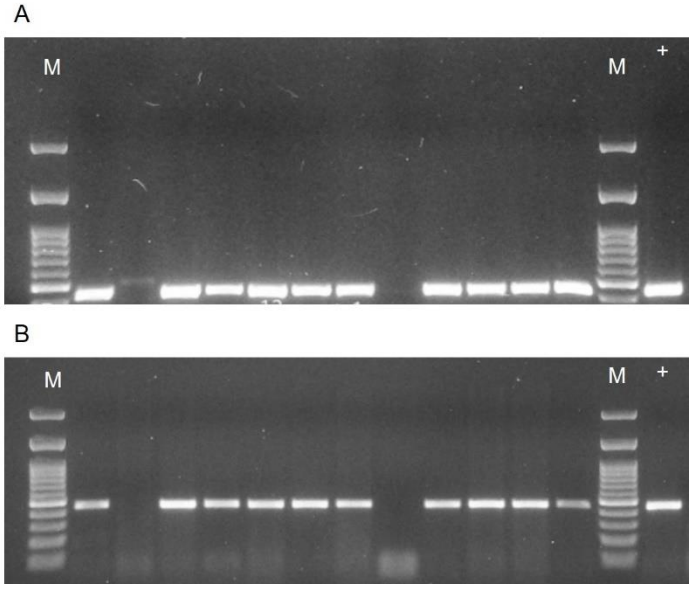

Figure 4.4 Example of the selection of *Ha* locus on the progenies of the three crosses. A) PinA PCR amplicons; B) PinB PCR amplicons. M indicates DNA ladder 100 bp (ExcelBand™ 100 bp DNA Ladder); + indicates positive control Soft Sv.

4.3.3 Selection of SSIIa null mutants

SSIIa *null* genotype harbours null mutations in both the homoeoalleles coding for the enzyme starch synthase IIa. In detail, the *SSIIa-A1* harbours a 289 bp deletion in exon I; while the *SSIIa-B1* presents a 175 bp insertion within the exon VIII (**Shimbata et al. 2005**) (**Figure 4.5**).

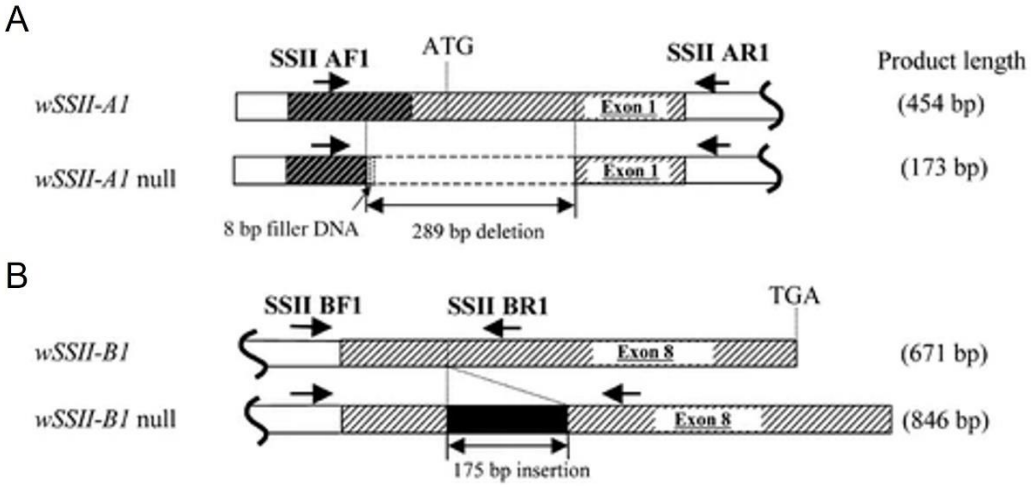

Figure 4.5 Mutations in A)*SSIIa-A1* homeoallele; B)*SSIIa-B1* hoemoallele. Arrows show the positions of primers. Broken lines indicate the deletions in null *SSIIa-A1* allele, and a filled box indicates the insertion in the null *SSIIa-B1* allele. The fragment size obtained using the indicated primer set is shown in brackets at the right of each allele (Modified by Shimbata et al. 2005).

PCR analyses were performed as reported in section 4.2.3 of "Materials and methods". The primer pairs designed for the *SSIIa-A1* homeoallele amplify a region of 454 bp in the wild-type and 173 bp in the mutant. Likewise, the primer pair designed for *SSIIa-B1* homeoallele produces an amplicon of 671 bp, in the wild-type and 846 bp in the mutant. Both markers are codominant, therefore it is possible to distinguish among heterozygous, homozygous and wild-type genotypes (**Figure 4.6**).

The selected Soft Sv/Sv SSIIa lines were then used for the biochemical characterization of amylose content.

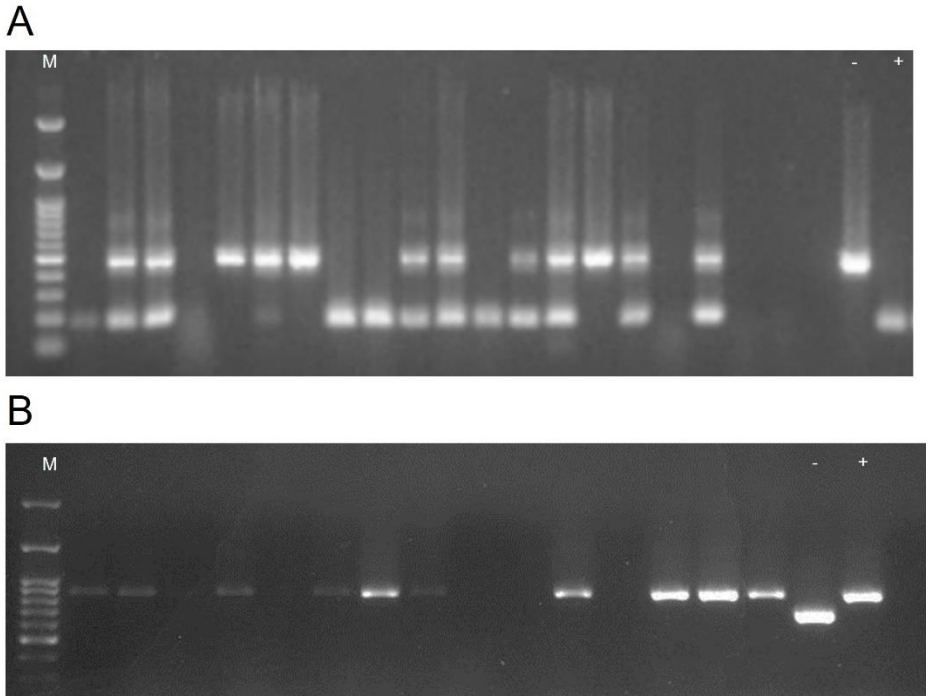

Figure 4.6 Visualization of PCR amplification products for A)*SSIIa-A1* and B)*SSIIa-B1* homeoalleles. M indicates DNA ladder 100 bp (ExcelBand™ 100 bp DNA Ladder); + indicates positive control null Sv SSIIa mutant; - indicates the negative control Sv wild-type.

4.3.4 Selection of SBEIIa null mutants

The SBEIIa null mutant has a nonsense mutation in both homeoalleles. In detail, in *SBEIIa-A1* allele, G>A transition generated a premature stop codon (TGA) in the twelfth exon; in *SBEIIa-B1* allele instead, the premature stop codon (TGA) occurred in the eighth exon (**Figure 4.7**).To identify mutations in segregating progeny of the cross Soft Sv x Sv SBEIIa, a MAS strategy was developed using HRM-genotyping.
Amplicons from the first PCR (401 bp and 552 bp, for *SBEIIa-A1* and *SBEIIa-B1* homeoalleles, respectively) were diluted 60-fold and used as templates for the nested PCR. HRM analysis was performed through the Light Scanner instrument (Idaho Technology, Inc.) which analyses the melting curves and distinguishes among heterozygous, homozygous and wild-type genotypes for both the homeoalleles (**Figure 4.8**).
The analysis led to identify five F_2 homozygous double null mutant lines for *SBEIIa* genes.
Among these, only in three lines, the Soft character resulted stable.
The three selected Soft Sv/Sv SBEIIa genotypes were then characterized at biochemical level.

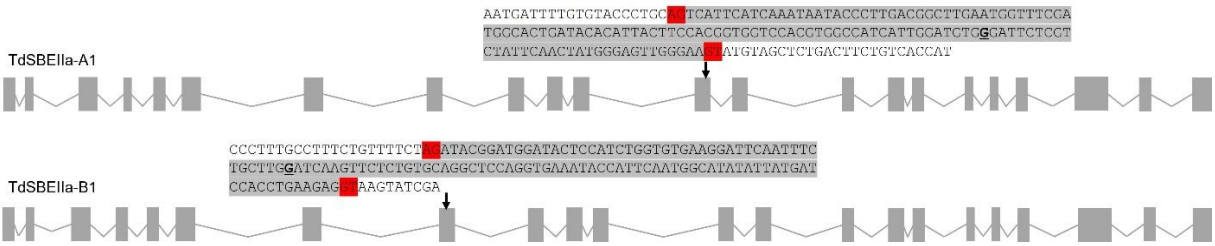

Figure 4.7 Gene structures of the two *SBEIIa* homeoalleles in durum wheat. Grey rectangles represent exons, grey lines represent introns. Black arrows indicate the position of the mutation in exon. The sequence of the exon presenting the mutation indicated in bold underlined is reported above the gene structure.

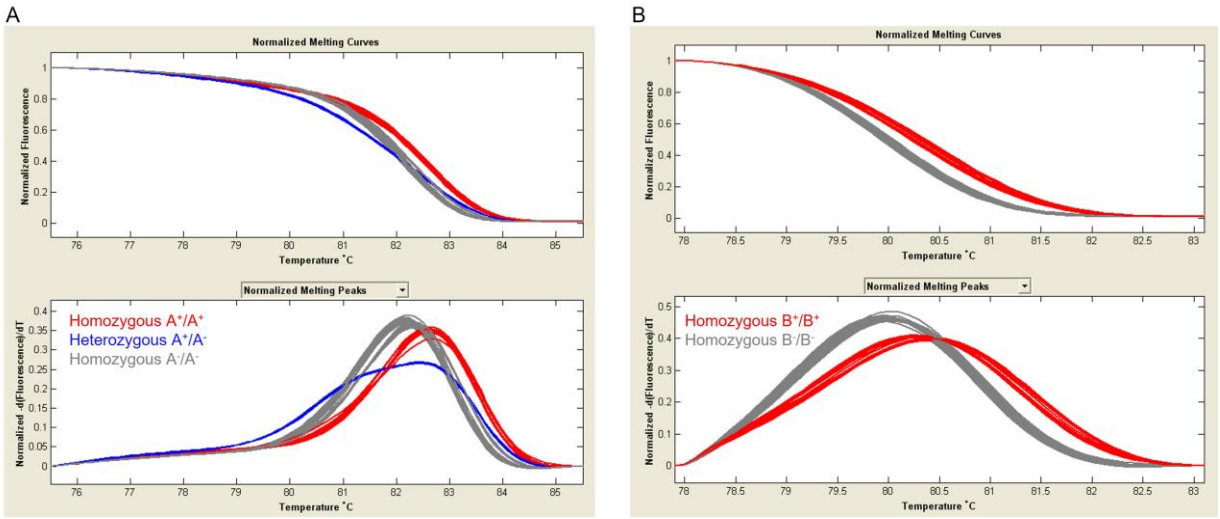

Figure 4.8 HRM- genotyping of the F_2 progenies from the cross Soft Sv x Sv SBEIIa. A) HRM analysis on the *SBEIIa-A1* homeoallele; B) HRM analysis on the *SBEIIa-B1* homeoallele.

4.3.5 Selection of GBSSI mutants

GBSSI mutants were selected by a qualitative colorimetric assay that determines the presence of amylose. GBSSI represents the only enzyme involved in the synthesis of amylose. Gene silencing alters the amylose/amylopectin ratio resulting in genotypes with highly reduced amylose levels (**Edwards et al., 2002**).
The results confirmed the presence of the waxy mutations in three lines selected through MAS (data not shown). The three lines showed, a similar behaviour compared to Sv GBSSI, used as a control (**Figure 4.9**).

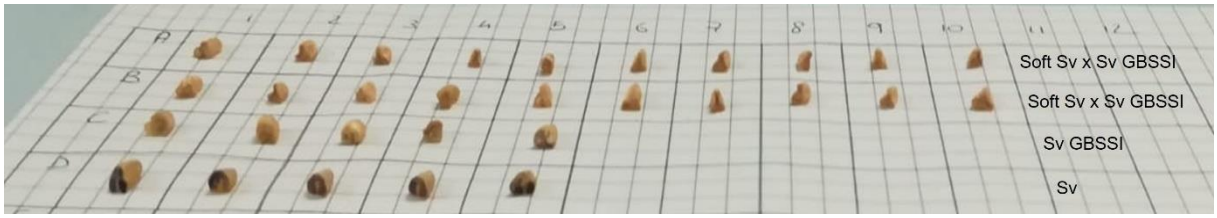

Figure 4.9 Example of half seeds of the colorimetric assay with Lugol's. The only samples in which iodine solution reacts with amylose are the positive controls Sv wild-type.

4.3.6 Biochemical characterization of selected lines

The selected lines Soft Sv/ Sv GBSSI, Soft Sv/ Sv SSIIa, Soft Sv/ Sv SBEIIa were characterized through biochemical analyses.

As expected, the mutant lines developed in this work contained different levels of amylose in their grains. The genotypes with Sv SBEIIa mutations showed elevated levels of amylose compared to the controls Svevo and Soft Sv. The amylose content was comparable with the parental genotype Sv SBEIIa which had an amylose content of about 70% of the total starch in grains. As expected, the *GBSSI* genotypes showed the lower content of amylose (almost equal to 0%). An intermediate value of amylose was measured in two genotypes (Sv SSIIa and Soft Sv/Sv SSIIa) carrying the mutations on the *SSIIa* genes (**Figure 4.10**).

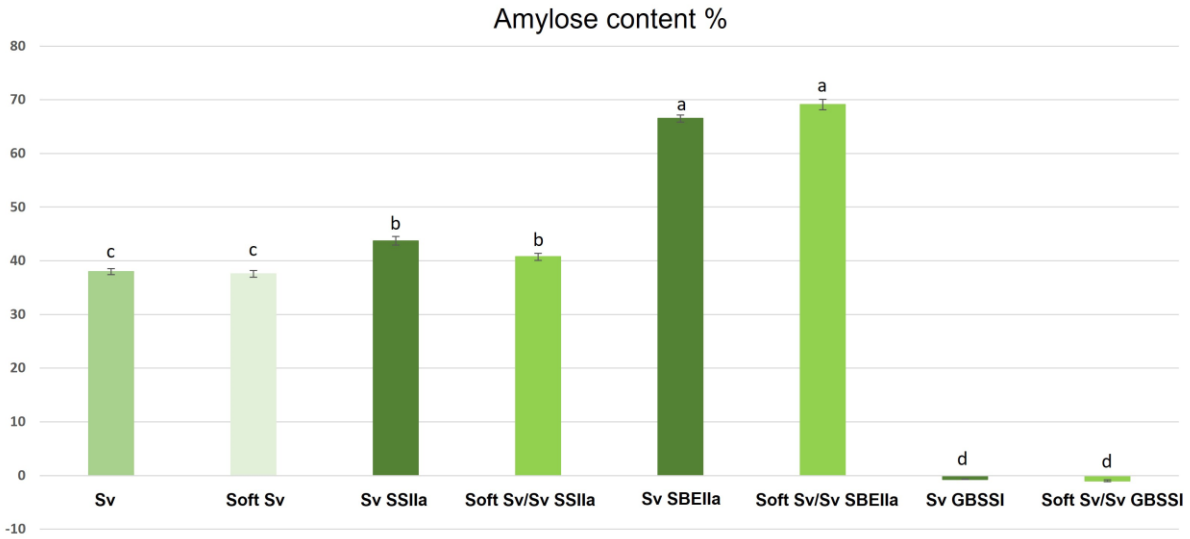

Figure 4.10 Analysis of amylose content (%) in the selected mutant lines, parental lines (Soft Sv , Sv SSIIa, Sv SBEIIa, Sv GBSSI) and control Sv wild-type. The mean of N =3 independent

replicates is reported; error bars indicate standard error. Different letters indicate significantly different values. Tukey HSD test p-value< 0.01.

The biochemical characterization consisting in the determination of the total starch content, resistant starch, β-glucans and arabinoxylans were only carried out on the lines with sufficient quantities. In particular, the lines Soft sv/ Sv SSIIa was not considered for this study as the grain was preserved for the multiplication in the greenhouse.
The total starch content was similar in all the lines analysed, except for the mutant lines carrying the SBEIIa mutation. As expected the content of resistant starch was higher in these lines compared to the other ones. The amount of β-glucans was significantly higher either in high amylose or low amylose genotypes. The Soft Sv had values similar to the control Svevo. The content of arabinoxylans was similar between the high amylose genotypes and the control Svevo; whereas it was lower in the Soft Sv, Sv GBSSI and Soft Sv/Sv GBSSI (**Table 4.3**).

Table 4.3 Biochemical characterization of the mutant lines in comparison to the parental lines (Soft Sv, Sv SBEIIa, Sv GBSSI) and the control Svevo. The mean of N =3 independent replicates is reported. Different letters indicate significantly different values. Tukey HSD test p-value< 0.01.

Lines	Total Starch (%)	Resistant Starch (%)	β-Glucans (mg/g)	Arabinoxylans (mg/g)
Sv	48.79± 0.97 a	0.79± 0.17 c	0.30± 0.01 d	53.33± 2.00 a
Soft Sv	50.95± 0.72 a	0.38± 0.01 d	0.28± 0.01 d	36.25± 1.57 b
Sv SBEIIa	45.64± 0.50 b	3.7± 0.04 b	0.46± 0.01 b	51.86± 3.78 a
Soft Sv/Sv SBEIIa	47.11± 0.54 b	5.1± 0.03 a	0.57± 0.01 a	44.27± 2.01 ab
Sv GBSSI	50.76± 0.69 a	0.23± 0.02 d	0.37± 0.008 c	38.42± 3.7 b
Soft Sv/Sv GBSSI	53.28± 1.38 a	0.28± 0.06 d	0.43± 0.005 b	34.84± 0.27 b

4.3.7 Analysis of seeds hardness

Seeds hardness was evaluated in the three selected genotypes compared to the parental lines and the control Svevo through SKCS analysis.
The hardness index (HI) was similar among Sv SSIIa, Soft Sv/Sv SSIIa and Svevo and higher in the high amylose parental Sv SBEIIa genotype. Differently, the Sv GBSSI mutant showed lower HI than Svevo and this value was similar to that of Soft Sv. Noteworthy all the high amylose soft starch mutants highlighted higher HI if compared to Soft Sv and a significant reduction of hardness was observed in the Soft Sv/Sv SBEIIa and Soft Sv/Sv GBSSI lines

compared to their respective starch mutant parent lines (Sv SBEIIa and Sv GBSSI). The sole exception was constituted by the Soft Sv/Sv SSIIa mutant: here no differences were found with Svevo and Sv SSIIa (**Figure 4.11**).

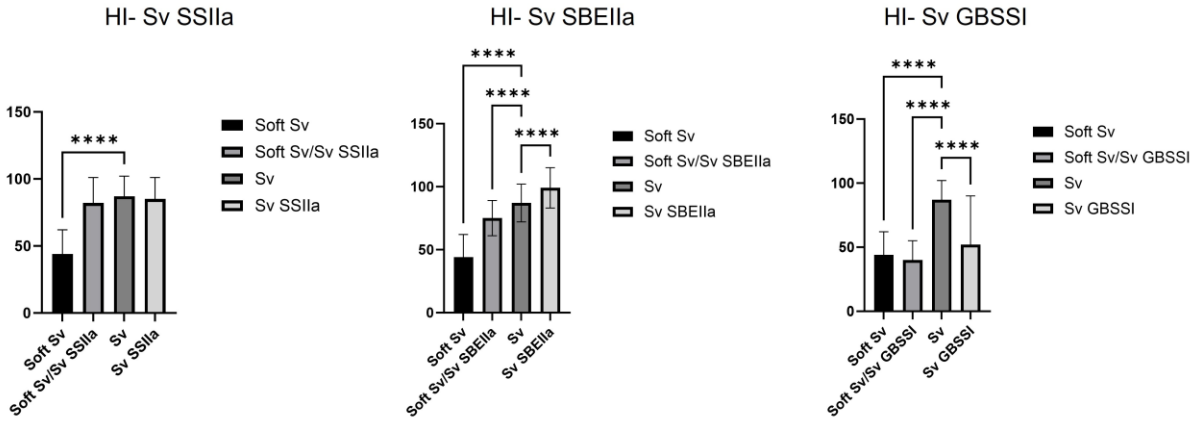

Figure 4.11 HI of the mutant lines in comparison to the parental lines (Soft Sv , Sv SSIIa, Sv SBEIIa, Sv GBSSI) and the control Sv wild-type. The mean 300 seeds is reported; error bars indicate standard deviation. * indicate significantly different values. Tukey HSD test p-value< 0.01.

4.4 Discussion and conclusions

The ever-growing world population and the consequences of the climate changes led the scientific research to focus on two main objectives: 1) improvement of grain yield and 2) sustainability. Over the past decade, the reduction of the 'triple burden of malnutrition' represented a key objective for the improvement of nutritional quality. The goal of the scientific research should be to create a system of sustainable food production that meets the needs of the world population both in terms of calories and nutritional quality (**Sands et al., 2009**).

The research here discussed concerns the development of three durum wheat genotypes in which novel properties have been combined in the health-functional profile of the derived foods and in the milling characteristics of the grain. These genotypes fit perfectly into the current framework described and have excellent potential in nutritional terms, technological quality and sustainability.

The project involves a set of durum wheat genotypes, in which the amylose/amylopectin ratio has been modified. Modifications to the starch composition, the major component of wheat flour, can have a deep effect on the nutritional and technological characteristics of the end products. These genotypes were, therefore, the subject of a further improvement breeding program focused on modifying the seed hardness associated with grinding efficiency and sustainability.

In detail, two high amylose genotypes Sv SSIIa and Sv SBEIIa and a low amylose genotype Sv GBSSI, previously developed (**Lafiandra et al., 2010**; **Sestili et al., 2015**; **Botticella et al., 2016**), were crossed with Soft Sv (**Morris et al., 2011**). Through a MAS strategy, three lines for the following durum wheat genotypes were selected: Soft Sv/ Sv SSIIa, Soft Sv/ Sv SBEIIa and Soft Sv/ Sv GBSSI.

These lines were fully characterized at biochemical level. As expected amylose content was increased in genotypes carrying the mutations on *SSIIa* and *SBEIIa* genes. Inversely amylose content was strongly reduced (up to 0%) in genotypes with the genetic background of Sv GBSSI. Since resistant starch is positively correlated with amylose content, it was markedly enhanced in the high- amylose genotypes, in agreement with previous works (**Slade at al., 2012**; **Sestili et al., 2015**; **Botticella et al., 2016**; **Botticella et al., 2018**).

Despite the improved nutritional qualities and the potential application in different final end uses, information on the technological properties of high amylose wheat is still limited. In a recent work, the study of milling and bread-making quality of bread *null* SSIIa mutants showed a significant reduction in flour yield. Furthermore, bread made by the flour of SSIIa mutants showed a significantly smaller volume compared to the control (**Hogg and Giroux, 2019**).

To date, an altered and increased texture was observed in high amylose grains (**Hogg et al., 2017**; **Schonhofen et al., 2017**; **Botticella et al., 2018**). Similarly, **Clarke et al., 2008** reported an increased grain hardness in the barley SSIIa mutant. SKCS analysis confirmed a correlation

between the amylose content and grain hardness, except for Sv SSIIa genotypes where the HI was similar to the control (Svevo).

In conclusion, we obtained new interesting genotypes due to the combination of the elevated nutritional properties typical of starch mutants and the innovative technological properties due to the introgression of the soft trait.

Future analyses will be necessary to determine the technological characteristics of the developed genotypes. The set of materials here produced will be precious to investigate the relationship between starch composition and seed texture, two important quality traits, in durum wheat.

CHAPTER 5

Enhancing grain size in durum wheat high amylose mutants to improve yield

Abstract

In recent years the incidence of diet-related diseases is increased and numerous breeding programs focused on the production of crops with improved nutritional value. In this context, the high amylose wheat is attracting the attention of several food industries for the production of low glycaemic food products. In fact, it has been well established that there is a correlation between the amount of amylose in flour and the amount of resistant starch (RS) in foods. RS is a particular fraction that escapes the digestion in the stomach playing a role similar to dietary fiber in the prevention of numerous diseases as colon cancer, diabetes, obesity and cardiovascular disorders.

In this scenario, the research presented aims to improve the yield in an high amylose durum wheat genotype. The study involved a durum wheat high amylose genotype produced in previous breeding programs (Svevo SSIIa^{-}). This mutant line had mutations in the *SSIIa* genes, key enzymes of amylopectin biosynthesis, that affected starch composition (the amylose is increased up to 45%) and structure (reduction of short amylopectin chains). However, one of the main issues detected in the high amylose mutant line is a decrease in the agronomic performances that drastically affected their yield and the spread on the market. Recently it was reported that the silencing of *TaGW2-A1* allele has positive effects on grain size, weight and yield. For this reason, the Kronos GW2-A1^{-} mutant was crossed with Svevo SSIIa^{-}.

The selected genotypes Kronos GW2-A1^{-}/Svevo SSIIa^{-} were characterized at biochemical, agronomic and molecular levels, demonstrating that the introgression of GW2-A1 mutation had positive effects on grain size and yield without to alter the elevated nutritional value associated to the mutants SSIIa.

KEYWORDS

Nutritional Quality, Fiber, Durum Wheat, High Amylose, Resistant Starch, Grain Weight 2 (GW2), Yield

5.1 Introduction

One of the major challenges of the Agenda 2030 for Sustainable Development is the reduction by one-third of premature mortality due to non-communicable diseases (NCDs) (Sustainable Development Goal 3 -SDG3) by 2030 (**Bennet et al., 2018**). NCDs are chronic diseases, i.e. heart and respiratory diseases, stroke, cancer, diabetes and obesity, that disproportionately affect people in low- and middle-income countries, where they are the leading causes of death (**WHO, 2016**; **Williams et al., 2018**). Although NCDs tend to manifest in adulthood, many have their origins in lifestyle behaviours and are the result of a combination of genetic, physiological, environmental and behavioural factors. The main risk factors contributing to the onset of NCDs include unhealthy diet, physical inactivity, and tobacco and alcohol use (**Benziger et al., 2016**; **WHO, 2017**). At this regard it is well-known that a healthy diet can reduce the risk of non-communicable diseases. Recently great interest was aroused by foods enriched in resistant starch (RS). RS is a starch fraction that escapes digestion in the stomach and small intestine and is fermented in the large bowel by human microflora and transformed into short-chain fatty acids (SCFA) as butyrate and propionate that low the pH in the lumen playing an important protective role against the onset of colorectal cancer (**Topping and Clifton, 2001**). In addition, owing to the low glycaemic index, foods with resistant starch can help to prevent important common diseases such as type II diabetes and obesity (**Birt et al., 2013**; **Raigond et al., 2015**). The starch is composed of two glucan homopolymers (amylose and amylopectin) that have the same backbone but differ in the degree of polymerization and ramification. Amylose is smaller (10^3-10^4 DP) than amylopectin (10^4-10^6 DP) and is mainly linear (D-glucose molecules are linked through α(1→4) glycosidic linkages); differently, amylopectin is characterized by several branching chains due to the presence of α(1→6) glycosidic linkages.

A successful strategy to increase RS in foods is to alter the starch composition by raising the amount of amylose in raw materials. Recently some breeding programs focused on the production of bread and durum wheat with an increased amylose/amylopectin ratio (reviewed in **Botticella et al., 2021**). The main targets were two genes involved in amylopectin biosynthesis: the *Starch Synthase IIa* (*SSIIa*) and the *Starch Branching Enzyme IIa* (*SBEIIa*). The silencing of *SSIIa* increased significantly the amount of amylose (up to 40-45%) compared to the wild-type either in bread or durum wheat (**Yamamori et al., 2000; Botticella et al., 2016**). Similarly, the elimination of *SSIIa* in barley *sex6* mutant promoted amylose content up to 50% (**Morell et al., 2003; Sparla et al., 2014**). Inactivation of *SBEIIa* by RNA interference raised amylose content to more than 75% in bread and durum wheat (25–30% in the wild-type) (**Regina et al., 2006; Sestili et al., 2010**). The same genes were also targeted by a TILLING approach and the obtained mutant lines showed an altered starch composition both in bread and durum wheat (**Botticella et al., 2018; Slade et al., 2012; Sestili et al., 2015**): amylose content

was increased up to 55–70% in the two SBEIIa mutants derived from bread wheat cultivars Express and Cadenza, respectively; similarly, the suppression of *SBEIIa* in durum wheat cultivar cv. Svevo led to the production of a genotype with an increased amount of amylose (52%). Although the high amylose wheats, above described, are very promising and interesting at nutritional level for their health properties, they are less performant at agronomic level. Pleiotropic effects were ascertained in some high amylose starch genotypes, among the more frequent a decrease in total starch content with a yield penalty. The most penalized genotypes regarding yield are the SSIIa mutants. **Botticella and colleagues (2016)** reported a reduction in yield parameters in a set of fourteen SSIIa mutant sister lines compared to the control. In detail the hectoliter weight and 1,000 grain weight were reduced at a variable extent from 10% to 20% and total starch in the range 25-45%.
The spread of the high amylose flour/semolina on the world market could contribute to prevent the diffusion of noncommunicable diseases but the unfavourable agronomic performances of the high amylose genotypes make them difficult to market. A possible strategy to improve the agronomic trait is the introgression of yield-associated alleles in such genotypes. At this purpose a promising gene is the *Grain Weight 2* (*GW2*) which encodes a RING-type protein exhibiting E3 ubiquitin ligase activity and is involved in the regulation of cell division (**Song et al., 2007**). The suppression of a homeoallele (*GW2-A1*) accelerated grain filling, leading to an increase in grain weight and width (**Song et al., 2007**). Recently, the screening of a wheat TILLING population allowed to identify several mutants in the allele *TaGW2-A1*, including a transition (G>A) in the splicing site of V exon (**Simmonds et al., 2016**). This transition is responsible in the increase of the seed width (+2.8%), length (+2.1%) and TGW (+6.6%) in durum wheat.
In this work, the starch mutant line Svevo SSIIa$^-$ was crossed with a Kronos TILLING GW2-A1$^-$ mutant with the aim to obtain durum wheat genotypes with improved nutritional value and good agronomic traits.

5.2 Materials and methods

5.2.1 Plant materials

An *in silico* study performed on the platform WheatTILLING available at the University of Davis (https://dubcovskylab.ucdavis.edu/home; **Krasileva et al., 2017**) allowed to identify a durum wheat mutant line possessing deleterious mutation on the *TdGW2-A1* homeoallele. The line Kronos 3898 had a splice site mutation that determine a transition G>A in the GT site of exon III of *TdGW2-A1*. The starch mutant (Svevo SSIIa$^-$), previously described in the Chapter 4, was crossed with the mutant Kronos GW2-A1$^-$. F_1 generation was self-pollinated and the selection of the different genotypes was conducted on the derived F_2 and F_3 progenies. Seedlings of durum wheat cultivars Svevo, the parental mutant genotypes Svevo SSIIa$^-$ and Kronos GW2-A1$^-$ along with the genotypes obtained by the cross were vernalized at 4°C for 4

weeks. Then the plants were grown in a regime of 20–28°C during the light period (16 h) and 16–24°C during the dark period (8h) in a growing chamber; the light intensity was 300 µE m^{-2} s^{-1}.

5.2.2 DNA extraction

Genomic DNA was extracted from leaves of F_2 and F_3 progenies of Kronos GW2-A1$^-$ X Svevo SSIIa$^-$ cross and controls according to **De Kochko and Hamon (1990)**, with some modifications. The samples were grinded and homogenized with liquid nitrogen to obtain a fine powder. 500 µl of extraction buffer (100 mM Tris, 50 mM EDTA and 500 mM NaCl) were added to the samples along with 2% SDS. After mixed thoroughly, the samples were incubated at 65°C for 10 min enabling cellular lysis. 150 µl of 5M Potassium Acetate were added to precipitate cellular debris and SDS-protein complex. After centrifugation at 13,500 rpm for 15 min in a refrigerated centrifuge at 4°C, the supernatant was transferred to a new Eppendorf tube with 2 volumes of 2-propanol and keep on ice for 15 min for facilitating the DNA precipitation. The pellet obtained through centrifugation at 13,500 rpm for 10 min was washed twice with 70% ethanol. The dried pellet was resuspended in 50 µl of 10 mM Tris, 1 mM EDTA, pH 8 solution and used for Polymerase Chain Reaction (PCR).

5.2.3 PCR amplification of *SSIIa* and *GW2* genes

In order to identify the homozygous mutants derived from the cross (Kronos GW2-A1$^-$ X Svevo SSIIa$^-$), a Marker Assisted Selection (MAS) assay based on PCR and HRM-genotyping was developed. PCR for *SSIIa* genes were performed with different primers pairs (**Shimbata et al., 2005**) reported in **Table 5.1**. The reactions were conducted in a final volume of 10 µl containing 2X GoTaq® G2 Hot Start Colorless Master Mix (Promega, Madison, USA), 0.5 µM of each primer, 20 ng of template DNA and nuclease-free water up to 10 µl volume. The PCR conditions were: an initial denaturation at 95°C for 2 min, followed by 38 cycles at 95°C for 30 sec, 61°C for 30 sec, 72°C for 1 min and a final extension at 72°C for 5 min.
Touch-down PCR method was used to amplify *SSIIa-A1* homeoallele, on the following conditions: 95°C for 5 min, followed by 9 cycles at 95°C for 30 sec, 72°C for 30 sec with an increment decreasing of 1°C per cycle, 72°C for 1 min. After these steps 29 cycles at 95°C for 30 sec, 63°C for 30 sec, 72°C for 1 min and a final extension at 72°C for 5 min were performed. Regarding the detection of the SNP on *GW2-A1* homeoallele, HRM analysis was carried out through a nested PCR strategy using primer pairs reported in **Table 5.1**. Touch-down PCR was used to amplify a portion of the gene containing the SNP, on the following conditions: 95°C for 5 min, followed by 5 cycles at 95°C for 30 sec, 65°C for 30 sec with an increment decreasing of 1°C per cycle, 72°C for 30 sec. After these steps 33 cycles at 95°C for 30 sec, 60°C for 30 sec, 72°C for 30 sec and a final extension at 72°C for 5 min were performed. The first PCR

reaction was diluted 60-fold and 2 µl were used as a template for the second PCR reaction for HRM analysis. The second reaction was carried out according to **Sestili et al. (2015)** in 96-well Frame-Star plates (4titude Ltd., Surrey, UK) overlaid with 10 µl of mineral oil (Sigma-Aldrich, St. Louis, MO, USA). The melting curves were analysed by the Light Scanner instrument (Idaho Technology, Inc.).

Table 5.1 List of genes and primers used for PCR.

Id primer	Sequence	T annealing	Amplicon size	Use	Gene
SSIIAF1	TGCGTTTACCCCACAGAGCAC	63°C	173 bp	PCR	*SSIIa-A1*
SSIIAR1	ACGCGCCATACAGCAAGTCATAA				
SSIIBF1	ATTTCTTCGGTACACCATTGGCTA	61°C	846 bp	PCR	*SSIIa-B1*
SSIIBR1	TGCCGCAGCAGCATGCC				
GWA-Till F2	GTGCTCTTGACCGGCTTGC	64°C	1335 bp	1st round PCR	*GW2-A1*
GWA-Till R2	GGTACGAATGGCATATGGATTTTCTTGC				
GTY3898F	CCAACTCATACTGCTCGACC	60°C	51 bp	2nd round PCR	
GTY3898R	AGAACAGAGATGGTATGAAGGA				

5.2.4 Isolation of starch granules and determination of amylose content

Starch granules were isolated from half seeds as described by **Zhao and Sharp (1996)** with some modifications. The half kernels without embryos were grinded, placed in tubes containing 1 ml of dH_2O and left at 4°C overnight. The following day the samples were vortexed and centrifuged for 5 minutes at 13,000 rpm. After the centrifugation the supernatant was removed, 300 ml of dH_2O were added to the pellet and mixed with a pestle in order to form the gluten. The starch granules in suspension were transferred in a new tube containing 1 ml of 5 M NaCl and centrifuged for 5 minutes at 13,000 rpm. The supernatant was discarded and the steps repeated twice. Each sample was washed three times with 1 ml of dH_2O. After each wash, the samples were vortexed, centrifuged for 5 minutes at 13,000 rpm and the supernatant removed. Finally, the pellet was washed with 1 ml of acetone and the samples centrifuged at 13,000 rpm for 3 minutes. The starch granules isolated were left to dry for one day at room temperature and stored at 4°C.

The amylose content was determined from a 15 mg of purified starch using a colorimetric assay based on the iodine–amylose reaction (**Chrastil, 1987**). Briefly 2 ml of 1M NaOH and 4 ml dH_2O were added to starch samples then placed in a boiling water bath for 30 minutes. During incubation, samples were vortexed at least three times in order to avoid gel lumps. After cooling, two tubes were prepared for each sample with 5 ml of TCA 0,5%, 100 µl of the starch solution and 50 µl of 0.01 N KI/I_2 mixture. After 20 min of incubation the absorbance of the

samples was read at 610 nm. A standard curve was generated from a mixture of potato amylose (Fluka, Neu-Ulm, Germany) and amylopectin from maize (Sigma Aldrich, St. Louis, MO). Each value represents the mean of three biological replicates ± standard error. Three technical replicates were carried out for each biological replicate.

5.2.5 Analysis of total starch, resistant starch, β-glucan and arabinoxylan

Total starch, resistant starch and β-glucan contents were determined from whole flour samples using commercial kits supplied by Megazyme (Irishtown, Ireland). Total starch and resistant starch were determined using the protocol specified for 'samples containing also resistant starch'. Total arabinoxylan contents were determined using a colorimetric method (**Finnie et al., 2006**). Ten mg of flour were weighed in Pyrex tubes. 4 mL of dH_2O and 20 mL of freshly prepared extraction solution (Glacial acetic acid, HCl, Fluoroglucinol 20% and Glucose 1.75%) were added to each tube. The samples were placed in a boiling water bath for 25 minutes and vortexed after 10 and 20 min. The absorbance of the samples was read at 510 and 552 nm. A standard curve was generated from a mixture of D-Xilose (Sigma Aldrich, St. Louis, MO) at different concentration. The total arabinoxylan contents were calculated as follow: $TOT - AX\ \left(\frac{mg}{g}\right) = \frac{\mathrm{A(552-510)-\ q}}{\mathrm{m}} * 100.$

Each value represents the mean of three biological replicates ± standard error. Three technical replicates were carried out for each biological replicate.

5.2.6 Phenotypic analyses

Phenotypic analyses were performed on a sample of 60 kernels for each genotype described in the section "Plant materials" using the SmartGrain software (**Tanabata et al., 2012**) (www.kazusa.or.jp/phenotyping/smartgrain/index.htmL). For each genotype the following traits were analysed: weight of 100 grains (HGW), seed surface area (AS), perimeter length (PL), length (L) and width (W).

5.2.7 Quantitative Real Time PCR (qRT-PCR)

The experimental field trial was carried out at University of Tuscia (Viterbo, Italy) during the 2021-2022 growing season. Immature seeds of the Kronos GW2-A1$^-$/Svevo SSIIa$^-$ selected mutants along with the parental lines of the cross (Kronos GW2-A1$^-$ and Svevo SSIIa$^-$) were collected at 14 and 21 Days Post Anthesis (DPA) and stored at -80°C. Total RNA was extracted using the Spectrum Plant Total RNA kit (Sigma-Aldrich, St. Louis, USA) following manufacturer's instructions. One µg of the extracted RNA was used as template for the synthesis of cDNA, following the protocol of the QuantiTect Reverse Transcription Kit (Qiagen, Hilden, Germany). One microlitre of the cDNA prepared was used for qRT-PCR in a

final volume of 15 µl. qRT-PCR were performed in the CFX 96 Real-TimePCR Detection System device (Bio-Rad Hercules, CA, USA). The reactions were prepared with 2X SsoAdvUniver SYBR GRN SMX (Bio-Rad Hercules, CA, USA) and 0.5 µM of each primer. The qRT-PCR program had the following conditions: 95°C for 3 min, followed by 39 cycles at 95°C for 10 sec and 60°C for 30 sec. A melting curve was generated over the range 75–95°C, with 0.5°C increments at 5 s/step. Transcript quantification was enabled by CFX manager software. Three biological replicates were analysed for each genotype, and each biological replicate was represented by three technical replicates. The list of genes analysed, along with the housekeeping β-actin gene, and the used primers are shown in **Table 5.2**.

Table 5.2 List of genes and primers used for qRT-PCR.

ID primer	Sequence	T Annealing	Amplicon Size	Gene
TdGW2A_rtF	CATGGGTGCTGCGGAAAG	60°C	166 bp	*TdGW2-A1*
TdGW2A_rtR	CCCCGCATCCACCACAAT			
GBSSI_rtF	CGGCATGGACGTCAGCGAGT	60°C	147 bp	*TdGBSSI*
GBSSI_rtR	AGGGGCACCTTCCGGTCCAC			
SSIIa_rtF	GTTCTCCCTGGTGCAAAACA	60°C	157 bp	*TdSSIIa*
SSIIa_rtR	GCAGCCTTGTAGTATTTTCGGA			
SBEIIa_rtF	GCACCAGTATGTTTCACGGA	60°C	173 bp	*TdSBEIIa*
SBEIIa_rtR	CAAAGAGTGCATCGTCGGAG			
ADPG_rtF	GGCCATCGAGCACTTCACTTAC	60°C	136 bp	*TdADPG*
ADPG_rtR	ATAGGTGCACAGGGTTGAGG			
Susy2_rtF	CGTCTGGGAGTATGTGAGGG	60°C	187 bp	*TdSusy2*
Susy2_rtR	GTTGCCAATGGACTTCGACA			
UGP_rtF	GGAGCAGCGATCAGGTTCTT	60°C	193 bp	*TdUGPase*
UGP_rtR	TGAACTCAGGACCAAGCTCA			
RUB3_rtF	CAAAGAGGAGACGGACTACC	60°C	189 bp	*TdRUB3*
RUB3_rtR	GTGTGGTCTCGTAAAGCAGG			
E3_rtF	GCAGGATAGCATCGGTGAT	60°C	128 bp	*TdE3*
E3_rtR	AGCAGTAGAGGTGGCCGC			
RFP_rtF	ATCCCCAAGCCGGTCATC	60°C	143 bp	*TdRFP*
RFP_rtR	CGCTCCTTGACCTCCTCG			
cACT_F	GGAATGGTCAAGGCTGGTT	60°C	200 bp	*TdActin*
cACT_R	CTCCATGTCATCCCAGTTGC			

5.3 Results

5.3.1 Pyramiding of SSIIa and GW2-A1 mutations

The mutations on the *SSIIa* homeoalleles were previously reported by **Shimbata et al. (2005)**. In detail, the *SSIIa-A1* and *SSIIa-B1* had a 289 bp deletion in the first exon and a 175 bp insertion within the eighth exon, respectively.
The Kronos 3898 line had a splice site mutation on the third exon of GW2-A1 allele, that affects its functionality (**Figure 5.1**).
To pyramid the mutation on the *SSIIa* genes and the *GW2-A1* null allele, the following cross was carried out: Kronos GW2-A1^{-} X Svevo SSIIa^{-}. The selection of the mutant lines was performed on the F_2 and F_3 generations of the cross using the MAS strategies based on PCR (for *SSIIa* mutations) and HRM-genotyping (for *GW2-A1*) described in the section "Material and Methods".
The screening of F_2 and F_3 progenies permitted to obtain ten sister lines Kronos GW2-A1^{-} /Svevo SSIIa^{-} characterized by the presence of *null* homozygous mutations on the *SSIIa-A1*, *SSIIa-B1* and *GW2-A1* genes (**Figure 5.2**).

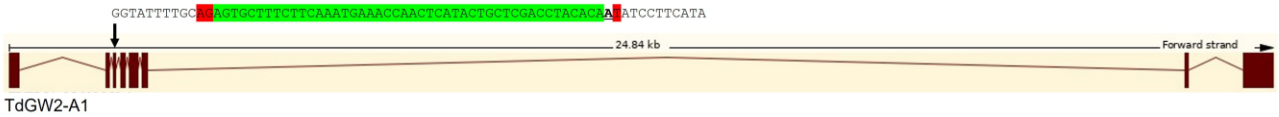

Figure 5.1 Gene structures of *GW2-A1* homeoallele in durum wheat. Intron-exon organization from Ensembl Plants (TRITD6Av1G091060). Black arrow indicates the position of the mutation in exon III. The sequence of the exon presenting the mutation indicated in bold underlined is reported above the gene structure.

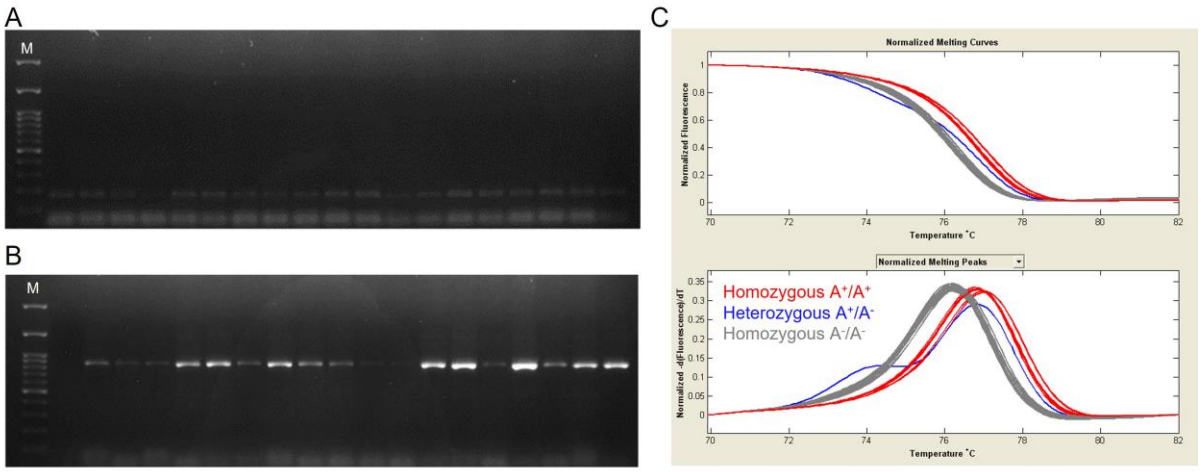

Figure 5.2 Screening of F_2 progeny of the Kronos GW2-A1$^-$ X Svevo SSIIa$^-$ cross. A) Visualization of PCR amplification products for *SSIIa-A1* and B) *SSIIa-B1* homeoalleles. M indicates DNA ladder 100 bp (ExcelBand™ 100 bp DNA Ladder) C) HRM-genotyping of the *GW2-A1* homeoallele.

5.3.2 Biochemical characterization of Kronos GW2-A1$^-$/Svevo SSIIa$^-$ genotypes

Biochemical analyses were performed on the selected genotypes Kronos GW2-A1$^-$/Svevo SSIIa$^-$ compared to the parental lines Svevo SSIIa$^-$, Kronos GW2-A1$^-$ and Svevo wild-type grown in field at University of Tuscia (Viterbo, Italy) in growing seasons 2020-2021 and 2021-2022 (**Table 5.3**). Biochemical analyses showed the same behaviour in the two analysed years. As expected, the amylose content was higher in the lines in which the *SSIIa* genes are silenced. In detail, the genotypes Kronos GW2-A1$^-$/Svevo SSIIa$^-$ had values of amylose similar to Svevo SSIIa$^-$, but significantly raised (20%, average of the two seasons) compared to the control Svevo wild-type. Similarly, the resistant starch was increased more than 10-fold in Svevo SSIIa$^-$ and Kronos GW2-A1$^-$/Svevo SSIIa$^-$ compared to Svevo. The analyses also highlighted an increase in β-glucans and arabinoxylans either in Kronos GW2-A1$^-$/Svevo SSIIa$^-$ or Svevo SSIIa$^-$ compared to Kronos GW2-A1$^-$ and Svevo. Unexpectedly the total starch content was not increased in the genotype Kronos GW2-A1$^-$/Svevo SSIIa$^-$ and even decreased compared to the parent line Svevo SSIIa$^-$ in the season 2020-2021. The reduction of total starch was probably due to the environmental conditions, in particular to the drought and the lack of rain during the grain filling in the season 2020-2021.

Table 5.3 Biochemical analyses carried out on Kronos GW2-A1$^-$/Svevo SSIIa$^-$ mutants, parental lines (Svevo SSIIa$^-$, Kronos GW2-A1$^-$) and wild-type (Svevo). The mean of N =3 independent replicates is reported. Different letters within the growing season indicate significantly different values. Tukey HSD test p-value< 0.01.

	Lines	Amylose (%)	Total Starch (%)	Resistant Starch (%)	β-Glucan (mg/g)	Arabinoxylans (mg/g)
FIELD 2020-2021	**Svevo**	32.05± 0.65 d	62.70± 1.06 a	0.21± 0.005 b	0.35± 0.06 b	54.41± 1.64 b
	Svevo SSIIa$^-$	44.03± 0.56 a	45.49± 1.98 b	2.09± 0.03 a	1.02± 0.10 a	70.65± 2.59 a
	Kronos GW2-A1$^-$	37.07± 1.00 c	57.58± 0.75 a	0.43± 0.02 b	0.30± 0.03 b	65.77± 1.94 a
	Kronos GW2-A1$^-$/Svevo SSIIa$^-$	40.99± 0.68 b	38.60± 0.86 c	2.32± 0.027 a	1.04± 0.05 a	74.83± 0.79 a
FIELD 2021-2022	**Svevo**	31.49± 0.29 b	48.79± 2.91 a	0.79± 0.17 b	0.29± 0.01 b	53.33± 2.00 b
	Svevo SSIIa$^-$	43.00± 0.39 a	28.93± 0.71 b	3.21± 0.09 a	0.88± 0.03 a	80.59± 2.71 a
	Kronos GW2-A1$^-$	33.20± 2.25 b	51.18± 0.83 a	1.17± 0.41 b	0.30± 0.01 b	54.29± 1.61 b
	Kronos GW2-A1$^-$/Svevo SSIIa$^-$	42.12± 0.50 a	25.44± 0.60 b	3.11± 0.14 a	0.98± 0.03 a	93.79± 6.47 a

5.3.3 Phenotypic Analyses of Kronos GW2-A1$^-$/Svevo SSIIa$^-$ genotypes

Phenotypic analyses of seed traits were carried out on F_2 and F_3 progenies of Kronos GW2-A1$^-$/Svevo SSIIa$^-$ compared to the parental lines Svevo SSIIa$^-$, Kronos GW2-A1$^-$ and Svevo. The following parameters were measured: hundred grain weight (HGW), area size (AS), perimeter length (PL), length (L) and width (W). The first measurements were made on seeds of plants grown in greenhouse during the season 2020-2021 (**Table 5.4**). The same phenotypic measurements were also performed on the same genotypes grown in field at University of Tuscia (Viterbo, Italy) in two growing seasons (2020-2021 and 2021-2022) (**Table 5.4**).
Noteworthy it is evident an improvement of grain size in the genotype Kronos GW2-A1$^-$/Svevo SSIIa$^-$ compared to the Svevo SSIIa$^-$. The comparison between the parental line Svevo SSIIa$^-$ and Kronos GW2-A1$^-$/Svevo SSIIa$^-$ highlighted a significant increase for all the parameters in the last one either for the plants grown in greenhouse or field; however, these values were lower if compared to the parental line Kronos GW2-A1$^-$ and the control Svevo (**Figure 5.3**).

Table 5.4. Phenotypic analyses carried out on Kronos GW2-A1$^-$/Svevo SSIIa$^-$ mutants, parental lines (Svevo SSIIa$^-$, Kronos GW2-A1$^-$) and wild-type (Svevo) grown in greenhouse and in field (seasons 2020-2021 and 2021-2022). The mean of N =3 independent replicates is reported. Different letters indicate significantly different values. Tukey HSD test p-value< 0.01.

	Lines	HGW (g)	AS (mm^2)	PL (mm)	L (mm)	W (mm)
GREENHOUSE 2020-2021	**Svevo**	4.27± 0.11 b	19.33± 0.36 b	20.19± 0.20 a	8.44± 0.08 a	2.99± 0.02 b
	Svevo SSIIa⁻	2.40± 0.08 d	11.73± 0.39 d	15.32± 0.21 c	6.14± 0.09 c	2.34± 0.05 d
	Kronos GW2-A1⁻	6.13± 0.04 a	22.48± 0.43 a	19.84± 0.18 a	7.75± 0.07 b	3.76± 0.04 a
	Kronos GW2-A1⁻/Svevo SSIIa⁻	3.82± 0.03 c	16.23± 0.58 c	18.73± 0.30 b	7.60± 0.11 b	2.70± 0.05 c
FIELD 2020-2021	**Svevo**	4.58± 0.15 b	19.27± 0.41 a	18.75± 0.85 a	7.98± 0.08 a	3.15± 0.04 a
	Svevo SSIIa⁻	2.62± 0.12 d	13.66± 0.31 b	17.160± 0.21 b	6.90± 0.07 b	2.42± 0.04 c
	Kronos GW2-A1⁻	5.41± 0.19 a	18.04± 0.31 a	19.06± 0.23 a	7.65± 0.09 a	3.04± 0.04 a
	Kronos GW2-A1⁻/Svevo SSIIa⁻	3.48± 0.10 c	17.22± 0.51 a	19.20± 0.27 a	7.85± 0.11 a	2.78± 0.05 b
FIELD 2021-2022	**Svevo**	4.20± 0.04 b	19.75± 0.44 b	19.58± 0.20 a	8.01± 0.09 a	3.20± 0.04 c
	Svevo SSIIa⁻	2.24± 0.03 d	13.85± 0.39 d	17.49± 0.24 b	7.28± 0.09 b	2.28± 0.04 d
	Kronos GW2-A1⁻	4.80± 0.02 a	17.31± 0.53 c	19.61± 0.24 a	7.99± 0.10 a	3.73± 0.06 a
	Kronos GW2-A1⁻/Svevo SSIIa⁻	3.59± 0.08 c	22.13± 0.45 a	20.65± 0.19 a	8.29± 0.07 a	3.50± 0.06 b

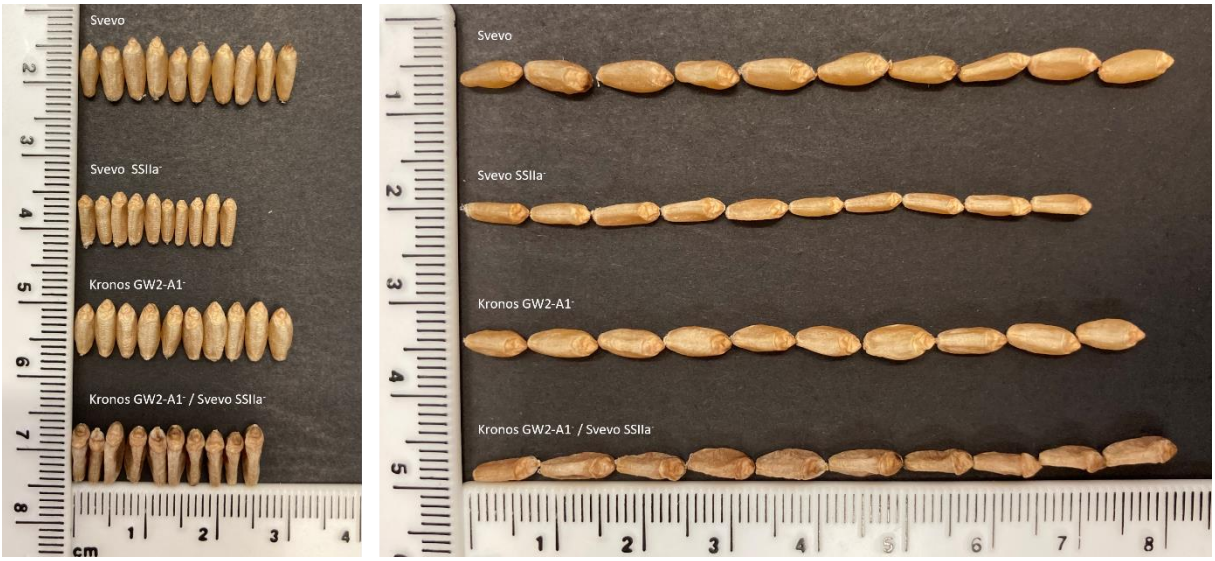

Figure 5.3 Seed width and length comparison among Kronos GW2-A1⁻/Svevo SSIIa⁻ mutants, the controls (Svevo SSIIa⁻, Kronos GW2-A1⁻) and Svevo wild-type. Field materials 2021-2022.

5.3.4 Expression Analysis of Kronos GW2-A1⁻/Svevo SSIIa⁻ genotypes

The study of gene expression was carried out on a set of major genes involved in the starch biosynthetic pathway and potential candidate genes belonging to the family of RING-type E3

ligases. To evaluate if the introgression of the mutant allele *GW2-A1* had an effect on these genes, the comparison of relative expression was among Svevo SSIIa$^-$ (used as control), Kronos GW2-A1$^-$ and Kronos GW2-A1$^-$/Svevo SSIIa$^-$. The list of genes analysed and the primers used are reported, along with the housekeeping gene β-actin, in **Table 5.2**. Among the selected genes, there are three encoding enzymes/proteins involved in the conversion of sucrose into ADP-glucose and viceversa: sucrose synthase (Susy2), UDP-glucose pyrophosphorylase (UGPase) and ADP-glucose transporter (AGPG-t). The last one is required for the import of cytosolic ADP-glucose into the amyloplast for starch biosynthesis (**Kleczkowski, 1996**; **Cakir et al., 2016**).

Susy2, *UGPase* and *ADPG-t* were up-regulated in Kronos GW2-A1$^-$/Svevo SSIIa$^-$ and Kronos GW2-A1$^-$ at 14 DPA compared to the control Svevo SSIIa$^-$. A different trend was observed at 21 DPA where *Susy2* and *ADPG-t* resulted strongly downregulated in both genotypes, whereas the transcripts of *UGPase* were similar to the control (Svevo SSIIa$^-$) (**Figure 5.4**). Regarding the expression of *GW2-A1*, it was not differentially expressed except for the genotype Kronos GW2-A1$^-$ at 21 DPA where it was upregulated (2-fold).

With regard to genes involved in starch biosynthesis, no difference was detected for the *GBSSI* in both genotypes compared to the control in both developmental stage. The transcript abundance of *SSIIa* was higher in Kronos GW2-A1$^-$ compared to control at 14 DPA, whereas no difference was observed at 21 DPA and in the genotype Kronos GW2-A1$^-$/Svevo SSIIa$^-$. An upregulation of *SBEIIa* was detected in both genotypes at 14 DPA. No differences were observed in the expression levels of the same gene at 21 DPA.

Lastly a set of genes belonging to the RING-type E3 ligase family was chosen for the expression analysis as these genes are potential candidates regulating high amylose starch biosynthesis in bread wheat **(Parveen et al. 2021)**. The *RUB3* (TraesCS3B02G461900) gene was not differentially expressed in the mutant lines Kronos GW2-A1$^-$/Svevo SSIIa$^-$ and Kronos GW2-A1$^-$ compared to Svevo SSIIa$^-$ either at 14 DPA or 21 DPA. Differently a significant up-regulation was observed for the *EU3* gene (TraesCS5A02G049400) in both the genotypes and developmental stages; in detail, the transcript abundance was 3-fold at 14 DPA and 8-fold at 21 DPA higher in Kronos GW2-A1$^-$ and 2-fold and 3.5 fold in Kronos GW2-A1$^-$/Svevo SSIIa$^-$ compared to the control. The *RFP* gene (TraesCS6B02G286500) was up-regulated in both genotypes at 21 DPA compared to the control, whereas no difference was detected at 14 DPA (**Figure 5.4**).

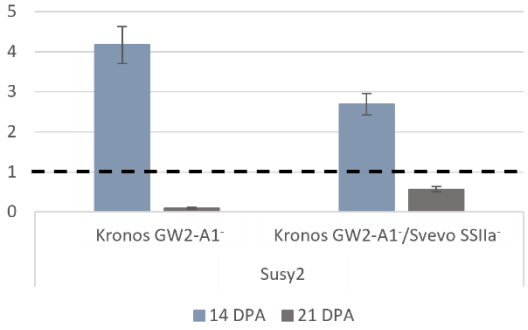
5
4
3
2
1
0
Kronos GW2-A1-
Kronos GW2-A1-/Svevo SSIIa-
Susy2
14 DPA
21 DPA

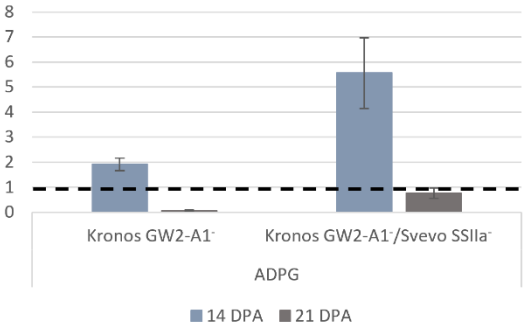
8
7
6
5
4
3
2
1
0
Kronos GW2-A1-
Kronos GW2-A1-/Svevo SSIIa-
ADPG
14 DPA
21 DPA

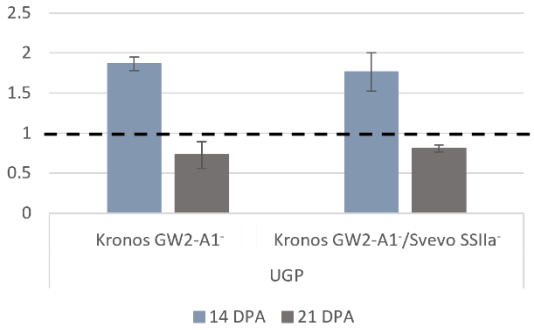
2.5
2
1.5
1
0.5
0
Kronos GW2-A1-
Kronos GW2-A1-/Svevo SSIIa-
UGP
14 DPA
21 DPA

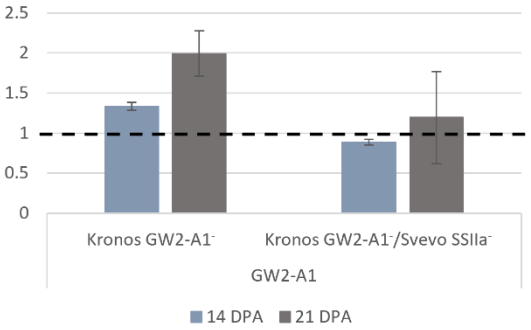
2.5
2
1.5
1
0.5
0
Kronos GW2-A1-
Kronos GW2-A1-/Svevo SSIIa-
GW2-A1
14 DPA
21 DPA

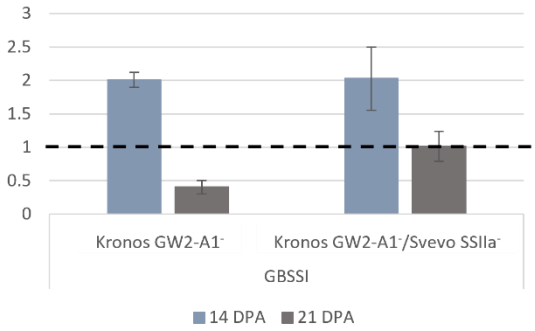
3
2.5
2
1.5
1
0.5
0
Kronos GW2-A1-
Kronos GW2-A1-/Svevo SSIIa-
GBSSI
14 DPA
21 DPA

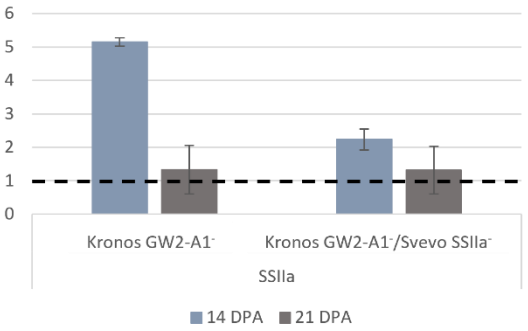
6
5
4
3
2
1
0
Kronos GW2-A1-
Kronos GW2-A1-/Svevo SSIIa-
SSIIa
14 DPA
21 DPA

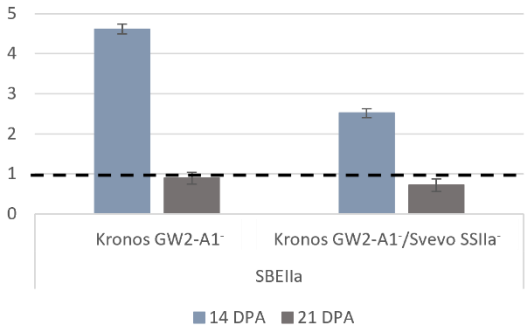
5
4
3
2
1
0
Kronos GW2-A1-
Kronos GW2-A1-/Svevo SSIIa-
SBEIIa
14 DPA
21 DPA

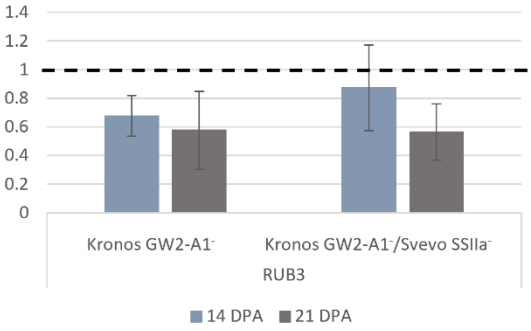
1.4
1.2
1
0.8
0.6
0.4
0.2
0
Kronos GW2-A1-
Kronos GW2-A1-/Svevo SSIIa-
RUB3
14 DPA
21 DPA

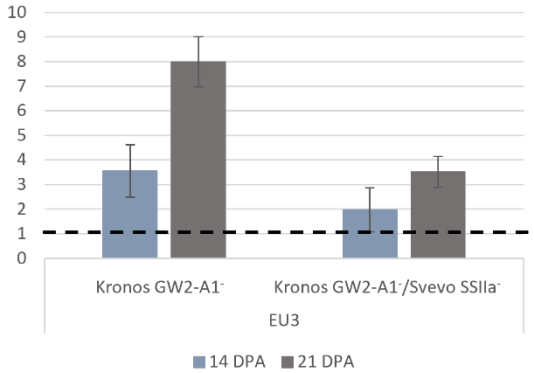
10
9
8
7
6
5
4
3
2
1
0
Kronos GW2-A1-
Kronos GW2-A1-/Svevo SSIIa-
EU3
14 DPA
21 DPA

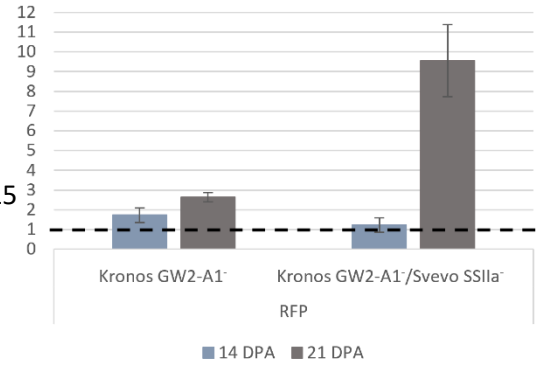
12
11
10
9
8
7
6
5
4
3
2
1
0
Kronos GW2-A1-
Kronos GW2-A1-/Svevo SSIIa-
RFP
14 DPA
21 DPA

Figure 5.4 Relative expression of genes involved in the starch biosynthetic pathway and potential candidate genes belonging to the family of RING-type E3 ligases. The levels of gene expression were determined in relation to the transcription levels of Svevo SSIIa$^-$. The bar graph represents the mean of three biological replicates, each one made of three technical replicates. The dotted line indicates the relative transcription value of the control Svevo SSIIa$^-$ (established at 1). Standard error is indicated above each bar.

5.4 Discussion and conclusion

Non-Communicable Diseases (NCDs) are the leading cause of death worldwide and are the result of a combination of genetic, physiological, environmental and behavioural factors. The main NCDs are cardiovascular diseases (such as heart attack and stroke), cancer, chronic respiratory diseases (such as chronic obstructive pulmonary disease and asthma), diabetes and obesity. The World Health Organization (WHO) indicated blood pressure, overweight/obesity, hyperglycemia, hyperlipidemia as metabolic factors that increase the risk of chronic diseases (**WHO 2022**, https://www.who.int/news-room/fact-sheets/detail/noncommunicable-diseases) and suggested that most of NCDs can be prevented by a correct lifestyle and balance eating habits. In this contest the spread of functional foods (such as those enriched in resistant starch) on the market can constitute a valid tool to achieve the goal. Several efforts have been done to obtain wheat with elevated nutritional value, as the modulation of the ratio amylose/amylopectin that permitted to obtain flour and semolina enriched in RS. There is strong interest by food industry for foods enriched in RS due to their low glycemic profile and prebiotic functionality in the intestine (**Sestili et al., 2015**; **Lockyer and Nugent, 2017**; **Botticella et al., 2021**). In fact, these raw materials have been used to produced functional foods and to carry out interesting in vivo studies that confirmed the positive effects of their consumption on human health, i.e. in the prevention of type 2 diabetes, obesity and colorectal cancer.

However, to be successful cultivated by farmers the high amylose genotypes must be improved in yield as among the pleiotropic effects the most problematic is undoubtedly the one related to yields due to the shrunken kernels. The continuous increase in global population, the effects of climate change, and the decreasing availability of arable land, pose a real threat to global food security. In this scenario, improving crop yield to feed more people has always been the primary goal of agriculture research.

Grain yield is a complex quantitative trait that is determined by various loci and genetic pathways in plants. In wheat grain yield is expressed as the product of different sub-traits such as number of spikes per plant, number of spikelet per spikes, grain number per spikes, grain weight and number of fertile spikes per unit area (**Sreenivasulu and Schnurbusch, 2012**).

In rice, GW2 represents the one of the main QTL that regulates the width and the weight of the seeds. It results to be a negative regulator of cell division (**Song et al., 2007**). Conflicting results

were observed in wheat studying the ortholog of *OsGW2*. In studies carried out on bread and durum wheat, the identification of polymorphisms in the nucleotide sequence led to mutations which determined an increase in the seeds size and weight (**Su et al., 2011**; **Yang et al., 2012**; **Jaiswal et al., 2015**; **Simmonds et al., 2016**. Similarly, transgenic lines, in which the *TaGW2* gene was silenced through RNAi technique, showed seeds with larger weight and width than control plants, confirming that the TaGW2 protein is a negative regulator of seed size (**Hong et al., 2014**).

The research presented aims to combine the health effects of high amylose genotypes with an improved yield. The project involves a durum wheat genotype with a high amylose content in the background of cv. Svevo. With the aim of mitigating the negative effects on yield associated to the presence of mutations on the *SSIIa* genes, the mutant Svevo SSIIa$^-$ was crossed with the Kronos GW2-A1$^-$mutant.

Ten sister lines (Kronos GW2-A1$^-$/Svevo SSIIa$^-$) were selected and characterized at biochemical and molecular level. These lines confirmed a content of amylose and resistant starch higher compared to the controls, in agreement with previous works reporting the silencing of the *SSIIa* genes in durum wheat (**Hogg et al., 2013**; **Hogg et al., 2015**; **Botticella et al., 2016**). Noteworthy along to the amylose and resistant starch content the main non starch polysaccharides, arabinoxylan and b-glucan, both accumulated in the kernel, were also elevated in the whole flour if compared to the control (Svevo). Arabinoxylan and b-glucan are the main component of dietary fiber whose consumption is considered beneficial for human health. So in future perspective it could be interesting to evaluate the synergic effect of different compounds of dietary fibre (resistant starch, arabinoxylan and b-glucan) detected in the Kronos GW2-A1$^-$/Svevo SSIIa$^-$ genotypes.

Regarding yield, the sister lines Kronos GW2-A1$^-$/Svevo SSIIa$^-$ showed a significant improvement of all traits associated to kernel size compared to the parental line Svevo SSIIa$^-$, except for total starch that was decreased. This last observation confirmed that *GW2-A1* gene has a role as repressor of the cell division in the kernel, but also suggested a potential role in the activation or regulation of genes involved in starch biosynthesis. Although the grain size and weight were significantly improved compared to Svevo SSIIa$^-$, the values were yet lower than Svevo and Kronos GW2-A1$^-$, highlighting the necessity to continue in the breeding program. Given the reduction in starch content, possible targets could be the transcription factors involved in the activation or repression of key genes of starch synthesis.

The study of gene expression based on the comparison between the parental Svevo SSIIa$^-$ and Kronos GW2-A1$^-$/Svevo SSIIa$^-$ was carried out to verify whether the mutations had pleiotropic effects on starch biosynthetic genes and potential candidate genes belonging to the family of RING-type E3 ligases,

The genes encoding Susy2, UGPase and ADPG-t were chosen as they are key control points of carbon partitioning, acting upstream of starch synthesis. The analysis of transcript abundance

revealed an up-regulation of *Susy2* and *ADPG-t* in Kronos GW2-A1^{-}/Svevo SSIIa^{-} at 14 DPA compared to Svevo SSIIa^{-}. This result is in agreement with previous works (**Clarke et al., 2008**; **Botticella et al., 2018)**, where *Susy2* resulted up-regulated in mutant lines lacking SSIIa activity respectively in barley and bread wheat. Although the up-regulation of *ADPG-t* suggests an increased rate of transport of ADP-glucose to the amyloplast, total starch remained unaltered or reduced.

Previous studies reported that GW2 is involved in grain size and weight in rice (**Song et al., 2007**) and wheat possibly by regulating the expression of starch biosynthetic pathway genes (**Geng et al., 2017**). The suppression of *TdGW2* in durum wheat cv. Svevo through RNAi increased the starch content by 10–40%, width by 4–13% and surface area by 3–5%, suggesting an active role of GW2 RING finger E3 ligase in starch biosynthesis (**Sestili et al., 2019**). **Parveen et al. (2021)** performed a genome-wide analysis of RING-type E3 ligase family in order to study the putative role of RING protein in amylose biosynthesis. Except for the gene TraesCS3B02G461900 encoding a RING protein, not affected in the expression analysis in selected mutant lines Kronos GW2-A1^{-}/Svevo SSIIa^{-} and Kronos GW2-A1^{-} compared to Svevo SSIIa^{-}, the other two genes TraesCS5A02G049400 and TraesCS6B02G286500 were up-regulated in the analysed genotypes. According to **Parveen et al. (2021)** the RING protein gene TraesCS6B02G286500 was found to be extremely up-regulated at later seed developmental stages (21 DPA) when amylose biosynthesis is high hence they might possibly act as positive regulators for amylose biosynthesis.

In conclusion, this study allowed to obtain durum wheat mutants in which the negative yield-related traits associated to the presence of mutations on the *SSIIa* genes are compensated through the silencing of *TdGW2-A1*, a negative regulator of grain yield. The Kronos GW2-A1^{-}/Svevo SSIIa^{-} mutants demonstrated that introgression of the GW2-A1 mutation had a good effect on grain size and yield without affecting the improved nutritional value associated with high-amylose genotypes. The high nutritional value together with an improved yield represent two important traits that combined in a single genotype can be used for genetic improvement programs to satisfy the demand that the scientific community is facing.

References

Aggarwal, S., Kumar, A., Bhati, K. K., Kaur, G., Shukla, V., Tiwari, S., & Pandey, A. K. (2018). RNAi-mediated downregulation of inositol pentakisphosphate kinase (IPK1) in wheat grains decreases phytic acid levels and increases Fe and Zn accumulation. *Frontiers in plant science*, *9*, 259.

Aiken, R. M., & Smucker, A. J. M. (1996). Root system regulation of whole plant growth. *Annual review of phytopathology*, *34*(1), 325-346.

Akhunov, E. D., Akhunova, A. R., Linkiewicz, A. M., Dubcovsky, J., Hummel, D., Lazo, G., ... & Dvorak, J. (2003). Synteny perturbations between wheat homoeologous chromosomes caused by locus duplications and deletions correlate with recombination rates. *Proceedings of the National Academy of Sciences*, *100*(19), 10836-10841.

Ali, N., Paul, S., Gayen, D., Sarkar, S. N., Datta, K., & Datta, S. K. (2013). Development of low phytate rice by RNAi mediated seed-specific silencing of inositol 1, 3, 4, 5, 6-pentakisphosphate 2-kinase gene (IPK1). *PloS one*, *8*(7), e68161.

Ariza-Nieto, M., Blair, M. W., Welch, R. M., & Glahn, R. P. (2007). Screening of iron bioavailability patterns in eight bean (Phaseolus vulgaris L.) genotypes using the Caco-2 cell in vitro model. *J. of Agricultural and Food Chemistry*, *55*(19), 7950-7956.

Bennett, J. E., Stevens, G. A., Mathers, C. D., Bonita, R., Rehm, J., Kruk, M. E., ... & Ezzati, M. (2018). NCD Countdown 2030: worldwide trends in non-communicable disease mortality and progress towards Sustainable Development Goal target 3.4. *The lancet*, *392*(10152), 1072-1088.

Benziger, C. P., Roth, G. A., & Moran, A. E. (2016). The global burden of disease study and the preventable burden of NCD. *Global heart*, *11*(4), 393-397.

Beres, B. L., Rahmani, E., Clarke, J. M., Grassini, P., Pozniak, C. J., Geddes, C. M., ... & Ransom, J. K. (2020). A systematic review of durum wheat: Enhancing production systems by exploring genotype, environment, and management (G× E× M) synergies. *Frontiers in Plant Science*, *11*, 568657.

Bhati, K. K., Aggarwal, S., Sharma, S., Mantri, S., Singh, S. P., Bhalla, S., ... & Pandey, A. K. (2014). Differential expression of structural genes for the late phase of phytic acid biosynthesis in developing seeds of wheat (Triticum aestivum L.). *Plant Science*, *224*, 74-85.

Bhati, K. K., Alok, A., Kumar, A., Kaur, J., Tiwari, S., & Pandey, A. K. (2016). Silencing of ABCC13 transporter in wheat reveals its involvement in grain development, phytic acid accumulation and lateral root formation. *Journal of Experimental Botany*, *67*(14), 4379-4389.

Bhave, M., & Morris, C. F. (2008). Molecular genetics of puroindolines and related genes: allelic diversity in wheat and other grasses. *Plant molecular biology*, *66*, 205-219.

Birt, D. F., Boylston, T., Hendrich, S., Jane, J. L., Hollis, J., Li, L., ... & Whitley, E. M. (2013). Resistant starch: promise for improving human health. *Advances in nutrition*, *4*(6), 587-601.

Botticella, E., Sestili, F., Hernandez-Lopez, A., Phillips, A., & Lafiandra, D. (2011). High resolution melting analysis for the detection of EMS induced mutations in wheat Sbella genes. *BMC Plant Biology*, *11*(1), 1-14.

Botticella, E., Sestili, F., Ferrazzano, G., Mantovani, P., Cammerata, A., D'Egidio, M. G., & Lafiandra, D. (2016). The impact of the SSIIa null mutations on grain traits and composition in durum wheat. *Breeding science*, *66*(4), 572-579.

Botticella, E., Sestili, F., Sparla, F., Moscatello, S., Marri, L., Cuesta-Seijo, J. A., ... & Lafiandra, D. (2018). Combining mutations at genes encoding key enzymes involved in starch synthesis affects the amylose content, carbohydrate allocation and hardness in the wheat grain. *Plant Biotechnology Journal*, *16*(10), 1723-1734.

Botticella, E., Savatin, D. V., & Sestili, F. (2021). The triple jags of dietary fibers in cereals: How biotechnology is longing for high fiber grains. *Frontiers in Plant Science*, *12*, 745579.

Boyer, C. D., & Preiss, J. (1978). Multiple forms of starch branching enzyme of maize: evidence for independent genetic control. *Biochemical and biophysical research communications*, *80*(1), 169-175.

Burge, C., & Karlin, S. (1997). Prediction of complete gene structures in human genomic DNA. *Journal of molecular biology*, *268*(1), 78-94.

Bushuk, W. (1998). Wheat breeding for end-product use. *Euphytica*, *100*, 137-145.

Cakir, B., Shiraishi, S., Tuncel, A., Matsusaka, H., Satoh, R., Singh, S., ... & Okita, T. W. (2016). Analysis of the rice ADP-glucose transporter (OsBT1) indicates the presence of regulatory processes in the amyloplast stroma that control ADP-glucose flux into starch. *Plant physiology*, *170*(3), 1271-1283.

Celletti, S., Pii, Y., Mimmo, T., Cesco, S., & Astolfi, S. (2016). The characterization of the adaptive responses of durum wheat to different Fe availability highlights an optimum Fe requirement threshold. *Plant Physiology and Biochemistry*, *109*, 300-307.

Cerino Badone, F., Amelotti, M., Cassani, E., & Pilu, R. (2012). Study of low phytic acid1-7 (lpa1-7), a new ZmMRP4 mutation in maize. *Journal of Heredity*, *103*(4), 598-605.

Chang, J. M., Di Tommaso, P., Taly, J. F., & Notredame, C. (2012). Accurate multiple sequence alignment of transmembrane proteins with PSI-Coffee. *BMC bioinformatics*, *13*, 1-7.

Chantret, N., Salse, J., Sabot, F., Rahman, S., Bellec, A., Laubin, B., ... & Chalhoub, B. (2005). Molecular basis of evolutionary events that shaped the hardness locus in diploid and polyploid wheat species (Triticum and Aegilops). *The Plant Cell*, *17*(4), 1033-1045.

Chaudhary, J., Deshmukh, R., & Sonah, H. (2019). Mutagenesis approaches and their role in crop improvement. *Plants*, *8*(11), 467.

Chen, J., & Raymond, K. (2008). Beta-glucans in the treatment of diabetes and associated cardiovascular risks. *Vascular health and risk management*, *4*(6), 1265-1272.

Chrastil, J. (1987). Improved colorimetric determination of amylose in starches or flours. *Carbohydrate research*, *159*(1), 154-158.

Clarke, B., Liang, R., Morell, M. K., Bird, A. R., Jenkins, C. L. D., & Li, Z. (2008). Gene expression in a starch synthase IIa mutant of barley: changes in the level of gene transcription and grain composition. *Functional & integrative genomics*, *8*, 211-221.

Colombo, F., Paolo, D., Cominelli, E., Sparvoli, F., Nielsen, E., & Pilu, R. (2020). MRP transporters and low phytic acid mutants in major crops: Main pleiotropic effects and future perspectives. *Frontiers in plant science*, *11*, 1301.

Cominelli, E., Confalonieri, M., Carlessi, M., Cortinovis, G., Daminati, M. G., Porch, T. G., ... & Sparvoli, F. (2018). Phytic acid transport in Phaseolus vulgaris: A new low phytic acid mutant in the PvMRP1 gene and study of the PvMRPs promoters in two different plant systems. *Plant Science*, *270*, 1-12.

Cominelli, E., Pilu, R., & Sparvoli, F. (2020a). Phytic acid and transporters: what can we learn from low phytic acid mutants?. *Plants*, *9*(1), 69.

Cominelli, E., Galimberti, M., Pongrac, P., Landoni, M., Losa, A., Paolo, D., ... & Sparvoli, F. (2020b). Calcium redistribution contributes to the hard-to-cook phenotype and increases PHA-L lectin thermal stability in common bean low phytic acid 1 mutant seeds. *Food Chemistry*, *321*, 126680.

Cornell, H. J. (2012). The chemistry and biochemistry of wheat. In *Breadmaking* (pp. 35-76). Woodhead Publishing.

Dalmo, R. A., & Bøgwald, J. (2008). ß-glucans as conductors of immune symphonies. *Fish & shellfish immunology*, *25*(4), 384-396.

De Kochko, A., & Hamon, S. (1990). A rapid and efficient method for the isolation of restrictable total DNA from plants of the genus Abelmoschus. *Plant Molecular Biology Reporter*, *8*, 3-7.

De Vita, P., & Taranto, F. (2019). Durum wheat (Triticum turgidum ssp. durum) breeding to meet the challenge of climate change. *Advances in Plant Breeding Strategies: Cereals*: Volume 5, 471-524.

Dubcovsky, J., & Dvorak, J. (2007). Genome plasticity a key factor in the success of polyploid wheat under domestication. *Science*, *316*(5833), 1862-1866.

DuPont, F. M., & Altenbach, S. B. (2003). Molecular and biochemical impacts of environmental factors on wheat grain development and protein synthesis. *Journal of cereal science*, *38*(2), 133-146.

Dvorak, J., McGuire, P. E., & Cassidy, B. (1988). Apparent sources of the A genomes of wheats inferred from polymorphism in abundance and restriction fragment length of repeated nucleotide sequences. *Genome*, *30*(5), 680-689.

Dvorak, J., Terlizzi, P. D., Zhang, H. B., & Resta, P. (1993). The evolution of polyploid wheats: identification of the A genome donor species. *Genome*, *36*(1), 21-31.

Edwards, A., Vincken, J. P., Suurs, L. C., Visser, R. G., Zeeman, S., Smith, A., & Martin, C. (2002). Discrete forms of amylose are synthesized by isoforms of GBSSI in pea. *The Plant Cell*, *14*(8), 1767-1785.

Evers, T., & Millar, S. (2002). Cereal grain structure and development: some implications for quality. *Journal of cereal science*, *36*(3), 261-284.

FAO, IFAD, UNICEF, WFP, and WHO. (2019). The State of Food Security and Nutrition in the World 2019. Safeguarding Against Economic Slowdowns and Downturns. Rome: FAO. Available online at: http://www.fao.org/3/ca5162en/ca5162en.pdf.

Faris, J. D. (2014). Wheat domestication: Key to agricultural revolutions past and future. *Genomics of Plant Genetic Resources: Volume 1. Managing, sequencing and mining genetic resources*, 439-464.

Feldman, M. (2001). Origin of cultivated wheat. *The world wheat book: a history of wheat breeding*, 3-53.

Feldman, M., Levy, A., Chalhoub, B., & Kashkush, K. (2012). Genomic plasticity in polyploid wheat. *Polyploidy and genome evolution*, 109-135.

Finnie, S. M., Bettge, A. D., & Morris, C. F. (2006). Influence of cultivar and environment on water-soluble and water-insoluble arabinoxylans in soft wheat. *Cereal Chemistry*, *83*(6), 617-623.

Frischmeyer, P. A., & Dietz, H. C. (1999). Nonsense-mediated mRNA decay in health and disease. *Human molecular genetics*, *8*(10), 1893-1900.

Frittelli, A., Botticella, E., Palombieri, S., Masci, S., Celletti, S., Fontanella, M. C., ... & Sestili, F. (2023). The suppression of TdMRP3 genes reduces the phytic acid and increases the nutrient accumulation in durum wheat grain. *Frontiers in Plant Science*, *14*, 46.

Fu, J., Peterson, K., Guttieri, M., Souza, E., & Raboy, V. (2008). Barley (Hordeum vulgare L.) inositol monophosphatase: gene structure and enzyme characteristics. *Plant Molecular Biology*, *67*, 629-642.

Garcia Molina, M. D., Botticella, E., Beleggia, R., Palombieri, S., De Vita, P., Masci, S., ... & Sestili, F. (2021). Enrichment of provitamin A content in durum wheat grain by suppressing β-carotene hydroxylase 1 genes with a TILLING approach. *Theoretical and Applied Genetics*, *134*, 4013-4024.

Garg, M., Sharma, N., Sharma, S., Kapoor, P., Kumar, A., Chunduri, V., & Arora, P. (2018). Biofortified crops generated by breeding, agronomy, and transgenic approaches are improving lives of millions of people around the world. *Frontiers in Nutrition*, *5*, 12.

Geng, J., Li, L., Lv, Q., Zhao, Y., Liu, Y., Zhang, L., & Li, X. (2017). TaGW2-6A allelic variation contributes to grain size possibly by regulating the expression of cytokinins and starch-related genes in wheat. *Planta*, *246*, 1153-1163.

Gilchrist, E., & Haughn, G. (2010). Reverse genetics techniques: engineering loss and gain of gene function in plants. *Briefings in functional genomics*, *9*(2), 103-110.

Giroux, M. J., & Morris, C. F. (1997). A glycine to serine change in puroindoline b is associated with wheat grain hardness and low levels of starch-surface friabilin. *Theoretical and Applied Genetics*, *95*, 857-864.

Global indicator framework for the Sustainable Development Goals and targets of the 2030 Agenda for Sustainable Development. Available at: https://unstats.un.org/sdgs/indicators/Global%20Indicator%20Framework%20after%202022%20refinement_Eng.pdf (Accessed March 2023).

Grases, F., Prieto, R. M., & Costa-Bauza, A. (2017). Dietary phytate and interactions with mineral nutrients. *Clinical aspects of natural and added phosphorus in foods*, 175-183.

Graybosch, R. A. (1998). Waxy wheats: Origin, properties, and prospects. *Trends in Food Science & Technology*, *9*(4), 135-142.

Guttieri, M., Bowen, D., Dorsch, J. A., Raboy, V., & Souza, E. (2004). Identification and characterization of a low phytic acid wheat. *Crop Science*, *44*(2), 418-424.

Guttieri, M. J., Peterson, K. M., & Souza, E. J. (2006). Agronomic performance of low phytic acid wheat. *Crop Science*, *46*(6), 2623-2629.

Hazard, B., Zhang, X., Naemeh, M., & Dubcovsky, J. (2014). Registration of durum wheat germplasm lines with combined mutations in SBEIIa and SBEIIb genes conferring increased amylose and resistant starch. *Journal of plant registrations*, *8*(3), 334-338.

Hemery, Y., Rouau, X., Lullien-Pellerin, V., Barron, C., & Abecassis, J. (2007). Dry processes to develop wheat fractions and products with enhanced nutritional quality. *Journal of cereal science*, *46*(3), 327-347.

Hinsinger, P., Bengough, A. G., Vetterlein, D., & Young, I. M. (2009). Rhizosphere: biophysics, biogeochemistry and ecological relevance.

Hogg, A. C., Gause, K., Hofer, P., Martin, J. M., Graybosch, R. A., Hansen, L. E., & Giroux, M. J. (2013). Creation of a high-amylose durum wheat through mutagenesis of starch synthase II (SSIIa). *Journal of Cereal Science*, *57*(3), 377-383.

Hogg, A. C., Martin, J. M., Manthey, F. A., & Giroux, M. J. (2015). Nutritional and quality traits of pasta made from SSIIa null high-amylose durum wheat. *Cereal Chemistry*, *92*(4), 395-400.

Hogg, A. C., Martin, J. M., & Giroux, M. J. (2017). Novel ssIIa alleles produce specific seed amylose levels in hexaploid wheat. *Cereal Chemistry*, *94*(6), 1008-1015.

Hogg, A. C., & Giroux, M. J. (2019). Milling and baking quality of hexaploid spring wheat starch synthase IIa (ssIIa) mutants with elevated amylose content. *Cereal Chemistry*, *96*(3), 532-544.

Hong, Y., Chen, L., Du, L. P., Su, Z., Wang, J., Ye, X., ... & Zhang, Z. (2014). Transcript suppression of TaGW2 increased grain width and weight in bread wheat. *Functional & integrative genomics*, *14*, 341-349.

Hua, K., Zhang, J., Botella, J. R., Ma, C., Kong, F., Liu, B., & Zhu, J. K. (2019). Perspectives on the application of genome-editing technologies in crop breeding. *Molecular Plant*, *12*(8), 1047-1059.

Huang, S., Sirikhachornkit, A., Su, X., Faris, J., Gill, B., Haselkorn, R., & Gornicki, P. (2002). Genes encoding plastid acetyl-CoA carboxylase and 3-phosphoglycerate kinase of the Triticum/Aegilops complex and the evolutionary history of polyploid wheat. *Proceedings of the National Academy of Sciences*, *99*(12), 8133-8138.

Hwang, J. U., Song, W. Y., Hong, D., Ko, D., Yamaoka, Y., Jang, S., ... & Lee, Y. (2016). Plant ABC transporters enable many unique aspects of a terrestrial plant's lifestyle. *Molecular plant*, *9*(3), 338-355.

Ibrahim, S., Saleem, B., Rehman, N., Zafar, S. A., Naeem, M. K., & Khan, M. R. (2022). CRISPR/Cas9 mediated disruption of Inositol Pentakisphosphate 2-Kinase 1 (TaIPK1) reduces phytic acid and improves iron and zinc accumulation in wheat grains. *Journal of Advanced Research*, *37*, 33-41.

Jaiswal, V., Gahlaut, V., Mathur, S., Agarwal, P., Khandelwal, M. K., Khurana, J. P., … & Gupta, P. K. (2015). Identification of Novel SNP in Promoter Sequence of TaGW2-6A Associated with Grain Weight and Other Agronomic Traits in Wheat (Triticum aestivum L.). *PLOS ONE*, *10*(6), e0129400.

Jeon, J. S., Ryoo, N., Hahn, T. R., Walia, H., & Nakamura, Y. (2010). Starch biosynthesis in cereal endosperm. *Plant physiology and Biochemistry*, *48*(6), 383-392.

Jongsutjarittam, O., & Charoenrein, S. (2014). The effect of moisture content on physicochemical properties of extruded waxy and non-waxy rice flour. *Carbohydrate Polymers*, *114*, 133-140.

Kadkol, G. P., & Sissons, M. (2016). Durum Wheat Overview, Reference Module in *Food Science*.

Kent, N. L. (1994). Kent's Technology of Cereals: An introduction for students of food science and agriculture. Elsevier.

Kilian, B., Martin, W., & Salamini, F. (2010). Genetic diversity, evolution and domestication of wheat and barley in the Fertile Crescent. *Evolution in Action: Case Studies in Adaptive Radiation, Speciation and the Origin of Biodiversity*, 137-166.

Kiran, A., Wakeel, A., Mahmood, K., Mubaraka, R., & Haefele, S. M. (2022). Biofortification of staple crops to alleviate human malnutrition: contributions and potential in developing countries. *Agronomy*, *12*(2), 452.

Kleczkowski, L. A. (1996). Back to the drawing board: redefining starch synthesis in cereals. *Trends in Plant Science*, *1*(11), 363-364.

Klein, M., Burla, B., & Martinoia, E. (2006). The multidrug resistance-associated protein (MRP/ABCC) subfamily of ATP-binding cassette transporters in plants. *FEBS letters*, *580*(4), 1112-1122.

Kolster, P. (1992). High molecular weight glutenin subunits of wheat: qualitative and quantitative variation in relation to bread-making quality. Wageningen University and Research.

Krasileva, K. V., Vasquez-Gross, H. A., Howell, T., Bailey, P., Paraiso, F., Clissold, L., ... & Dubcovsky, J. (2017). Uncovering hidden variation in polyploid wheat. *Proceedings of the National Academy of Sciences*, *114*(6), E913-E921.

Krishnan, H. B. (2008). Preparative procedures markedly influence the appearance and structural integrity of protein storage vacuoles in soybean seeds. *Journal of agricultural and food chemistry*, *56*(9), 2907-2912.

Krishnan, S., Ebenezer, G. A. I., & Dayanandan, P. (2001). Histochemical localization of storage components in caryopsis of rice (Oryza sativa L.). *Current Science*, 567-571.

Krishnappa, G., Singh, A. M., Chaudhary, S., Ahlawat, A. K., Singh, S. K., Shukla, R. B., ... & Solanki, I. S. (2017). Molecular mapping of the grain iron and zinc concentration, protein content and thousand kernel weight in wheat (Triticum aestivum L.). *PLoS One*, *12*(4), e0174972.

Kuo, H. F., Chang, T. Y., Chiang, S. F., Wang, W. D., Charng, Y. Y., & Chiou, T. J. (2014). Arabidopsis inositol pentakisphosphate 2-kinase, AtIPK1, is required for growth and modulates phosphate homeostasis at the transcriptional level. *The Plant Journal*, *80*(3), 503-515.

Kurowska, M., Daszkowska-Golec, A., Gruszka, D., Marzec, M., Szurman, M., Szarejko, I., & Maluszynski, M. (2011). TILLING-a shortcut in functional genomics. *Journal of applied genetics*, *52*, 371-390.

Lafiandra, D., Sestili, F., D'Ovidio, R., Janni, M., Botticella, E., Ferrazzano, G., ... & DeAmbrogio, E. (2010). Approaches for modification of starch composition in durum wheat. *Cereal chemistry*, *87*(1), 28-34.

Lambers, H., Shane, M. W., Cramer, M. D., Pearse, S. J., & Veneklaas, E. J. (2006). Root structure and functioning for efficient acquisition of phosphorus: matching morphological and physiological traits. *Annals of botany*, *98*(4), 693-713.

Lee, H. S., Lee, D. H., Cho, H. K., Kim, S. H., Auh, J. H., & Pai, H. S. (2015). InsP6-sensitive variants of the Gle1 mRNA export factor rescue growth and fertility defects of the ipk1 low-phytic-acid mutation in Arabidopsis. *The Plant Cell*, *27*(2), 417-431.

Levy, A. A., & Feldman, M. (2022). Evolution and origin of bread wheat. *The Plant Cell*, *34*(7), 2549-2567.

Li, Z., Chu, X., Mouille, G., Yan, L., Kosar-Hashemi, B., Hey, S., ... & Rahman, S. (1999). The localization and expression of the class II starch synthases of wheat. *Plant physiology*, *120*(4), 1147-1156.

Li, W., Huang, L., & Gill, B. S. (2008). Recurrent deletions of puroindoline genes at the grain hardness locus in four independent lineages of polyploid wheat. *Plant physiology*, *146*(1), 200-212.

Linde-Laursen, I., Heslop-Harrison, J. S., Shepherd, K. W., & Taketa, S. (1997). The barley genome and its relationship with the wheat genomes. A survey with an internationally agreed recommendation for barley chromosome nomenclature. *hereditas*, *126*(1), 1-16.

Liu, E., Pimpin, L., Shulkin, M., Kranz, S., Duggan, C. P., Mozaffarian, D., & Fawzi, W. W. (2018). Effect of zinc supplementation on growth outcomes in children under 5 years of age. *Nutrients*, *10*(3), 377.

Lochlainn, S. Ó., Amoah, S., Graham, N. S., Alamer, K., Rios, J. J., Kurup, S., ... & Broadley, M. R. (2011). High Resolution Melt (HRM) analysis is an efficient tool to genotype EMS mutants in complex crop genomes. *Plant Methods*, *7*, 1-9.

Lockyer, S., & Nugent, A. P. (2017). Health effects of resistant starch. *Nutrition bulletin*, *42*(1), 10-41.

Lockyer, S., White, A., & Buttriss, J. L. (2018). Biofortified crops for tackling micronutrient deficiencies–what impact are these having in developing countries and could they be of relevance within Europe?. *Nutrition Bulletin*, *43*(4), 319-357.

Lopez, H. W., Leenhardt, F., Coudray, C., & Remesy, C. (2002). Minerals and phytic acid interactions: is it a real problem for human nutrition?. *International journal of food science & technology*, *37*(7), 727-739.

López-Bucio, J., Cruz-Ramırez, A., & Herrera-Estrella, L. (2003). The role of nutrient availability in regulating root architecture. *Current opinion in plant biology*, *6*(3), 280-287.

Lowe, N. M. (2021). The global challenge of hidden hunger: Perspectives from the field. *Proceedings of the Nutrition Society*, *80*(3), 283-289.

Ludwig, Y., & Slamet-Loedin, I. H. (2019). Genetic biofortification to enrich rice and wheat grain iron: from genes to product. *Frontiers in Plant Science*, *10*, 833.

Mangueze, A. V. D. J., Pessoa, M. F., Silva, M. J., Ndayiragije, A., Magaia, H. E., Cossa, V. S., ... & Ramalho, J. C. (2018). Simultaneous zinc and selenium biofortification in rice. Accumulation, localization and implications on the overall mineral content of the flour. *Journal of cereal science*, *82*, 34-41.

Manjeru, P., Van Biljon, A., & Labuschagne, M. (2019). The development and release of maize fortified with provitamin A carotenoids in developing countries. *Critical reviews in food science and nutrition*, *59*(8), 1284-1293.

Martin, C. R., Rousser, R., & Brabec, D. L. (1993). Development of a single-kernel wheat characterization system. *Transactions of the ASAE*, *36*(5), 1399-1404.

Martínez-Moreno, F., Ammar, K., & Solís, I. (2022). Global changes in cultivated area and breeding activities of durum wheat from 1800 to date: A historical review. *Agronomy*, *12*(5), 1135.

Mayer, K. F., Martis, M., Hedley, P. E., Šimková, H., Liu, H., Morris, J. A., ... & Stein, N. (2011). Unlocking the barley genome by chromosomal and comparative genomics. *The Plant Cell*, *23*(4), 1249-1263.

McCallum, C. M., Comai, L., Greene, E. A., & Henikoff, S. (2000). T argeting I nduced L ocal L esions IN G enomes (TILLING) for plant functional genomics. *Plant physiology*, *123*(2), 439-442.

Meis, S. J., Fehr, W. R., & Schnebly, S. R. (2003). Seed source effect on field emergence of soybean lines with reduced phytate and raffinose saccharides. *Crop Science*, *43*(4), 1336-1339.

Montpetit, B., Thomsen, N. D., Helmke, K. J., Seeliger, M. A., Berger, J. M., & Weis, K. (2011). A conserved mechanism of DEAD-box ATPase activation by nucleoporins and InsP6 in mRNA export. *Nature*, *472*(7342), 238-242.

Morell, M. K., Kosar-Hashemi, B., Cmiel, M., Samuel, M. S., Chandler, P., Rahman, S., ... & Li, Z. (2003). Barley sex6 mutants lack starch synthase IIa activity and contain a starch with novel properties. *The Plant Journal*, *34*(2), 173-185.

Morita, M. T., Kato, T., Nagafusa, K., Saito, C., Ueda, T., Nakano, A., & Tasaka, M. (2002). Involvement of the vacuoles of the endodermis in the early process of shoot gravitropism in Arabidopsis. *The Plant Cell*, *14*(1), 47-56.

Morris, C. F. (2002). Puroindolines: the molecular genetic basis of wheat grain hardness. *Plant molecular biology*, *48*, 633-647.

Morris, C. E., & Sands, D. C. (2006). The breeder's dilemma—yield or nutrition?. *Nature biotechnology*, *24*(9), 1078-1080.

Morris, C. F., Simeone, M. C., King, G. E., & Lafiandra, D. (2011). Transfer of soft kernel texture from Triticum aestivum to durum wheat, Triticum turgidum ssp. durum. *Crop Science*, *51*(1), 114-122.

Morris, C. F. (2019). Development of soft kernel durum wheat. *Front. Agric. Sci. Eng*, *6*, 273-278.

Muthayya, S., Rah, J. H., Sugimoto, J. D., Roos, F. F., Kraemer, K., & Black, R. E. (2013). The global hidden hunger indices and maps: an advocacy tool for action. *PloS one*, *8*(6), e67860.

Nagy, R., Grob, H., Weder, B., Green, P., Klein, M., Frelet-Barrand, A., ... & Martinoia, E. (2009). The Arabidopsis ATP-binding cassette protein AtMRP5/AtABCC5 is a high affinity inositol hexakisphosphate transporter involved in guard cell signaling and phytate storage. *Journal of Biological Chemistry*, *284*(48), 33614-33622.

Nakamura, T., Yamamori, M., Hirano, H., Hidaka, S., & Nagamine, T. (1995). Production of waxy (amylose-free) wheats. *Molecular and General Genetics MGG*, *248*, 253-259.

Nalam, V. J., Vales, M. I., Watson, C. J., Kianian, S. F., & Riera-Lizarazu, O. (2006). Map-based analysis of genes affecting the brittle rachis character in tetraploid wheat (Triticum turgidum L.). *Theoretical and Applied Genetics*, *112*, 373-381.

O'Dell, B. L., De Boland, A. R., & Koirtyohann, S. R. (1972). Distribution of phytate and nutritionally important elements among the morphological components of cereal grains. *Journal of Agricultural and Food Chemistry*, *20*(3), 718-723.

Oladosu, Y., Rafii, M. Y., Abdullah, N., Hussin, G., Ramli, A., Rahim, H. A., ... & Usman, M. (2016). Principle and application of plant mutagenesis in crop improvement: a review. *Biotechnology & Biotechnological Equipment*, *30*(1), 1-16.

Olson, R., Gavin-Smith, B., Ferraboschi, C., & Kraemer, K. (2021). Food fortification: The advantages, disadvantages and lessons from sight and life programs. *Nutrients*, *13*(4), 1118.

Oltmans, S. E., Fehr, W. R., Welke, G. A., Raboy, V., & Peterson, K. L. (2005). Agronomic and seed traits of soybean lines with low–phytate phosphorus. *Crop Science*, *45*(2), 593-598.

Orth, R. A., & Shellenberger, J. A. (1988). Origin, production, and utilization of wheat. *Wheat chemistry and technology*, *3*, 1-14.

Osborne, B. G., & Anderssen, R. S. (2003). Single-kernel characterization principles and applications. *Cereal Chemistry*, *80*(5), 613-622.

Pagès, L., Bernert, M., & Pagès, G. (2020). Modelling time variations of root diameter and elongation rate as related to assimilate supply and demand. *Journal of Experimental Botany*, *71*(12), 3524-3534.

Pareyt, B., Finnie, S. M., Putseys, J. A., & Delcour, J. A. (2011). Lipids in bread making: Sources, interactions, and impact on bread quality. *Journal of Cereal Science*, *54*(3), 266-279.

Parry, M. A., Madgwick, P. J., Bayon, C., Tearall, K., Hernandez-Lopez, A., Baudo, M., ... & Phillips, A. L. (2009). Mutation discovery for crop improvement. *Journal of Experimental Botany*, *60*(10), 2817-2825.

Parveen, A., Rahim, M. S., Sharma, A., Mishra, A., Kumar, P., Fandade, V., ... & Roy, J. (2021). Genome-wide analysis of RING-type E3 ligase family identifies potential candidates regulating high amylose starch biosynthesis in wheat (Triticum aestivum L.). *Scientific Reports*, *11*(1), 11461.

Pasricha, S. R., Low, M., Thompson, J., Farrell, A., & De-Regil, L. M. (2014). Iron supplementation benefits physical performance in women of reproductive age: a systematic review and meta-analysis. *The Journal of nutrition*, *144*(6), 906-914.

Péret, B., Clément, M., Nussaume, L., & Desnos, T. (2011). Root developmental adaptation to phosphate starvation: better safe than sorry. *Trends in plant science*, *16*(8), 442-450.

Pilu, R., Landoni, M., Cassani, E., Doria, E., & Nielsen, E. (2005). The maize lpa241 mutation causes a remarkable variability of expression and some pleiotropic effects. *Crop Science*, *45*(5), 2096-2105.

Pont, C., Murat, F., Guizard, S., Flores, R., Foucrier, S., Bidet, Y., ... & Salse, J. (2013). Wheat syntenome unveils new evidences of contrasted evolutionary plasticity between paleo-and neoduplicated subgenomes. *The Plant Journal*, *76*(6), 1030-1044.

Prom-u-Thai, C., Dell, B., Thomson, G., & Rerkasem, B. (2003). Easy and rapid detection of iron in rice grain. *ScienceAsia*, *29*, 203-207.

Quagliata, G., Abdirad, S., Celletti, S., Sestili, F., & Astolfi, S. (2023). Screening of Triticum turgidum genotypes for tolerance to drought stress. *Plant Physiology and Biochemistry*, *194*, 271-280.

Raboy, V. (2009). Approaches and challenges to engineering seed phytate and total phosphorus. *Plant Science*, *177*(4), 281-296.

Raboy, V. (2020). Low phytic acid crops: Observations based on four decades of research. *Plants*, *9*(2), 140.

Rahman, S., Li, Z., Batey, I., Cochrane, M. P., Appels, R., & Morell, M. (2000). Genetic alteration of starch functionality in wheat. *Journal of Cereal Science*, *31*(1), 91-110.

Rahman, S., Regina, A., Li, Z., Mukai, Y., Yamamoto, M., Kosar-Hashemi, B., ... & Morell, M. K. (2001). Comparison of starch-branching enzyme genes reveals evolutionary relationships among isoforms. Characterization of a gene for starch-branching enzyme IIa from the wheat D genome donor Aegilops tauschii. *Plant Physiology*, *125*(3), 1314-1324.

Rahman, S., Bird, A., Regina, A., Li, Z., Ral, J. P., McMaugh, S., ... & Morell, M. (2007). Resistant starch in cereals: exploiting genetic engineering and genetic variation. *Journal of Cereal Science*, *46*(3), 251-260.

Raigond, P., Ezekiel, R., & Raigond, B. (2015). Resistant starch in food: a review. *Journal of the Science of Food and Agriculture*, *95*(10), 1968-1978.

Ramzan, Y., Hafeez, M. B., Khan, S., Nadeem, M., Batool, S., & Ahmad, J. (2020). Biofortification with zinc and iron improves the grain quality and yield of wheat crop. *International Journal of Plant Production*, *14*, 501-510.

Ranhotra, G. S. (1994). Wheat: contribution to world food supply and human nutrition. *Wheat: Production, Properties and Quality*, 12-24.

Regina, A., Kosar-Hashemi, B., Li, Z., Pedler, A., Mukai, Y., Yamamoto, M., ... & Rahman, S. (2005). Starch branching enzyme IIb in wheat is expressed at low levels in the endosperm compared to other cereals and encoded at a non-syntenic locus. *Planta*, *222*, 899-909.

Regina, A., Bird, A., Topping, D., Bowden, S., Freeman, J., Barsby, T., ... & Morell, M. (2006). High-amylose wheat generated by RNA interference improves indices of large-bowel health in rats. *Proceedings of the National Academy of Sciences*, *103*(10), 3546-3551.

Regvar, M., Eichert, D., Kaulich, B., Gianoncelli, A., Pongrac, P., Vogel-Mikuš, K., & Kreft, I. (2011). New insights into globoids of protein storage vacuoles in wheat aleurone using synchrotron soft X-ray microscopy. *Journal of Experimental Botany*, *62*(11), 3929-3939.

Riemer, E., Pullagurla, N. J., Yadav, R., Hansjosten, L., Priyanshi, R., ... & Laha, D., (2022). Regulation of plant biotic interactions and abiotic stress responses by inositol polyphosphates. *Frontiers in Plant Science*, 2835.

Roberts, D. P., & Mattoo, A. K. (2019). Sustainable crop production systems and human nutrition. *Frontiers in Sustainable Food Systems*, *3*, 72.

Sakamura, T. (1918). Kurze Mitteilung ueber die Chromosomenzahlen und die Verwandtschaftsverhältnisse der Triticum-arten. *Shokubutsugaku Zasshi*, *32*(379), en150-en153.

Samtiya, M., Aluko, R. E., & Dhewa, T. (2020). Plant food anti-nutritional factors and their reduction strategies: an overview. *Food Production, Processing and Nutrition*, *2*, 1-14.

Sands, D. C., Morris, C. E., Dratz, E. A., & Pilgeram, A. L. (2009). Elevating optimal human nutrition to a central goal of plant breeding and production of plant-based foods. *Plant Science*, *177*(5), 377-389.

Schönhofen, A., Zhang, X., & Dubcovsky, J. (2017). Combined mutations in five wheat STARCH BRANCHING ENZYME II genes improve resistant starch but affect grain yield and bread-making quality. *Journal of Cereal Science*, *75*, 165-174.

Seal, C. J., Nugent, A. P., Tee, E. S., & Thielecke, F. (2016). Whole-grain dietary recommendations: the need for a unified global approach. *British Journal of Nutrition*, *115*(11), 2031-2038.

Secco, D., Bouain, N., Rouached, A., Prom-u-Thai, C., Hanin, M., Pandey, A. K., & Rouached, H. (2017). Phosphate, phytate and phytases in plants: from fundamental knowledge gained in Arabidopsis to potential biotechnological applications in wheat. *Critical reviews in biotechnology*, *37*(7), 898-910.

Sestili, F., Janni, M., Doherty, A., Botticella, E., D'Ovidio, R., Masci, S., ... & Lafiandra, D. (2010). Increasing the amylose content of durum wheat through silencing of the SBEIIa genes. *BMC Plant Biology*, *10*, 1-12.

Sestili, F., Botticella, E., & Lafiandra, D. (2014). TILLING for improved starch composition in wheat. *Genomics of Plant Genetic Resources: Volume 2. Crop productivity, food security and nutritional quality*, 467-487.

Sestili, F., Palombieri, S., Botticella, E., Mantovani, P., Bovina, R., & Lafiandra, D. (2015). TILLING mutants of durum wheat result in a high amylose phenotype and provide information on alternative splicing mechanisms. *Plant Science*, *233*, 127-133.

Sestili, F., Pagliarello, R., Zega, A., Saletti, R., Pucci, A., Botticella, E., ... & Lafiandra, D. (2019). Enhancing grain size in durum wheat using RNAi to knockdown GW2 genes. *Theoretical and Applied Genetics*, *132*, 419-429.

Sestili, F., Garcia-Molina, M. D., Gambacorta, G., Beleggia, R., Botticella, E., De Vita, P., ... & Lafiandra, D. (2019). Provitamin A biofortification of durum wheat through a TILLING approach. *International journal of molecular sciences*, *20*(22), 5703.

Shayanmehr, S., Rastegari Henneberry, S., Sabouhi Sabouni, M., & Shahnoushi Foroushani, N. (2020). Drought, climate change, and dryland wheat yield response: An econometric approach. *International Journal of Environmental Research and Public Health*, *17*(14), 5264.

Shears, S.B. (2001). Assessing the omnipotence of inositol hexakisphosphate. *Cellular signalling*, *13*(3), 151-158.

Sheoran, S., Kumar, S., Ramtekey, V., Kar, P., Meena, R. S., & Jangir, C. K. (2022). Current status and potential of biofortification to enhance crop nutritional quality: an overview. *Sustainability*, *14*(6), 3301.

Shevkani, K., Singh, N., Bajaj, R., & Kaur, A. (2017). Wheat starch production, structure, functionality and applications—a review. International Journal of Food Science & Technology, 52(1), 38-58.

Shewry, P. R., Napier, J. A., & Tatham, A. S. (1995). Seed storage proteins: structures and biosynthesis. *The plant cell*, *7*(7), 945.

Shewry, P. R., Halford, N. G., & Lafiandra, D. (2003). Genetics of wheat gluten proteins. *Advances in genetics*, *49*, 111-184.

Shewry, P. R. (2009). Wheat. *Journal of experimental botany*, *60*(6), 1537-1553.

Shi, J., Wang, H., Schellin, K., Li, B., Faller, M., Stoop, J. M., ... & Glassman, K. (2007). Embryo-specific silencing of a transporter reduces phytic acid content of maize and soybean seeds. *Nature biotechnology*, *25*(8), 930-937.

Shimbata, T., Nakamura, T., Vrinten, P., Saito, M., Yonemaru, J., Seto, Y., & Yasuda, H. (2005). Mutations in wheat starch synthase II genes and PCR-based selection of a SGP-1 null line. *Theoretical and Applied Genetics*, *111*(6), 1072-1079.

Silva, V. M., Putti, F. F., White, P. J., & Dos Reis, A. R. (2021). Phytic acid accumulation in plants: Biosynthesis pathway regulation and role in human diet. *Plant Physiology and Biochemistry*, *164*, 132-146.

Simmonds, J., Scott, P., Brinton, J., Mestre, T. C., Bush, M., Del Blanco, A., ... & Uauy, C. (2016). A splice acceptor site mutation in TaGW2-A1 increases thousand grain weight in tetraploid and hexaploid wheat through wider and longer grains. *Theoretical and Applied Genetics*, *129*, 1099-1112.

Simons, K. J., Fellers, J. P., Trick, H. N., Zhang, Z., Tai, Y. S., Gill, B. S., & Faris, J. D. (2006). Molecular characterization of the major wheat domestication gene Q. *Genetics*, *172*(1), 547-555.

Singh, R., Tiwari, R., Sharma, D., Tiwari, V., & Sharma, I. (2014). Mutagenesis for wheat improvement in the genomics era. *J. Wheat Res.(JWR)*, *6*, 120-125.

Slade, A. J., Fuerstenberg, S. I., Loeffler, D., Steine, M. N., & Facciotti, D. (2005). A reverse genetic, nontransgenic approach to wheat crop improvement by TILLING. *Nature biotechnology*, *23*(1), 75-81.

Slade, A. J., McGuire, C., Loeffler, D., Mullenberg, J., Skinner, W., Fazio, G., ... & Knauf, V. C. (2012). Development of high amylose wheat through TILLING. *BMC plant biology*, *12*(1), 1-17.

Sofi, F., Abbate, R., Gensini, G. F., & Casini, A. (2010). Accruing evidence on benefits of adherence to the Mediterranean diet on health: an updated systematic review and meta-analysis. *The American journal of clinical nutrition*, *92*(5), 1189-1196.

Song, X. J., Huang, W., Shi, M., Zhu, M. Z., & Lin, H. X. (2007). A QTL for rice grain width and weight encodes a previously unknown RING-type E3 ubiquitin ligase. *Nature genetics*, *39*(5), 623-630.

Sourdille, P., Perretant, M. R., Charmet, G., Leroy, P., Gautier, M. F., Joudrier, P., ... & Bernard, M. (1996). Linkage between RFLP markers and genes affecting kernel hardness in wheat. *Theoretical and Applied Genetics*, *93*, 580-586.

Sparla, F., Falini, G., Botticella, E., Pirone, C., Talamè, V., Bovina, R., ... & Trost, P. (2014). New starch phenotypes produced by TILLING in barley. *PloS one*, *9*(10), e107779.

Sparvoli, F., Cominelli, E. (2014). Phytate transport by MRPs. In *Plant ABC transporters* (pp. 19-38). Springer, Cham, p.19-38.

Sparvoli, F., & Cominelli, E. (2015). Seed biofortification and phytic acid reduction: a conflict of interest for the plant?. *Plants*, *4*(4), 728-755.

Spinoni, J., Vogt, J. V., Naumann, G., Barbosa, P., & Dosio, A. (2018). Will drought events become more frequent and severe in Europe?. *International Journal of Climatology*, *38*(4), 1718-1736.

Šramková, Z., Gregová, E., & Šturdík, E. (2009). Chemical composition and nutritional quality of wheat grain. *Acta chimica slovaca*, *2*(1), 115-138.

Sreenivasulu, N., & Schnurbusch, T. (2012). A genetic playground for enhancing grain number in cereals. *Trends in plant science*, *17*(2), 91-101.

Stammers, A. L., Lowe, N. M., Medina, M. W., Patel, S., Dykes, F., Perez-Rodrigo, C., ... & Moran, V. H. (2015). The relationship between zinc intake and growth in children aged 1–8

years: a systematic review and meta-analysis. *European journal of clinical nutrition*, *69*(2), 147-153.

Stevenson-Paulik, J., Bastidas, R. J., Chiou, S. T., Frye, R. A., & York, J. D. (2005). Generation of phytate-free seeds in Arabidopsis through disruption of inositol polyphosphate kinases. *Proceedings of the National Academy of Sciences*, *102*(35), 12612-12617.

Su, Z., Hao, C., Wang, L., Dong, Y., & Zhang, X. (2011). Identification and development of a functional marker of TaGW2 associated with grain weight in bread wheat (Triticum aestivum L.). *Theoretical and Applied Genetics*, *122*, 211-223.

Surget, A., & Barron, C. (2005). Histologie du grain de blé. *Industries des céréales*, (145), 3-7.

Tamura, K., Stecher, G., & Kumar, S. (2021). MEGA11: molecular evolutionary genetics analysis version 11. *Molecular biology and evolution*, *38*(7), 3022-3027.

Tanabata, T., Shibaya, T., Hori, K., Ebana, K., & Yano, M. (2012). SmartGrain: high-throughput phenotyping software for measuring seed shape through image analysis. *Plant physiology*, *160*(4), 1871-1880.

Teng, W., Deng, Y., Chen, X. P., Xu, X. F., Chen, R. Y., Lv, Y., ... & Li, Z. S. (2013). Characterization of root response to phosphorus supply from morphology to gene analysis in field-grown wheat. *Journal of experimental botany*, *64*(5), 1403-1411.

Thompson, J., Biggs, B. A., & Pasricha, S. R. (2013). Effects of daily iron supplementation in 2-to 5-year-old children: systematic review and meta-analysis. *Pediatrics*, *131*(4), 739-753.

Tidiane Sall, A., Chiari, T., Legesse, W., Seid-Ahmed, K., Ortiz, R., Van Ginkel, M., & Bassi, F. M. (2019). Durum wheat (Triticum durum Desf.): Origin, cultivation and potential expansion in Sub-Saharan Africa. *Agronomy*, *9*(5), 263.

Till, B. J., Reynolds, S. H., Greene, E. A., Codomo, C. A., Enns, L. C., Johnson, J. E., ... & Henikoff, S. (2003). Large-scale discovery of induced point mutations with high-throughput TILLING. *Genome research*, *13*(3), 524-530.

Till, B. J., Cooper, J., Tai, T. H., Colowit, P., Greene, E. A., Henikoff, S., & Comai, L. (2007). Discovery of chemically induced mutations in rice by TILLING. *BMC plant biology*, *7*, 1-12.

Topping, D. L., & Clifton, P. M. (2001). Short-chain fatty acids and human colonic function: roles of resistant starch and nonstarch polysaccharides. *Physiological reviews*, *81*(3), 1031-1064.

Vance, C. P., Uhde-Stone, C., & Allan, D. L. (2003). Phosphorus acquisition and use: critical adaptations by plants for securing a nonrenewable resource. *New phytologist*, *157*(3), 423-447.

Vasconcelos, M. W., Gruissem, W., & Bhullar, N. K. (2017). Iron biofortification in the 21st century: setting realistic targets, overcoming obstacles, and new strategies for healthy nutrition. *Current Opinion in Biotechnology*, *44*, 8-15.

Venegas, J., Guttieri, M. J., Boehm Jr, J. D., Graybosch, R., Bai, G., St. Amand, P. C., ... & Baenziger, P. S. (2022). Genetic architecture of the high-inorganic phosphate phenotype derived from a low-phytate mutant in winter wheat. *Crop Science*, *62*(3), 1228-1241.

Verma, S. K., Kumar, S., Sheikh, I., Malik, S., Mathpal, P., Chugh, V., ... & Dhaliwal, H. S. (2016). Transfer of useful variability of high grain iron and zinc from Aegilops kotschyi into wheat through seed irradiation approach. *International Journal of Radiation Biology*, *92*(3), 132-139.

Vitamin and Mineral Nutrition Information System (VMNIS). 2022. https://www.who.int/teams/nutrition-and-food-safety/databases/vitamin-and-mineral-nutrition-information-system. Accessed August 2022.

Von Grebmer, K., Saltzman, A., Birol, E., Wiesman, D., Prasai, N., Yin, S., ... & Sonntag, A. (2014). *Synopsis: 2014 global hunger index: The challenge of hidden hunger* (Vol. 83). Intl Food Policy Res Inst.

Wani, S. H., Gaikwad, K., Razzaq, A., Samantara, K., Kumar, M., & Govindan, V. (2022). Improving zinc and iron biofortification in wheat through genomics approaches. *Molecular Biology Reports*, *49*(8), 8007-8023.

White, P. J., & Broadley, M. R. (2009). Biofortification of crops with seven mineral elements often lacking in human diets–iron, zinc, copper, calcium, magnesium, selenium and iodine. *New Phytologist*, *182*(1), 49-84.

Wicker, T., Taudien, S., Houben, A., Keller, B., Graner, A., Platzer, M., & Stein, N. (2009). A whole-genome snapshot of 454 sequences exposes the composition of the barley genome and provides evidence for parallel evolution of genome size in wheat and barley. *The Plant Journal*, *59*(5), 712-722.

Willett, W. C., Sacks, F., Trichopoulou, A., Drescher, G., Ferro-Luzzi, A., Helsing, E., & Trichopoulos, D. (1995). Mediterranean diet pyramid: a cultural model for healthy eating. *The American journal of clinical nutrition*, *61*(6), 1402S-1406S.

Williams, J., Allen, L., Wickramasinghe, K., Mikkelsen, B., Roberts, N., & Townsend, N. (2018). A systematic review of associations between non-communicable diseases and socioeconomic status within low-and lower-middle-income countries. *Journal of global health*, *8*(2).

Wittwer, C. T., Reed, G. H., Gundry, C. N., Vandersteen, J. G., & Pryor, R. J. (2003). High-resolution genotyping by amplicon melting analysis using LCGreen. *Clinical chemistry*, *49*(6), 853-860.

World Health Organization. (2006). *Guidelines on food fortification with micronutrients*. World Health Organization.

World Health Organization. (2016). *World Health Statistics 2016 [OP]: Monitoring Health for the Sustainable Development Goals (SDGs)*. World Health Organization.

World Health Organization. (2017). *Preventing noncommunicable diseases (NCDs) by reducing environmental risk factors* (No. WHO/FWC/EPE/17.01). World Health Organization.

Xu, X. H., Zhao, H. J., Liu, Q. L., Frank, T., Engel, K. H., An, G., & Shu, Q. Y. (2009). Mutations of the multi-drug resistance-associated protein ABC transporter gene 5 result in reduction of phytic acid in rice seeds. *Theoretical and applied genetics*, *119*, 75-83

Xynias, I. N., Mylonas, I., Korpetis, E. G., Ninou, E., Tsaballa, A., Avdikos, I. D., & Mavromatis, A. G. (2020). Durum wheat breeding in the Mediterranean region: Current status and future prospects. *Agronomy*, *10*(3), 432.

Yamamori, M., Nakamura, T., Endo, T. R., & Nagamine, T. (1994). Waxy protein deficiency and chromosomal location of coding genes in common wheat. *Theoretical and applied genetics*, *89*, 179-184.

Yamamori, M., Fujita, S., Hayakawa, K., Matsuki, J., & Yasui, T. (2000). Genetic elimination of a starch granule protein, SGP-1, of wheat generates an altered starch with apparent high amylose. *Theoretical and Applied Genetics*, *101*, 21-29.

Yang, Z., Bai, Z., Li, X., Wang, P., Wu, Q., Yang, L., ... & Li, X. (2012). SNP identification and allelic-specific PCR markers development for TaGW2, a gene linked to wheat kernel weight. *Theoretical and Applied Genetics*, *125*, 1057-1068.

Zhao, X. C., & Sharp, P. J. (1996). An improved 1-D SDS–PAGE method for the identification of three bread wheat «Waxy» proteins. *Journal of Cereal Science*, *23*(2), 191-193.